DANMARKS OG GRØNLANDS GEOLOGISKE UNDERSØGELSE RAPPORT 2011/95

Contribution to predictions of stratigraphy and reservoir properties in the Eastern Norwegian-Danish Basin

Report to Universitetet i Oslo, UiO

L. H. Nielsen, R. Weibel, L. Kristensen, K. Dybkjær,
P. Japsen, M. Olivarius, T. Bidstrup
& A. Mathiesen

GEOLOGICAL SURVEY OF DENMARK AND GREENLAND
MINISTRY OF CLIMATE AND ENERGY

GEUS

DANMARKS OG GRØNLANDS GEOLOGISKE UNDERSØGELSE RAPPORT 2011/95

Contribution to predictions of stratigraphy and reservoir properties in the Eastern Norwegian-Danish Basin

Report to Universitetet i Oslo, UiO

L. H. Nielsen, R. Weibel, L. Kristensen, K. Dybkjær,
P. Japsen, M. Olivarius, T. Bidstrup
& A. Mathiesen

Compiled and edited by Lars Henrik Nielsen

GEOLOGICAL SURVEY OF DENMARK AND GREENLAND
MINISTRY OF CLIMATE AND ENERGY

GEUS

Preface

This report compiles essential information and data relevant for the assessment of the storage potential of CO_2 in the eastern part of the Norwegian-Danish Basin. The report is prepared as a contribution to the project ”Kortlægning af mulighederne for lagring af CO_2 i østlige Nordsø, Skagerrak og på land i Danmark” headed by “Universitet i Oslo”. The aim is to provide a framework for extrapolation of Danish data to the study area.

The report contains geological aspects relevant for predictions of the undrilled stratigraphy and the potential reservoirs in the study area and provides a framework for interpretation of seismic data. It contains a summary of the geological development of the eastern Norwegian-Danish Basin and the Fennoscandian Border Zone including the Farsund Basin; descriptions and evaluation of potential reservoir sandstones including data on their petrography and diagenesis based on Danish well information; a series of comments regarding the expected stratigraphy in the study area, and a discussion of Neogene uplift and exhumation.

Based on core descriptions and sedimentological interpretations supported by new biostratigraphic and geochemical analyses of samples from the IKU/Sintef core 13/1-U-1, correlation to the sequence stratigraphic framework established in Danish wells is presented.

Parts of the content have previously been presented and reported to the project group at the University in Oslo.

1. Summary

The Mesozoic succession of the Norwegian-Danish Basin contains several formations with sandstones that may be potential reservoirs for CO_2 storage (Anthonsen and Nielsen 2008; Anthonsen et al. 2009, 2011; Frykmann et al. 2009). These include the Triassic Bunter Sandstone and Skagerrak Formations, the Upper Triassic–Lower Jurassic Gassum Formation, the Middle Jurassic Haldager Sand Formation, and the mainly Jurassic Frederikshavn Formation. Additional storage potential may locally occur in the Upper Jurassic Flyvbjerg Formation. Investigations have shown that among these formations, the potential of the Gassum and Haldager Sand Formations is probably the highest. This is related to their distribuition and burial depths, the potential storage volume, the presence of overlying cap rocks with suitable seal capacity and the presence of large structures at suitable depths.

Both reservoirs are expected to be present in the Skagerrak area and in the Farsund Basin except on marked salt structures. They are probably sealed by Lower and Upper Jurassic marine mudstones with large lateral continuity and excellent sealing capacity.

Based on the detailed depositional models and the sequence stratigraphic framework established for the Danish part of the basin (Nielsen 2003), and the Danish well data on reservoir and cap rock properties reported here, it is possible to defined predictive models and interpretations for undrilled areas in the basin based on available seismic data.

Parts of the basin have experienced pronounced uplift and erosion. The exhumation began between 45 and 20 Ma according to new AFTA data, and may reach ca. 1 km or more for the Farsund Basin. The amount of uplift needs to be considered when the properties of reservoir and cap rocks are predicted in undrilled areas as the maximal burial depths are greater than the present day burial depth.

The report thus contains information on structural development, stratigraphy, sedimentology, petrography, diagenesis and exhumation which have been compiled from various internal sources at GEUS in order to provide a platform for detailed discussion among the project participants. The scope has been to provide data for the project group for its common efforts toward predictions of undrilled stratigraphy in the areas seleceted by “Universitetet I Oslo”.

2. Introduction

The objectives of this report are to compile relevant information and data on the structural-stratigraphic development of the eastern Norwegian-Danish Basin in order to contribute to establishment of a geological framework for interpretations of the seismic data in the study area and to qualify predictions of reservoir properties.

The geological development of the central and eastern part of the Norwegian-Danish Basin and Fennoscandian Border Zone is described. When possible, comments regarding the expected development and stratigraphy of the virtually undrilled Farsund Basin is provided based on the current understanding of the regional pattern. Seismic data from the Farsund Basin has not been available for the study except for a few published sections. Particular emphasis is placed on the Late Triassic–Late Jurassic development as the potential reservoirs and most promising cap rocks were formed during this period. Interpretations of depositional environments are displayed on regional well-log panels and paleogeographic maps. Based on a detailed description of the established geological model for this part of the stratigraphy and interpretations of the IKU/Sintef core wells northeast of the Farsund Basin (including new biostratigraphic, palynofacies and geochemical analyses of 13/1-U-1), specific proposals regarding the anticipated geology of the Farsund Basin are given for each stratigraphic interval discussed.

An interpretation including net/gross ratios of the Upper Triassic Gassum and Middle Jurassic Haldager reservoirs, which are the most promising reservoirs in the area, is provided. Additional reservoirs known in the Norwegian-Danish Basin and Fennoscandian Border Zone are briefly described.

The significant Neogene exhumation in the area is discussed based on a large number of vitrinite reflectance measurements, AFTA data and shale velocity anomalies in an attempt to contribute to the estimation of exhumation in the eastern Norwegian-Danish Basin. Tables with well picks of formations and sequence stratigraphic surfaces are enclosed.

3. Exploration history

The Mesozoic succession of the Danish part of the Norwegian–Danish Basin and the Fennoscandian Border Zone has been target for exploration activities since 1935 and is known from c. 60 deep wells drilled for hydrocarbons, geothermal energy or gas storage (Fig. 3.1) (Sorgenfrei & Buch 1964; Nielsen & Japsen 1991). Only poor indications of hydrocarbons have been encountered. The Mesozoic has likewise been tested in the Norwegian part of the basin and border zone in c. 10 wells also with poor results; however the succession has not yet been drilled in the Farsund Basin except for well 11/5-1 located on a salt structure in the western part of the basin and the shallow core wells drilled on the northern flanck of the basin.

In the central to eastern part of the Norwegian-Danish Basin and Fennoscandian Border Zone the principal hydrocarbon play models have been the sandstones of the Upper Triassic Gassum Formation or the Middle Jurassic Haldager Sand and Bryne formations charged from source rocks within the Lower Jurassic (Fjerritslev Formation) or the Upper Jurassic–Lower Cretaceous (Børglum, Frederikshavn, Tau and Mandal formations). These plays have been tested by more than 30 wells placed on structures or pinch-outs formed by salt movements or faults. No or only weak indications of active petroleum systems have been encountered, and the principal source rock, the F-III and F-IV members of the Fjerritslev Formation, is immature to marginally mature in the wells drilled. The wells have mainly been drilled on structures, but seismic data support a relatively shallow burial depth. Sufficient burial of the source rocks prior to Late Cretaceous–Paleogene inversion events and Neogene exhumation may have occurred in local deep areas, such as the Farsund Basin where indications of an active petroleum system is found as structural aligned seafloor potmarks.

The DUC Group drilled four wells south of the Farsund Basin, the F-1 well (1968), J-1 (1970), K-1 (1970), and Inez-1 (1977) (Fig. 3.1). The F-1, K-1 and Inez-1 wells are located in the Norwegian-Danish Basin, while J-1 is located on the down-thrown side of the Fjerritslev Fault in the Fjerritslev Trough, which is part of the larger Sorgenfrei-Tornquist Zone that also includes the Farsund Basin. All four wells tested the Haldager and the Gassum reservoirs. Both reservoirs were present at c. 1050–2050 m of depths overlain by marine mudstones with seal capacity. Later, the Statoil Group drilled the Felicia-1/1A well (1987) on a Rotliegend target situated on the upthrown side of the Fjerritslev Fault. The well tested also a large structure present at top Triassic level (Hanstholm structure), but in an unfavourable position some 700 m down flank of the structure. The well encountered the Haldager and Gassum reservoirs and additional sandstones in the Flyvbjerg Formation (Upper Jurassic).

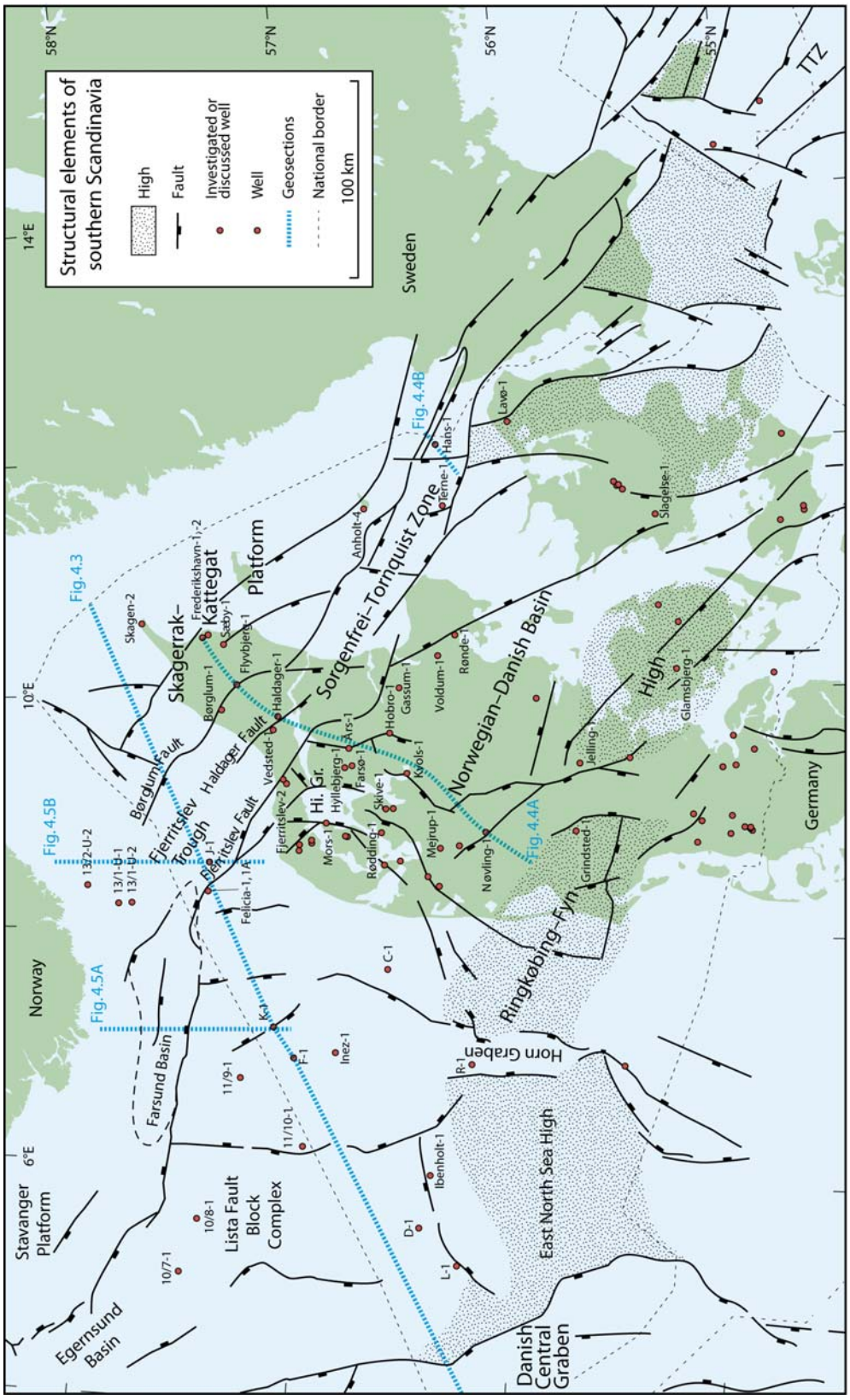

Figure 3.1.

Map displaying position of wells, interpreted seismic sections shown in section, and principal structural elements including the Farsund and Egernsund basins. The wells named have been included in the study or are mentioned in the report.

On the Norwegian side the well 11/9-1 (Elf Norway, 1976) tested the Triassic section on a large salt structure 30–35 km south of the Farsund Basin (Fig. 3.1). The well started out in the Triassic and was terminated in Zechstein salt at 1972 m. The well 11/10-1 (Phillips Petroleum, 1969) is situated c. 60 km southwest of the Farsund Basin and was terminated in the Triassic Skagerrak Formation at 2430 m without encountering the Haldager Sand or Gassum reservoirs or the Fjerritslev cap rock as the Upper Jurassic unconformably overlies the Triassic (Rhaetian). The 10/8-1 well (Elf 1971) located some 50 km west-southwest of the Farsund Basin was terminated at 2861 m in the Zechstein. The well encountered a good Middle Jurassic Haldager reservoir unconformably overlying the Triassic. The 10/7-1 well (Esso Norway, 1992) is located some 75 km west of the Farsund Basin and proved good reservoir sandstones in the Bryne/Haldager Sand Formation and the Sandnes/Flyvbjerg Formation. The Middle Jurassic sandstones unconformably overlie the Zechstein. The 11/5-1 well (Norsk Hydro 2007) located in the Farsund Bassin proved the presence of Middle Jurassic sandstones unconformably overlying Zechstein.

In summary, none of the five Norwegian wells encountered the Lower Jurassic Fjerritslev Formation (cap rock), which suffers from deep erosion in the area, especially on structures, owing to the uplift of the Ringkøbing-Fyn High and regional tilting of the Norwegian-Danish Basin in early Middle Jurassic time (Andsbjerg et al. 2001; Nielsen 2003). The Haldager Sand Formation was confirmed as a potential reservoir; however, the reservoir may be missing, on the highest structures. Reservoir sandstones were furthermore proved in the Upper Jurassic Flyvbjerg Formation similar to the Felicia-1 well and to wells in the Fjerritslev Trough and the Skagerrak-Kattegat Platform.

4. Tectonic setting

4.1 Principal structures

The eastern part of the Norwegian-Danish Basin is a WNW–ESE trending intracratonic, Permian–Cenozoic structure bounded by elevated Precambrian basement blocks of the Ringkøbing-Fyn High to the south and the Fennoscandian Border Zone to the north and east (Figs 3.1, 4.1, 4.2)(Sorgenfrei & Buch 1964; EUGENO-S Working Group 1988; Michelsen & Nielsen 1991, 1993; Vejbæk 1997; Nielsen 2003). The Ringkøbing-Fyn High separates the Norwegian-Danish Basin from the North German Basin and was probably formed contemporaneously with the Norwegian-Danish Basin as an area of less crustal stretching. The Fennoscandian Border Zone demarcates the transition from the basin to the stable Precambrian Baltic Shield to the north and east. It comprises the Skagerrak-Kattegat Platform that westward passes into the Stavanger Platform northeast of the Egernsund Basin (Figs 3.1, 4.1, 4.2). On the Skagerrak-Kattegat Platform the Mesozoic section is relatively undisturbed; it onlaps tilted fault blocks with Precambrian crystaline basement, Lower Palaeozoic and Lower Permian strata and wedges out toward the northeast (Figs 4.3, 4.4A). The Sorgenfrei-Tornquist Zone is a highly block-faulted 30–50 km wide zone that runs SE–NW from the Rønne Graben in the Baltic Sea across southern Sweden through Kattegat and northern Jylland to Skagerrak, where it turns westward across the Norwegian shelf (Figs 3.1, 4.1–4.5). The zone includes, among others, the deep Fjerritslev Trough with a Zechstein–Mesozoic succession that locally reaches more than 9 km in thickness and the shallower Farsund Basin, where the Zechstein–Mesozoic section reaches slightly more than 6 km in places.

4.2 Rifting

The principal rifting phase of the Norwegian-Danish Basin and the Sorgenfrei-Tornquist Zone including the Farsund Basin is marked by tilted fault blocks with basement rocks and Lower Palaeozoic strata unconformably overlain by Permian rocks (Figs 4.3–4.5)(Liboriussen et al. 1987; Vejbæk 1989, 1997; Michelsen & Nielsen 1991, 1993; Jensen and Schmidt 1993; Vejbæk & Britze 1994; Christensen & Korstgård 1994). The crests of the fault blocks are deeply truncated and this top-pre Zechstein surface is the deepest regional surface that can be mapped by reflection seismic data in the Norwegian-Danish Basin and the Fennoscandian Border Zone. The surface is relatively flat and smooth indicating pronounced erosion prior to the Zechstein transgression. The unconformity is penetrated by wells, which show the occurrence of Precambrian crystalline rocks on the Ringkøbing–Fyn High (Glamsbjerg-1, Grindsted-1, Ibenholt-1 and Jelling-1) and the Skagerrak–Kattegat Platform (Frederikshavn-1) and Lower Palaeozoic sedimentary rocks in the Norwegian-Danish Basin and Fennoscandian Border Zone (Figs 3.1, 4.1)(Nøvling-1, Rønde-1, Slagelse-1 and Terne-1; Sorgenfrei & Buch 1964; Poulsen 1969, 1974; Christensen 1971, 1973; Larsen 1971, 1972; Michelsen & Nielsen 1991, 1993; Nielsen & Japsen 1991). The

shallow IKU/Sintef corehole 13/2-U-2 encountered Silurian strata subcropping the Quaternary northeast of the Farsund Basin (Fig. 3.1). These wells all cut the unconformity on footwall blocks or on hangingwall block crests, where deep erosion has occurred, thus making an accurate dating of the rifting impossible. In contrast, the Hans-1 and Sæby-1 wells are located in the deep hangingwalls of tilted fault blocks close to the footwall fault. In Sæby-1, on the Skagerrak–Kattegat Platform, the unconformity separates Triassic sediments from syn-rift Rotliegend volcaniclastic rocks. In the Sorgenfrei–Tornquist Zone, Hans-1 penetrates a pre-rift succession of clastic sediments and extrusive volcanic rocks, of presumed Late Carboniferous age (Fig. 4.4B). The succession is overlain by a thick Rotliegend syn-rift prism of alluvial conglomerates and sandstones and lacustrine mudstones. The syn-rift succession is overlain by marginal to non-marine Zechstein deposits. In the nearby Terne-1 well, Upper Carboniferous intrusive volcanic rocks occur, and the volcanic rocks in Hans-1 and Terne-1 seem to be roughly contemporaneous with the earliest volcanic rocks in the Oslo Graben and dolerite dykes in southern Sweden (Bergström *et al.* 1982; Ro *et al.* 1990). The principal phase of rifting of the Norwegian-Danish Basin and the Fennoscandian Border Zone is thus interpreted to have occurred in the Late Carboniferous – Early Permian at the same time as, or slightly later than, rifting of the Oslo Graben (Ro et al. 1990; Michelsen & Nielsen 1991, 1993).

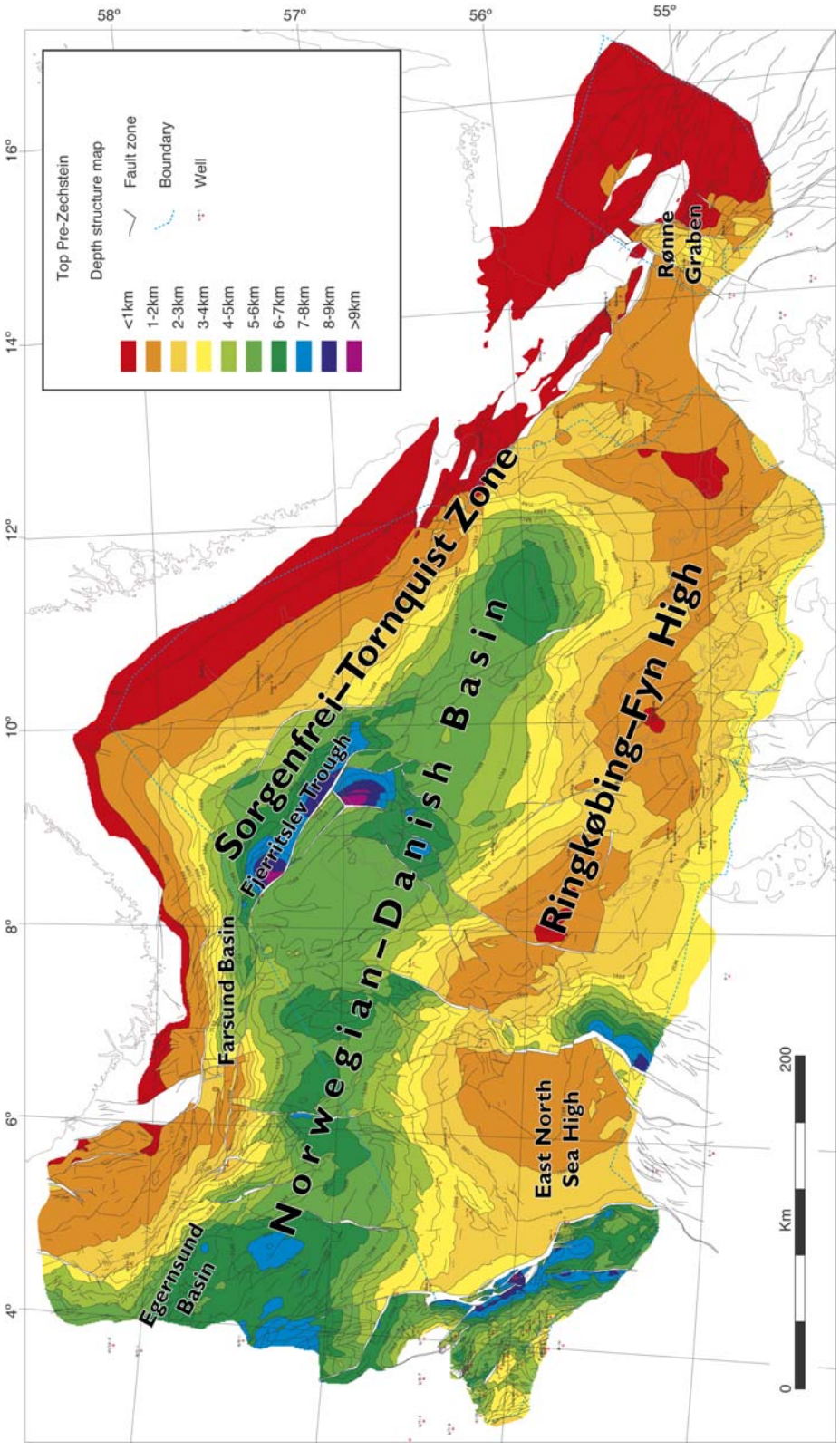

Figure 4.1. *Depth structure map of the top pre-Zechstein surface, the deepest surface that can be mapped regionally by conventional seismic data. Note the large thickness in the Fjerritslev Trough and the Himmerland Graben situated just south of the Fjerritslev Trough. Note also that the depth in the Farsund Basin is similar to or slightly shallower than the main basin (modified from Vejbæk 1977).*

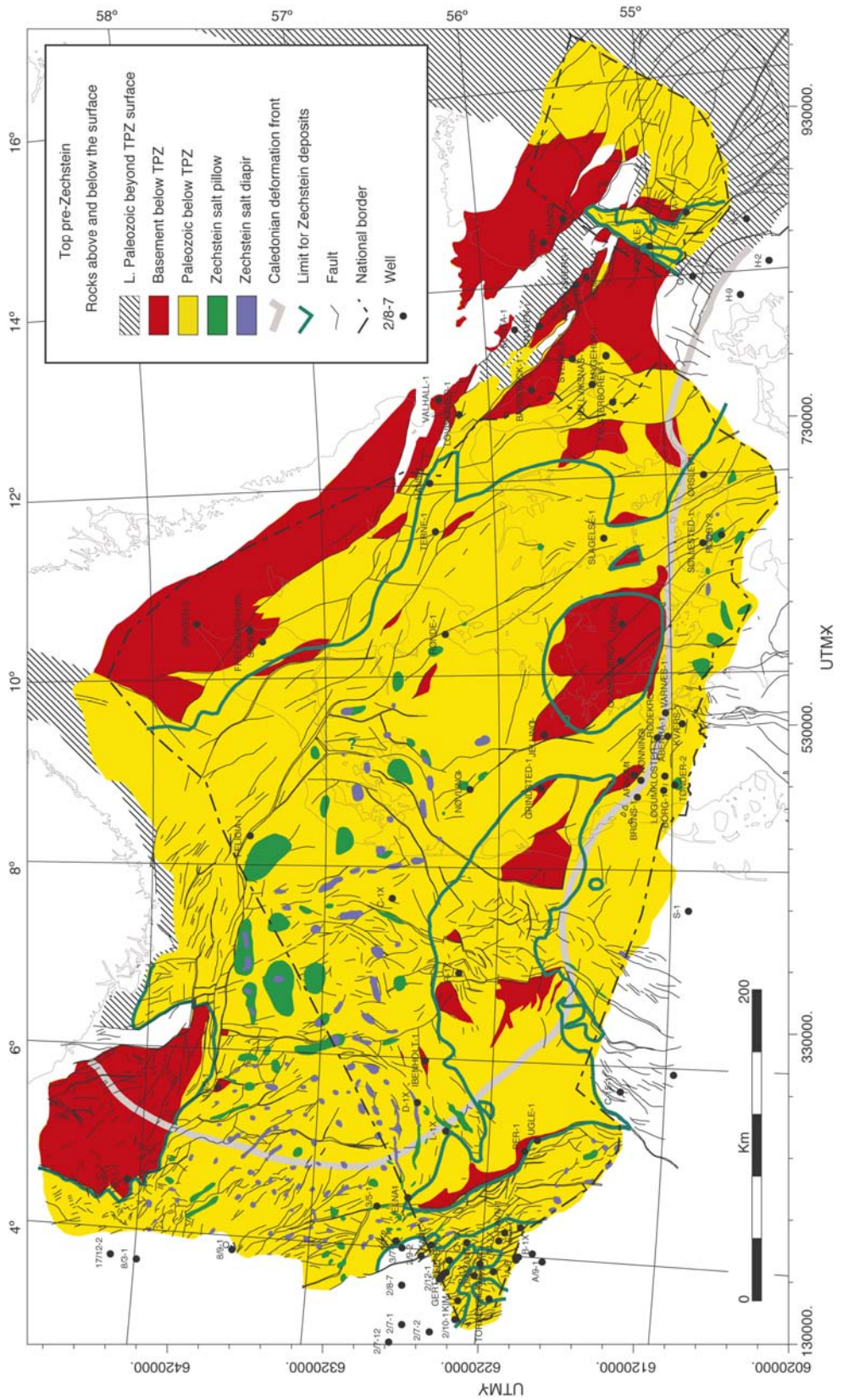

Figure 4.1B. *The map displays the rocks below the top-pre Zechstein surface and the known salt structures. Note the green line indicating the limit of the Zechstein deposits (from Vejbæk 1997).*

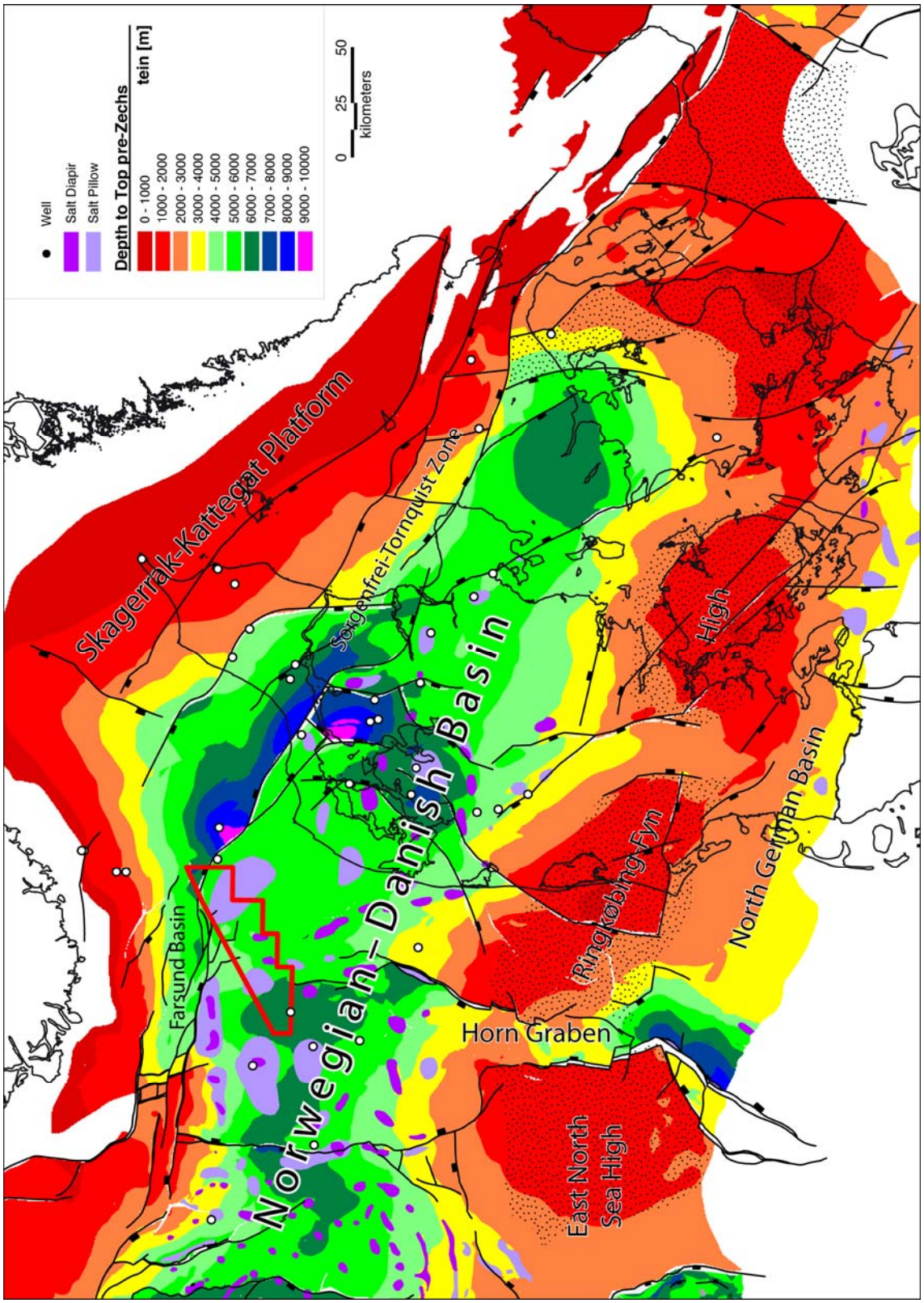

Figure 4.2. *Depth structure map of the top-Pre Zechstein surface with positions of wells and salt diapirs and pillows (modified from Vejbæk 1997).*

4.3 Post-rifting

The tilted fault block crests are deeply truncated by the mid-Permian unconformity showing that regional post-rift thermal subsidence was somewhat delayed (Vejbæk 1997). The unconformity that defines the basis of the post-rift sequence is overlain by a relatively complete succession of Zechstein salts and carbonates, Triassic clastics, carbonates and salts, Jurassic–Lower Cretaceous clastics, Upper Cretaceous chalks and Cenozoic clastics that attains a thickness of 5–6.5 km along the basin axis. A similar thickness of the post-rift succession is found in the Farsund Basin, where the succession is more than 3 sec (TWT) thick in places corresponding to slightly more than 6 km (Jensen & Schmidt 1994; Vejbæk & Britze 1994), whereas the succession attains more than 9 km locally in the Fjerritslev Trough and the Himmerland Graben (Fig. 4.1). Isochore maps of the Triassic and Jurassic – Lower Cretaceous successions show a relatively uniform regional thickness over most of the basin except for areas influenced by local halokinetic movements, indicating relatively uniform thermal subsidence (Vejbæk 1989, 1997; Britze & Japsen 1991; Japsen & Langtofte 1991). Although the thick Upper Permian – Triassic succession indicates rapid subsidence that exceeds normal thermal contraction, a prolonged or new rifting phase is precluded by the general lack of pronounced extensional faulting in the Mesozoic succession, and phase-transformations in the deep crust have been proposed to explain the rapid early post-rift subsidence (Vejbæk 1989, 1997). The evaporitic and continental facies show that the basin was never under-filled with accommodation below sea level in spite of the rapid subsidence. The great thickness of the Mesozoic in the Himmerland Graben and the Fjerritslev Trough were facilitated by transtensional strike-slip movements in the Sorgenfrei–Tornquist Zone or large-scale salt movements (Pegrum 1984; Vejbæk 1989; Christensen & Korstgård 1994; Mogensen 1994, 1996). Local growth of salt structures influenced the Mesozoic deposition.

4.4 Middle Jurassic exhumation

The Ringkøbing-Fyn High was uplifted significantly in early Middle Jurassic time and the Danish Basin became tilted to the northeast (Michelsen 1978; Koch 1983; Andsbjerg *et al*. 2001; Nielsen 2003). The uplift and tilting caused a progressively deeper erosive truncation of the Lower Jurassic and Triassic across the basin toward the Ringkøbing-Fyn High, where erosion removed the entire Lower Jurassic and much of the Triassic on the most elevated parts of the high (Fig. 5.2). In contrast, subsidence continued during Middle Jurassic time in the Sorgenfrei-Tornquist Zone shown by well sections in the Øresund region, in Kattegat (Terne-1, Anholt-4), and in the Fjerritslev Trough (Børglum-1, Fjerritslev-2, Flyvbjerg-1, J-1, Haldager-1, Vedsted-1) but at a much lower rate than in Triassic–Early Jurassic times (Fig. 4.6). Danish well-sections in the Skagerrak-Kattegat Platform (Frederikshavn-1,-2,-3, Skagen-2, Sæby-1) indicate that only limited erosion occurred north of the Fjerritslev Through during this phase. A sequence stratigraphic interpretation of the succession in the shallow IKU/Sintef corehole 13/1-U-1 based on preliminary GEUS studies including sedimentology, biostratigraphy and source rock screening analysis conforms with this pattern (Fig. 5.7), which strongly supports the assumption that the Farsund Basin followed the pattern with a phase of reduced subsidence during Middle Jurassic time in the Sorgenfrei-Tornquist Zone. Based on this and the geosections in Fig. 4.5 it is thus pro-

posed that the Late Triassic–Early Cretaceous subsidence of the Farsund Basin mirrored the pattern indicated by the “Fjerritslev Trough” and the “Skagerrak-Kattegat Platform” curves in Fig 4.6, which differs from that proposed for the Jurassic by Jensen and Schmidt (1993; their Fig. 6).

4.5 Inversion and Neogene exhumation

Regional subsidence gradually resumed during late Middle Jurassic–Late Jurassic times and tectonic tranquillity generally prevailed except for local salt movements until inversion occurred in the Sorgenfrei-Tornquist Zone. A Late Cretaceous–Paleogene age is generally accepted for the inversion, which is interpreted to be caused by compression related to a change in the regional stress field from extensional to compressional related to the Alpine deformation and opening of the North Atlantic (Liboriusen *et al*. 1987; Ziegler 1990; Michelsen & Nielsen 1991, 1993; Mogensen & Korstgård 2003). However, the inversion may have occurred in several phases and it is assumed that the inversion began in Turonian time or earlier in the southeast with 2–3 km of uplift in the Scania-Bornholm area, and propagated north-westward with a decreasing intensity of deformation (Berthelsen 1992; Mogensen & Jensen 1994; Michelsen 1997). After cessation of the inversion a new quiet tectonic phase began with regional subsidence of the greater North Sea Basin. Contemporaneously with the regional down-warping of southern Scandinavia, significant uplift and erosion began to influence parts of the Norwegian-Danish Basin and the Ringkøbing-Fyn High in Neogene time (Japsen 1993; Jensen & Schmidt 1993; Japsen et al. 2002a,b).

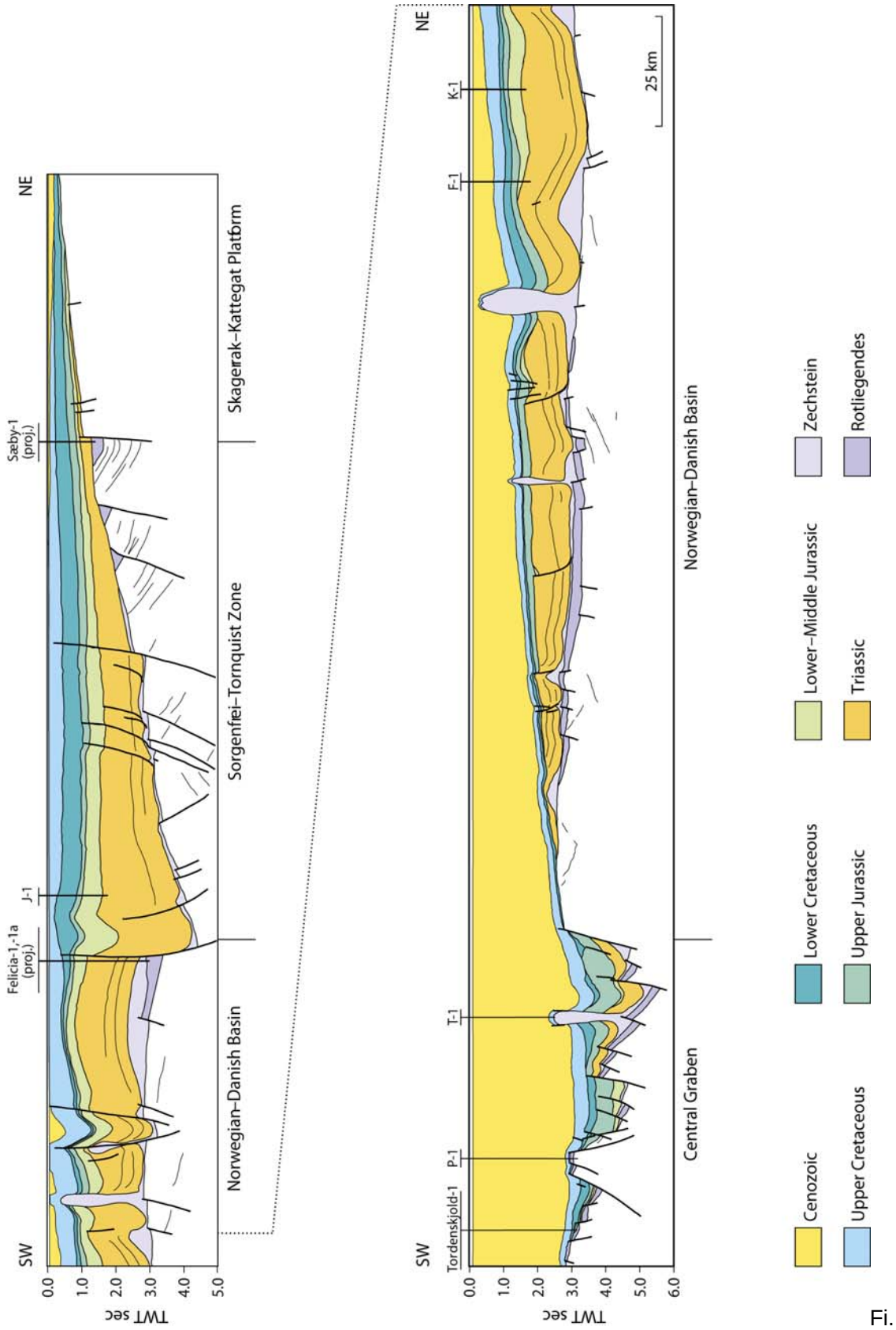

Fi.

Figure 4.3.. *Regional geosection from the Central Graven in the southwest to the Skagerrak-Kattegat Platform in the northeast. Position is marked on Fig. 3.1.*

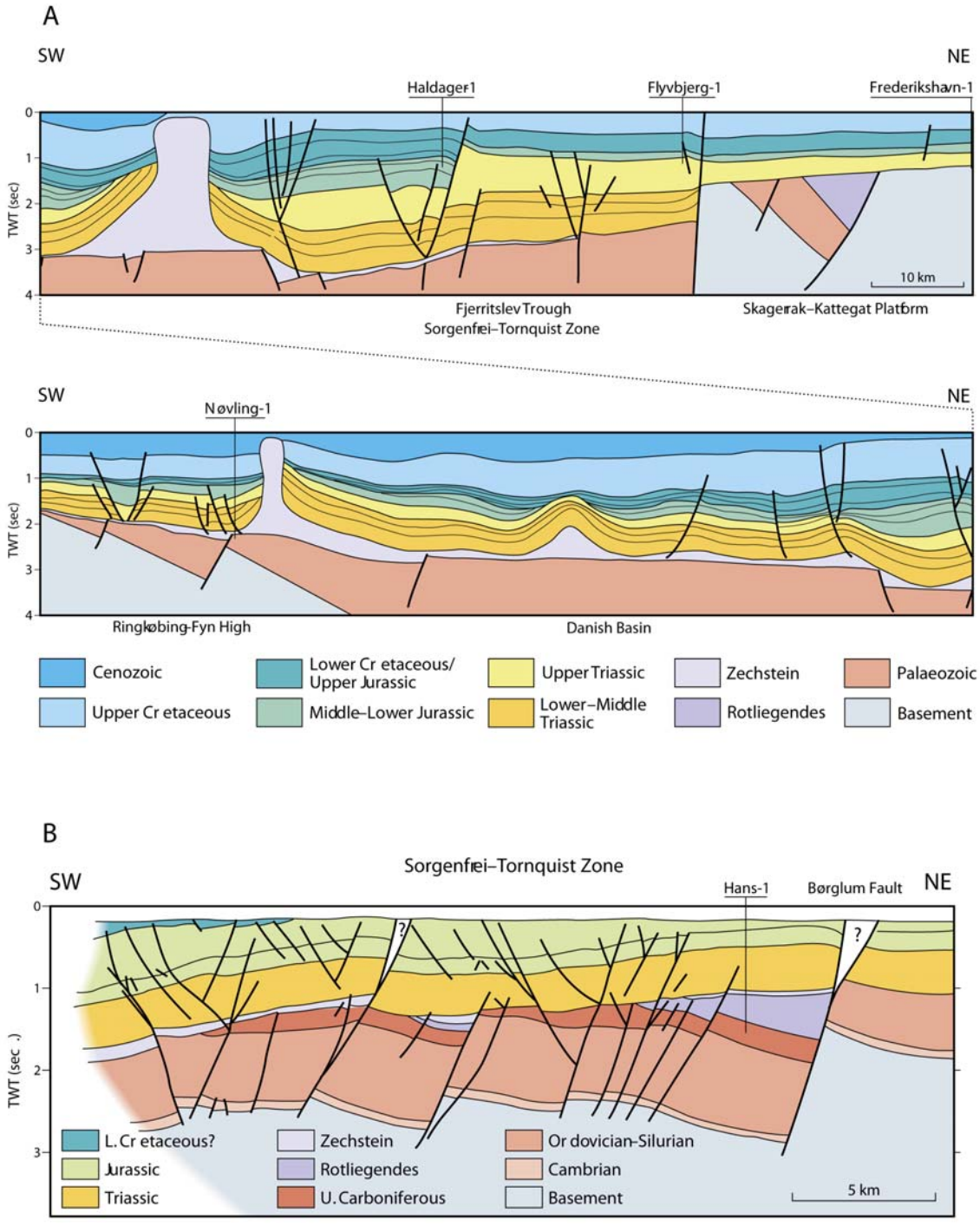

Figure 4.4 (A) *Regional geosection across the Danish part of the Norwegian-Danish Basin. (B) Geosection from Kattegat through the Hans-1 well; note Palaeozoic fault blocks. Position of sections are marked on Fig. 3.1 (modified from Michelsen & Nielsen 1991).*

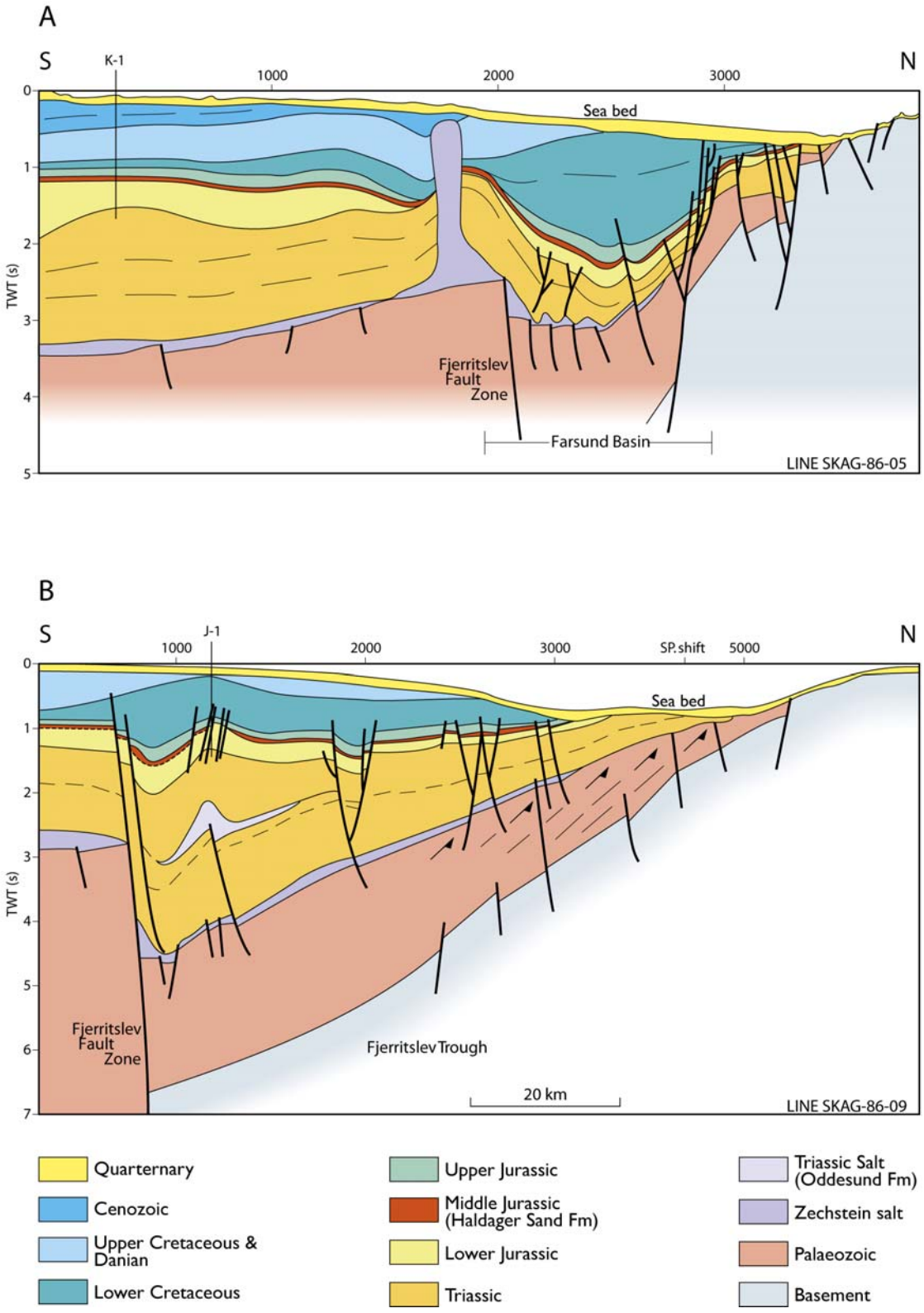

Figure 4.5. (A) *Geosection trending north-south from the Norwegian-Danish Basin across the Fjerritslev Fault and Farsund Basin. The Middle Jurassic Haldager reservoir overlying the Lower Jurassic cap rocks is marked in red. Note Palaeozoic fault blocks overlain by Zechstein salt. (B) Geosection from the Fjerritslev Trough. Positions are marked on Fig. 3.1 (modified from Jensen & Schmidt 1993).*

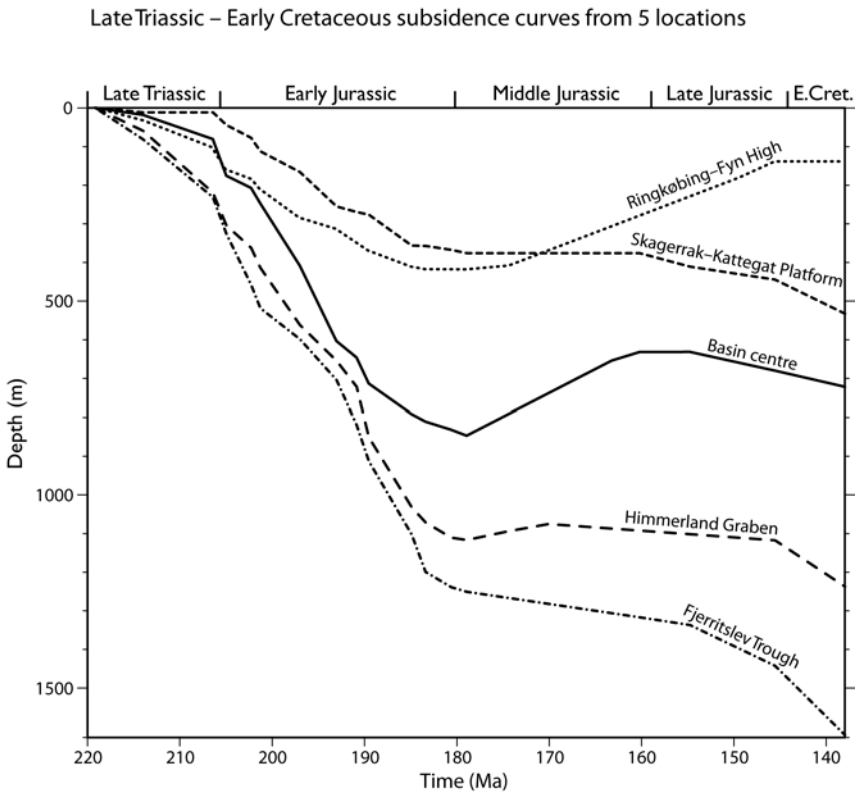

Figure 4.6. *Subsidence curves for the Late Triassic–Early Cretaceous constructed for different structural elements/subbasins within the Norwegian-Danish Basin, Skagerrak-Kattegat Platform and Ringkøbing-Fyn High based on a high-resolution sequence stratigraphic break-down. The Farsund Basin is expected to follow a trend between the trends of the Fjerritslev Trough and the Skagerrak-Kattegat Platform with a slow subsidence in Middle Jurassic time (from Nielsen 2003).*

5. Depositional development and stratigraphy

The main emphasis in this chapter is placed on a detailed description of Late Triassic–Late Jurassic development as the principal reservoir and cap rocks in the eastern Norwegian-Danish Basin were formed during this period of time. The lithostratigraphy of the Norwegian-Danish Basin and the Danish Central Graben is shown in Fig. 5.1. A sequence stratigraphic interpretation of the Upper Triassic–Upper Jurassic succession is presented in detail in order to justify proposed interpretations of the virtually undrilled succession in the Farsund Basin. Fig. 5.2 shows a time stratigraphic scheme across the Norwegian-Danish Basin perpendicular to the principal structural strike with interpreted sequence stratigraphic key-surfaces, lithostratigraphy and depositional environments. A series of well-log panels have been constructed across the basin to illustrate the depositional facies, and these are used to predict facies in the Skagerrak area (Figs 5.2–5.6, 5.8, 5.10). A dip log panel across the basin exemplifies the lithostratigraphy (Fig. 5.12), and it is expected that a profile across the Farsund Basin to the centre of the Norwegian-Danish Basin would be comparable to this. A series of paleogeographic maps illustrate the overall depositional pattern at selected Jurassic time steps (5.13).

5.1 Zechstein evaporites

The deposition of the post-rift succession was initiated in Late Permian times with deposition of thick Zechstein evaporites in most of the Norwegian-Danish Basin over the peneplained structural relief. Marginal facies were developed along parts of Ringkøbing-Fyn High in Late Permian time and as the Lower Triassic Bunter Shale Formation seems to rest on deeply weathered basement in the Grindsted-1 well it is likely that the high formed a barrier between the Southern and Northern Zechstein basins (Ziegler 1982; Stemmerik et al. 1987; Vejbæk 1997). The Zechstein deposits form a continuous cover in most of the basin and the later mobilisation of salt have caused the formation of significant salt structures such as pillows and diapirs, of which some occur within the licence area (Figs 4.1B, 4.2). The continued growth of salt structures influenced the Mesozoic deposition significantly in places. Toward the east the evaporites disappear and are replaced by thin clastic Zechstein deposits as shown by the Terne-1 and Hans-1 wells in the Sorgenfrei-Tornquist Zone (Michelsen & Nielsen 1991, 1993). Farther northwest in the Sorgenfrei-Tornquist Zone evaporites are present in the Fjerritslev Trough and the Farsund Basin (e.g. Liboriussen et al. 1987; Jensen & Schmidt 1993; Christensen & Korstgård 1994; Vejbæk 1997). In Felicia-1A the Zechstein salt and carbonates attain 447 m.

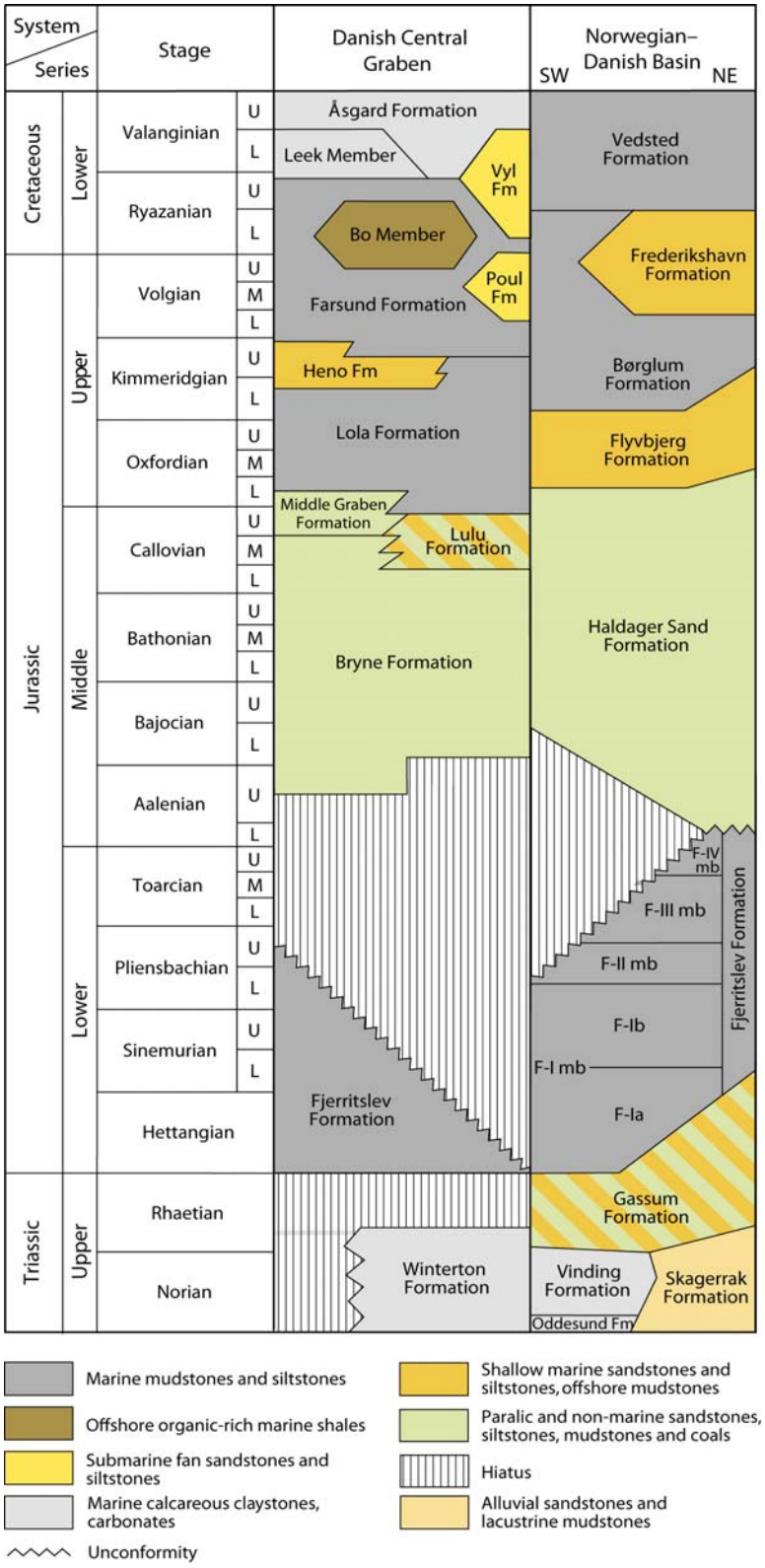

Figure 5.1 *Lithostratigraphy of the Upper Triassic–Lower Cretaceous in the Norwegian-Danish Basin. For reference the stratigraphy of the Danish Central Graben is included (from Michelsen et al. 2003).*

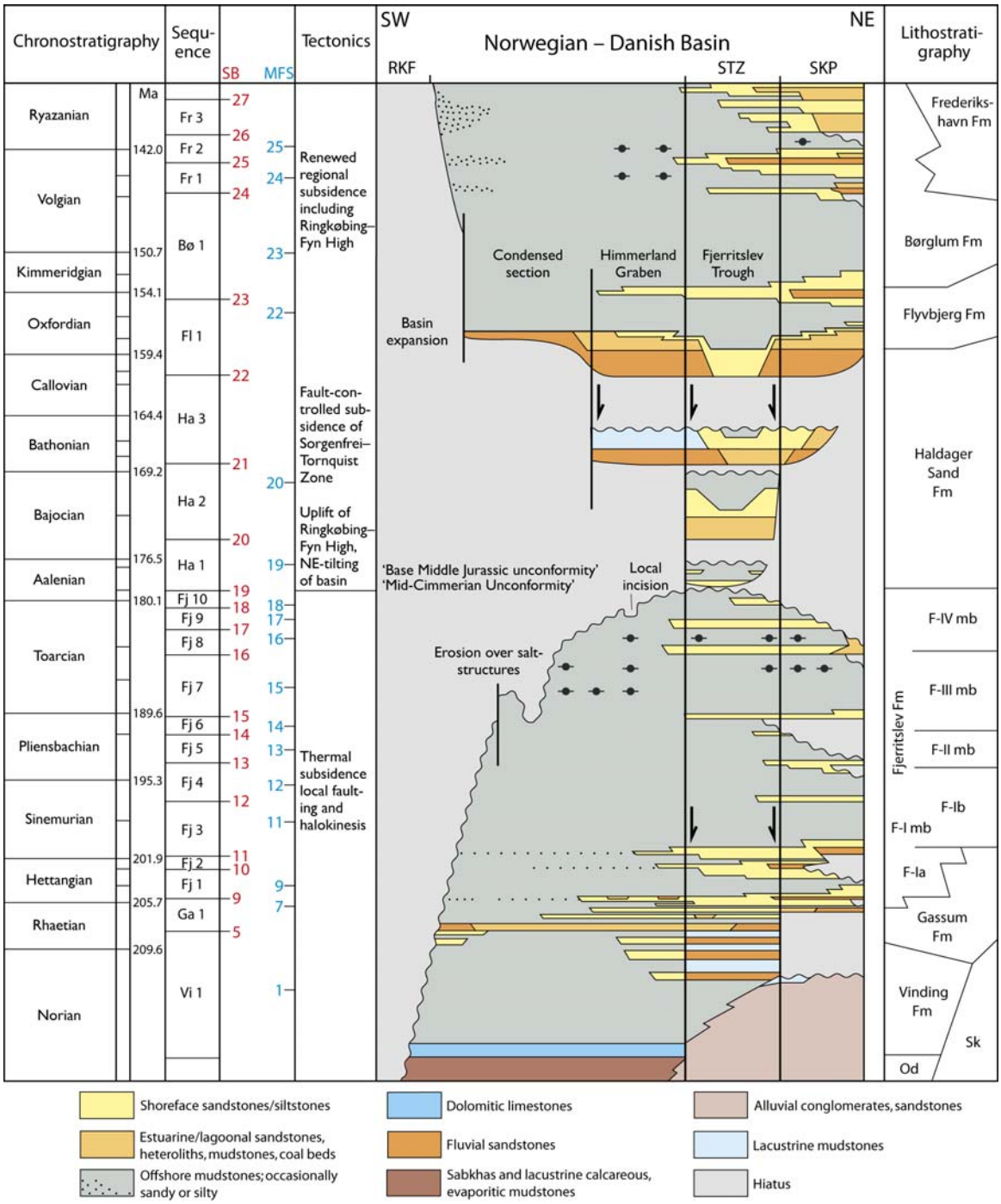

Figure 5.2 *Time stratigraphic scheme trending SW–NE across the Norwegian-Danish Basin showing age, lithostratigraphy, interpreted sequence stratigraphy and depositional environments. Sequence stratigraphic key-surfaces are included with numbered sequence boundaries shown in red (SB) and maximum flooding surfaces shown in blue (MFS). SBs define bases and tops of named sequences. The main tectonic events are indicated. Note the significant Middle Jurassic Unconformity that cuts deep to the southwest and is onlapped through time as the area of subsidence expanded (modified after Nielsen 2003).*

5.2 Early–Middle Triassic clastic deposition

In Early Triassic time the depositional environment changed to more continental conditions. Similarity in depositional facies in the North German and Norwegian-Danish basins indicate that connections between the two basins occasionally existed (Bertelsen 1978; Michelsen & Clausen 2002). Three facies provinces have been differentiated – the Central Graben Province, the Germano-type Province and the Northern Province; the latter covers the area of interest (Bertelsen 1980). The change from the Germano-type facies province to the northern facies province occurs in the southern part of the Norwegian-Danish Basin and seems to follow roughly the northern flank of the Ringkøbing-Fyn High as the facies drilled in the Jelling-1 and Grindsted-1 wells located on the high belong to the Germano-type, whereas the sections encountered in the Stenlille-19 and Nøvling-1 wells represent an intercalation of the two facies types (Michelsen & Clausen 2002). The Germano-type formations (the Bunter Shale, Bunter Sandstone, Ørslev, Falster and Tønder formations) may be traced farther northward to the Mors-1 well, where the encountered section reflects a transition to the contemporaneous Skagerrak Formation, that dominates along the northern and eastern basin margin (Bertelsen 1980; Nielsen & Japsen 1991). The Bunter Shale and Bunter Sandstone formations may be identified in Felicia-1A, whereas the remaining Germano-type formations here are replaced by the Skagerrak Formation. The Bunter Sandstone Formation may also be identified in the Terne-1 well where the lower 155 m of the Triassic succession consists mainly of fine-grained, well sorted sandstones. On the Skagerrak-Kattegat Platform the Lower–Middle Triassic deposits are all referred to the Skagerrak Formation, which here seems to include large parts of the Upper Triassic as well (Frederikshavn-1,-2,-3 and Sæby-1 wells).

It is thus expected that the Lower–Middle Triassic and most of the Upper Triassic in the Farsund Basin belongs to the Skagerrak Formation, while the basal Lower Triassic in parts of the Skagerrak area may include a thin Bunter Shale Formation and a thicker Bunter Sandstone Formation overlain by the Skagerrak Formation similar to the sections in Felicia-1A and Mors-1.

The Bunter Sandstone Formation mainly consists of red-brown and yellow-brown, medium to fine-grained, well sorted sandstones with intraformational claystone clasts and thin mudstone beds (Bertelsen 1980; Pedersen & Andersen 1980; Completion report Felicia-1/1A). The sand was supplied from the Baltic Shield and was mainly deposited in ephemeral braided fluvial channels in a dry dessert environment. Eolian dune sand and mud deposited in short-lived lakes may constitute minor proportions of the formation, especially in the southern part of the basin. Up-section and toward the northern and north-eastern basin margin the Bunter Sandstone Formation passes into the Skagerrak Formation, which include the heterogenous succession of interbedded conglomerates, sandstones, siltstones and claystones that occur along the northern and north-eastern margin of the Norwegian-Danish Basin. These deposits were mainly deposited as alluvial fans along the basin margins and rapid lateral facies changes are expected to occur.

5.3 Late Triassic clastics and evaporites

In Late Triassic time the climate changed to arid or semi-arid, and deposition of red-brown, brown, variegated, calcareous, anhydritic and pyritic mudstones and siltstones with thin beds of dolomitic limestones and marls commenced in sabkhas and ephemeral lakes. In the central and deep part of the basin more permanent lakes were established. The deposits are included in the Carnian–Early Norian Oddesund Formation, which passes into the Skagerrak Formation toward the basin margins to north and northeast. In the type section in the Mors-1 well, the formation is subdivided into 3 informal members, the O_1, O_2 and O_3 members amounting to 475 m. The O_2 member contains evaporites including two halite units, 73 m and 87 m thick (Bertelsen 1980). The formation is also recognised in the Felicia-1/1A well, where the 541 m thick formation includes a c. 400 m thick O_2 member with a c. 70 m thick lower halite unit and an upper c. 60 m thick, heterogeneous halite unit with claystones and dolomites. Halite beds within the Oddesund Formation is also interpreted to be present in the Fjerritslev Trough, where mobilisation of Oddesund salt is thought to cause the dome structure at the J-1 well location (Fig. 4.5B) (Liboriussen et al. 1987; Jensen & Schmidt 1993). An alternative or complementary interpretation advocates that the salt dome was enhanced by Zechstein salt, which intruded the Triassic section along faults in Late Triassic time (Christensen & Kortsgård 1994).

Assuming that the Triassic section in the Farsund Basin is much thinner compared to the Norwegian-Danish Basin and the Fjerritslev Trough as indicated by Fig. 4.5A, it is most likely that sandstones and mudstones of the Skagerrak Formation were deposited in the Farsund Basin contemporaneously with deposition of Oddesund Formation in more distal and deeper areas.

5.4 Late Triassic marine flooding

A gradual change to more humid conditions took place in Late Triassic time, partly due to formation of a large epicontinental sea. Deposition of lacustrine and sabkha mudstones (Oddesund Fm) was terminated by the Early Norian marine transgression that probably came from the south. The transgression led to deposition of oolitic limestones succeeded by marlstones and fossiliferous claystones of the Vinding Formation, typically 40–100 m thick in most of the basin (Figs 5.1, 5.2, 5.3)(Bertelsen 1978, 1980; Nielsen 2003). At its maximum late Norian extent, the shallow sea covered most of the Norwegian-Danish Basin and the Ringkøbing-Fyn High, whereas deposition of fluvial arkosic sands and lacustrine muds of the Skagerrak Formation continued in the Sorgenfrei–Tornquist Zone and on the Skagerrak-Kattegat Platform. The facies transition from the marine Vinding Formation to the continental deposits of the Skagerrak Formation seems to occur close to the Norwegian-Danish border in parts of the Skagerrak area as the Vinding Formation is identified in the K-1 well (41 m) and Felicia-1 well (c. 140 m), whereas the Skagerrak Formation takes over in the F-1 well. The Skagerrak Formation also dominates in the Fjerritslev Trough (J-1, Fjerritslev-2, Vedsted-1) and on the Skagerrak-Kattegat Platform, the Vinding Formation is thus expected to be absent in the Farsund Basin.

After the maximum transgression, a phased regression followed, and shoreface and fluvial sands of the lower Gassum Formation were deposited in stepwise more basinward positions intercalated with clays of the upper Vinding Formation in the basin centre. Deposi-

tion of fluvial sand and lacustrine mud of the Skagerrak Formation continued in the Fjerritslev Trough (Figs 5.2, 5.3). The regression culminated in the early Rhaetian with the formation of an extensive, fluvial-incised sequence boundary (SB 5, Figs 5.2, 5.3). Non-deposition or erosion probably occurred on the Skagerrak–Kattegat Platform. When sea level rose again, fluvial–estuarine deposits, up to 30 m thick in the basin centre, were deposited above the sequence boundary before widespread marine flooding occurred. The transgression continued but was punctuated by two short-term, forced regressions that led to deposition of widespread shoreface sand sheets encased in offshore mud. The transgression reached its maximum in the latest Rhaetian, when the Norwegian-Danish Basin, the Sorgenfrei–Tornquist Zone, the Skagerrak–Kattegat Platform and the Ringkøbing–Fyn High were covered by the sea (MFS 7 in Figs 5.2–5.4).

This general development is also shown by the sections in the F-1, K-1 and Felicia-1 wells where fluvial and shoreface sandstones alternate with thinner mudstones in the upper Gassum Formation above SB 5. A similar alternation with dominance of sandstones is thus expected in parts of the Skagerrak area. The latest Rhaetian maximum flooding event (MFS 7) is distinct in F-1 and Felicia-1 (Fig. 5.5), and since the event influenced the entire basin including the basin margin in southern Sweden and the Skagerrak-Kattegat Platform, it is expected that it can be traced to the Farsund Basin as a thin unit of marine mudstones intercalated with sandstones in the upper Gassum Formation. The lower part of the Gassum Fm (the section below SB 5), however, seems to be absent in F-1 and K-1 owing to erosion during formation of SB 5 or non-deposition caused by lack of sufficient accommodation. In Felcia-1 the lower part of the Gassum Formation seems thickly developed probably owing to deposition in a rim syncline to a close salt structures (Fig. 5.5). It is emphasised, however, that the detailed sequence stratigraphic breakdown of the Gassum Formation in these wells is not constrain by biostratigraphic data in the same degree as in most of the other well-sections in the basin.

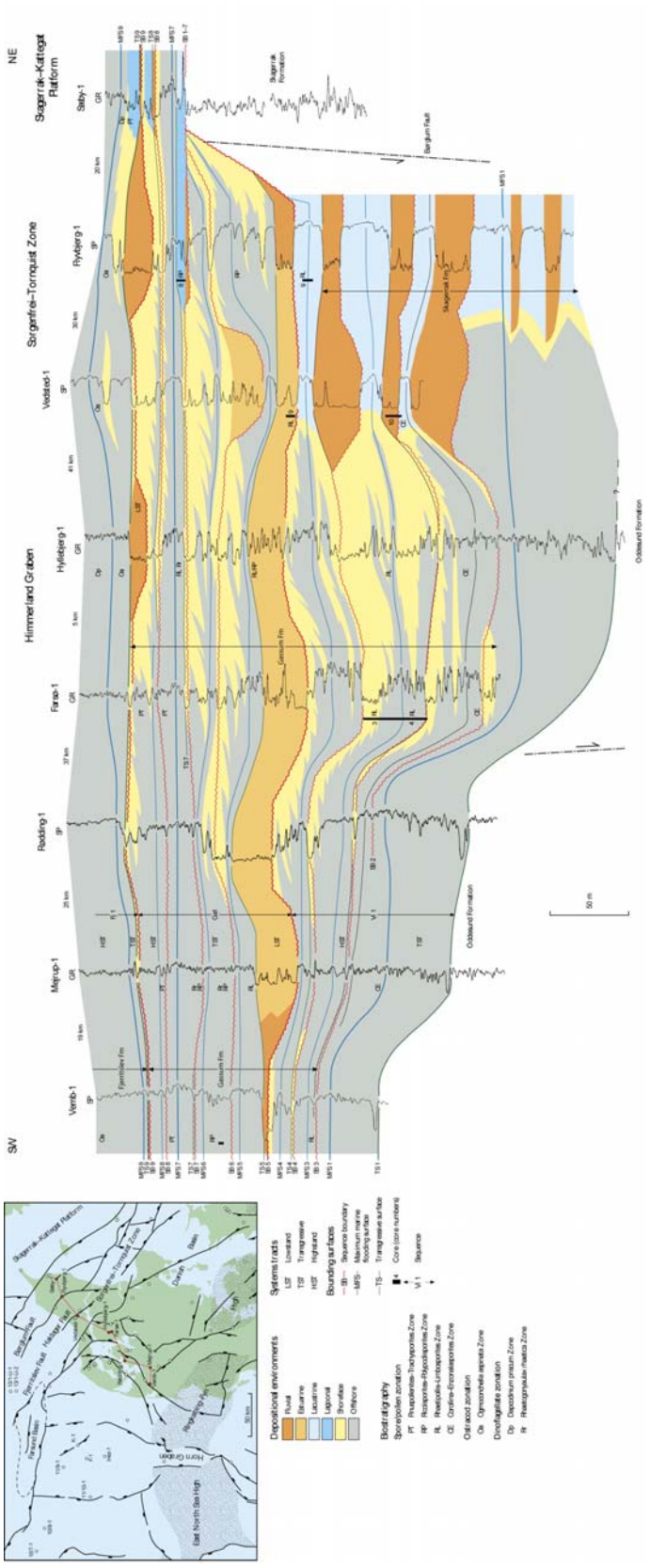

Figure 5.3 *Well log panel trending SW–NE across the basin showing the Norian–Hettangian depositional environments of the Vinding, Skagerrak, Gassum and lowermost Fjerritslev formations (Nielsen 2003)*

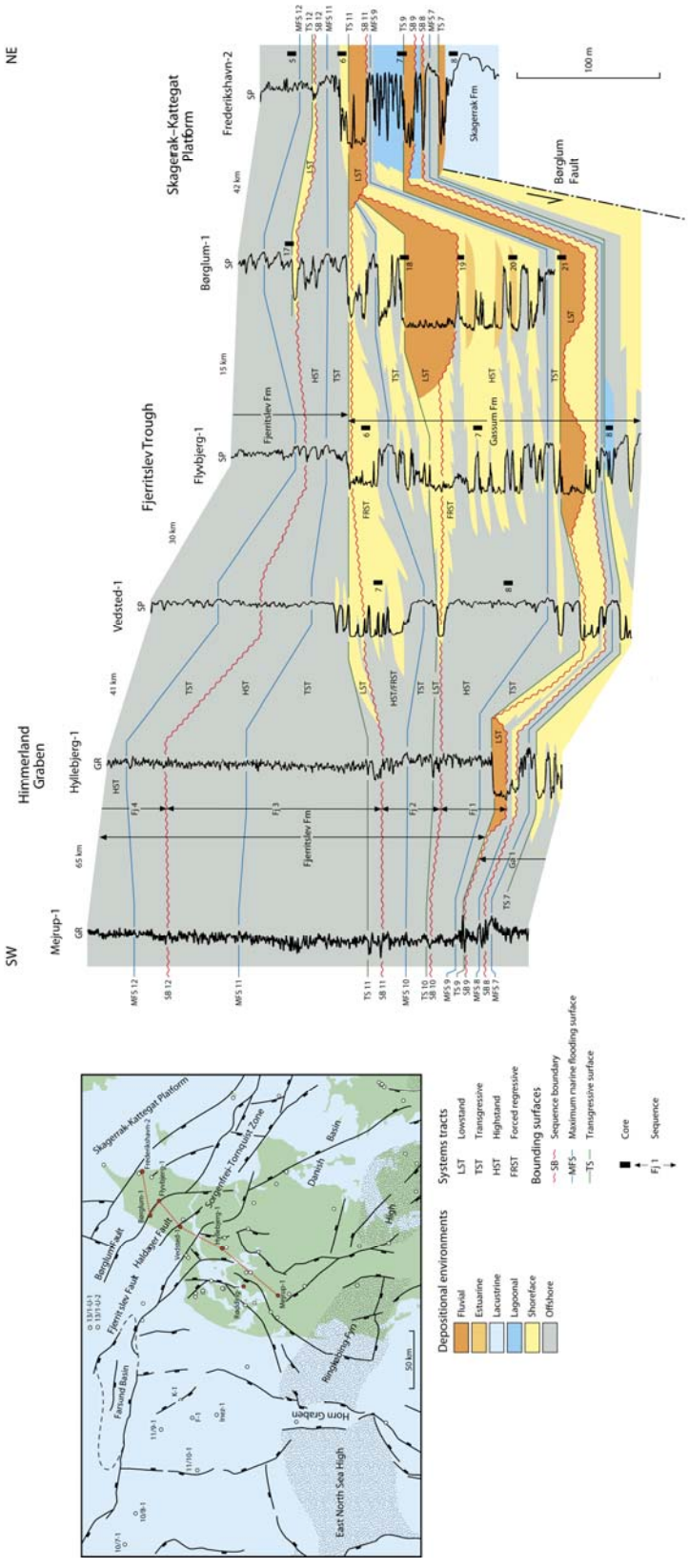

Figure 5.4 *Well log panel trending SW–NE across the basin showing the Rhaetian–Sinemurian depositional environments of the upper Gassum and lower Fjerritslev formations (Nielsen 2003).*

5.5 Hettangian – Early Pliensbachian transgression and basin expansion

The latest Rhaetian extensive flooding heralded the change to the subtropical to warm-temperate and humid climate that characterised the Jurassic period where large quantities of clay supplied to the basin due to weathering of Palaeozoic shales and granitic basement of the Baltic Shield. The Jurassic transgression was briefly interrupted by two phases of coastal progradation that caused deposition of two thin regressive shoreface sand sheets, which constitute the uppermost part of the Gassum Formation over much of the Norwegian-Danish Basin. The regression culminated with coastal progradation far into the basin accompanied by fluvial erosion and incision in the Himmerland Graben, the Fjerritslev Trough and the Skagerrak-Kattegat Platform (SB 9; Figs 5.2, 5.4). Hereafter the regional transgression continued (TS 9; the early Hettangian Planorbis Zone) and fully marine mudstones belonging to the F-Ia unit of the Fjerritslev Formation overlie the sandy Gassum Formation in most of the Norwegian-Danish Basin probably including parts of the Skagerrak area as indicated by interpretation of the sections in F-1, K-1 and Felicia-1 wells (Figs 5.5). This is probably also the case along the southern margin of the Farsund Basin, while shoreface sandstones may prevail along the northern margin similar to the successions in the Flyvbjerg-1 and Børglum-1 wells (Fig. 5.4). The mudstones have a low content of ostracods, foraminifera and infaunal bivalves and a high content of land-derived organic matter. In the northeastern part of the Sorgenfrei–Tornquist Zone aggrading parasequences of fluvial and shoreface sands with subordinate offshore muds were deposited, while lagoonal parasequences were formed in places on the Skagerrak–Kattegat Platform. The transgression peaked in the early and late Hettangian (MFS 9 & 10), interrupted by a short-term regression in the middle Hettangian (SB 10, Figs 5.2, 5.4).

The deposition of transgressive paralic deposits along the basin margin was interrupted briefly by a fall in sea level soon after the Hettangian–Sinemurian boundary. This resulted in fluvial incision on the Skagerrak-Kattegat Platform, while regressive shoreface sand was deposited in the Fjerritslev Trough (SB 11, Figs 5.2, 5.4). The thin fine-grained sandstone stringers in the basal Fjerritslev Formation in the Felicia-1 and J-1 wells are probably related to this event (Fig. 5.5; Encl. 1); they may have a weak influence on the sealing capacity of the lowermost Fjerritslev Formation in the eastern and northern most part of the Skagerrak area. Farther basinward, heteroliths and silty mudstones were deposited above the conformable part of the sequence boundary. A rapid sea-level rise followed in the earliest Sinemurian (upper part of the Bucklandi Zone) and transgressive marine muds of the F-Ib unit finally overstepped fluvial and marine sands of the Gassum Formation in the Sorgenfrei–Tornquist Zone and on the Skagerrak–Kattegat Platform. The coarse-grained, shell-bearing sandstone at the base of the shallow corehole 13/1-U-1 (at c. 292 m) is probably the ravined top of the Gassum Formation overlain by Lower Sinemurian transgressive marine mudstones of the basal Fjerritslev Formation according to the sequence stratigraphic interpretation of GEUS (Fig. 5.7A). Following this it is assumed that the deposition of coastal and shallow marine sands also came to an end along the northern margin of the Farsund Basin at this time. Thin lagoonal sediments were formed during the Hettangian–Early Sinemurian transgressions in places on the Skagerrak-Kattegat Platform and similar sediments may be present in the Farsund Basin, but are considered to be of limited distribution and thickness.

The early Sinemurian transgression led to deposition of up to 150 m of uniform mudstones in the basin, showing a marked thinning towards the northern and northeastern basin margin (Sequence Fj 3 in Figs 5.2, 5.4, 5.6). In the Late Sinemurian, a minor sea-level fall caused a slight basinward progradation of distal coastal parasequences on the Skagerrak–Kattegat Platform and in parts of the Sorgenfrei–Tornquist Zone. This progadational event is expected to be represented also in the Farsund Basin and may be suggested by the slight upward coarsening trend seen in the 13/1-U-1 core at ca. 260–255 m (Fig. 5.7A). The After this minor excursion, the overall Early Jurassic sea-level rise continued, and reached a maximum in the latest Sinemurian. In the centre of the basin, the diversity and abundance of the ostracod fauna decreased and infaunal bivalves and some of the epifaunal bivalves disappeared due to reduced oxygen conditions. A gradual decrease in the rate of sea-level rise in the Early Pliensbachian Jamesoni Zone caused a distinct basinward progradation of shoreface clinoform sandstones on the Skagerrak–Kattegat Platform, which may also be found in the Farsund Basin.

The regression culminated in the middle Early Pliensbachian (early Ibex Zone) and the deposition changed from fine-grained mud (F-Ib unit) to silty and sandy heteroliths (F-IIa beds, SB 13; Figs 5.2, 5.6; Michelsen 1989; Nielsen 2003). On the Skagerrak–Kattegat Platform deposition of shallow marine shoreface sand ceased for some time due to submarine or subaerial erosion and bypass. This event may be marked in the Farsund Basin by somewhat coarser-grained beds within the marine mudstones and is probably shown by the 13/1-U-1 core at ca. 213–192 m. When the sea level started to rise again, deposition of fine-grained mud resumed in the basin (lower part of F-IIb beds), while backstepping parasequences of marine sand were succeeded by transgressive mud on the Skagerrak–Kattegat Platform. Peak transgression was reached in the late Early Pliensbachian Davoei Zone. The biostratigraphic analyses conducted by GEUS (Section 10) suggest that this event is shown by the mudstones at ca. 188–181 m in the 13/1-U-1 core. Thereafter, the rate of sea-level rise decreased and a coarsening-upwards succession of mud and fine-grained heteroliths were deposited in the Norwegian-Danish Basin and probably also in the Farsund Basin (middle part of F-IIb) as indicated by the 13/1-U-1 core from ca. 181–162.6 m (Figs 5.7A & B).

5.6 Late Pliensbachian – Early Aalenian sea-level fluctuations

Significant erosion took place on the Skagerrak–Kattegat Platform during a sea level fall in the early Late Pliensbachian Margaritatus Zone (SB 14; Figs 5.2, 5.6). Basinward, in the Fjerritslev Trough and in the Norwegian-Danish Basin, deposition changed to silty and sandy mud and fine-grained sand, showing pronounced thinning over some salt-structures possibly reflecting shallow water depths (upper part of F-IIb and F-IIc beds; Michelsen 1989). The event can be traced to F-1, K-1 and Felcia-1, where it is marked by a change to sandy mudstones. The new biostratigraphic results (Section 10) support the GEUS interpretation of the IKU/Sintef 13/1-U-1 core, which suggests that the event corresponds to the fluvial erosion surface at 162.6 m (Fig. 5.7A & B marked as SB 14). It is thus likely that the event is recorded in the Farsund Basin as a sandstone intercalation, which shows fining and thinning toward the south.

The ensuing sea-level rise commenced in the Margaritatus Zone and reached a peak in the late Late Pliensbachian (early Spinatum Zone). Marine silty mud was deposited in the

basin, while muddy marine sand with bivalves was deposited in the Fjerritslev Trough and presumably also in the Farsund Basin. Deposits from this period are absent on the Skagerrak–Kattegat Platform due to bypass or later erosion (Figs 5.2, 5.6). The interpreted SB 14 in 13/1-U-1 is overlain by a sandstone with rootlets and a thin coal bed (c. 162.6–159 m), and this succession is interpreted to represent the transgressive phase that raised the base level along the basin margin.

A subsequent sea-level fall culminated in the late Spinatum Zone with the formation of a widespread marine regressive surface of erosion and deposition of 5–10 meters of lowstand shoreface sandstones in the central parts of the Fjerritslev Trough (SB 15 in Figs 5.2, 5.6), whereas Lower Pliensbachian strata were eroded on the Skagerrak–Kattegat Platform. The erosion surface at c. 159 m in 13/1-U-1 is interpreted as an amalgamated sequence boundary and ravinement surface (SB 15 and TS 15 in Fig. 5.7A & B) overlain by a transgressive succession of shallow marine sandstones. The sequence boundary was cut during sea-level fall and lowstand and was later subjected to transgressive marine erosion. It is thus expected that the event is recorded in the Farsund Basin as a shoreface or fluvial sandstone similar to the succession in the Fjerritslev Trough (Fig. 5.6).

The ensuing sea-level rise caused marine flooding over the entire basin at the Pliensbachian–Toarcian boundary, including the Sorgenfrei–Tornquist Zone, the Skagerrak–Kattegat Platform, and the Farsund Basin. The transgression reached its maximum in the Early Toarcian Falciferum Zone (MFS 15 in Figs 5.2, 5.6). Due to oxygen-poor conditions, the ostracod fauna disappeared and an increasing amount of amorphous marine matter was preserved making the mudstones favourable for hydrocarbon generation in parts of the basin. The new biostratigraphic analysis of the 13/1-U-1 core (see Chapter 10) indicate that the sandstones from c. 159–148 m were deposited during this transgressive event that culminated with the deposition of c. 6 m of silty mudstones 148–142 m (Fig. 5.7A & B). The mudstones show increased TOC values and contain type II kerogen, and based on the evidences provided by the new biostratigraphy and geochemical analyses perform by GEUS it is proposed that the mudstones were deposited during the Early Toarcian sea level maximum that influenced deposition along the margin of the depositional basin (MFS 15)(Figs 5.2, 5.6, 5.7A & B). A similar influence is seen at margin far to the southeast at Bornholm (Koppelhus and Nielsen 1994; Hesselbo et al. 2000).

During the remainder of the Early Jurassic and in the Early Aalenian Opalinum Zone (Early Middle Jurassic), a succession of up to 150 m of marine mudstones was deposited in the Sorgenfrei–Tornquist Zone. Interbedded with the mudstones occur three shoreface sandstones, 5–15 m thick overlying regressive marine erosion surfaces; these sandstones were deposited during sea-level falls. Similar shoreface sandstones are expected to be present in the Farsund Basin. In F-1, K-1 and Felicia-1 the stratigraphic level containing the sandstones is eroded by the Base Middle Jurassic Unconformity, but since the amount of erosion decreases northward toward the Farsund Basin (Fig. 5.8) it is likely that the sandstones will be present closer to the basin.

5.7 Late Early – Middle Jurassic uplift and erosion

The Ringkøbing–Fyn High and most of the Norwegian-Danish Basin were uplifted in late Early Jurassic – early Middle Jurassic times, and the Triassic – Lower Jurassic successions

were eroded on the highest parts of the Ringkøbing–Fyn High (Fig. 5.8). The Lower Jurassic was deeply eroded in the uplifted area north of the high, whereas erosion did not reach such deep levels closer to the Sorgenfrei–Tornquist Zone. In the fault-bounded Sorgenfrei–Tornquist Zone, where subsidence still occurred but at a much smaller rate than before, the dramatic change in basin configuration is shown by a shift from offshore mudstones of the F-IV Member (Fjerritslev Fm) to shallow marine sandstones (Haldager Sandstone Fm; Figs 5.2, 5.6, 5.9, 5.10). The sandstones overlie a marine, forced regressive erosion surface dated to the top of the Lower Aalenian Opalinum Zone, thus contemporaneous with the greatest basin-ward shift in facies recorded from the Lower–Middle Jurassic in the North Sea. Hence, during the rest of the Aalenian, the Bajocian and the early Bathonian, deposition was more or less confined to the narrow zone bounded by the Fjerritslev and Børglum Faults and their south-eastward continuation in Kattegat, Øresund and southern Sweden. It is assumed that the west-ward continuation of the faults defining the southern margin (the Fjerritslev Fault) and the northern margin of the Farsund Basin also delineate an area of continued subsidence in Middle Jurassic time, thus preventing erosion of the potential source rocks in the upper Fjerritslev Formation.

The four Norwegian wells, 11/9-1, 11/10-1, 11/5-1,10/7-1 and 10/8-1 situated in the Norwegian-Danish Basin southwest and west of the Farsund Basin (Fig. 3.1) confirms the deep regional erosion of the Lower Jurassic, although their position on local structures have further enhanced the erosional hiatus. In the Egernsund Basin located on structural strike farther to the west the Fjerritslev Formation is also deeply truncated and absent in places.

The Fjerritslev Trough and presumably also the Farsund Basin received erosion material from the uplifted areas to the west and south west, and from the Baltic Shield to the north, making up the Haldager Sand Formation, 29–155 m thick in the well sections in the Fjerritslev Trough (Figs 5.2, 5.10). The formation is dominated by shoreface and fluvial sandstones interbedded with thin marine and lacustrine mudstones, and thin coaly beds in places. The new biostratigraphic breakdown of the IKU/Sintef core 13/1-U-1 (Fig. 10.1) indicates that Lower Toarcian mudstones of the Fjerritslev Formation are overlain by Bajocian–Bathonian coastal or delta plain deposits of the Haldager Sand Formation at ca. 142 m (Fig. 5.7A & B). The sequence stratigraphic interpretation of the 13/1-U-1 core thus indicates that the erosion surface at 142.2 m correlates to the Base Middle Jurassic Unconformity and the overlying sandstone succession, c. 142–122.3 m corresponds to the Haldager Sand Formation (Bryne Fm; Fig. 5.7A & B). The underlying sandstones, included in the Bryne Formation by IKU/Sintef, are here interpreted to represent intercalations in the Fjerritslev Formation similar to the sandstones seen in the sections from the Fjerritslev Trough and Skagerrak-Kattegat Platform (Figs 5.2, 5.6, 5.10).

The geological model presented here therefore predicts that the stratigraphic interval with the potential source rocks in the upper Fjerritslev Formation is formed and preserved in the Farsund Basin, and the interval is expected to be much thicker in the basin than in the 13/1-U-1 core located landward of the depocentre of the Farsund Basin. It is also expected that the Haldager Sand Formation is present in the Farsund Basin and dominated by relatively thick fluvial and marine sandstones (Fig. 4.5). Sandstone stringers are expected to be present at specific stratigraphic levels in the Fjerritslev Formation influencing the overall sealing capacity of the formation.

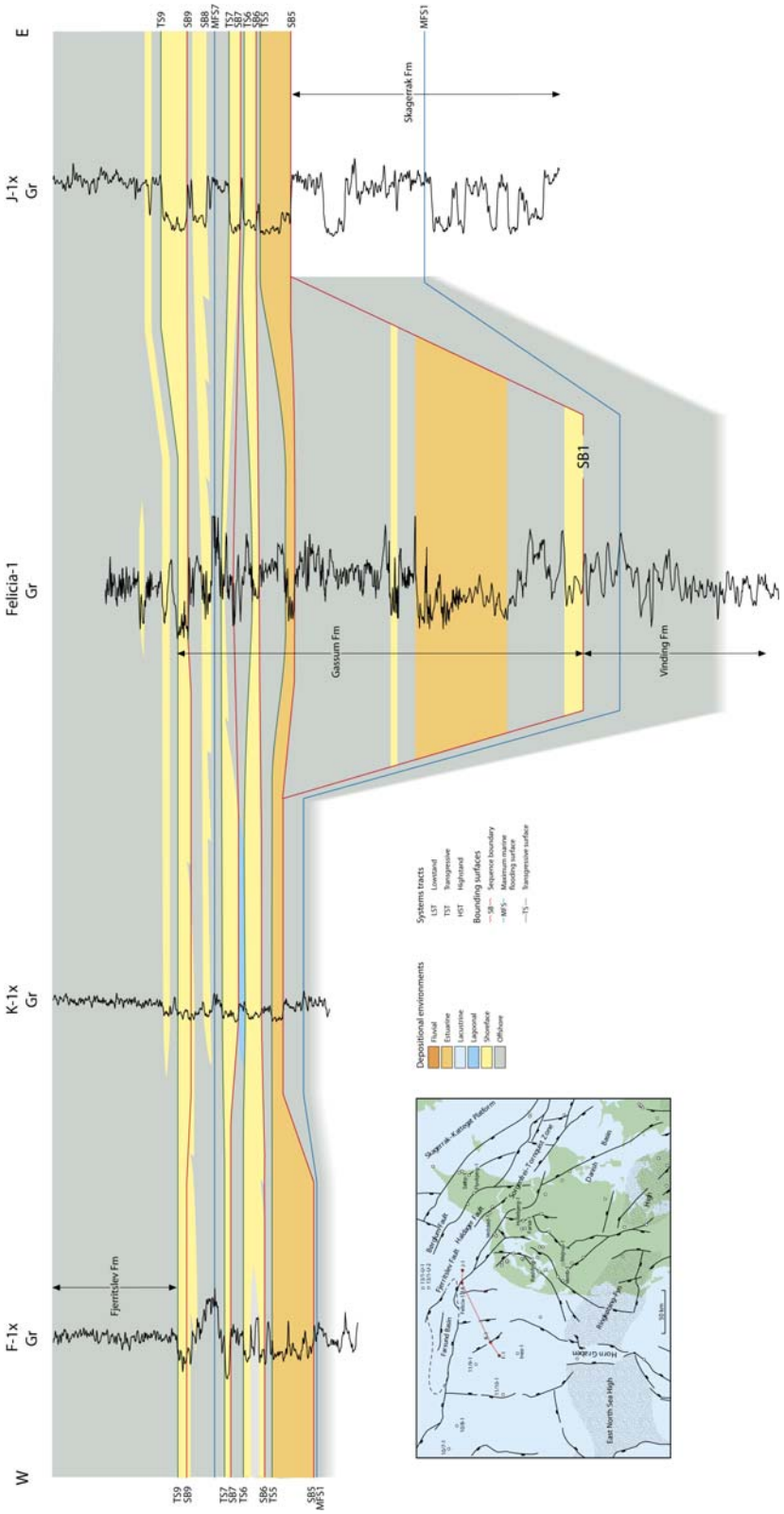

Figure 5.5 *Proposed interpretation of sequence stratigraphy and depositional environments of the Gassum reservoir in the wells F-1, K-1, Felicia-1 and J-1; oblique depositional dip section.*

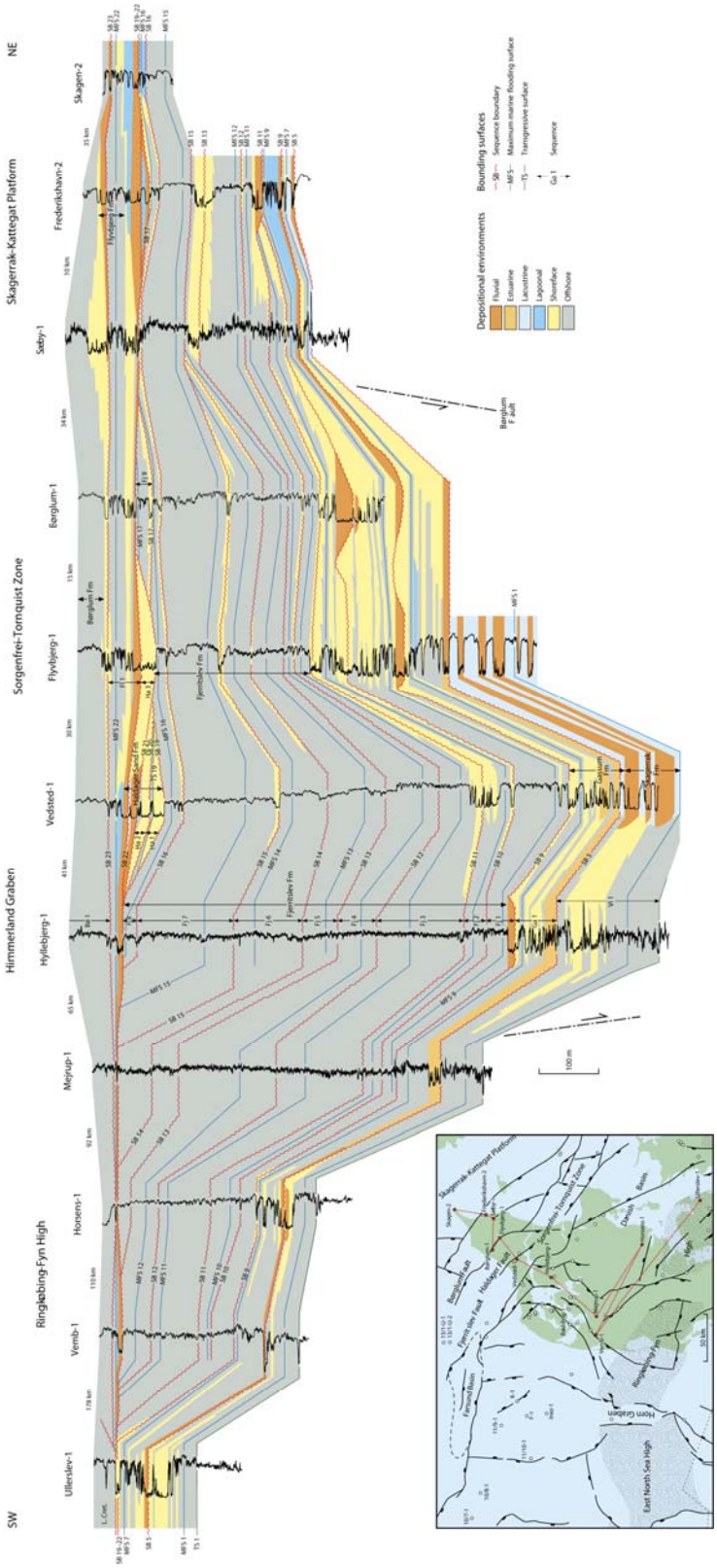

Figure 5.6. *Well log panel trending SW–NE across the basin showing the Norian–Oxfordian depositional environments of the Vinding, Skagerrak, Gassum, Fjerritslev, Haldager Sand, Flyvbjerg and Børglum formations. Note the pronounced erosional truncation at the amalgamated sequence boundary, SB 19-22 (Nielsen 2003).*

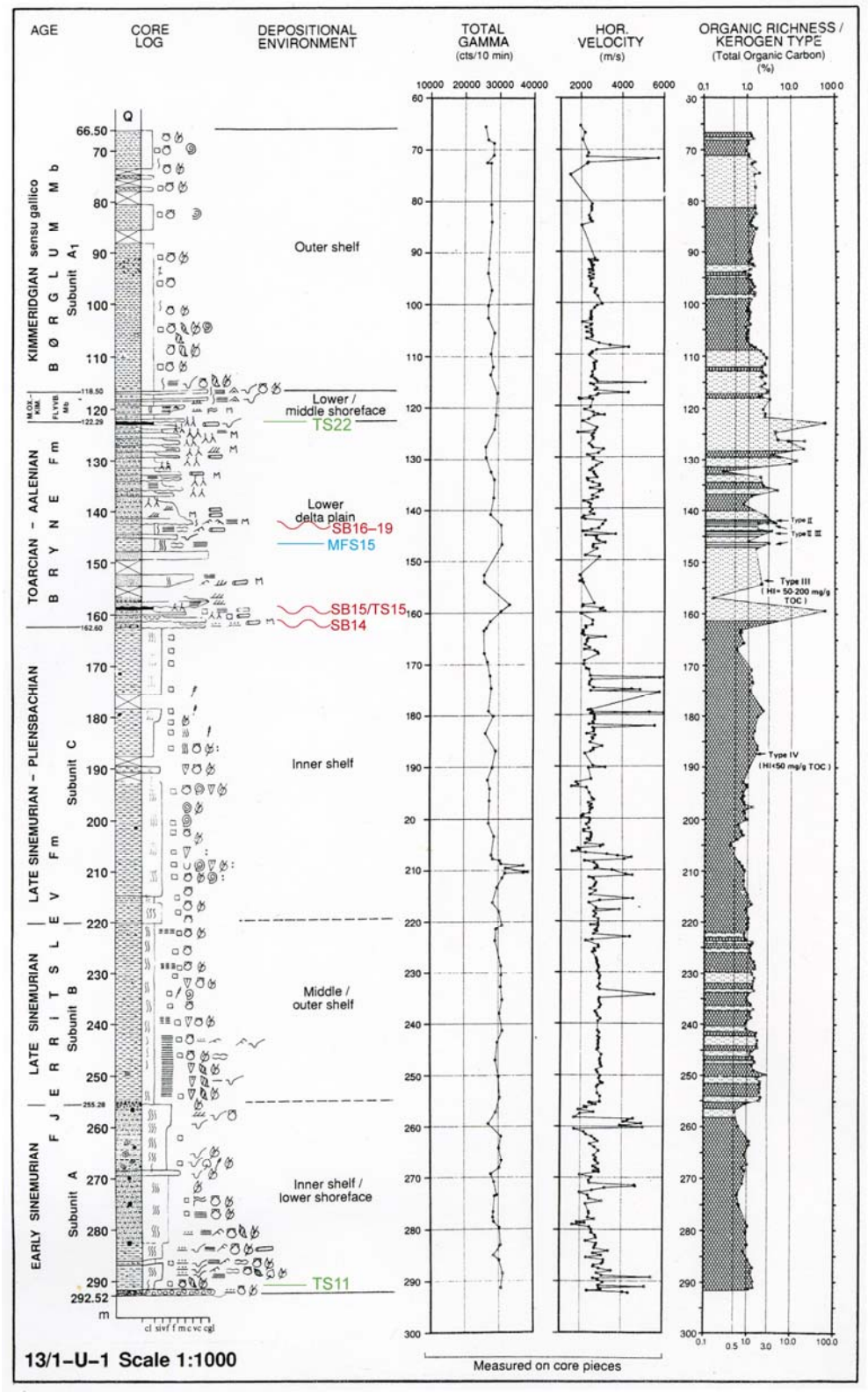

Figure 5.7A *The IKU/Sintef core from 13/1-U-1 with key sequence stratigraphic surfaces marked based on GEUS` interpretation. The interval from SB 14 to the amalgamated SB 16-19 is interpreted as equivalent to the Fjerritslev Formation, and the mudstones at 142–148 are regarded as deposited during the Early Toarcian flooding event (MFS 15) that resulted in formation of organic-rich mudstones in parts of the basin. The section from SB 16-19 to TS 22 is interpreted as the Haldager Sand Fm overlain by a thin Flyvbjerg Fm.*

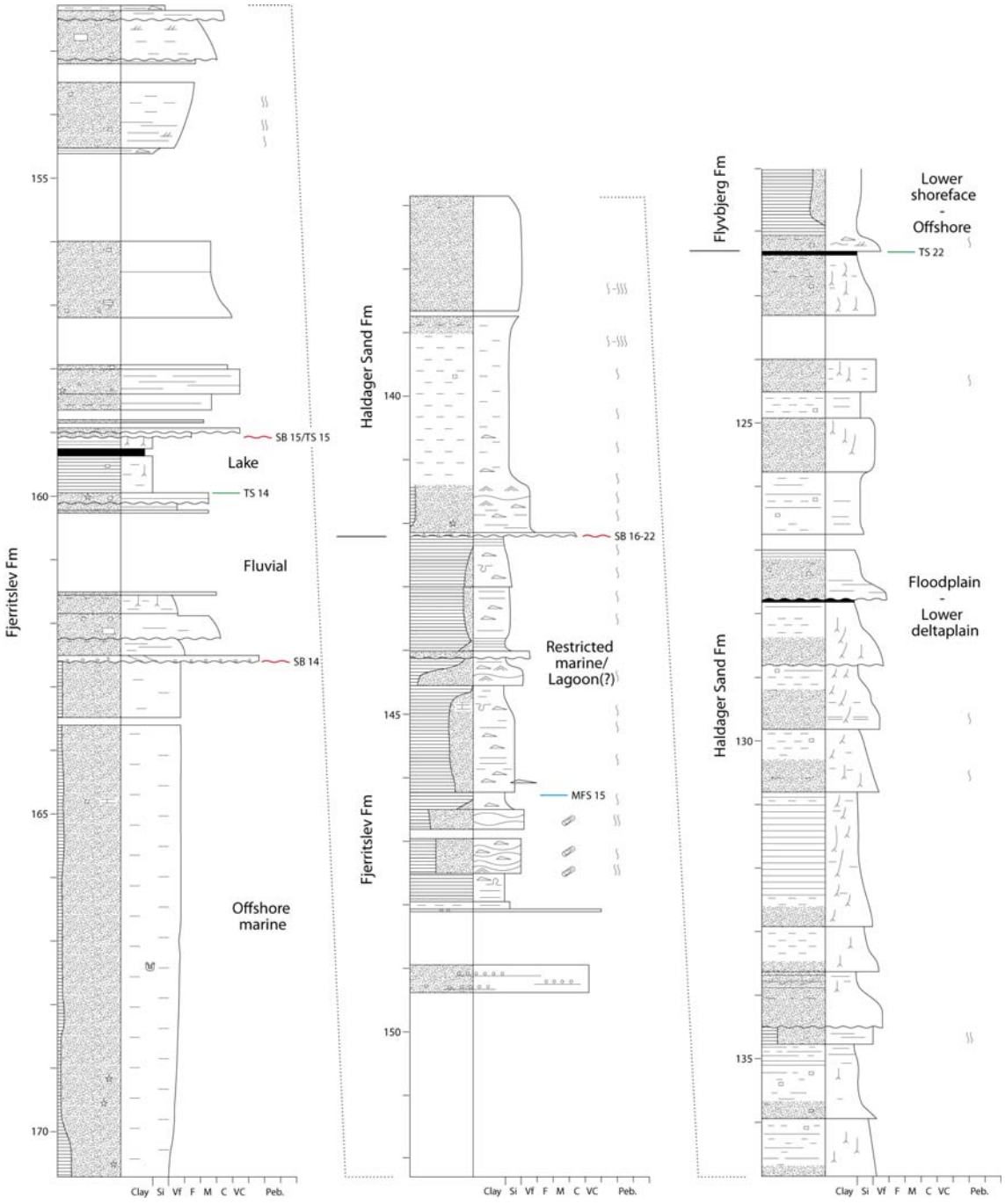

Figure 5.7B. *A blow-up of the upper part of the Lower Jurassic, the Middle Jurassic and the lowermost Upper Jurassic based on core logging by GEUS. Lower Toarcian mudstones with source rock potential are present at 148.2–142.2 based biostratigraphic, geochemical and sequence stratigraphic analyses by GEUS.*

5.8 Late Middle – Late Jurassic basin expansion

Regional subsidence resumed during late Middle Jurassic–Late Jurassic times and the area with deposition of shallow marine clastics gradually expanded as testified by the Upper Jurassic onlap on the Base Middle Jurassic Unconformity showing a significant younging of the onlap toward the southwest and northeast on both sides of the Sorgenfrei-Tornquist Zone (Fig. 5.11). The deposition overstepped the bounding faults of the Sorgenfrei-Tornquist Zone with deposition of Bathonian(?) braided fluvial sands on the Skagerrak–Kattegat Platform and in the Himmerland Graben. Shallow lagoons or lakes dominated at the 13/1-U-1 well; according to IKU these deposits are of Aalenian age based on poor evidence. However, the GEUS investigation indicates a Mid Bajocian–Bathonian age and the section is interpreted to record the general base-level rise that occurred at this time in the area.

The base level rise similary led to deposition of fluvial sandstones and lacustrine mudstones at the positions of the F-1, K-1 and Felicia-1 wells in Bathonian time, and 14–48 m of the Haldager Sand Formation accumulated here (Fig. 5.8).

Deposition also resumed at the wells 10/8-1 and 10/7-1 where Bathonian(?) sandstones of the Haldager Sand/Bryne Formation are preserved. A marine transgression close to the Callovian–Oxfordian boundary influenced most of the basin and accommodation space was also created in the former by-pass zone of the southern part of the basin and on the Skagerrak–Kattegat Platform, where fluvial sands were now deposited. During the Oxfordian, the sedimentation area was further enlarged and a north-eastward thickening wedge of transgressive, fossiliferous marine sand and mud was deposited above lagoonal deposits on the Skagerrak-Kattegat Platform (lower Flyvbjerg Fm; Figs 5.2, 5.10). Transgressive shoreface sand was also deposited at Felicia-1 (Fig. 5.8). The transgression peaked in mid-Oxfordian time with deposition of marine mudstones over most of the northern basin including the Fjerritslev Trough and Skagerrak-Kattegat Platform. A latest Oxfordian sea-level fall resulted in coastal progradation on the Skagerrak-Kattegat Platform and in the Fjerritslev Trough; fluvial and shallow marine sands were deposited, and a south-west prograding wedge was formed (upper Flyvbjerg Fm; Fig. 5.10).

The new biostratigraphic dating confirms the IKU/Sintef interpretation of the 13/1-U-1 core where the Haldager Sand Formation is overlain by 4 m of lower shoreface to offshore heteroliths belonging to the Flyvbjerg Formation (Fig. 5.7A & B). The Flyvbjerg Formation is thus expected to present in the Farsund Basin, where it is expected to be thicker and probably dominated by shoreface and fluvial sandstones in the lower and upper parts with a middle part of marine mudstones and siltstones similar to the sections in the Fjerritslev Trough.

Extensive marine flooding occurred in the Kimmeridgian, and sedimentation of marine mud (Børglum Formation) characterised the whole area, although the marked thinning towards the south-western part of the Norwegian-Danish Basin emphasises the reduced accommodation space here. The Børglum Formation is also present in the 13/1-U-1 and 13/1-U-2 coreholes with a thickness of more than 60 m (compared to 38–59 m in F-1, K-1 and Felicia-1), and is expected to be present in the Farsund Basin as well. During Volgian–Ryazanian times, the depositional environment was dominantly a shallow shelf with three–four major phases of coastal progradation (sequences Fr 1, Fr 2, Fr 3 of the Frederikshavn Fm, Fig. 5.2). Coastal and deltaic sandy deposits with interbedded marine mudstones accumulated on the Skagerrak-Kattegat Platform and in parts of the Sorgenfrei-Tornquist

Zone, while marine muds were deposited over much of the basin. The unit in 13/1-U-2 termed subunit C of the Børglum Formation by IKU/Sintef is better included in the lower part of Frederikshavn Formation (Fig. 5.7).

Jensen and Schmidt (1993) proposed that the Farsund Basin experienced increased subsidence in the Early Cretaceous (Fig. 4.5); this is also suggested by Mogensen & Korstgård (2003) and is supported by the relatively thick succession in the J-1 well compared to other wells. Depending on the time of onset of the higher rate of subsidence, the Frederikshavn Formation may be differently developed in the Farsund Basin from sections on the Skagerrak-Kattegat Platform and the Norwegian-Danish Basin. In Terne-1, situated in the Sorgenfrei-Tornquist Zone, the Frederikshavn Formation is thickly developed, mudstones dominate that possibly were deposited in a somewhat restricted brackish environment (Petersen et al. 2005). The same development could be possible in the Farsund Basin, and with increased subsidence the thermal maturity may be higher.

A general overview of the Upper Triassic–Lower Cretaceous lithostratigraphy across the Danish part of the basin is provided in Figure 5.12. This general pattern is also expected to be found in the Farsund Basin based on the geological model presented above, the geosection crossing the basin and the regional paleogeographic maps (Fig. 4.5A; 5.13).

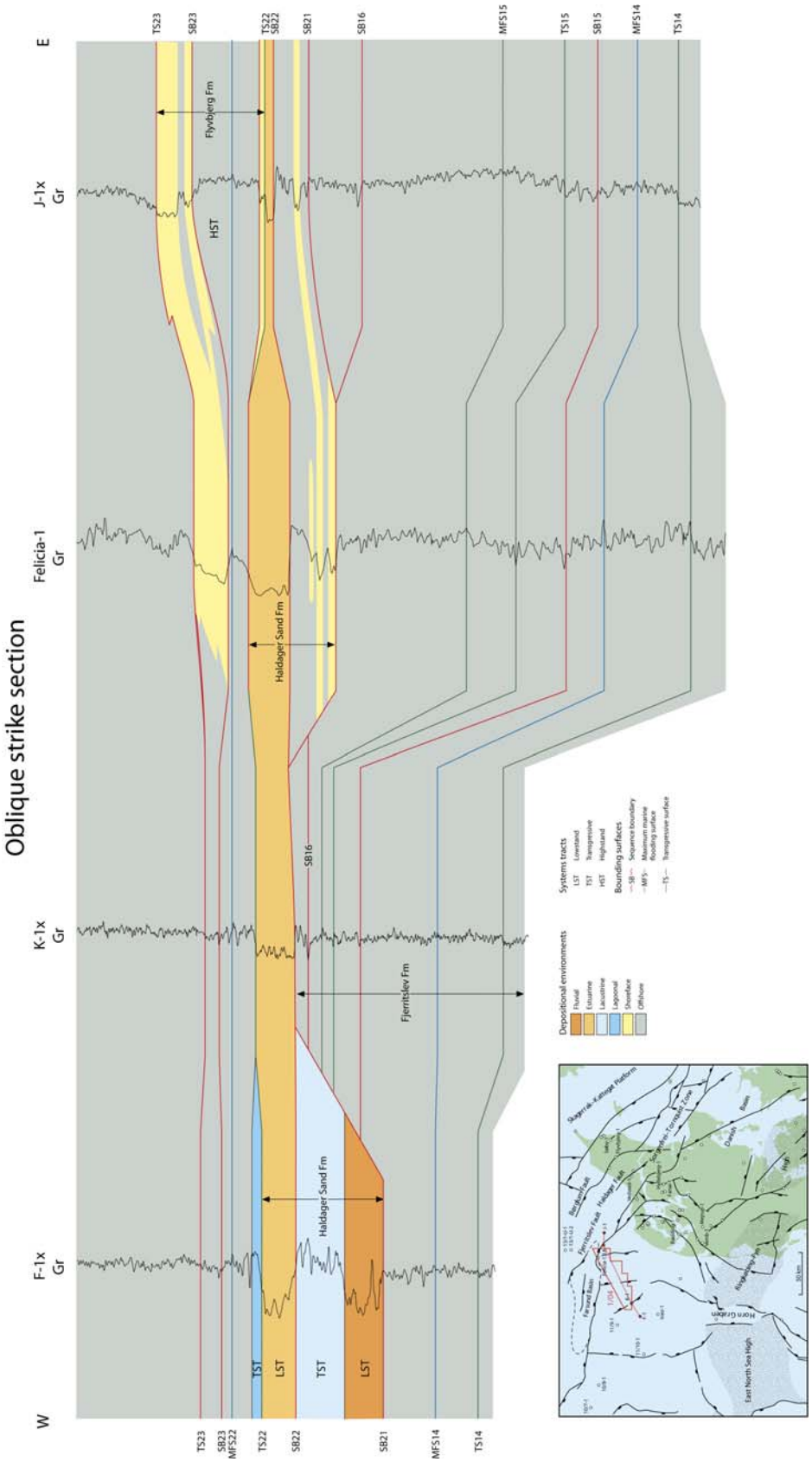

Figure 5.8. *Proposed interpretation of sequence stratigraphy and depositional environments of the Haldager reservoir in selected Skagerrak wells; oblique depositional dip section.*

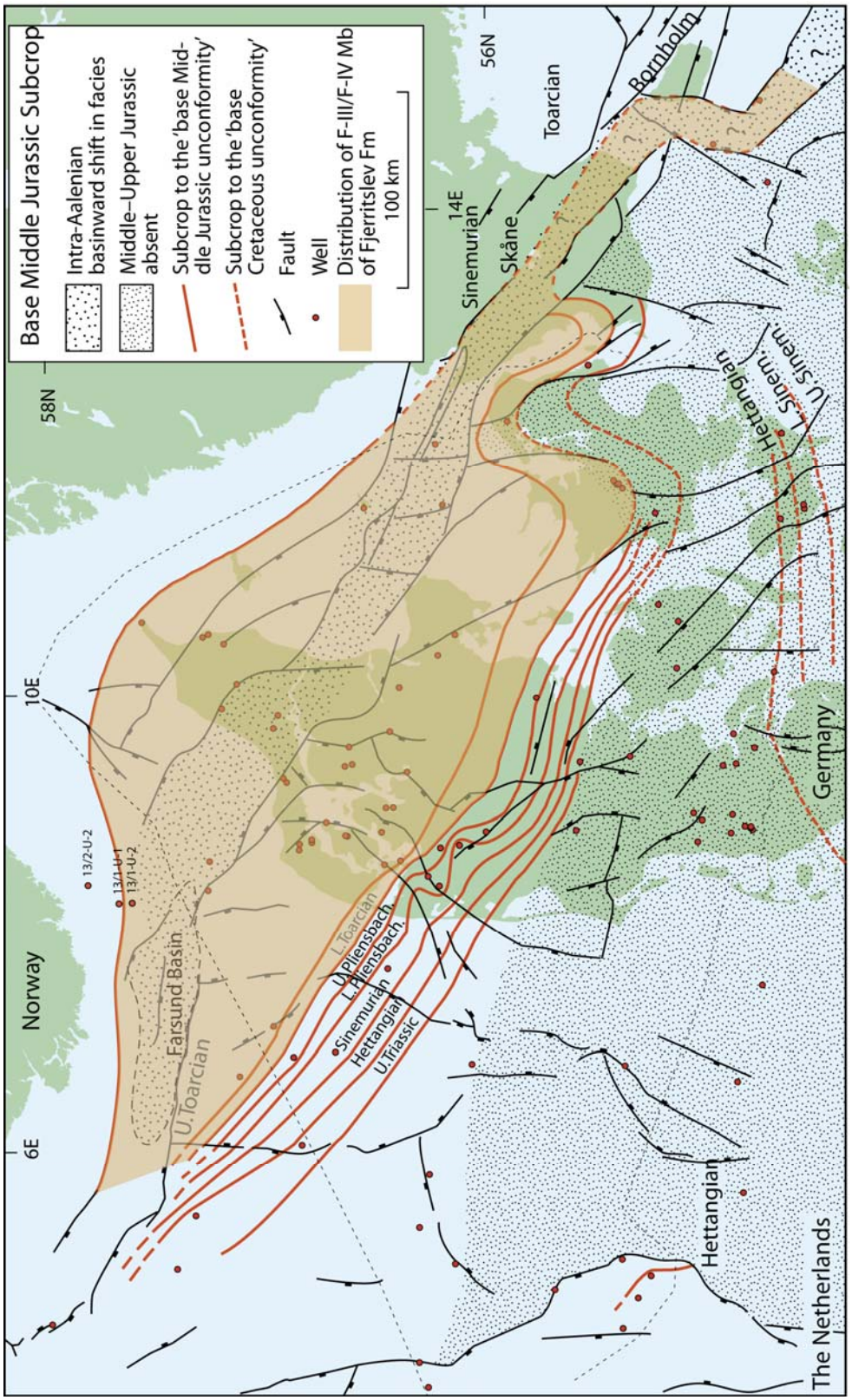

Figure 5.9. *Map showing the subcrop of the Base Middle Jurassic Unconformity and the distribution of the two upper units (F-III & F-IV mb) of the Lower Jurassic Fjerritslev Fm. The coarse dotted area indicates where the shift from marine mudstones to shallow marine sandstones or fluvial sandstones occurred in the Aalenian without major erosion (modified from Nielsen 2003).*

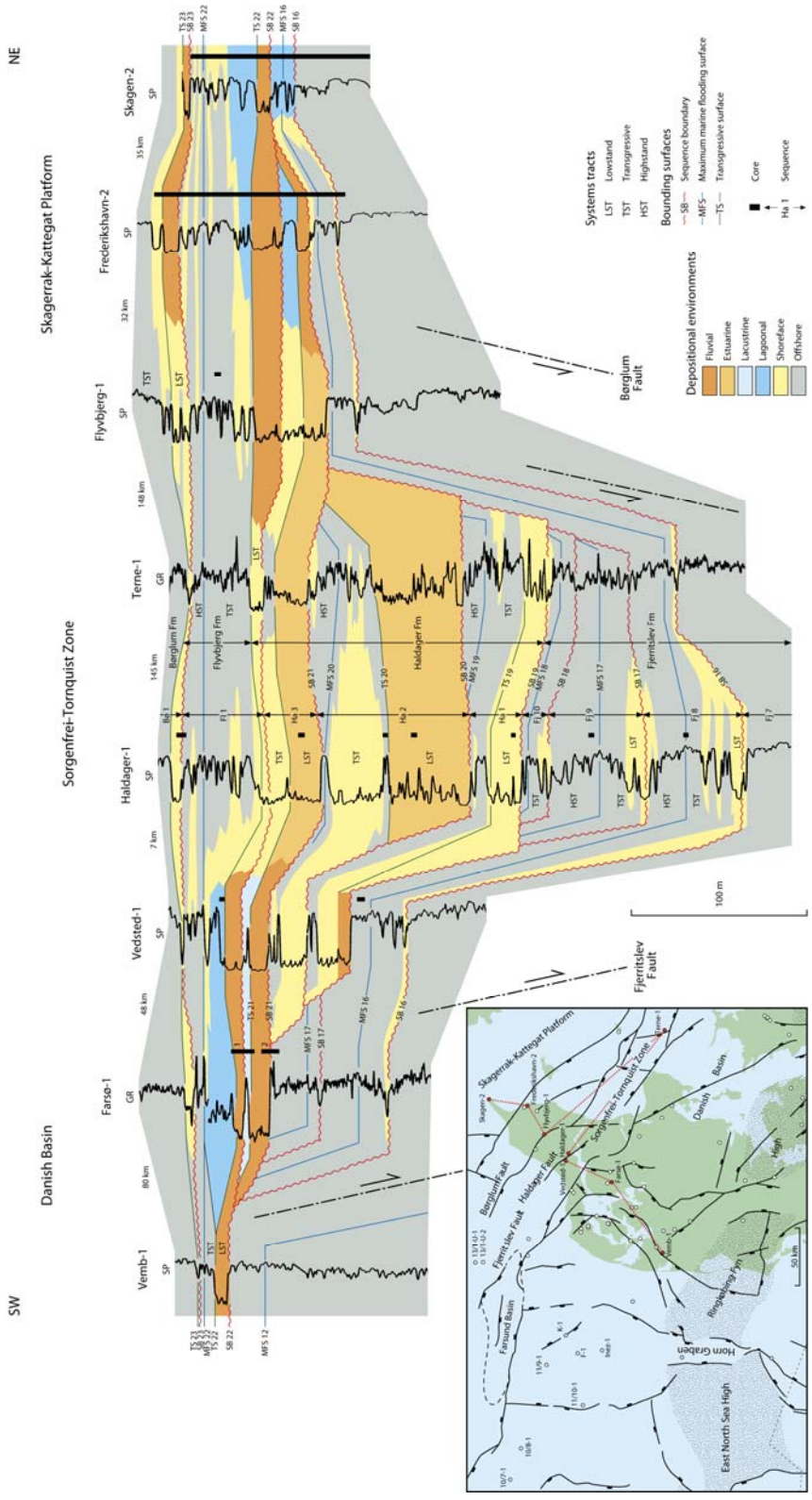

Figure 5.10. *Well log panel trending SW–NE across the basin showing the Toarcian–Oxfordian depositional environments of the upper Fjerritslev, Haldager Sand, Flyvbjerg and Børglum formations. Note the pronounced erosional truncation at the base of the Middle Jurassic marked by various sequence boundaries depending on the amount of erosion related to structural position (Nielsen 2003).*

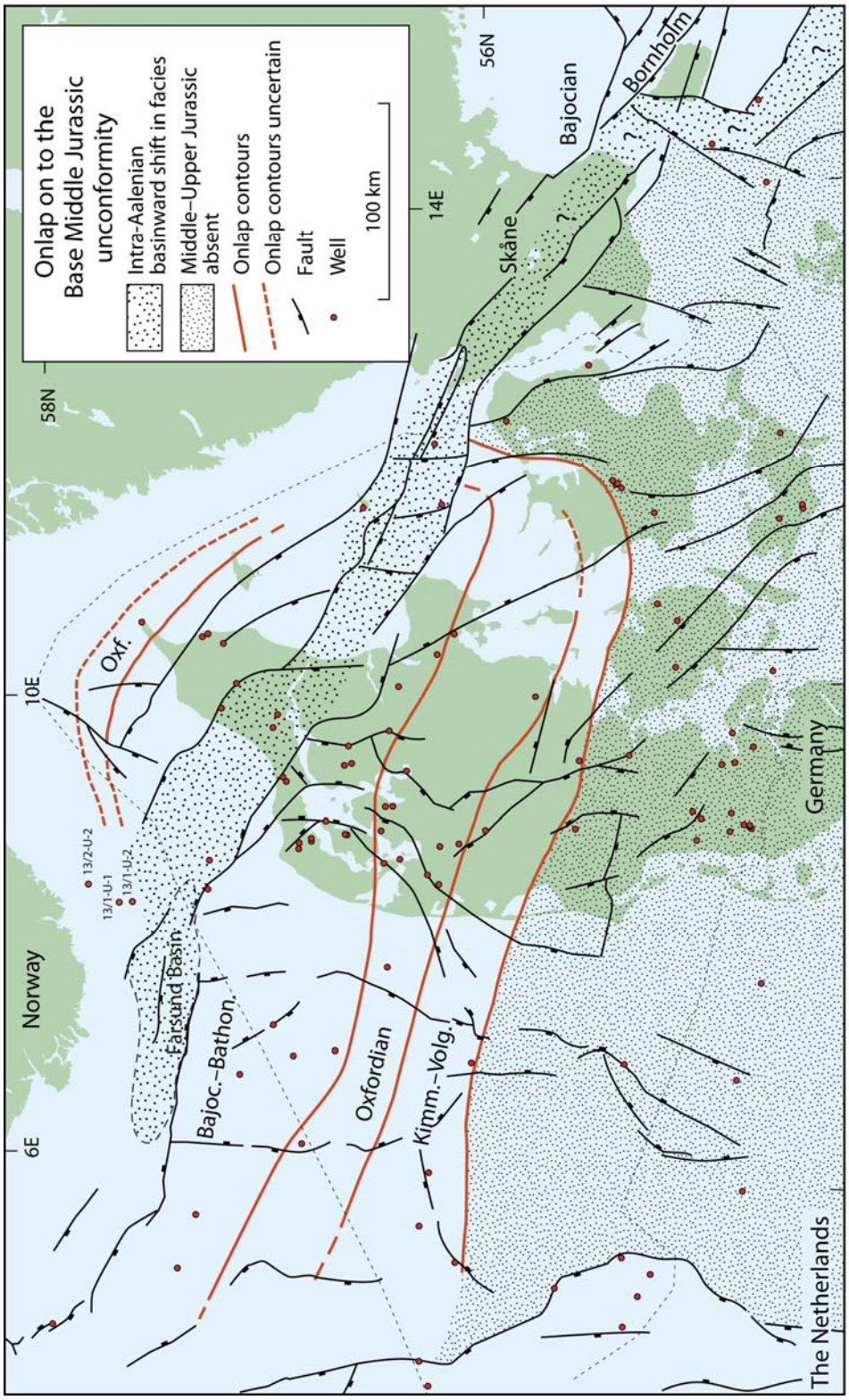

Figure 5.11. *Map showing the Upper Jurassic–Lower Cretaceous onlap to the Base Middle Jurassic Unconformity indicating the gradual expansion of the depositional area (Modified from Nielsen 2003).*

5.9 Early Cretaceous continued basin expansion

In Early Cretaceous times the area of marine deposition expanded further with coastal progradation from the north and northeast. Deposition of marine mudstones prevailed in most of the basin including the Sorgenfrei-Tornquist Zone, the Skagerrak-Kattegat Platform and most of the Ringkøbing High as indicated by Lower Cretaceous marine mudstones unconformably overlying Middle Triassic strata on the high. On the extreme westernmost and easternmost parts of the high deposition did not resume before the Late Cretaceous. The Lower Cretaceous mudstones with sandy intercalations being most common to the northeast are included in the Vedsted Formation, which shows a relatively systematic vertical variation in log-patterns that allow a subdivision into four units (Michelsen & Nielsen 1991). The uppermost unit contains a glauconite rich interval, up to 10 m thick in Sæby-1, which seems to be time equivalent to the redbrown, greyish, occasionally pyritic and glauconitic marls of the Rødby Formation. The Vedsted Formation is expected to be thickly developed in the Farsund Basin similar to the section in the J-1 well, if the basin was an Early Cretaceous depocentre as suggested by Jensen & Schmidt (1993).

5.10 Late Cretaceous–Danian Chalk deposition

In Late Cretaceous–Danian times a high sea level dominated and the Norwegian-Danish Basin, the Ringkøbing-Fyn High and the Fennoscandian Border Zone became covered by an epicontinental sea. The dry climate and low relief of the hinterland significantly reduced the clastic input, and biogenic, pelagic chalk deposition (with coccolith plates being the dominant constituent) occurred in the Norwegian-Danish Basin, the Ringkøbing-Fyn High and most of the Fennoscandian Border Zone. In the easternmost part of the basin and within the Fennoscandian Border Zone deposition of marine greensands ceased in late Cenomanian times and in the Early Turonian an intermittent deposition of marls and mudstones in parts of the basin came also to an end (Stenestad 1972; Surlyk 1980). Similar sands may occur proximal in the Farsund Basin. In central parts of the Norwegian-Danish Basin outer shelf coccolithic chalks accumulated at depths that may have been up to a few hundreds meters (Stenestad 1972; Surlyk & Håkansson 1999). Closer to the basin margins and over structural highs, chalks of the mid to inner shelf environment rich in bryozons and other bentic fossils were deposited. In more shallow water areas in the Fennoscandian Border Zone, benthos-rich chalks pass into bryozon wackestones and packstones occasionally developed as mound complexes, while skeletal grainstones and oyster bank carbonates formed closer to shorelines (Surlyk 1997). Hardgrounds and omission surfaces in the Maastrictian and Danian are most common in the shallower water sections. Centrally in the basin southwest of the Sorgenfrei-Tornquist Zone 1.5–2 km of chalk was deposited, while 500–750 m accumulated over the Ringkøbing-Fyn High. In the Sorgenfrei-Tornquist Zone including the Farsund Basin the original thickness of the chalks is masked by Late Cretaceous–Paleogene inversion and erosion (Liboriusen et al. 1987; Nielsen & Japsen 1991; Jensen & Schmidt 1993; Michelsen & Nielsen 1993; Erlström & Sivhed 2001). Seismic features such as northeastward onlaps, chaotic and hummocky reflection patterns in the chalk depocentres closely southwest of the Sorgenfrei-Tornquist Zone indicate syndepositional growth of the inversion structures. Parts of the zone probably became uplifted to or above sea level forming elongated islands from which chalky debris flows originated.

The inversion began in Coniacian time and accelerated rapidly during Santonian–Campanian time (the sub-Hercynian phase, Ziegler 1990), while decreased activity during Maastrichtian–Danian time was followed by pronounced inversion again in the Late Paleocene (the Laramide phase, Liboriusen et al. 1987; Ziegler 1990). These tectonic phases are also recorded on Bornholm, where shallow marine sands were deposited in Late–Middle Santonian time (the Bavnodde Greensand Fm) and in Scania where coarse-grained clastic deposition was especially significant during the Santonian–Campanian contemporaneously with the peak of inversion (the Lund Sandstone) (Surlyk 1980; Norling & Bergström 1987; Erlström 1994; Erlström et al. 1997). Marine, coarse-grained clastic deposition resumed again in the middle Maastrictian albeit at a much smaller scale (the Hansa Sandstone, Erlström 1990; Sivhed et al. 1999). Depending on the intensity of deformation in the Farsund Basin and north hereof, similar clastic wedges may be present within the Chalk Group.

5.11 Cenozoic clastic deposition and Neogene exhumation

After cessation of carbonate deposition in Paleocene time, fine-grained hemipelagic deep marine sedimentation took over in the Norwegian-Danish Basin and on the Ringkøbing-Fyn High. The north- and eastward limit of these fine-grained sediments is unknown due to later erosion, but parts of the Baltic shield were probably covered. In the Farsund Basin the Quaternary is subcropped by the Upper and Lower Cretaceous, and the original thickness and lithology of the Cenozoic is unknown.

In the basin volcanic ashes were deposited at the transition of the Paleocene–Eocene, and diatomites were laid down around salt structures in the central part of the basin where up-welling occurred (Bonde 1979; Pedersen 1981). The Paleogene succession is thickest immediately north of the Ringkøbing-Fyn High, where it is up to 300 m thick (Dinesen et al. 1977). Minor tectonic movements in Oligocene time reactivated former structural elements on the Ringkøbing-Fyn High and salt structures in the basin, and Paleogene sediments were eroded on elevated areas (Rasmussen 2004). Major clastic wedges began to build out from the Fennoscandian Shield in the Oligocene, while prodeltaic glauconite-rich clayey sediments were deposited further basinward. The deposition of coarse-grained sediments reached the southern part of the basin and the Ringkøbing-Fyn High in the Neogene (Larsen and Dinesen 1959; Friis et al. 1998; Rasmussen 2004). During the Early Miocene deltas prograded south-southwest and stacked deltaic deposits up to 300 m thick were formed. At the end of the Early Miocene, tectonic movements along older fault trends occurred resulting in pronounced coal accumulation in minor grabens (Koch 1989). A distinct flooding of the area took place in the Middle Miocene and deposition of clayey sediments prevailed in most of the Middle–Late Miocene. The flooding was partly due to the so-called Mid Miocene climatic optimum (Zachos et al. 2001) and partly due to increased subsidence of this part of the North Sea basin in the Late Miocene. Resumed delta progradation from the east and northeast occurred at the end of the Miocene (Rasmussen & Dybkjær 2005). The infilling of the North Sea basin continued during the Pliocene and up to 500 m of sediments were deposited in the Norwegian-Danish Basin during the Late Miocene and Pliocene (Overeem 2001).

Contemporaneously with the regional down-warping of southern Scandinavia, parts of the Norwegian-Danish Basin and Fennoscandian Border Zone including the Farsund Basin

were uplifted and eroded. This major tilting continued into the Quaternary (Japsen 1993; Jensen & Schmidt 1993; Japsen et al. 2002; Rasmussen et al. 2005).

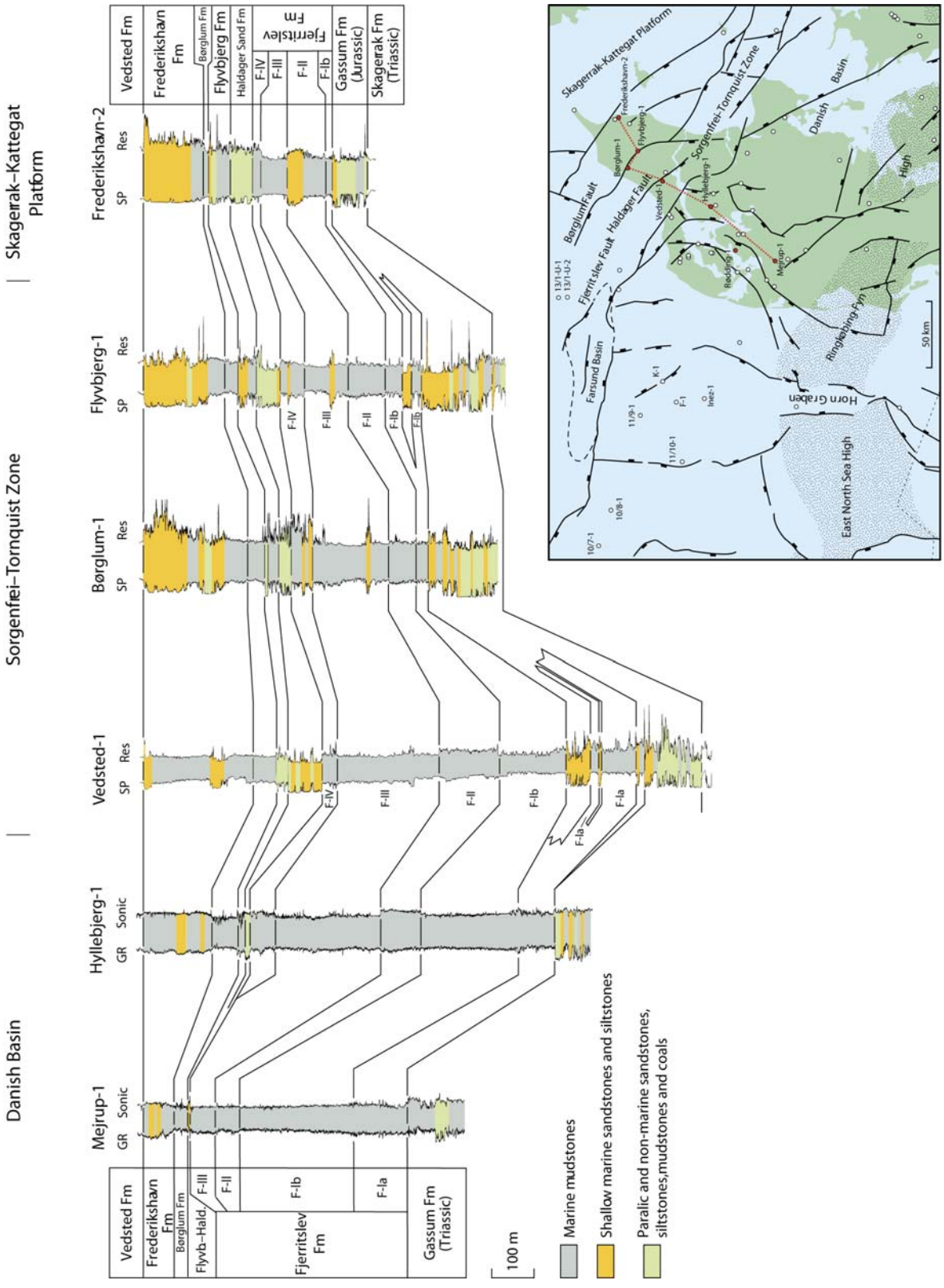

Figure 5.12. *Well log panel trending SW–NE across the basin showing the lithostratigraphy of the Upper Triassic–Lower Cretaceous. It is expected that a N–S trending panel across the Farsund Basin will show similar units (Michelsen et al. 2003).*

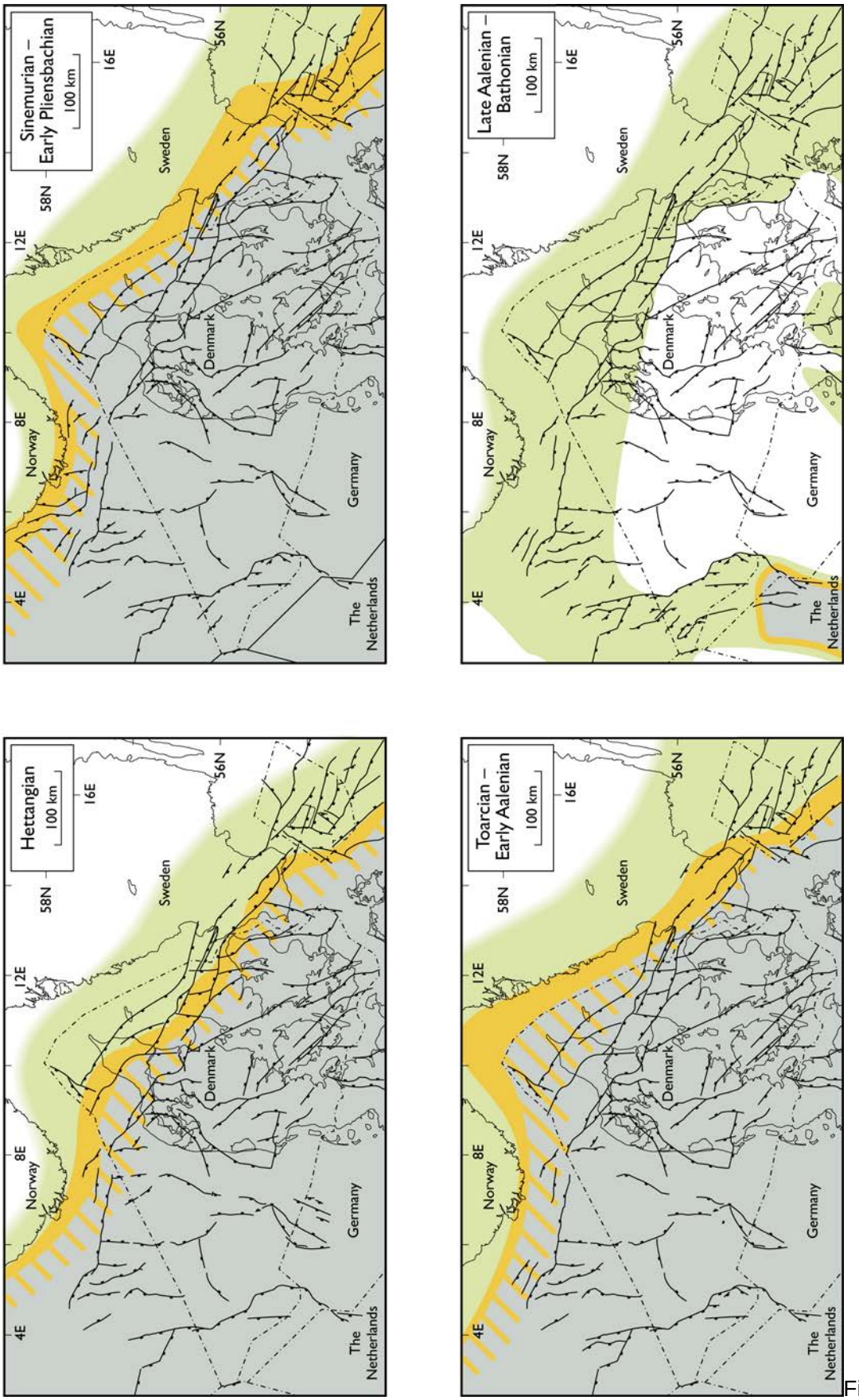

Fig.

Figure 5.13. *Paleogeographic maps showing the general depositional environment at specific Jurassic times (modified after Michelsen et al. 2003).*

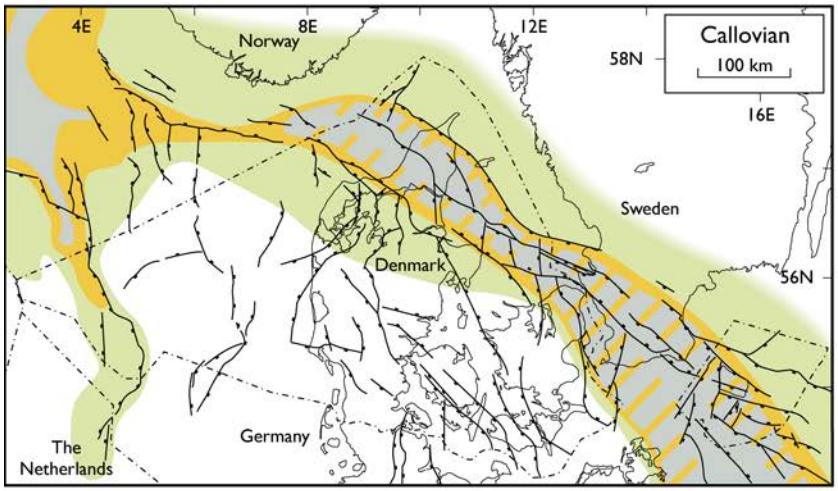

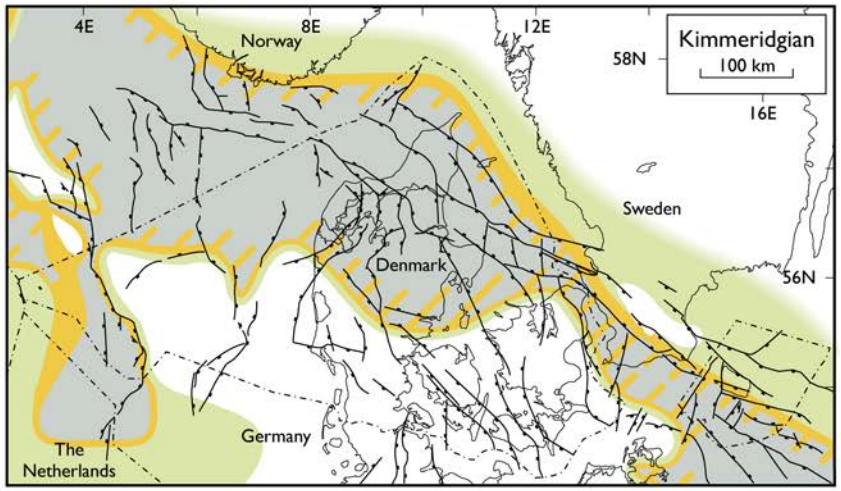

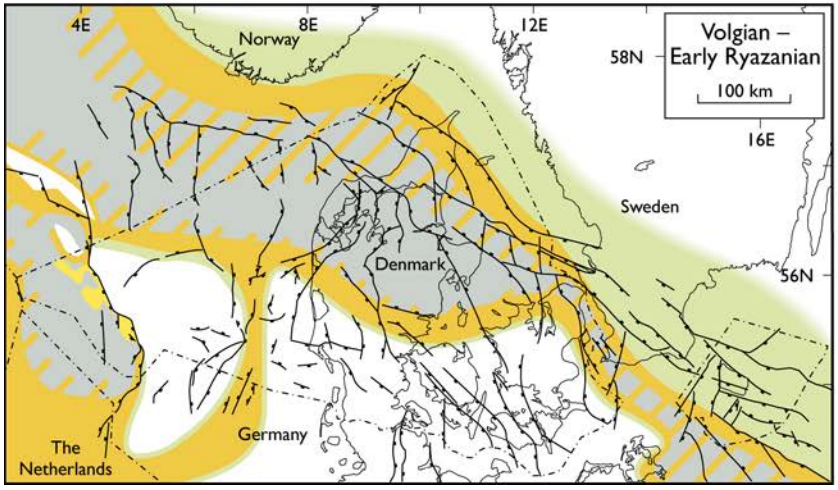

- Offshore marine (mud-dominated)
- Deep marine (sands, gravels)
- Shallow marine sandstones and siltstones
- Paralic and non-marine sandstones, siltstones, mudstones and coals
- Non-deposition/erosion

6. Characterisation of potential reservoirs

Reservoirs potentially suitable for CO_2 storage are found at several stratigraphic levels in the Mesozoic succession. Among these the Lower Triassic Bunter Sandstone Formation, the Triassic Skagerrak Formation, the Upper Triassic–lowermost Jurassic Gassum Formation and the Middle Jurassic Haldager Sand Formation (Fig. 6.1) constitute the principal reservoirs in the Danish part of the Norwegian-Danish Basin due to their distribution, burial depth and reservoir properties. The Bunter Sandstone Formation is not considered to be present along the northern and northeastern basin margins and is not considered further here. Cores are available from the formations as they have been the target for previous hydrocarbon and geothermal exploration activities. A number of samples were selected from the cores with the strategy of covering the variable petrographical composition of the formations. The variations reflect primary differences related to source areas and depositional environments and secondary alterations caused by different diagenetic development related to different burial depths in the basin and also lithology of the embracing formations. This strategy was followed in order to obtain the best possible overview of the potential chemical reactions, which subsequently may be the target of further in-depths studies. The three formations are described below.

6.1 Skagerrak Formation

The Skagerrak Formation was defined by Deegan & Scull (1977) to include the interbedded conglomerates, sandstones, siltstones and claystones that occur along the northern and north-eastern margin of the Norwegian-Danish Basin. These up to more than 2 km thick deposits are of Early–Late Triassic age and were mainly deposited as alluvial fans along the faulted basin margin. The alluvial fan deposits pass into braided river facies towards the central parts of the basin (Pedersen & Andersen 1980; Priisholm 1983). The lower part of Skagerrak the formation is probably contemporaneous with the Bunter Sandstone Formation, while the middle part is contemporaneous with the Ørslev, Falster, Tønder and Oddesund Formations that mainly occur centrally in the basin. These formations consist primarily of marine–brackish claystones, marls, carbonates and evaporites without significant reservoir potential; only the Tønder Formation may contain sandstones with some potential. At the time of deposition of the Skagerrak Formation, the climate was arid to semi-arid (Bertelsen 1980), consistent with the occurrence of the contemporaneously evaporitic deposits.

6.2 Gassum Formation

The Gassum Formation was redefined by Bertelsen (1978) to include the well to moderately sorted, fine to medium-grained sandstones occurring between the restricted marine mudstones of the Upper Triassic Vinding Formation and the marine mudstones of the Lower Jurassic Fjerritslev Formation. The Gassum Formation becomes younger stepwise towards north and east, being mainly of Rhaetian age in the central parts of the basin, while it is of Rhaetian–Early Sinemurian age along the basin margin in North Jylland, Kattegat and

eastern Sjælland. The Gassum Formation is widely distributed with thicknesses of 50–150 m in central and distal parts of the Danish part of the basin. The thickness increases to 170–200 m in the fault-bounded Himmerland Graben and the northern part of the Sorgenfrei-Tornquist Zone, while the thickness increases to more than 300 m in the southern part of the fault zone. In areas of significant salt movements an extraordinary large thickness of the formation is seen and the proportion of thick mudstones is larger probably reflecting topographic influence during deposition from the nearby large salt structures (e.g. Felicia-1). On the Skagerrak-Kattegat Platform the thickness decreases (10–80 m) and is absent on most of the Ringkøbing-Fyn High due to later uplift and erosion (Nielsen & Japsen 1991).

In the Himmerland Graben, Sorgenfrei-Tornquist Zone and Skagerrak-Kattegat Platform, sandstones are the dominant lithology, while the formation is sand-poor in the central parts of the basin (Mejrup-1, Vemb-1, and Vinding-1). The sandstones are predominantly well to moderately sorted, fine to medium-grained, occasionally coarse-grained and slightly pebbly, and range from very permeable to well-cemented. The shoreface sandstones occur as widespread sheets, 4–30 m thick separated by marine transgressive mudstones and lagoonal heteroliths. Thick fluvial-estuarine sandstones are primarily overlying the major SB 5.

The formation was deposited during a series of relative sea level falls and is dominated by shallow marine shoreface sandstones and fluvial-estuarine sandstones; offshore marine and lagoonal heteroliths and mudstones, and lacustrine claystones and thin coal seams constitute a significant but minor proportion of the formation (Nielsen 2003). The source area of the Gassum sand probably comprised reworked Bunter Sandstones in the south-eastern part of the basin, whereas more heterogeneous bedrock to the north and east supplied the sand to the northern and central parts of the basin causing a variable petrography of the formation. The formation records a general chance in climate from the dominantly arid to semi arid climate during the early–mid Triassic, which gradually became more humid during the Rhaetian as reflected in preservation of larger amounts of organic matter (Bertelsen, 1978).
In major parts of the basin the Gassum Formation is overlain by thick, uniform marine mudstones of the Fjerritslev Formation with large lateral continuity forming a highly competent caprock unit probably making the Gassum Formation one of the most promising reservoirs for CO_2 storage in the Danish subsurface.

6.3 Haldager Sand Formation

The Haldager Sand Formation was redefined by Michelsen (1989) to include the Middle Jurassic sandstones occurring between marine mudstones of the Lower Jurassic Fjerritslev Formation and marine mudstones and sandstones of the Upper Jurassic Flyvbjerg and Børglum formations. The distribution and thickness of the Haldager reservoir is strongly influenced by regional syn-depositional tectonism, local faulting and salt-structures. The formation overlies the regional "Base Middle Jurassic Unconformity" (also termed the Mid Cimmerian Unconformity, MCU) and is thickest developed in the Sorgenfrei-Tornquist Zone, where slow subsidence prevailed during the Middle Jurassic uplift phase, that af-

fected the Ringkøbing-Fyn High and most of the Danish part of the basin including the Skagerrak-Kattegat Platform and parts of Skåne (Nielsen 2003).

The regional depositional model for the Haldager reservoir is shown on Figures 5.6, 5.8, 5.10. Generally, the formation consists of thick fluvial and shallow marine sandstones interbedded with thin mudstones. In the Sorgenfrei-Tornquist Zone the formation consists of four fluvial-estuarine to shallow marine sandstone units separated by marine and lagoonal-lacustrine mudstones (Figs 5.6, 5.10). Outside the fault-bounded graben, the sandstones were mainly deposited by braided rivers, and are expected to be laterally coherent without significant primary hydraulic barriers. Anomalies with respect to facies and thickness occur locally in rim-synclines to salt-structures. The sediments were supplied from the north and east, but deep erosion of Triassic and older strata on the Ringkøbing-Fyn High and Lower Jurassic mudstones along the northern flank of the high added a substantial amount of material. As a result of the uplift of the Ringkøbing-Fyn High, high-energy braided rivers shed erosion products into the Sorgenfrei-Tornquist Zone, which experienced slow fault-controlled subsidence. The formation is thin and patchy distributed in the southern and south-western part of the basin with thickness below 10 m. In the more central parts of the basin the thickness increases to 25–50 m; in the Sorgenfrei-Tornquist Zone between the Fjerritslev and Børglum faults the thickness further increases to ca. 175 m. On the Skagerrak-Kattegat Platform the formation thins to 15–30 m. The sandstones are mostly medium to coarse-grained, slightly pebbly, well to moderately sorted sandstones and greywackes.

The Haldager Sand Formation is covered by the marine mudstones of the Børglum Formation with excellent sealing capacity and may locally be a promising reservoir for CO_2 storage in the Danish subsurface.

6.4 Samples

Mesozoic sediments onshore Denmark occur at a wide spectrum of burial depths making investigations of diagenetic evolution with burial depth possible. Cored intervals of the Skagerrak Formation have present day burial depth from 600 – 5100 m (Fig. 6.1). The corresponding maximum burial depths are ca. 1750 – 5900 m (with an estimated error of ± 200 m) corrected for Late Cretaceous to Early Palaeogene and Neogene uplift (Weibel 1999). Cores from the Gassum and Haldager Sand Formations represent burial depths from 550 to 3360 m (Fig. 6.2) and 450 – 2500 m (Fig. 6.3), respectively.

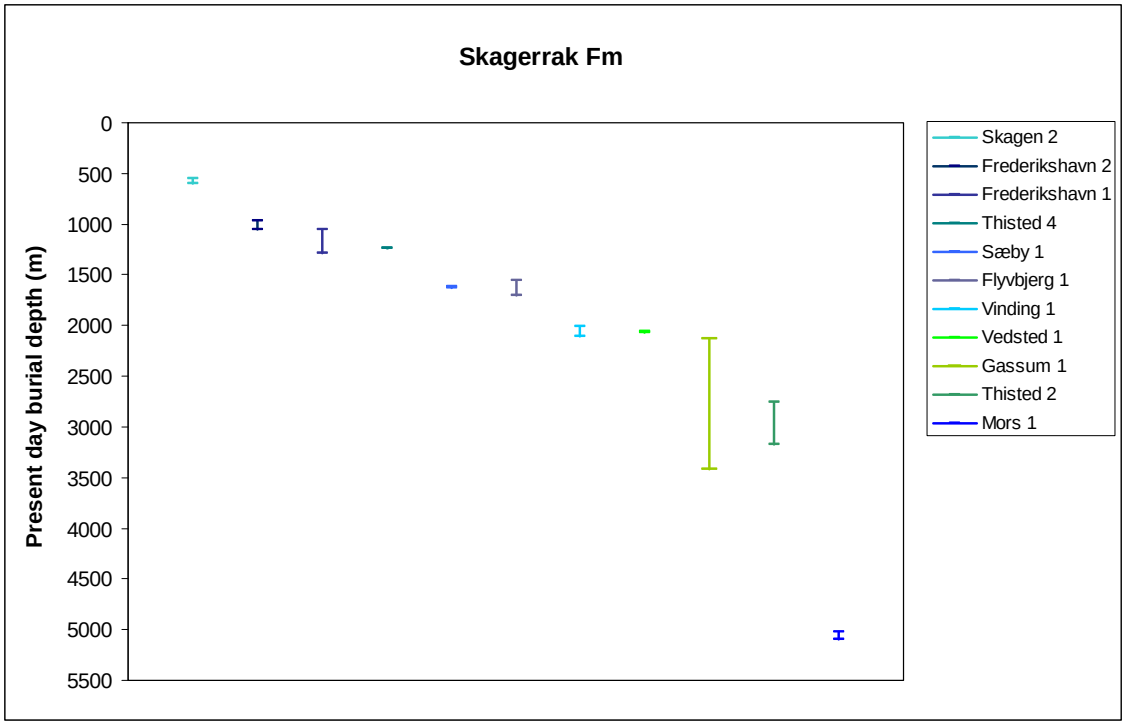

Figure. 6.1. *Cored intervals of the Skagerrak formation onshore Denmark*.

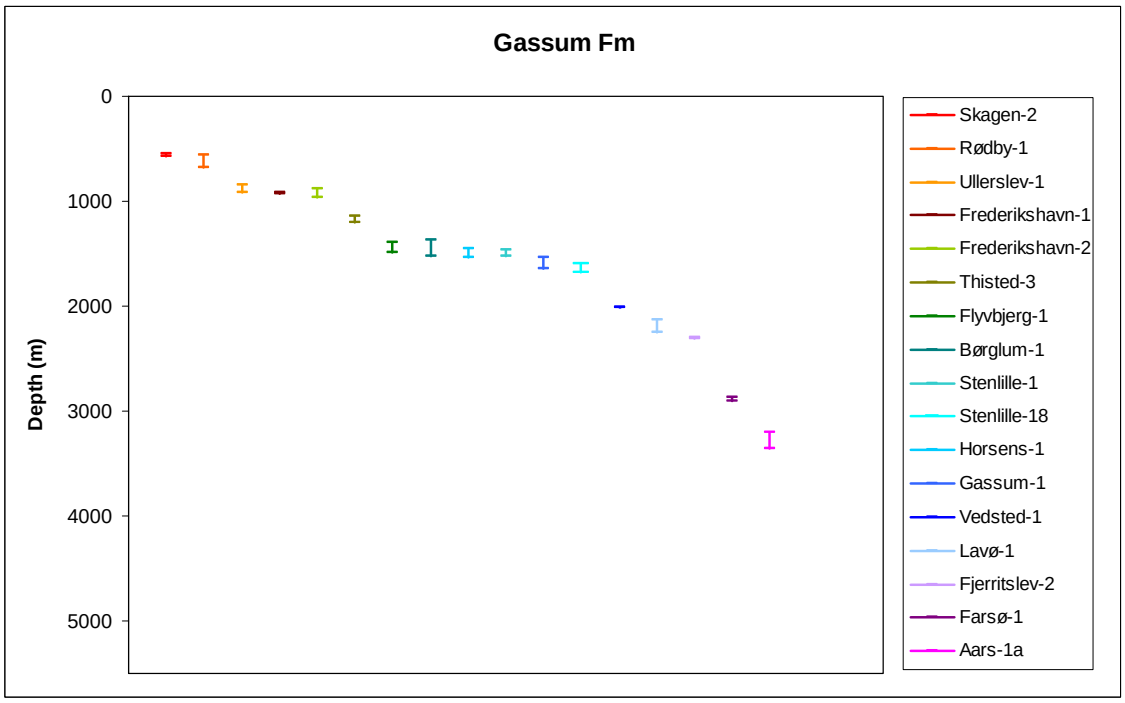

Figure. 6.2. *Cored intervals of the Gassum Formation onshore Denmark.*

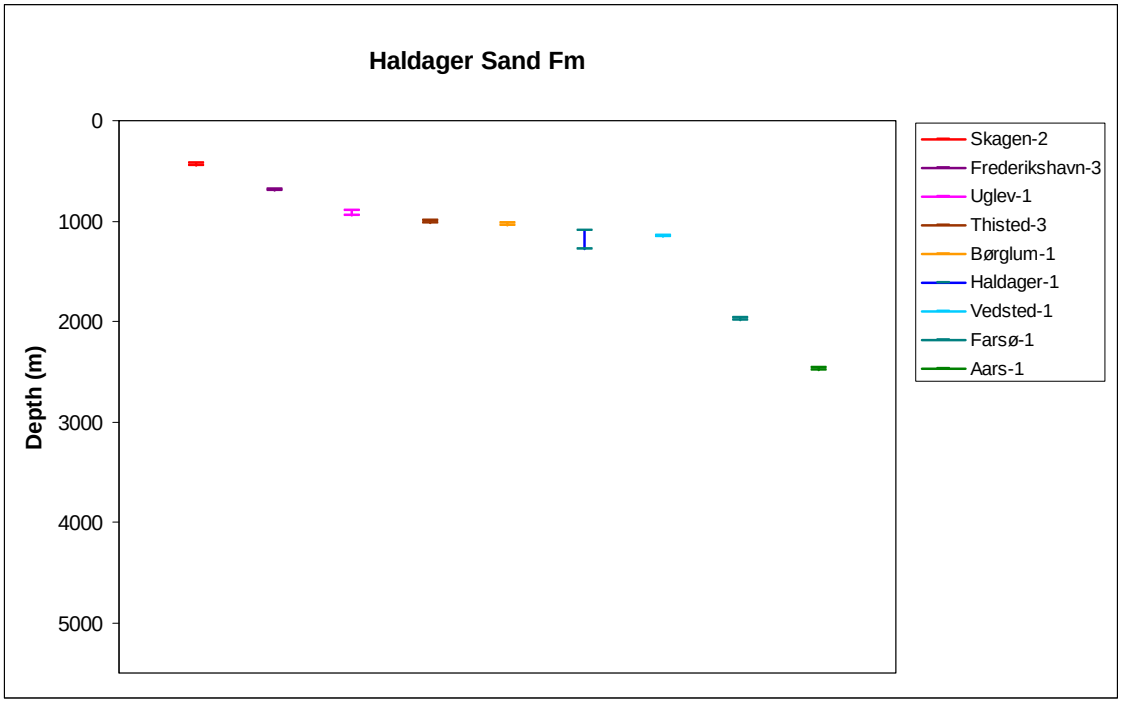

Figure. 6.3. *Cored intervals of the Haldager Sand Formation onshore Denmark.*

6.5 Laboratory methods

6.5.1 Petrography

Petrography was evaluated from transmitted light and reflected light microscopy of polished thin sections. The sedimentary rocks were impregnated with blue epoxy for easy identification of porosity. Half of the polished thin section was stained for easy recognition of K-feldspar. Modal compositions of the sandstones were obtained by counting minimum 300–500 points in each thin section. Supplementary studies of crystal morphologies and paragenetic relationships were performed on gold coated rock chips mounted on stubs and on carbon coated thin sections using a Phillips XL 40 scanning electron microscope (SEM). The scanning electron microscope was equipped with secondary electron detector (SE), back-scatter detector (BSE), cathodoluminescence detector (CL); and with a Thermo Nanotrace 30 mm^2 detector surface window and a Pioneer Voyager 2.7 10 mm^2 window Si(Li) detector energy dispersive X-ray analysis (EDX) system. The electron beam was generated by a tungsten filament operating at 17 kV and 50–60 µA.

6.5.2 Microprobe analysis

Feldspar composition was analysed on carbon-coated polished thin sections on a JEOL© JXA-8200 microprobe at an acceleration voltage of 15 kV and a beam current of 15 nA.

6.5.3 X-ray diffraction (clay and bulk mineralogy)

The clay fraction samples were separated by sieving and gravitational settling and prepared as smear slides. Bulk samples were mounted with random orientation. Samples were scanned on an automated Philips© PW 3710 X-ray diffractometer with automatic divergence slit, using graphite monochromated CuKα radiation. The clay specimens were scanned air-dried; ethylene glycolated at 60°C; and after heating at 500°C for one hour. Criteria for identification of clay minerals can be found in Weibel (1999). Quantification of major mineral phases was done by Rietveld analysis of x-ray diffractograms of bulk-rock samples, whereas the clay minerals were evaluated semi-quantitatively.

6.5.4 Porosity and permeability

The porosity and permeability were measured according to the API RP-40 standard (API 1998). Gas permeability was measured at a confining P ~ 2.8 MPa (400 psi), and at a mean N_2 gas pressure of ~ 1.5 bar (bar absolute) = 0.15 MPa (permeabilities below 0.05 mD were measured using a bubble flowmeter). He-porosity was measured unconfined.

6.6 Petrography and diagenesis

The detrital composition and authigenic formed minerals will be presented for each formation: Skagerrak Formation, Gassum Formation and Haldager Sand Formation. The detrital composition can be compared in several ways; in Figure 6.4 the amount of quartz, feldspar and rock fragments are compared according to the classification by McBride (1987). The mineralogical changes with burial depth will first be discussed for each formation prior to comparison of the diagenesis in the respective formations. The early diagnesis (eogenesis) is very different between the formations, as it is strongly tied to the depositional environment (Schmidt and McDonald, 1979). The diagenesis during increased burial depth (mesogenesis) comprise the changes when interstitial water is no longer controlled by the surface environment (Schmidt and McDonald, 1979) and is consequently strongly related to the stability and instablility of the detrital minerals (as well as their abundance). This can explain the remarkably degree of consistency in the diagenetic assemblages (illite, chlorite, ferroan carbonate, quartz cement and secondary porosity) formed at deep burial in sediment of a variety of environments and tectonic settings and it suggests that depth-related (mesogenetic) diagenetic processes conform to a pattern that may be predictable (Burley et al. 1985).

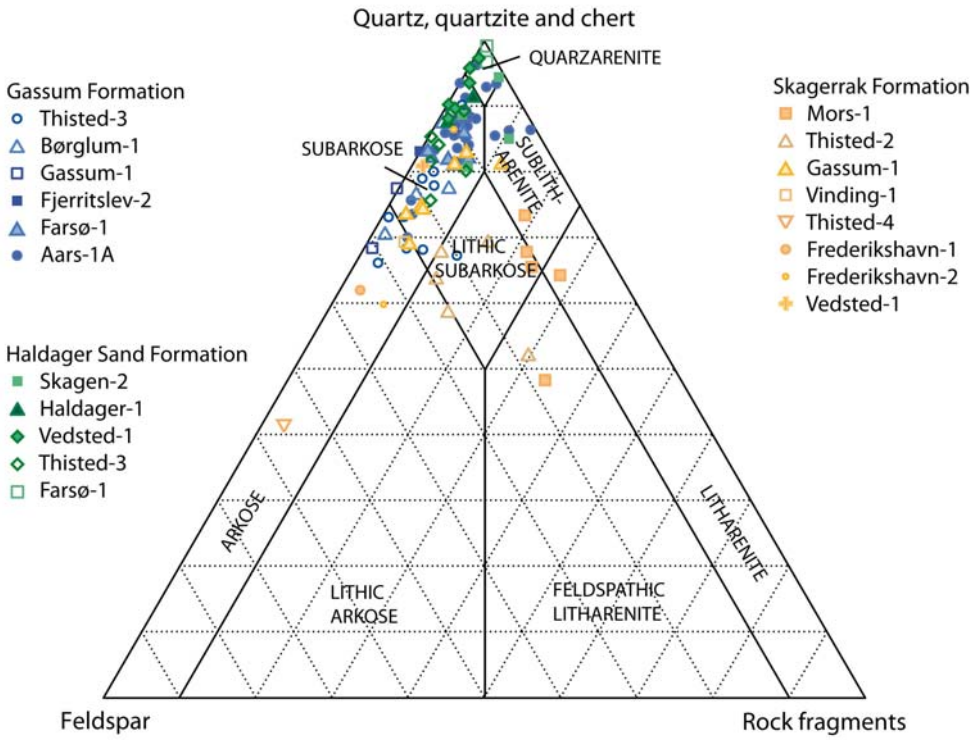

Figure. 6.4. *Ternary diagram showing the classification, according to McBride (1968), of the Danish Mesozoic onshore sandstones. Data for the Gassum Formation after Friis (1987).*

6.6.1 Skagerrak Formation

The alluvial fan and braided river deposits of the Triassic Skagerrak Formation has present day burial depths from 600–5000 m and total thicknesses up to 1700 meters (Nielsen & Japsen 1991; Mathiesen et al. 2009).

6.6.1.1 Detrital composition

The sediments are arkoses, lithic arkoses and subarkoses (Figs 6.4 & 6.5; Weibel 1998) according to the classification of McBride (1963). The sediments vary from fine-grained sandstones to conglomerates. The sorting is poor to moderate in the northeastern part of Denmark but the degree of sorting increases towards southwest. The grains are typically subangular to subrounded.

Monocrystalline quartz is the major framework grain, though polycrystalline quartz also occurs. The feldspar group is completely dominated by K-feldspar, though plagioclase grains have been identified. Alteration of feldspar grains includes dissolution, clay mineral or carbonate replacement, sericitisation and possible albitisation (only in the deeper reservoir sandstones, for example Thisted-2). Furthermore, a relatively high number of altered grains are probably altered feldspar grains.

The rock fragments are mainly igneous and rarely metamorphic, but volcanic rock fragments are common in a specific area (in the Mors-1, Thisted-2, Thisted-4 and Gassum-1 wells). Clay intraclasts that probably are rip-up clasts from overbank deposits occur in high abundance in few samples. Mica occurs in small amounts in most samples. Mica shows signs of oxidation, reduction (only in reduction spots), replacement by clay minerals or minor expansion due to precipitation of authigenic phases (hematite and anatase) between cleavage planes. Transparent (apatite, zircon, tourmaline, rutile, amphibole) and opaque heavy minerals are common accessory minerals, though they may be abundant in specific samples containing heavy mineral lamina. Opaque minerals may in specific samples be present in up to 20.3%. The alteration of opaque minerals includes among other leucoxene replacement of ilmenite and hematisation of magnetite (Weibel 1998; Weibel & Friis 2007).

6.6.1.2 Authigenic phases

The dominating porosity reducing cements in the Skagerrak Formation are carbonates and clays (Figs 6.6, 6.7 & 6.8). Clay minerals occur as pore-lining, pore filling cement as well as replacement of detrital grains, which, besides feldspar and mica, may include both volcanic rock fragments and heavy minerals. The clays are dominated by smectite in the shallow wells, whereas mixed-layer illite/smectite and illite become more abundant with increased burial depth (Weibel, 1999). Infiltration clays (Fig. 6.7A), probably of smectitic composition, are volumetrically important in rare samples. Authigenic illite appears as radiating crystals either pore lining or intragranular on remnants of almost completely altered detrital minerals (Figs 6.8C & D). Chlorite occurs as a late diagenetic pore filling cement and is clearly separated from illite by red coatings (Figs 6.8E & F). Kaolin dominates the clay mineral assem-

blage in the reduction spots and reduced areas, but is rare in the red host (Weibel 1998, 1999) (Figs 6.11 E & F).

Red coatings cover most detrital grains and are found in between some authigenic phases. The red colouration of the Skagerrak Formation origins from goethite in the shallow sandstones (< 2100 m), but from hematite in the deeper sandstones (>2700 m), where the goethite needles are pseudomorphous transformed into hematite (Weibel 1999; Weibel & Groberty 1999). Additionally hematite occurs as replacement of mica and amphiboles, syntaxial overgrowth on detrital hematite and as pore filling crystals arranged as rosettes which appear to be "doughnut" shaped in high resolution (SEM).

The carbonate cement is typically dolomite, which occurs either as rhombohedral-shaped crystals with distinct growth zones, or as pore filling poikilotopic and micritic cement, which may be replacive to other mineral phases (Figs 6.7E & F). The nucleation points for carbonate are altered plagioclase grains or clay intraclasts where they are present (Figs 6.7C & D). The micritic cement is common in between the cleavage planes of expanded mica, whereas the poikilotopic cement is pore filling and corrosive towards the other mineral phases. The pore filling carbonate often has a radiating extinction thereby resembling saddle dolomite. Occasionally the pore filling carbonate cement is calcite or ankerite (ankerite in the Vedsted-1 well; Appendix 1). Calcite corrodes the rims of the detrital minerals which "float" in the calcite matrix. Calcite occurs as both micritic and poikilotopic cements. The micritic cement exhibits several of the Alpha calcrete fabric elements described by Wright (1990). For example the calcite crystals form a radiating rim on the detrital grains in some of the shallow wells (Frederikshavn-1, -2, Skagen-2 and Flyvbjerg-1) (Fig. 6.7A).

Of minor volumetrically importance are quartz overgrowths and feldspar overgrowths. Syntaxial quartz overgrowths occur as prismatic or pore filling crystals. Prismatic authigenic quartz (occasionally bi-pyramidal authigenic quartz) occurs where relatively thick clay rims or red coatings cover the detrital grains (Figs 6.9A & B). Pore filling quartz occurs only in rare very fine-grained (siltstone - fine-grained sandstone) cross-stratified samples. Authigenic macroquartz encloses other authigenic phases, such as red coatings (Fig. 6.9D), anatase, illite rims, fibrous illite, feldspar, early carbonate rhomb and occasionally prismatic quartz as observed in the deepest well (Mors-1). Pressure solution and fractural healing in detrital quartz grains (and abundant authigenic quartz) are common phenomena in the Gassum-1 well, which has a lower content of ductile rock fragments and authigenic clay minerals (Fig. 6.9.F). Thick red coatings seem to have a prohibiting effect on the pressure solution.

Authigenic feldspars occur as syntaxial and rarely epitaxial overgrowths on detrital feldspar grains and as crystals precipitated on remnants of dissolved feldspars in the secondary porosity (Figs 6.10A, B & C). Authigenic feldspar encloses red coatings and illitic rims (Fig 6.10D). Feldspar overgrowths are more abundant than quartz overgrowths in the shallowest part of the cores from the Gassum-1 well, and in fine-medium grained samples in the Thisted-2 well.

Rare authigenic minerals include anatase, pyrite and anhydrite (Fig. 6.11). Titanium-oxides comprise leucoxene, which replaces detrital titanium-rich minerals, and single crystals of

anatase, which are precipitated in the pore space. Pyrite occurs as framboidal or euhedral cubic pore filling crystals or replacement of mica in the reduction spots (Figs 6.11C & D). Pyrite is commonly occurring together with kaolin. Crandallite group minerals occur as euhedral cubic pore filling crystals along the outer rim of reductions spots.

Anhydrite is the last authigenic phase and corrosive to all other mineral phases (Figs 6.11A & B). Anhydrite is very rare in the Skagerrak Formation.

Mechanical deformation of ductile grains such as mica, clay intraclasts and rock fragments is common in the deepest reservoir sandstones, whereas pressure solution of quartz occurs in sandstones with a low content of ductile grains.

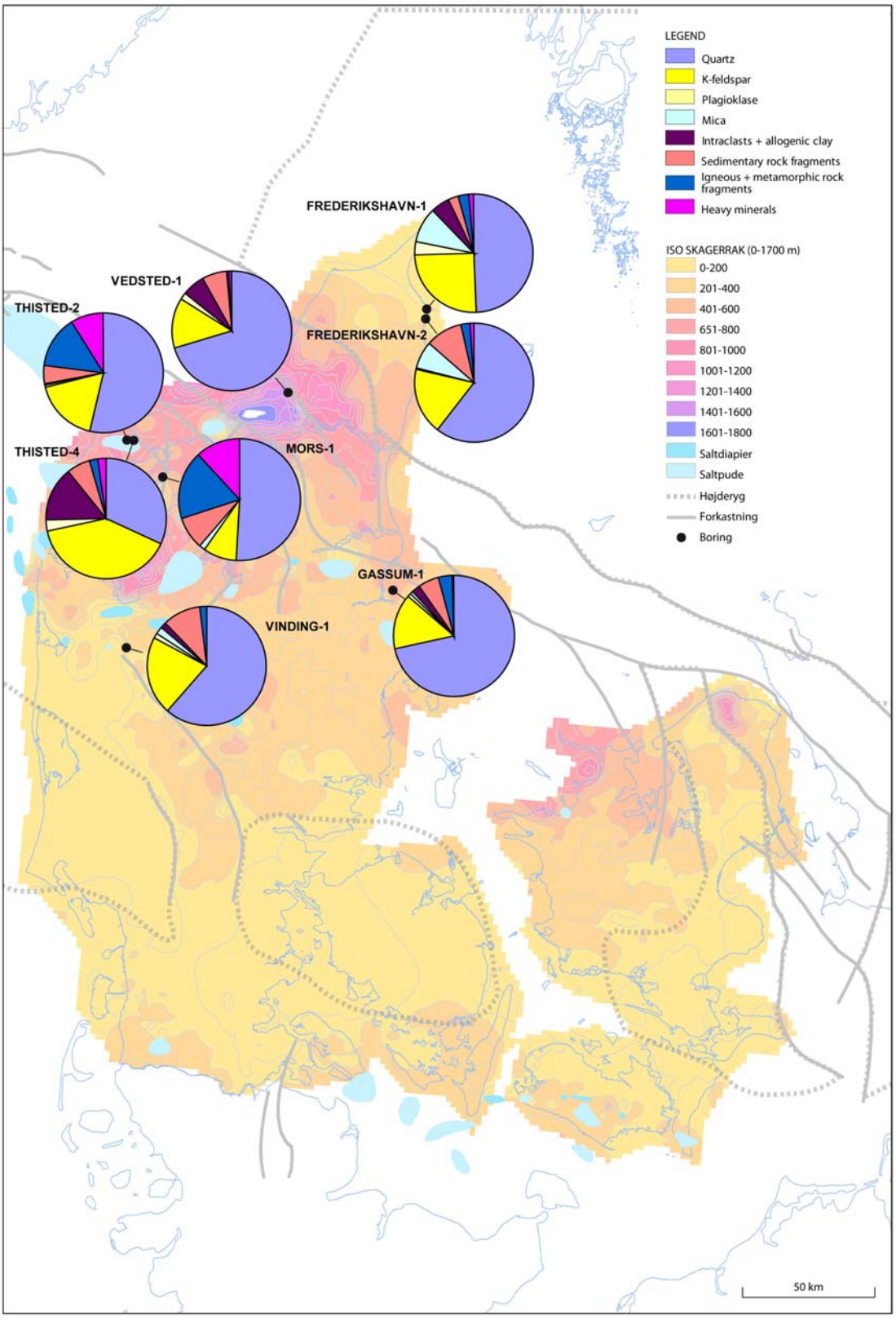

Figure. 6.5. *Average detrital composition of the Skagerrak Formation shown as pie diagrams for each analysed well on isopach map of the Bunter Sandstone and Skagerrak formations (modified after Mathiesen et al. 2009).*

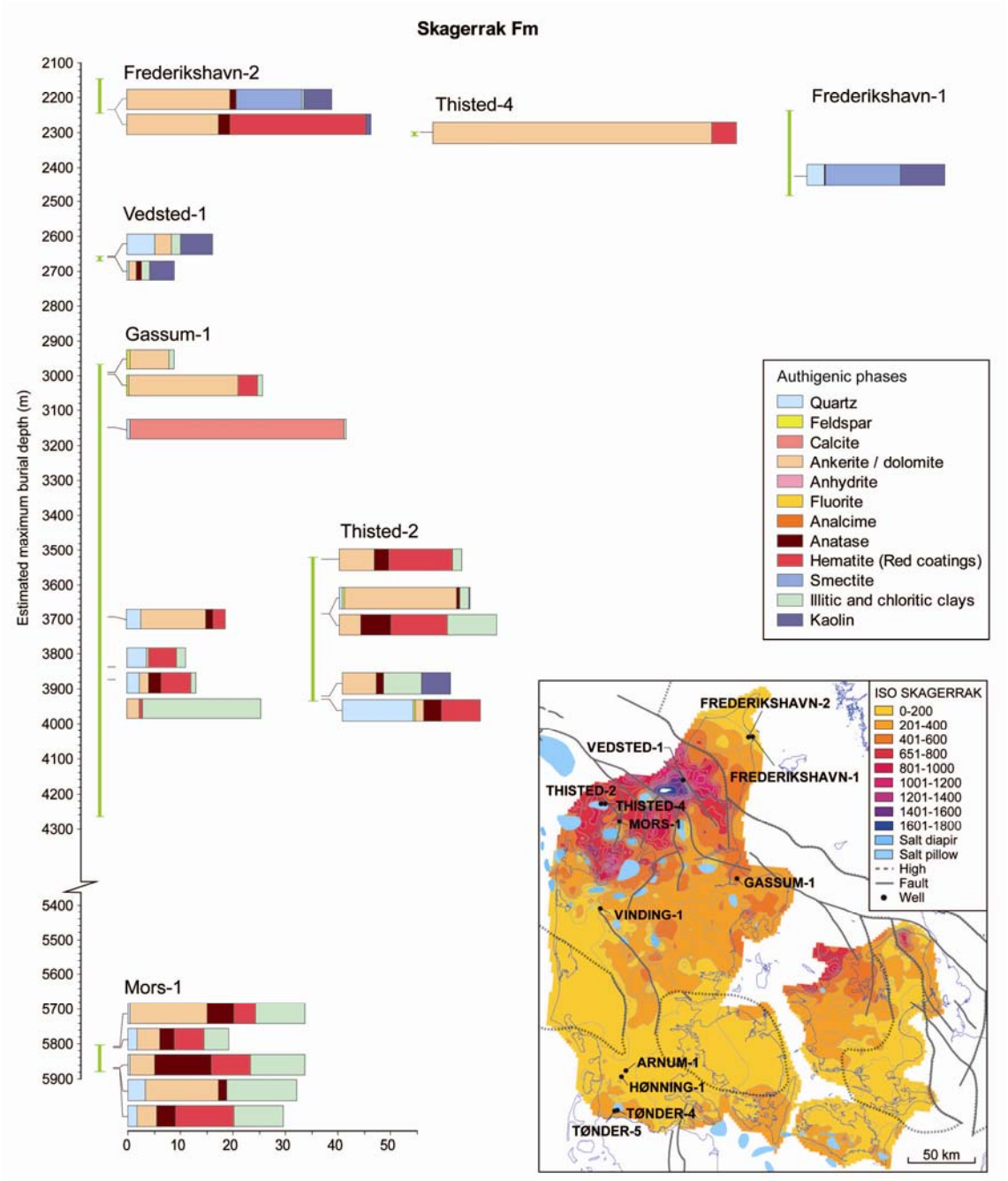

Figure. 6.6. *Authigenic phases, quantified by point counting, in the Skagerrak Formation for different wells and consequently different burial depths.*

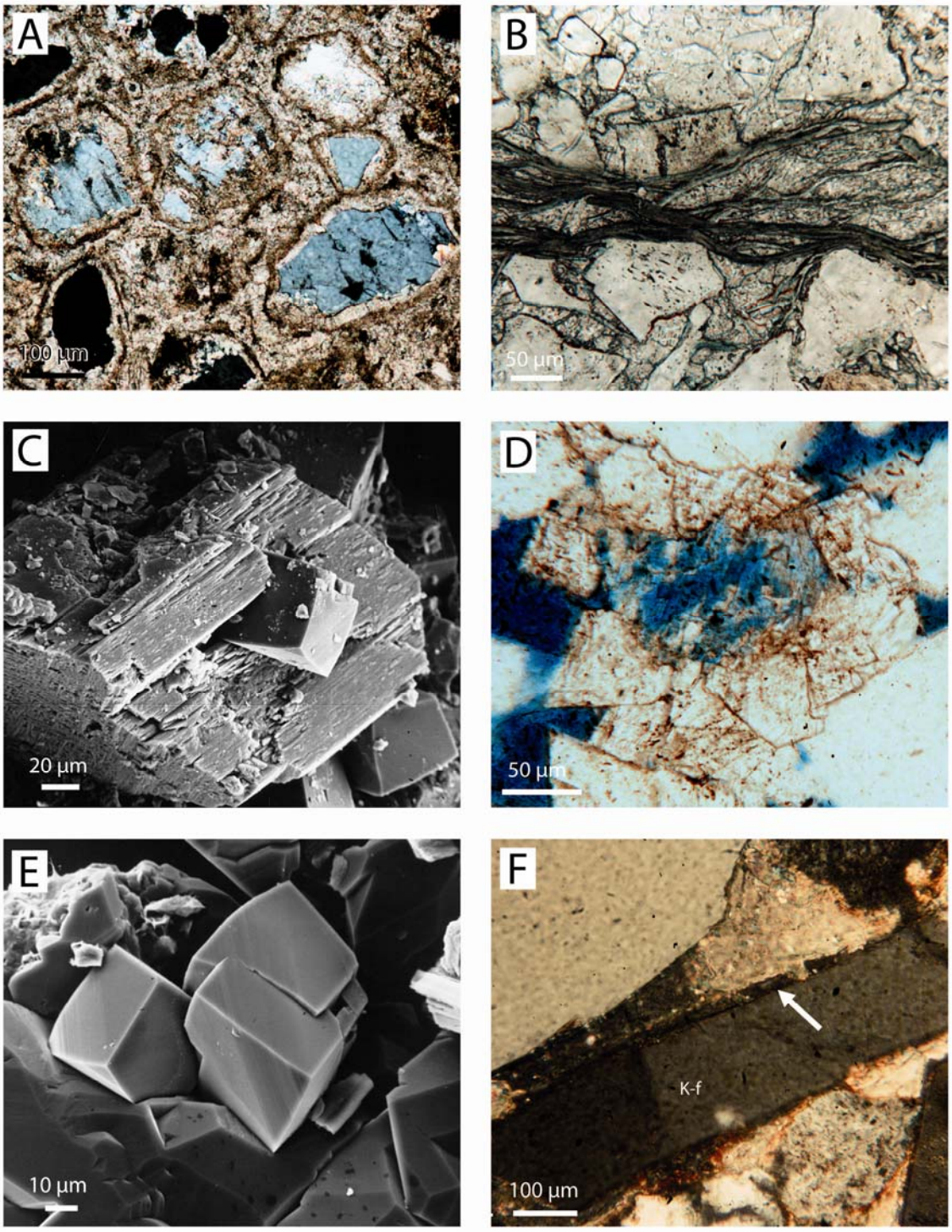

Figure. 6.7. *Carbonate diagenesis in the Skagerrak Formation. A. Calcrete showing radiating crystals on the detrital grains, Frederikshavn-2, 1050.95 m, crossed nicols. B. Early calcite cement precipitated between the cleavage planes of detrital chlorite, Gassum-1, 2153.73 m. C. Dolomite precipitation related to feldspar alteration. Gassum-1, 2153.71 m, scanning electron micrograph. D. Dolomite precipitation related to feldspar alteration, Gassum-1, 2153.40 m. E. Late dolomite precipitation after quartz overgrowth, Gassum-1, 2153.71 m, scanning electron micrograph. F. Late dolomite cement formed after feldspar overgrowth (marked by arrows) on detrital K-feldspar (K-f), Thisted-2, 2763.04 m.*

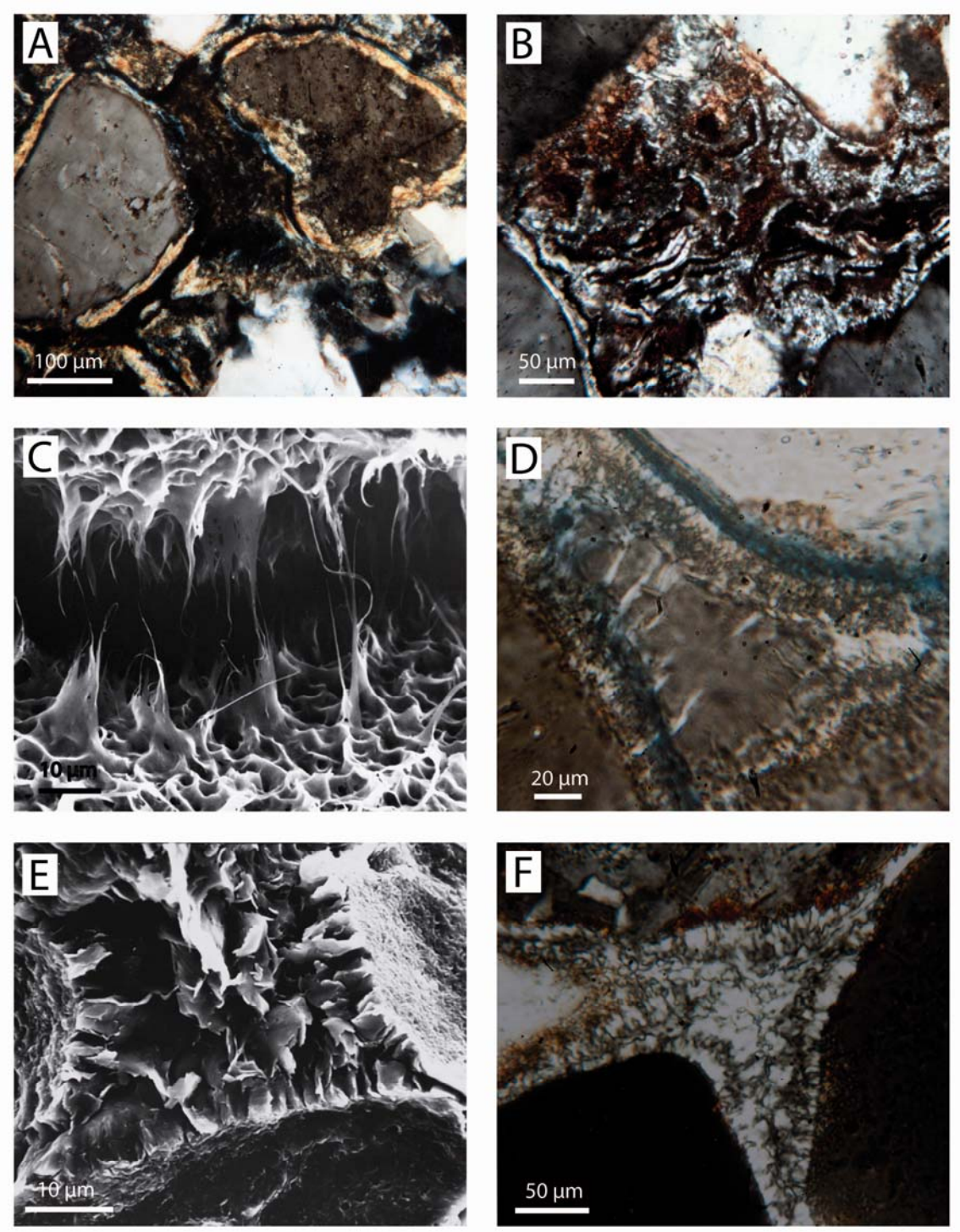

Figure. 6.8. *Clay minerals in the Skagerrak Formation. A. Smectitic infiltration clay orientated parallel to the detrital grain surface, Sæby-1, 1628.03 m, crossed nicols. B. Complete clay mineral and iron-oxide/hydroxide replacement of unstable silicate grain, Thisted-2, 2912.26 m, crossed nicols. C. Mixed-layer smectite/illte as indicated from their boxwork texture, from which illite whiskers grows, Thisted-2, 2761.40 m, scanning electron micrograph. D. Rim of illitic clay and illite whiskers prior to quartz cementation, Mors-1, 5081.93 m, crossed nicols. E. Rim of illitic clay preceding pore filling chloritic clays, Mors-1, 5032.22 m, scanning electron micrograph. F. Rim of illitic clay preceding pore filling chloritic clays, Mors-1, 5090.32 m, crossed nicols*.

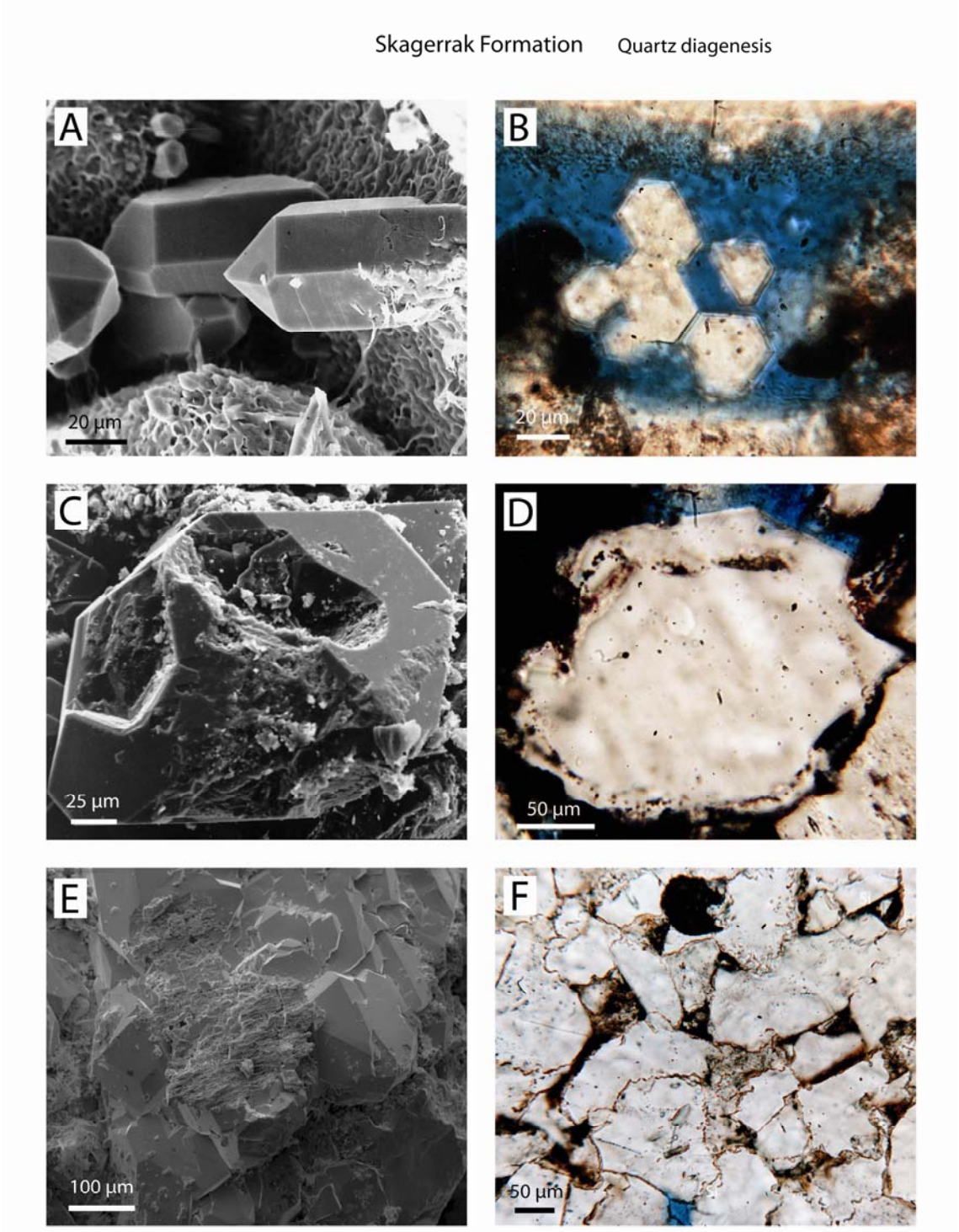

Figure. 6.9. *Quartz diagenesis in the Skagerrak Formation. A. Prismatic quartz outgrowths after thick clay coating, Thisted-2, 3162.29 m, scanning electron micrograph, B. Prismatic authigenic quartz in pore space, Thisted-2, 2919.33, C. Quartz overgrowths after iron-oxide/hydroxide coatings, Gassum-1, 2508.91 m, scanning electron micrograph, D. Quartz overgrowths after iron-oxide/hydroxide coatings Gassum-1, 2524.75 m, E. Quartz overgrowths enclosing partly dissolved feldspar, Vedsted-1, 2065.00 m, scanning electron micrograph, F. Pressure solution and sutured grain contacts between quartz grains, Gassum-1, 3122.48 m.*

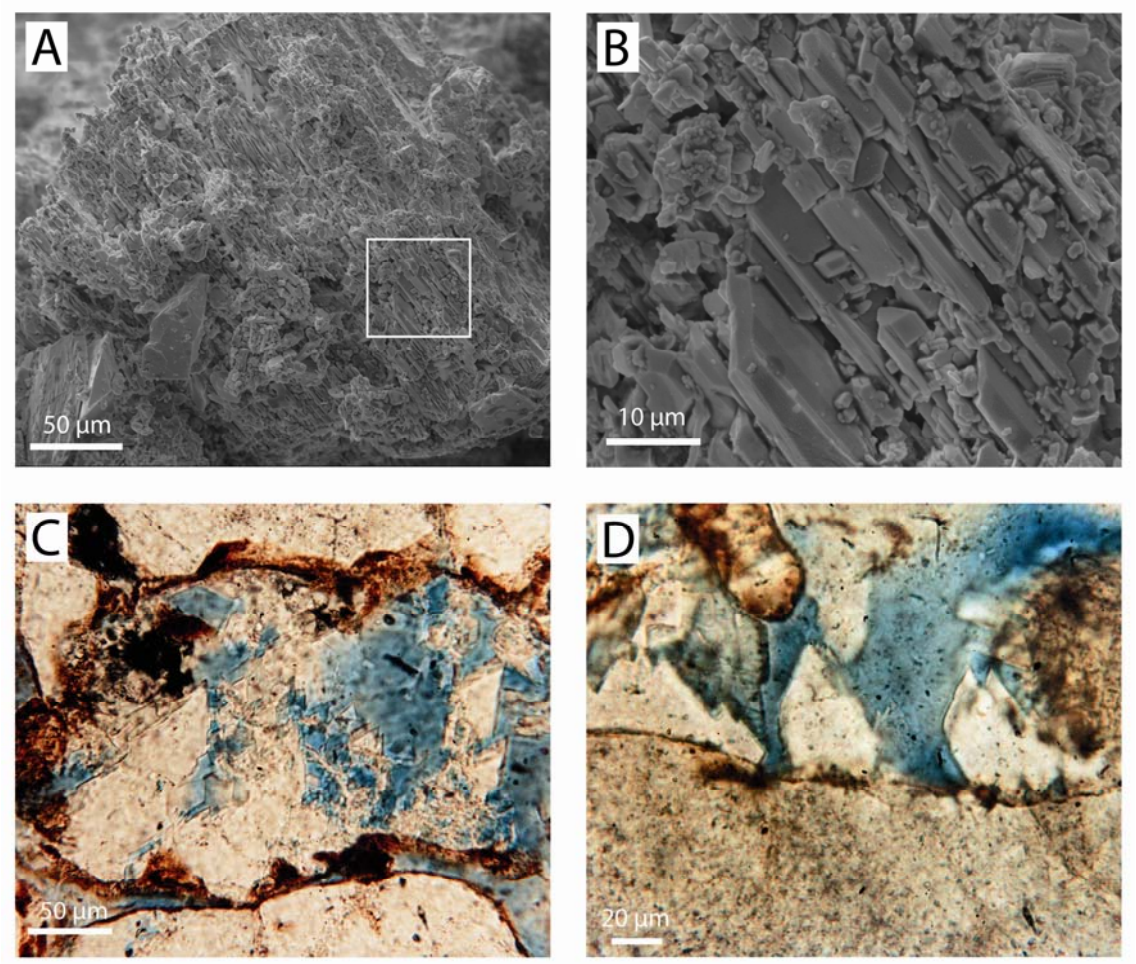

Figure. 6.10. *Feldspar alteration and authigenesis in the Skagerrak Formation. A. Partly dissolved detrital plagioclase with authigenic albite precipitations, Vedsted-1, 2064.94 m, scanning electron micrograph. B. Close up of A. C. Dissolution of feldspar (the iron-oxide/hydroxide coating marks to original size of the grain) and precipitation of feldspar (K-feldspar?), Thisted-2, 2764.62 m. D. Limited feldspar overgrowth formed after iron-oxide/hydroxide coating, Thisted-2, 2764.62 m.*

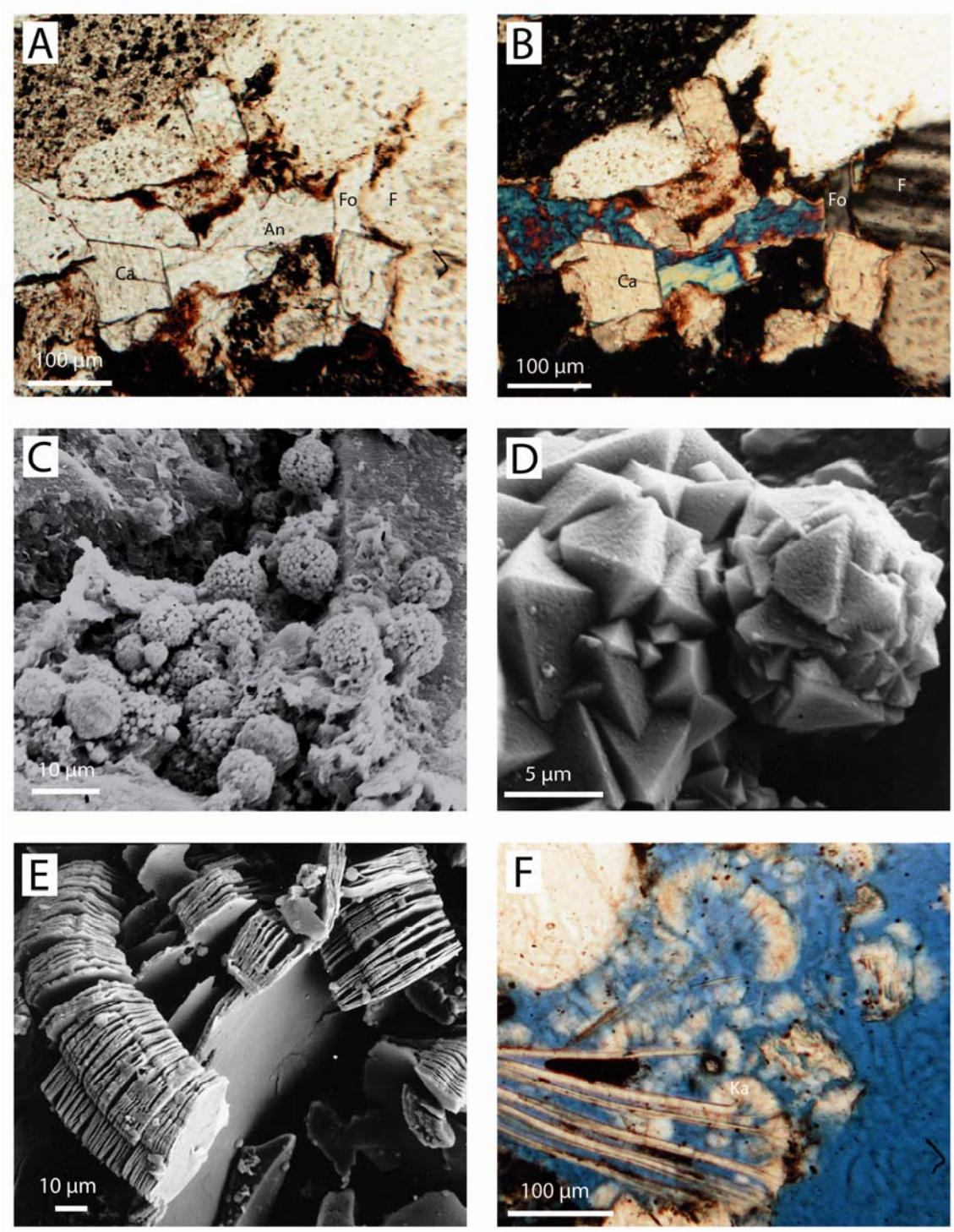

Figure. 6.11. *Minor authigenic phases in the Skagerrak Formation. A. Anhydrite (An) pore filling cement after carbonate cement (Ca) and feldspar overgrowth (Fo) on detrital feldspar (F), Thisted-2, 2763.04 m. B. As A, crossed nicols. C. Framboids of pyrite in reduction spot, Skagen-2, 562.00 m, scanning electron micrograph. D. Recrystallised framboids of pyrite in reduction spot, Gassum-1, 2153.73 m, scanning electron micrograph. E. Vermicular kaolinite, Frederikshavn-1, 1158.11 m, scanning electron micrograph. F. Kaolinite precipitated between the cleavage planes of muscovite, Sæby-1, 1613.25 m.*

6.6.1.3 Mineralogical changes with burial depth

The chronological order of these authigenic phases is shown in the paragenetic sequence of the Skagerrak Formation (Fig. 6.12).

Shortly after deposition of the Skagerrak Formation mineral alterations begin, such as dissolution of iron-magnesium silicates and leucoxene replacement of Fe-Ti oxides, which liberates iron. Due to the prevailing oxidising conditions in the interstitial water, a consequence of the arid to semi-arid climate during deposition of the Skagerrak Formation (Bertelsen 1980), direct precipitation of iron-oxides/hydroxides is promoted (Walker 1976; Durrance et al., 1978; Ixer et al., 1979, Weibel and Grobety, 1999). Direct precipitation of goethite occurs at shallow depths, whereas pseudomorphous transformation of goethite needles into hematite occurs in the deeper parts of the Skagerrak Formation (Weibel 1999; Weibel and Grobety 1999). Red coatings continued to precipitate into the early mesogenetic regime, as they can be observed between authigenic phases, such as mesogenetic quartz, dolomite and clays (Weibel 1998). Authigenic hematite is also recognised as overgrowths and replacement of other minerals.

The fact that the red pigments in most Mesozoic red sediments consist of hematite, whereas ferrihydrite and goethite are more common in younger sediments, has lead several authors (Van Houten 1961, Walker 1967, Schluger and Roberson 1975, Turner 1980) to the assumption that ferrihydrite and goethite ages into hematite. Though the Skagerrak Formation spans over approximately 30 Ma, it is all of Triassic age. Thus the transformation of goethite into hematite seems mainly to be temperature dependent (Weibel 1999, Weibel and Grobety, 1999).

Smectite is the dominant clay mineral of infiltration clays and ‘rip-up’ clasts from the shallow-buried part of the Skagerrak Formation. The honeycomb texture of illitic phases indicates transformation of smectite into mixed-layer illite/smectite and finally illite (Figs 6.8C & D; Weibel 1999). Transformation of smectite into random mixed-layer smectite-illite has occurred in the part of Skagerrak Formation exposed to estimated burial temperatures of 47–68°C (Weibel 1999). This is consistent with the findings of Sŕodoń (1984), who describes the transformation of smectite layers into illite layers in mixed-layer smectite-illite to begin at temperatures ~ 50°C, though the reaction rate may also depend on smectite chemistry and K-activity in the pore fluids (Chang et al. 1986; Ramseyer and Boles 1986). Ordered mixed-layer illite/smectite occurs in deep wells with an estimated burial temperature of > 74°C (Weibel 1999). Other investigations (Perry and Hower, 1970; Chang et al. 1986; Pearson and Small 1988; Pollastro 1993) suggest higher temperatures in the range of 90–125°C before ordering of mixed-layer illite/smectite takes place. This variation in temperatures may be a result of relatively high K-activity in the pore fluids possibly caused by K-rich brines from the underlying Zechstein evaporates. Authigenic illite, recognised by its fibrous appearance (Fig. 5.12C), occurs in samples exposed to maximum burial temperatures > 105°C (Weibel 1999).

Smectite transformation into random mixed-layer smectite/chlorite occurs at 58°C estimated minimum burial temperature, and into ordered mixed-layer chlorite/smectite (corrensite) at > 105°C in the Skagerrak Formation. Ordering of mixed-layer smectite/chlorite has been observed to take place at 60°C in sandstones and 70°C in shales (Chang et al. 1986)

whereas corrensite forms at temperatures > 100°C in mudrocks (Hillier 1993). Direct precipitation of chlorite may have been favoured by the liberated elements from the transformation of smectite into illite (see Burley 1984).

Kaolin is abundant in shallow wells where it is associated with alteration of muscovite and feldspars, but decreases in abundance with increased burial depth (Weibel 1999). A vermicular morphology is common in samples from shallow wells, whereas blocky crystal growth between the vermicular flakes occurs at increased burial depth; and at maximum burial depth kaolin has a blocky morphology. Formation of kaolin due to meteoric water flushing (Bjørlykke and Aagaard, 1992) can only be considered a possibility under the humid condition during deposition of the overlying Gassum Formation and in case of very slow burial. Recycling of the Skagerrak Formation during deposition of the Gassum Formation is another possible explanation. Replacement of vermicular kaolin with a more blocky morphology (probably dickite) begins at estimated burial temperatures < 75°C (Weibel 1999). Investigations by Ehrenberg et al. (1993) show that transformation of vermicular kaolinite to blocky dickite occurs at ~ 120°C, however this may reflect the completion temperature, whereas the 75°C reflects the onset of the transformation, which seems to be a gradual process, as described Beaufort et al. (1998).

Two or more episodes of quartz precipitation occur. The first formation of prismatic authigenic quartz outgrowths, rather than quartz overgrowths, probably reflects a limited silica concentration in the pore fluid as well as limited access to detrital quartz surfaces due to thick clay rims or red coatings. Thus authigenic clay rims and iron-oxide/hydroxide coatings inhibit quartz diagenesis, as previously described for chlorite (Ehrenberg, 1993) and illite (Storvold et al. 2002). Macroquartz is more abundant in the deeper wells (Mors-1, Thisted-2 and Gassum-1) probably reflecting increased liberation of silica from feldspar alteration, and from pressure solution in the samples with the lowest content of ductile fragments (mica, rock fragments) and authigenic clays. The sandstones in the Gassum-1 well generally have lower contents of ductile fragments and thinner red coatings, consequently fractural healing, pressure solution and thick quartz coatings are more abundant here. The quartz diagenesis is thus depending on the detrital composition and the previous diagenetic evolution as well as the burial depth.

The micritic carbonate cement is formed early diagenetic, as it exhibit displacive growth textures (between cleavage planes of expanded mica) and it forms rims of radiating crystals on detrital grains and is frame-work supporting. The carbonate thus exhibits several of the Alpha calcrete fabric elements described by Wright (1990). Calcrete is only found in relatively shallow parts of the Skagerrak Formation from the northeasternmost wells (Frederikshavn-1, -2, Skagen-2 and Flyvbjerg-1). Calcrete and dolocrete are common in the arid to semi-arid Triassic non-marine sediments (i.e. Mader 1983; Burley 1984). Calcrete was either not formed in the deeper part of the Skagerrak Formation or recrystallisation and growth of larger crystals at the expense of smaller may have taken place at deeper burial depths. Formation of calcrete can only take place if there is discontinued sedimentation and time enough for pedogenetic processes to be active. In marginal areas, dominated by ephemeral streams, mature calcretes developed, whereas in the distal, sandy braided stream environments with more continuous sedimentation poikilotopic and nodular cements formed instead (Burley 1984). Alluvial fan deposits characterise the Skagerrak Formation in

the proximal northeasternmost part of the Norwegian-Danish Basin, whereas braided stream deposits are more dominating towards the distal southwesternmost part of the basin. Lack of pedogenetic developments in the southwesternmost part may therefore best explain the observed lateral differences in the Skagerrak Formation.

Poikilotopic carbonate cement probably forms later. The pore filling carbonate often has a radiating extinction thereby resembling saddle dolomite. Saddle dolomite forms at temperatures higher than 60-80°C and lower than 90-160°C under the influence of pore fluids of higher salinity than seawater (Spötl and Pitman, 2009). Occasionally the poikilotopic carbonate cement is calcite or ankerite cement. Ankerite can form at temperatures similar to dolomite, i.e. 110-165°C in the Triassic Sherwood Sandstone Group, U.K. (Schmid et al. 2004).

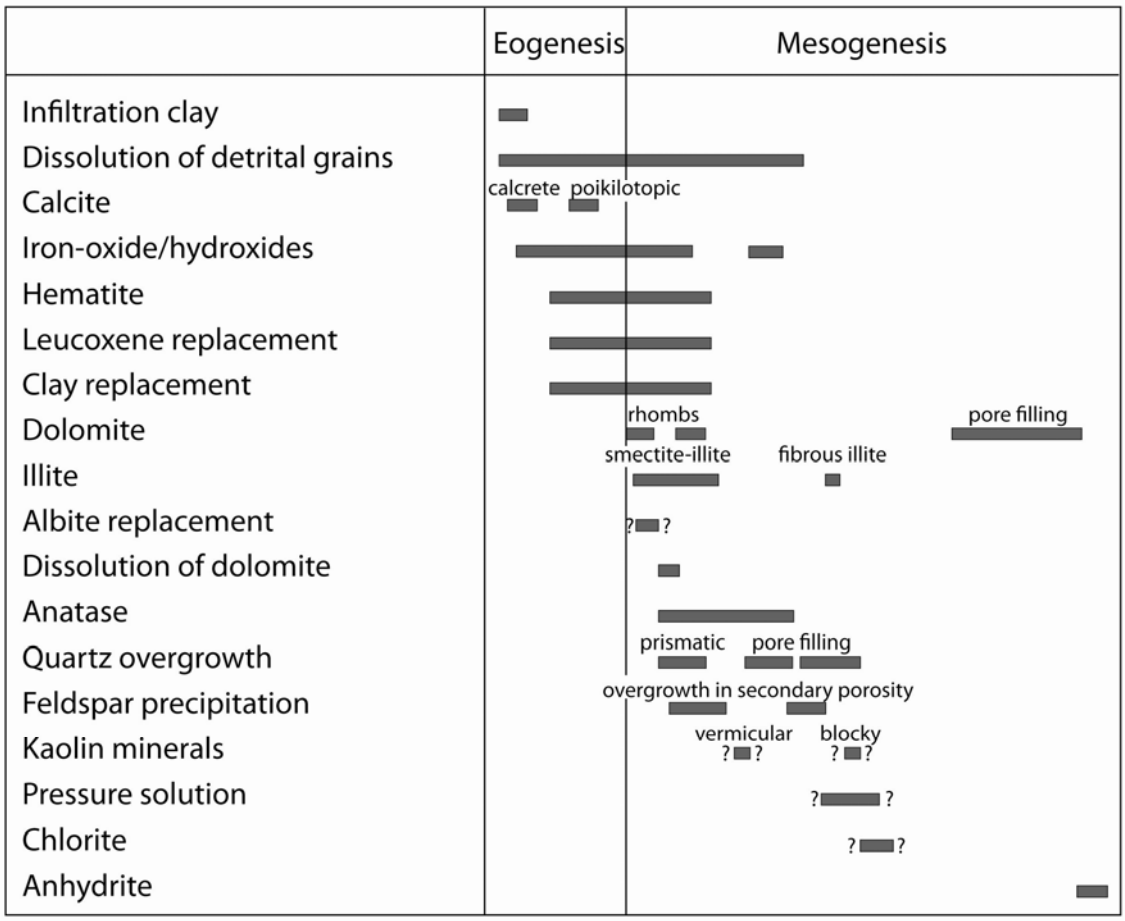

Figure. 6.12. *Diagenetic sequence for the Skagerrak Formation, simplified after Weibel (1998).*

6.6.2 Gassum Formation

The Upper Triassic – Lower Jurassic shallow marine and paralic sandstones of the Gassum Formation) are present in most of Denmark (Fig. 1; Nielsen 2003). It occurs with thicknesses up to 400 m (Mathiesen et al. 2009) and present day burial depths varying from 550–3350 m.

6.6.2.1 Detrital composition

The Gassum Formation comprises fine to medium-grained, well-sorted sand with occasional oversize clay clasts between otherwise subangular to subrounded detrital grains. Rare bimodal sorting of the sand can be found in samples from the Vedsted-1 well. The sandstones of the Gassum Formation are mainly subarkoses and arkoses (Figs 6.1 & 6.13; Friis 1987) according to the classification by McBride (1963). Monocrystalline quartz, with subordinate polycrystalline quartz, dominates the framework grains. The feldspar abundance varies across the Danish Subbasin and feldspar is relatively more abundant in the northwestern part than in the eastern part. K-feldspar is generally the dominating feldspar in the northern part of Denmark, whereas albite is characteristic in the eastern part of Denmark, i.e. in the Stenlille wells (Fig. 6.13; Appendix 2). Ca-rich plagioclase has not been identified. Alteration of feldspar grains includes partly dissolution, seritization, replacement by kaolin or carbonate and incipient albitisation in the deepest buried sandstones. Some oversize pores with clay-lining mould ("ghost rim") are inferred to originate from completely dissolved feldspar grains. Rock fragments are generally rare; the only exception being the very coarse-grained sandstones. Plutonic, micaceous metamorphic and sedimentary rock fragments are equally abundant. Mica is present in all samples and is commonly abundant in the fine-grained samples. Mica is dominated by muscovite with subordinate biotite and chlorite. Mica shows varying degree of alteration from expansion along cleavage planes caused by precipitation of authigenic minerals (e.g. siderite) to compaction along stylolites in the deepest wells. Organic matter occurs in most samples. Accessory minerals include tourmaline, rutile, zircon and opaque heavy minerals, the latter being dominated by ilmenite intensively altered to leucoxene.

6.6.2.2 Authigenic phases

The porosity reduction is mainly due to compaction in sandstones of burial depths down to 1500 m (Friis, 1987). The exception is occasionally extensive siderite precipitation in mica rich samples. At increasing burial depth quartz diagenesis, carbonate precipitation and feldspar alteration becomes important porosity influencing processes, whereas pyrite only locally may be important as pore filling cement (Figs 6.14, 6.15, 6.16, 6.17, 6.18, 6.19 & 6.20).

Siderite is the first authigenic phase and appears as occasional displacive spherulites and numerous rhombs (up to 15 µm large) in the open pore space or between cleavage planes of mica (preferentially biotite or chlorite) resulting in expansion of the micas original size (Fig. 6.15A, B & D). The last type of siderite has only been identified in shallow buried sandstones, where it may be a porosity reducing factor.

Pyrite is ubiquitous in all samples and may occur in three phases, first framboids, followed by euhedral crystals and presumably a tertiary pore filling cement (Fig. 6.16). Pyrite is

commonly associated with organic matter or altered Fe-bearing minerals e.g. ilmenite replaced by leucoxene. Pyrite framboids precipitate early diagenetic more or less simultaneously with the siderite rhombs, as pyrite framboids may occur enclosed in the siderite rhombs (Fig. 6.16C) or nucleated on them. Euhedral pyrite crystals enclose pyrite framboids and kaolin booklets (Figs 6.17D & E). Pore filling pyrite commonly encloses partly dissolved K-feldspar grains. Marcasite has been observed in a few samples, where it occurs as clusters of crystals and, locally, as pore filling cement and, occasionally, partly inside pyrite concretions.

Kaolin booklets typically fill the primary pores commonly adjacent to partly dissolved feldspar grains and more rarely within the intragranular porosity, i.e. the secondary porosity of feldspar and mica. Kaolin in oversize pores is inferred to represent replacement of detrital feldspar grains (Figs 6.17A, E & F). Extremely fine kaolin crystals form between the cleavage planes of mica, in particular muscovite, leading to expansion of its original size. Fine kaolin crystals may also occur in secondary porosity possibly as replacement of mica. Kaolin booklets may be enclosed in euhedral pyrite crystals, authigenic quartz and ankerite.

Authigenic quartz, as syntaxial overgrowths, is common in most samples (Figs 6.18 & 6.19). The amount of authigenic quartz may be underestimated, where there are no distinct boundary between the overgrowths and the detrital grain, i.e. poorly developed dust lines. However, the size of individual quartz overgrowths may be up to 100 µm on monocrystalline quartz grains (Friis 1987). Authigenic quartz encloses authigenic anatase, pyrite and clay minerals as chlorite, illite, kaolin (Figs 6.17, 6.18F, 6.19A & 6.20F), whereas barite and ankerite enclose authigenic quartz.

The carbonates (mainly ankerite; Appendix 1) can be pervasive in intensely cemented samples or appearing as rhombohedrons (typically calcite and siderite) in sporadic cemented parts (Figs 5.15C, D, E & F). Pore filling carbonate can be corrosive or replasive towards all other minerals. Siderite rhombehedrons, on the other hand, tend to have displasive growth and may occasionally in shallow buried sandstones form intensely cemented parts of the sediments. Calcite and siderite dominate in the Stenlille-18 well, whereas ankerite dominates some samples in the Vedsted-1 well. XRD analysis showed that dolomite is the dominating carbonate cement in the Aars-1 well (Krabbe & Nielsen 1984; Larsen 1986). However, microprobe analysis showed that the actual composition of the carbonate resembles ankerite more than dolomite (Friis 1987). Ankerite cement commonly encloses remnants of detrital albite. Siderite is abundant in the fine-grained facies (mudstones and the heterolithic sandy/silty-mudstones), whereas ankerite dominates the more coarse-grained facies with coarse to fine-grained sandstones (Friis 1987).

Volumetrically minor authigenic phases in the deep wells include illite, chlorite, pyrite, albite and K-feldspar. Chlorite is important, in specific samples, as pore lining and pore filling cement. Chlorite abundance is related to depositional environment in such a way that chlorite forms very thick coatings in offshore sandstones, but thinner coatings in shoreface and estuarine environments, and chloritic clay coatings have even been observed in fluvial deposits (Fig. 6.17F). Chlorite typically constitutes less than 2 % of the clay minerals (Schmidt 1985; Friis 1987).

Authigenic albite occurs as overgrowths and as crystals growing on remnants of partly dissolved detrital feldspar grains. Though authigenic albite is common in samples of intermediate or deep burial (i.e. from the Gassum-1 and deeper wells) it is of minor volumetric importance. Authigenic K-feldspar besides authigenic albite on detrital feldspar grains were described in samples with burial depths of more than 1500 m by Friis (1987).

Rare pore filling barite encloses authigenic quartz (Fig. 6.21A) and is enclosed in ankerite. Anatase occurs as replacement of detrital Fe-Ti oxides and as single crystals formed in the open pore space (Figs 6.21A, E & F). Rare apatite overgrowths occur on detrital apatite and rare monazite encloses kaolin and possibly authigenic albite (Fig 6.21C). Authigenic anatase, pyrite and crandallite group minerals occur in association with stylolites (Figs 6.21D & F).

Meniscus forming clays containing tiny barite and fluorite crystals, found in the Stenlille-18 and Stenlille-12 wells, are considered to be infiltrated drilling mud. The smectitic clays identified by XRD are probably drilling mud and consequently not part of the Gassum Formation.

6.6.2.3 Porosity and permeability

Primary porosities (from point counting) up to 34 % have been registered in the shallowest sandstones (in the Thisted-3 well, 1180 m). With increasing burial the average porosity decreases and the contribution from secondary porosity increases (up to 5 % in the Aars-1 well out of a total porosity of 10 %).

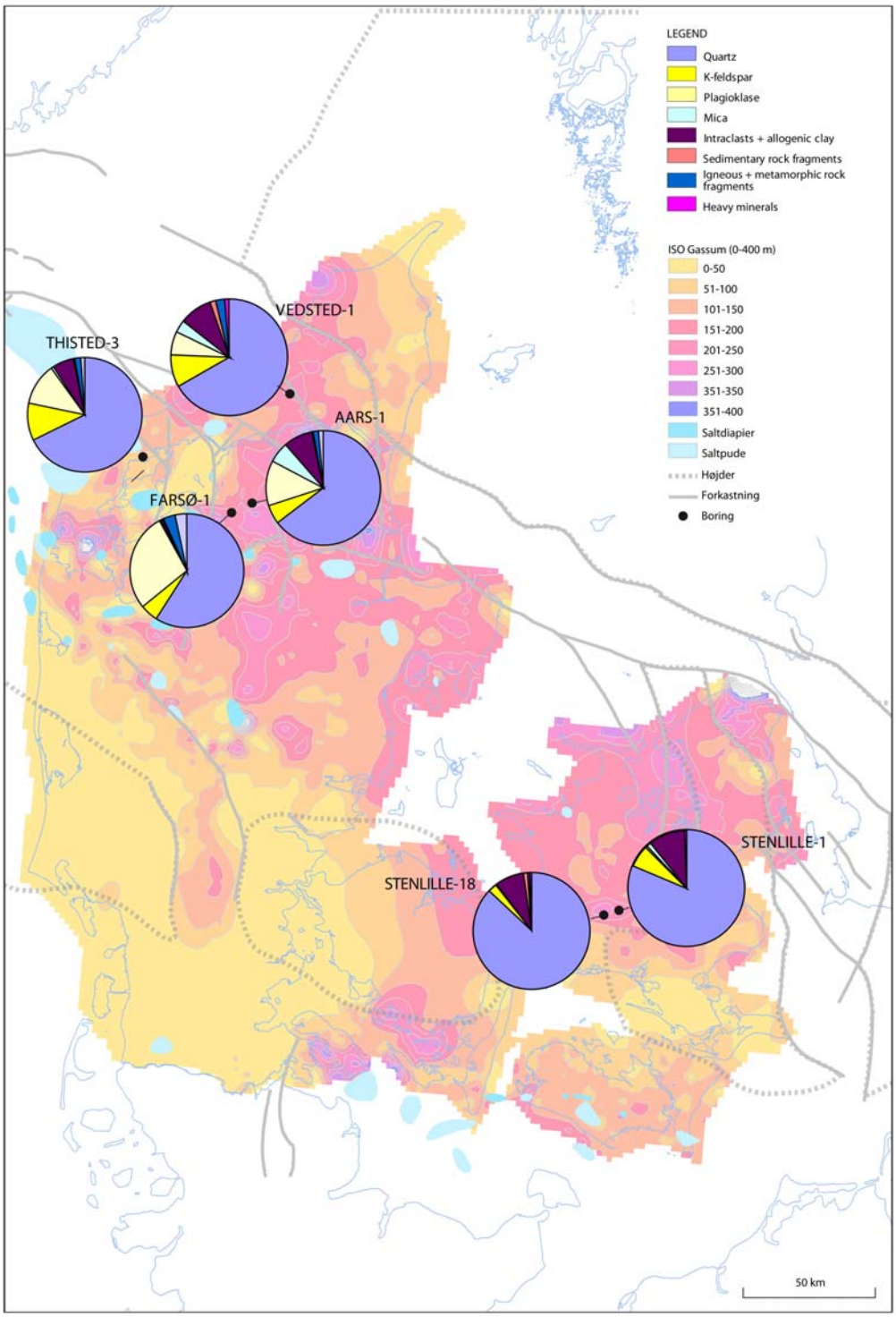

Figure. 6.13. *Average detrital composition of the Gassum Formation shown as pie diagrams for each analysed well on isopach map of the Gassum Formation (modified after Mathiesen et al. 2009).*

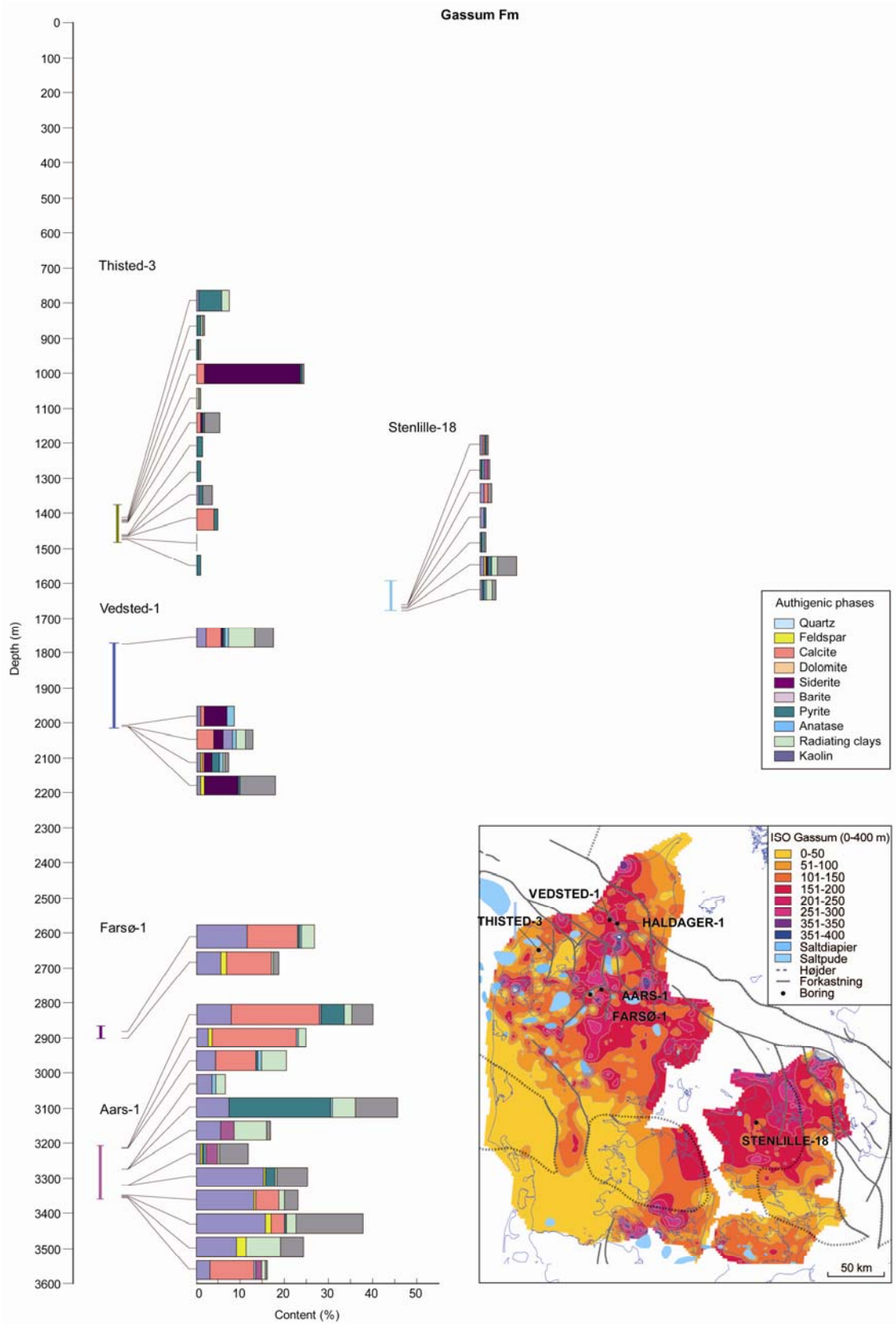

Figure. 6.14. *Authigenic phases, quantified by point counting, in the Gassum Formation for different wells and consequently different burial depths*.

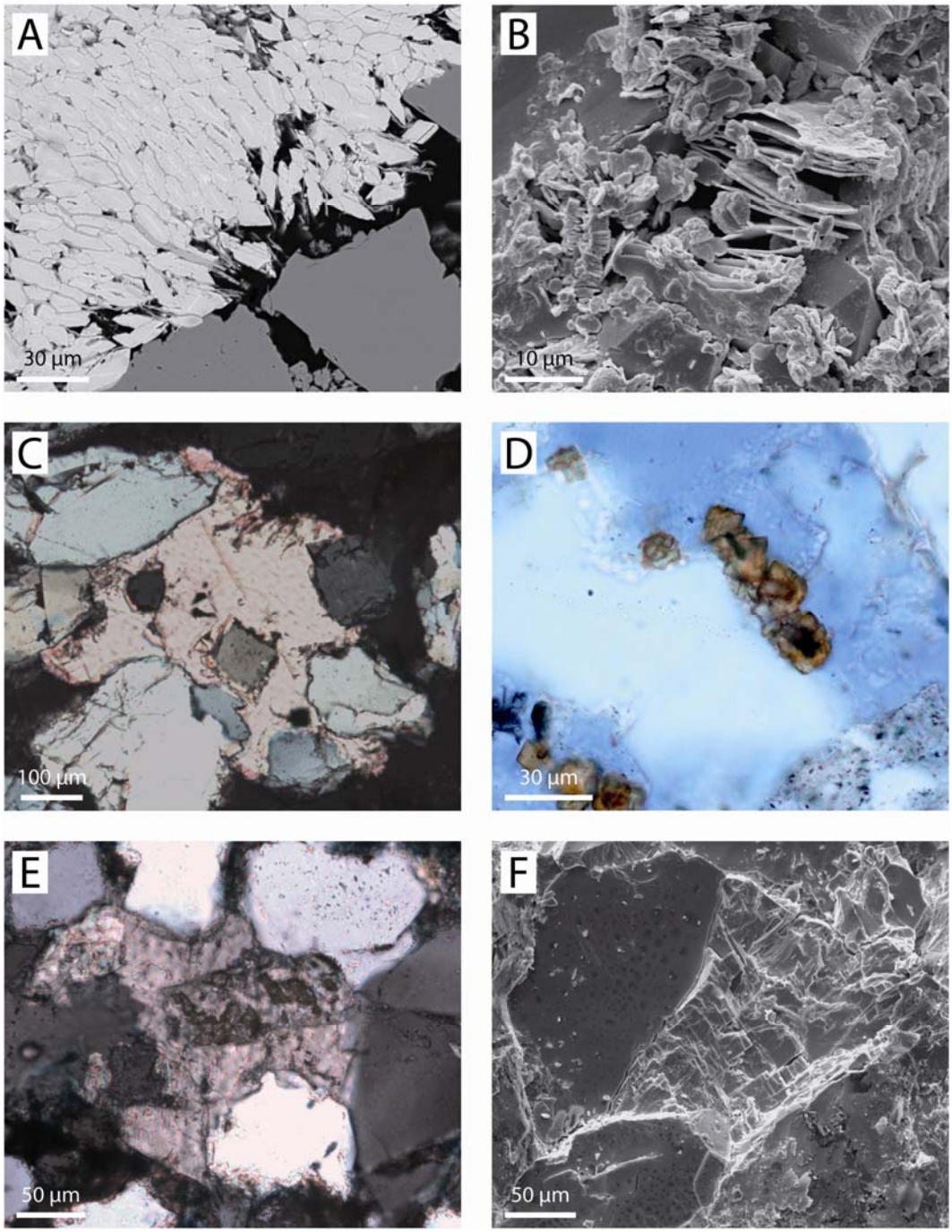

Figure. 6.15. *Carbonate diagenesis in the Gassum Formation. A. Siderite rhombs growing between the cleavage planes in mica, thereby expanding its size several times, Gassum-1, 1540.16 m, backscatter electron micrograph. B. Siderite growing between the cleavage planes in mica, Vedsted-1, 2010.12 m, scanning electron micrograph. C. Pore filling carbonate (calcite?) cement, Thisted-3, 1225.62 m, crossed nicols. D. Siderite cores with ankerite rims, Vedsted-1, 2009.69 m. E. Pore filling ankerite cement growing around partly dissolved K-feldspar (stained), Aars-1, 3215.70 m, crossed nicols. F. Pore filling ankerite cement around quartz grains, Aars-1, 3208.75 m, scanning electron micrograph.*

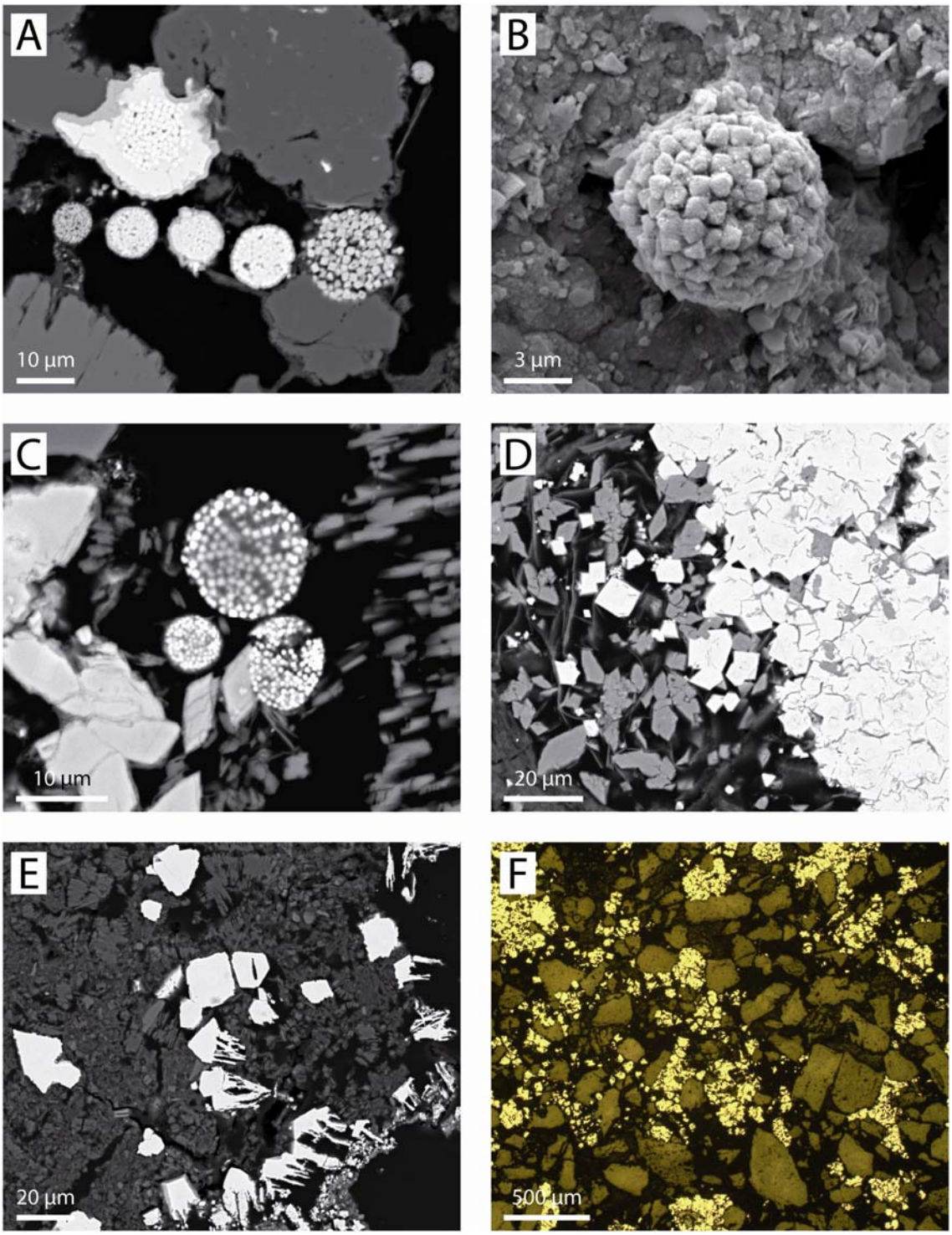

Figure. 6.16. *Pyrite diagenesis in the Gassum Formation. A. Pyrite framboids in a row and one pyrite framboid enclosed in euhedral pyrite, Frederikshavn-2, 925.61 m, backscatter electron micrograph. B. Pyrite framboid, Stenlille-18, 1662.47 m, scanning electron micrograph. C. Pyrite framboids, some enclosed in siderite rhombs, Gassum-1, 1540.16 m, backscatter electron micrograph. D. Euhedral and concretionary pyrite enclosing siderite rhombs, Frederikshavn-2, 885.85 m, backscatter electron micrograph. E. Euhedral pyrite enclosing kaolin crystals, Stenlille-18, 1662.07, backscatter electron micrograph. F. Pore filling pyrite, Thisted-3, 1211.25 m, reflected light*.

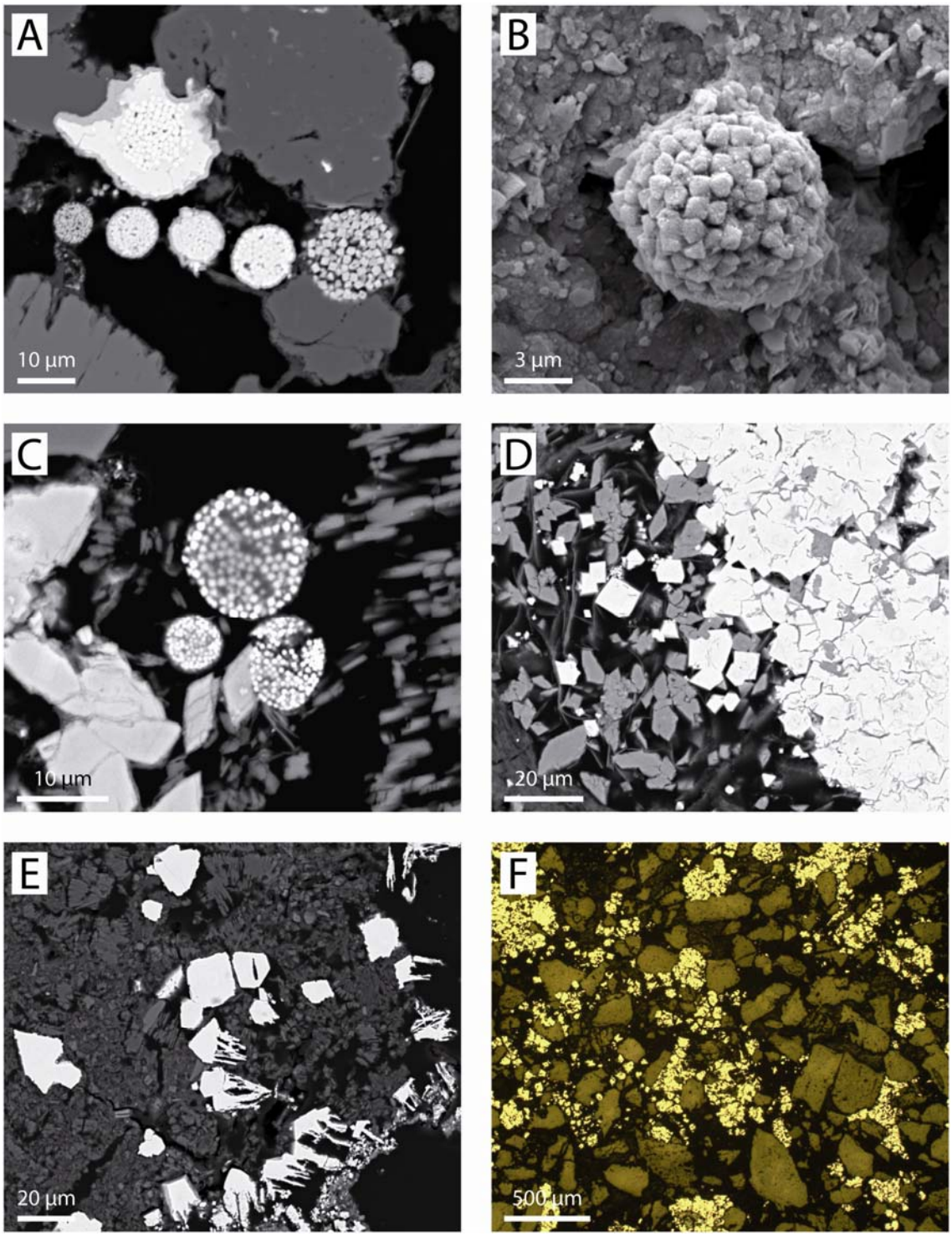

Figure. 6.17. *Clay minerals in the Gassum Formation. A. Kaolin and pyrite filling an oversized pore, Stenlille-18, 1662.45 m. B. Blocky dickite growing between vermicular kaolinite, Vedsted-1, 2010.12 m, scanning electron micrograph. C. Illite rims partly captured in authigenic quartz, Farsø-1, 2880.11, backscatter electron micrograph. D. Kaolin enclosed in authigenic quartz, Aars-1, 3208.72 m, backscatter electron micrograph. E. Moldic pores marked by illite rims and partly filled by kaolin minerals, Aars-1, 3321.52 m, crossed nicols. F. Chlorite rim around completely kaolin replaced grain, Aars-1, 3208.72 m, backscatter electron micrograph*.

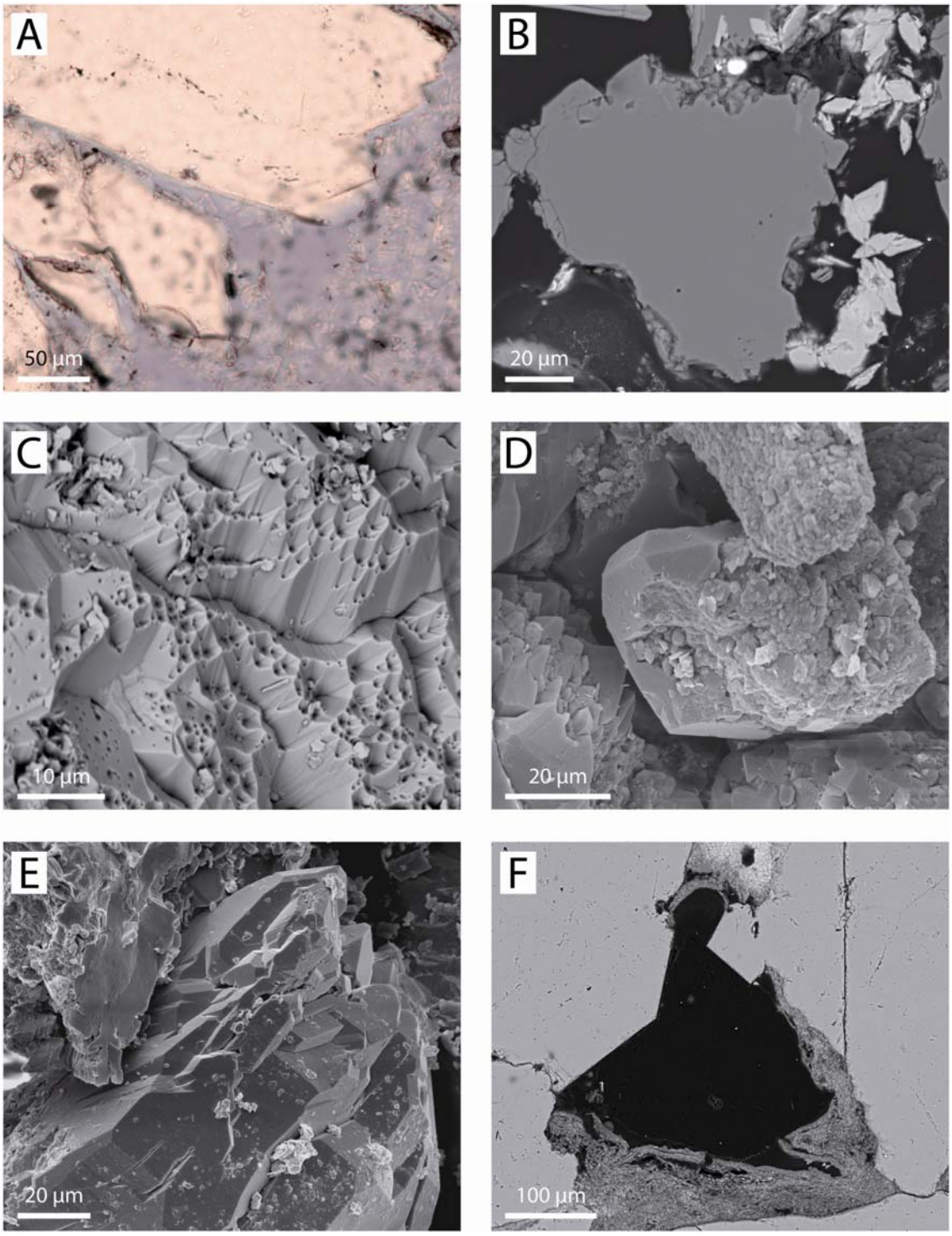

Figure 6.18. *Quartz diagenesis in the Gassum Formation. A. Small quartz overgrowth, Thisted-3, 1211.03 m. B. Small quartz overgrowths, Gassum-1, 1540.16 m, backscatter electron micrograph. C. Authigenic quartz in shape of 'quartz mountains', Thisted-3, 1225.62 m, scanning electron micrograph. D. Limited quartz overgrowths on detrital quartz, Thisted-3, 1173.68 m, scanning electron micrograph. E. Macroquartz completely covering the detrital quartz grain, Vedsted-1, 2010.12 m, scanning electron micrograph. F. Quartz overgrowths inhibited where thick chlorite coatings are present, Farsø-1, 2869.85 m, back-scatter electron micrograph.*

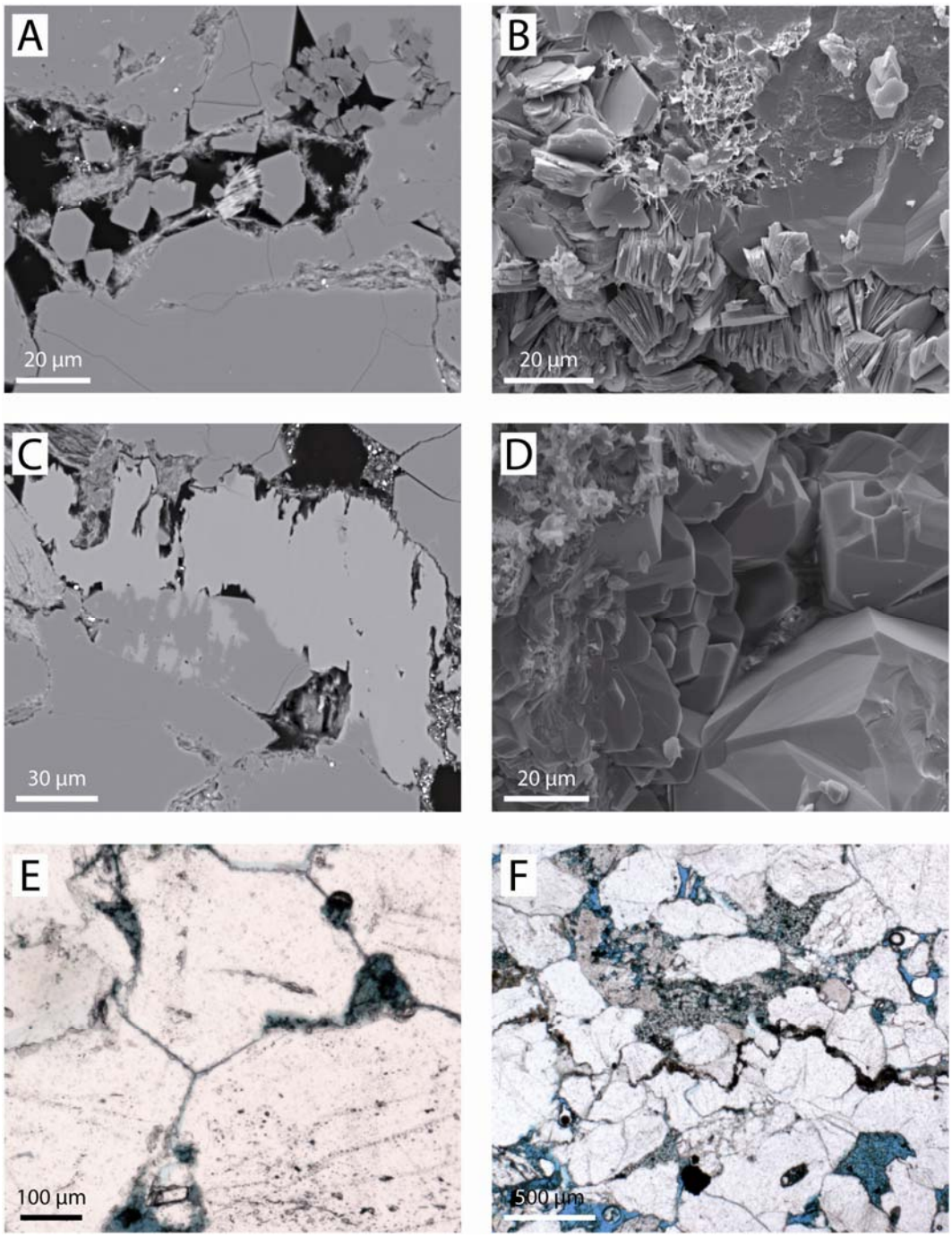

Figure 6.19. *Quartz diagenesis in the Gassum Formation. A. Authigenic quartz enclosing kaolin minerals and chlorite, which locally seem to inhibit the authigenic quartz growth, Aars-1, 3208.72 m, backscatter electron micrograph. B. Authigenic quartz enclosing illite and kaolin minerals, Aars-1, 3275.35 m, scanning electron micrograph. C. Authigenic quartz growing into secondary porosity after K-feldspar dissolution, Aars-1, 3208.72 m, backscatter electron micrograph. D. Macroquartz on all detrital quartz grains, Aars-1, 3208.40 m, scanning electron micrograph. E. Macroquartz completely closing the primary porosity, Aars-1, 3319.65 m. F. Stylolite marked by concentration of bending mica, Aars-1, 3277.45 m.*

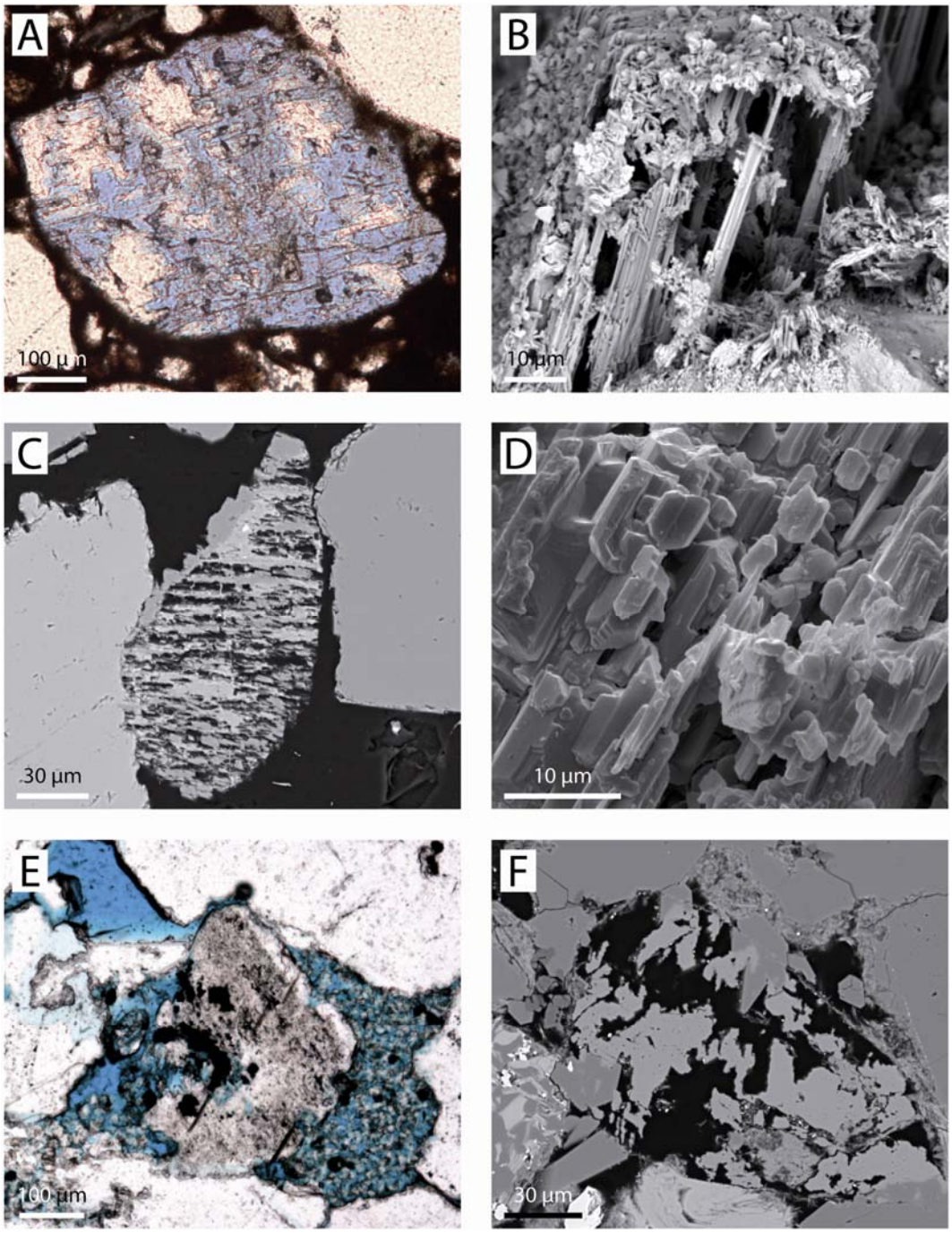

Figure 6.20. *Feldspar alteration and authigenesis in the Gassum Formation. A. Feldspar dissolution after pore filling siderite formation, Thisted-3, 1183.95 m. B. Intense feldspar dissolution, Thisted-3, 1233.38 m, scanning electron micrograph. C. Albite overgrowths on perthite remnants, where the intergrown K-feldspar is partly dissolved, Gassum-1, 1640.03 m, backscatter electron micrograph. D. Authigenic albite precipitated on partly dissolved feldspar, Vedsted-1, 2010.03 m, scanning electron micrograph. E. Feldspar overgrowth on partly altered feldspar grain, Aars-1, 3277.45 m. F. Secondary porosity after partly dissolved K-feldspar which original outline is marked by a chloritic rim. Authigenic quartz grows partly into the secondary porosity, Aars-1, 3208.72 m, backscatter electron micrograph.*

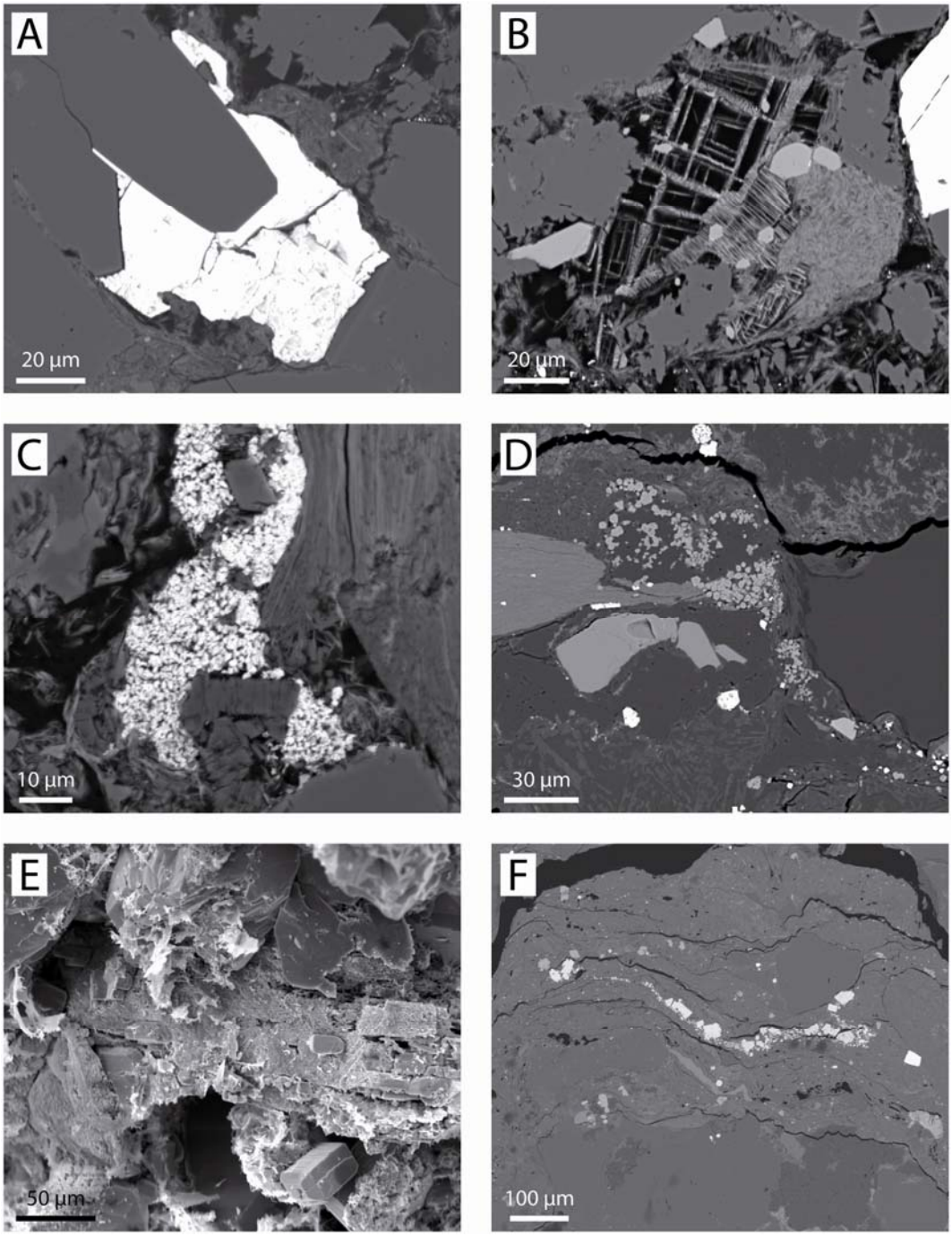

Figure 6.21. *Accessory authigenic phases in the Gassum Formation. A. Pore filling barite formed after authigenic quartz, illitic and chloritic rims, Aars-1, 3208.72 m, backscatter electron micrograph. B. Apatite precipitating after leucoxene replacement of Fe-Ti oxide, Aars-1, 3208.72 m, backscatter electron micrograph. C. Authigenic monazite enclosing kaolin and authigenic? albite, Vedsted-1, 2007.77 m, backscatter electron micrograph. D. Crandalite group minerals precipitated along stylolite zone, Aars-1, 3352.54 m, backscatter electron micrograph. E. Anatase on partly dissolved leucoxene, Aars-1, 3353.05 m, scanning electron micrograph. F. Pyrite and anatase precipitated in the stylolite zone, Aars-1, 3352.54 m, backscatter electron micrograph.*

6.6.2.4 Mineralogical changes with burial depth

The chronological order of the authigenic phases is shown in the paragenetic sequence of the Gassum Formation (Fig. 5.26).

In a vegetated humid environment, as during deposition of the Gassum Formation, the organic matter plays an important role in the eogenesis. Organic matter creates reducing conditions, under which iron is highly solvable, and it serves as an energy sources for microbes. Sulphate reducing bacteria promote the precipitation of pyrite framboids, which therefore commonly form near organic matter. Iron-oxides and -hydroxides (ferrihydrite, lepidocrosite, goethite and hematite) are unstable under the reducing conditions and are considered possible sources for pyrite framboids (Canfield et al. 1992). Textural evidence suggests that altered Fe-Ti oxides acts as an iron source for euhedral pyrite in the Gassum Formation during increased burial and probably only where iron sources are limited (possibly in deltaic or fluvial deposits). The pyrite formation slows down during burial, as less reactive organic matter is available and due to more slowly liberation of iron from detrital iron-rich minerals (Canfield et al. 1992). Concretionary pyrite precipitation in the Aars-1 well seems to have formed beneath a marine (transgressive) erosional boundary. The level containing pyrite concretions have probably been situated in the sulphate reducing regime for a longer period than comparative sediments. Ferric iron, which is highly solvable, is likely to migrate to such places of sulphate reduction (Berner 1969).

The displasive growth of siderite (spherulite and precipitation in between cleavage planes of mica; Fig. 5.19A) and its interaction with pyrite framboids emphasise its early diagenetic formation. Alternating pyrite and siderite precipitation occurs early diagenetic in the Gassum Formation and can be related to small changes in pH and Eh conditions or variations in CO_3^{2-} or H_2S saturation (Coleman & Raiswell 1981). Sulphate reducing bacteria can under specific conditions (in a consortium with microbial fermenters) reduce Fe^{3+} using hydrogen, formed during fermentation, instead of sulphate (Coleman 1993). During bacterial sulphate reduction, simple organic molecules (CH_2O) are oxidised to HCO^{3-}, which can precipitate as carbonates and siderite if the Fe-content is not limited. In this way, the same sulphate reducing bacteria may promote formation of pyrite or siderite depending on the associated microbial activity. Siderite is therefore not necessarily an indicator of methanogenic environments where little or no sulphate is present (as suggested by e.g. Thyne and Gwinn, 1994; Bailey et al., 1998) nor does alternating pyrite and siderite precipitation have to be explained by moving freshwater/seawater interface as a response to sea level changes (as suggested by Machemer and Hutcheon, 1988). Mica may have liberated iron during its alteration, or served as a protective site for the bacteria colony, which could explain the numerous siderite crystals that precipitate between the mica cleavage planes and result in expansion of mica to several times its original size.

The ankerite rims on the siderite cores in the Gassum Formation are clear evidence that with increased burial the Fe content of the pore fluids decreases and the carbonate cement becomes more Mg (and Ca) rich. This phenomenon is also known from fluvio-deltaic sediments from the Norwegian North Sea (Hammer et al. 2010) and from the Salam field (Egypt's Western Desert) (Rossi et al. 2001). A change from a brackish influenced pore water to more marine influenced pore water (for example by marine transgression of lagoonal sediments) could also lead to relatively increase of Mg, Mn and Ca in the siderite as

observed in spherulitic siderite in Holocene coastal deposits (Choi et al. 2003) and in siderite from fluvial-deltaic sediments under influence from marine waters (Rossi et al. 2001). The estimated temperatures (140-170°C) of ankerite formed at deep burial (c. 3500-4500 m) in Jurassic sandstone from Central North Sea (Hendry et al. 2000) seem to be rather high compared to the burial depth of sandstones containing ankerite cement in the Gassum Formation. The differences may come from a relatively longer period of ankerite precipitation in the Gassum Formation, though ankerite, similar to the Jurassic sandstone in the Central North Sea, is one of the last forming authigenic cements.

Preferential occurrence of chlorite in marine influenced sediments (thickest chlorite coating is observed in the offshore sandstones) suggests that chlorite formed early diagenetic by direct precipitation in the anoxic pore waters in an estuarine and marine environment (see Burley et al. 1985). Transformation of smectitic infiltration clays into chlorite, as the fluids evolve to become more Fe and Mg rich with increased burial (which could be related to elements liberated by smectite to illite transformations) is another possibility, which can explain chlorite in fluvial sandstones.

Variation in the feldspar composition between the northern and the eastern part of the Danish Subbasin (eastern part of the Norwegian-Danish Basin) is indicative of sediment source area differences. The sediment supply to the eastern part may have been dominated by high quartz contents from kaolinised basement for example in southern Sweden (Ahlberg et al. 2003), whereas the northern part may be characterised by a continued more northerly sediment source. Feldspar dissolution preferentially affects the plagioclase grains at shallow burial depth but also the K-feldspar grains at deeper burial depth. Variations in the degree of feldspar alteration within each sandstone sample are common in the Gassum Formation probably reflecting inherited chemical variations, crystallographic weaknesses etc. Secondary porosity, mainly the result of feldspar dissolution, may constitute up to 5 % of the total porosity of 11 % in the deepest buried sandstones from the Aars-1 well. However, in the deepest sandstones the intragranular porosity in feldspar grains is partly filled by authigenic phases (quartz or kaolin), including albite, which grows on the remnants of detrital feldspar (Figs 5.24D & F). This incipient albitisation process, where albite crystals grow along the cleavage planes in the parent K-feldspar grains with high intragranular porosity, occurs at 65-90°C in Jurassic-Lower Cretaceous sediments offshore Norway (Saigal et al. 1988). Whereas albitisation represented by blocky albite crystals and lack of any dissolution porosity in K-feldspar occurs at higher temperatures > 90°C (Saigal et al. 1988). Other investigations also point towards albitisations of both plagioclase and K-feldspar taking place at higher temperatures (120-160°C, Boles and Ramseyer 1988; 120-150°C, Baccar et al. 1993; 100-130°C, Mansurbeg et al. 2008). Different reactivity of feldspar grains to albitization can be caused by variation in amounts of grain surface areas in contact with pore fluid, degree of fracturing, chemical composition and structural state (Ramseyer et al. 1991). Carbonate probably formed as by-product of albitisation (Morad et al. 1990), which explains why ankerite cement is commonly associated with feldspar.

Kaolin typically precipitates close to altered feldspar grains, and over-size pores filled completely by kaolin probably represent completely altered feldspar grains. Flushing of meteoric water shortly after deposition is responsible for dissolution of feldspar grains and precipitation of kaolin (see Bjørlykke 1998). The fresh water is diluted on most ionic species

and therefore causes dissolution of the feldspar grains and other unstable grains, which leads to formation of kaolin. This process is likely to occur in the fluvial, lacustrine and deltaic environment, however not in the marine sediments.

The intensity of quartz diagenesis increases with burial depth, from being characterised by quartz mountains (see Weibel et al. 2010 for a detailed description) in shallow sandstones (for example in the Thisted-3 well, 1180 m; Fig. 5.22C), to large quartz overgrowths (macroquartz) in the deeper buried samples (for example the Farsø-1 well, 2900 m and the Aars-1 well, 3300 m; Figs 5.23 D & E) and follows the typical diagenetic trend of increasing authigenic quartz abundance with burial for marine influenced sandstones (Bjørlykke et al. 1986, Land & Fisher 1987, Ehrenberg 1990, Weibel et al. 2010). Pressure solution of quartz and sutured grain contacts are limited to deeper buried sediments (in the Gassum-1 and Aars-1 wells). Sutured quartz grain contacts (microstylolites) occur in the Jurassic Brent Group at depths greater than 2700 m and temperatures higher than c. 100°C (Harris 1992). Stylolites only occur in the fluvial deposits in the Aars-1 well at large burial depths of 3280 m (Fig. 5.23F). These sediments are characterised by only small amounts of ductile grains and limited amounts of authigenic clay coatings.

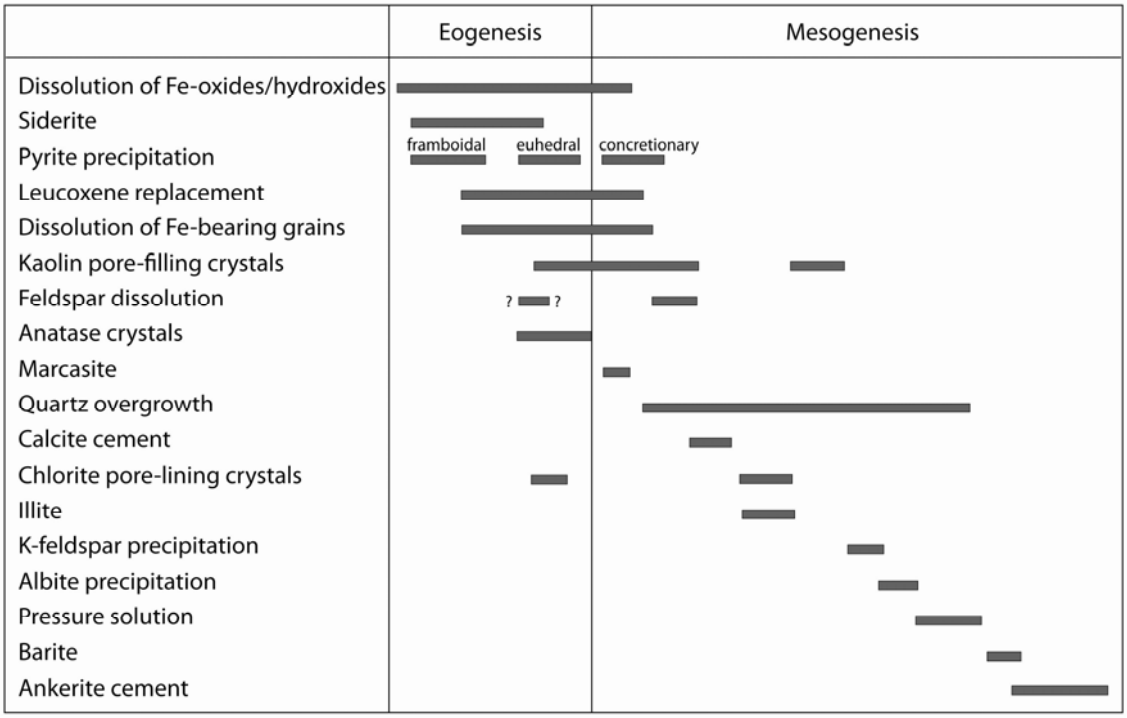

Figure 6.22. *Diagenetic sequence for the Gassum Formation, modified after Friis (1987).*

6.6.3 Haldager Sand Formation

The Middle Jurassic fluvial, estuarine and shallow marine sandstones of the Haldager Sand Formation) occur in restricted areas in the northern part of Denmark (Fig. 1; Nielsen 2003). It has thicknesses up to 200 m (Mathiesen et al. 2009) and present day burial depth of 400–2500 m.

6.6.3.1 Detrital composition

The Haldager Sand Formation is characterized by quartz arenites and subordinate subarkoses (Fig 5.1 & 5.27). Quartz dominates the framework grains. K-feldspar is more common than plagioclase, which is extremely rare in the deepest buried sediments. Sparse rock fragments are of plutonic, metamorphic or sedimentary origin. Organic matter is abundant in some samples and commonly concentrated together with mica. Mica is dominated by muscovite. A characteristic kaolinitised muscovite is found in most samples of the Haldager Sand Formation, but not in the Gassum Formation. Heavy minerals are dominated by a very stable assemblage (zircon, tourmaline, rutile). Occasionally samples have abundant intraclasts and allogenic clays, some of which may be infiltration of drilling mud.

6.6.3.2 Authigenic phases

The porosity reduction is low in the shallow buried Haldager Sand Formation and mainly due to compaction, as the amount of authigenic phases is very low compared to the other formations (compare Fig. 5.28 with 5.18). Kaolin is the most abundant authigenic phase (Fig. 5.29). Quartz, siderite, pyrite, iron-oxide/hydroxides and anatase are minor but common authigenic phases (Figs 6.26 & 6.27).

Kaolin is strongly related to alteration of K-feldspar, and it forms intragranular in cracks and along cleavages planes, as well as in the adjacent pore spaces (Figs 6.25A, B, C & D). Intense kaolin alteration of muscovite is also common (Figs 6.25E & F). Kaolin precipitates between the cleavage planes of mica thereby expanding its original size. Pore filling kaolin occurs in spotted areas of the deepest samples, but most of the pore space remains open. Kaolin forms after framboidal pyrite (Fig. 6.26C) and prior to quartz overgrowths (Fig. 6.27D).

Framboidal pyrite is the first authigenic phase to form and is occasionally associated with organic matter. Framboidal pyrite commonly occurs with an outer oxidation rim (6.26C). Euhedral pyrite encloses framboidal pyrite and occasionally occurs with internal round dissolution voids (Figs 6.26B &E). Euhedral pyrite commonly forms around altered Fe-Ti oxides (Fig. 6.26F).

Authigenic quartz (quartz mountains) occurs on detrital quartz grains and locally they may merge together to thin quartz overgrowths (Fig. 6.27).

6.6.3.3 Porosity and permeability

Changes in the reservoir properties with increasing burial depth are mainly the result of mechanical compaction, as only limited amounts of authigenic phases such as siderite, pyrite and calcite occur. Generation of secondary porosity by feldspar dissolution has only minor influence.

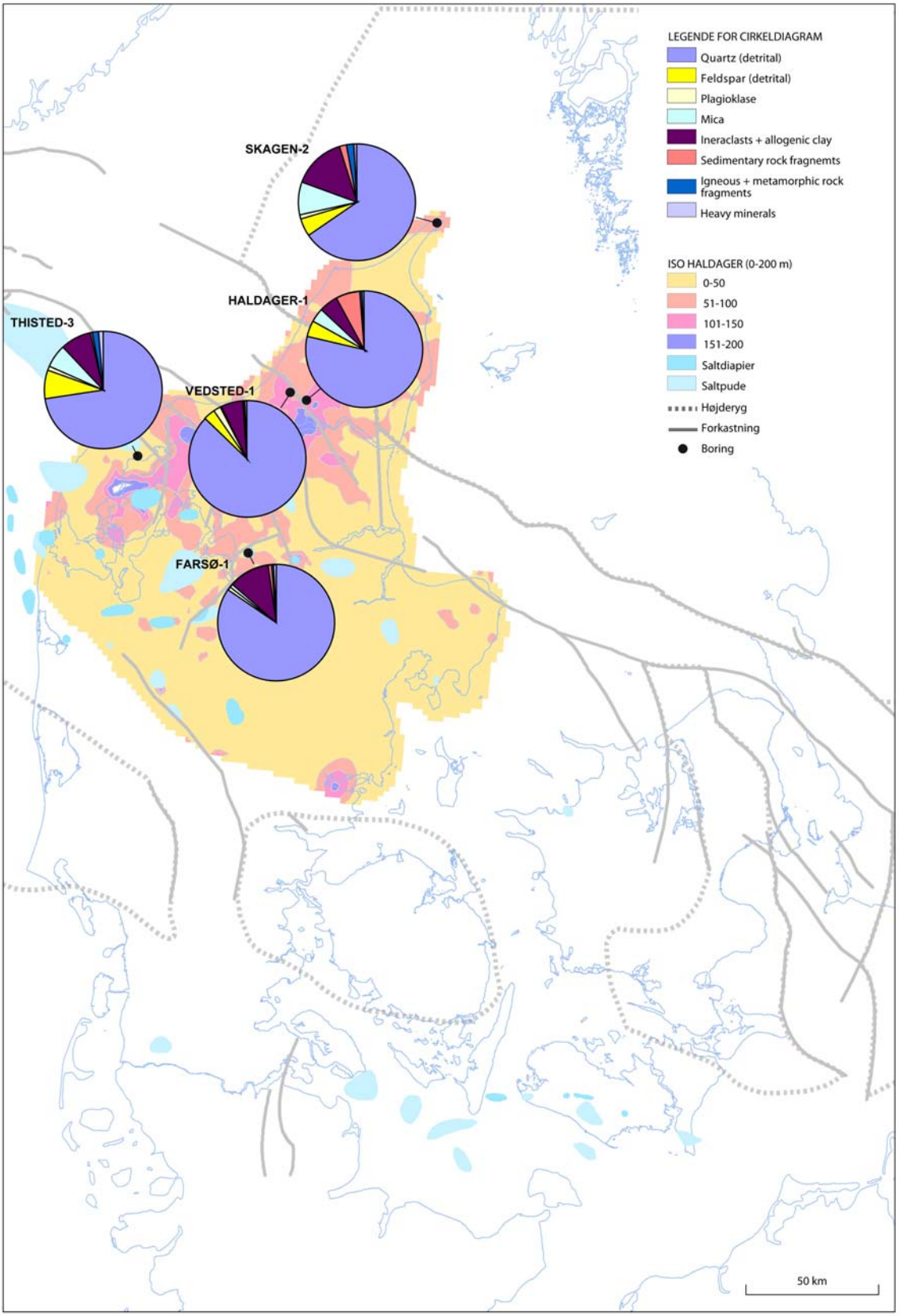

Figure 6.23. *Average detrital composition of the Haldager Sand Formation shown as pie diagrams for each analysed well on isopach map of the Haldager Sand Formation (modified after Mathiesen et al. 2009).*

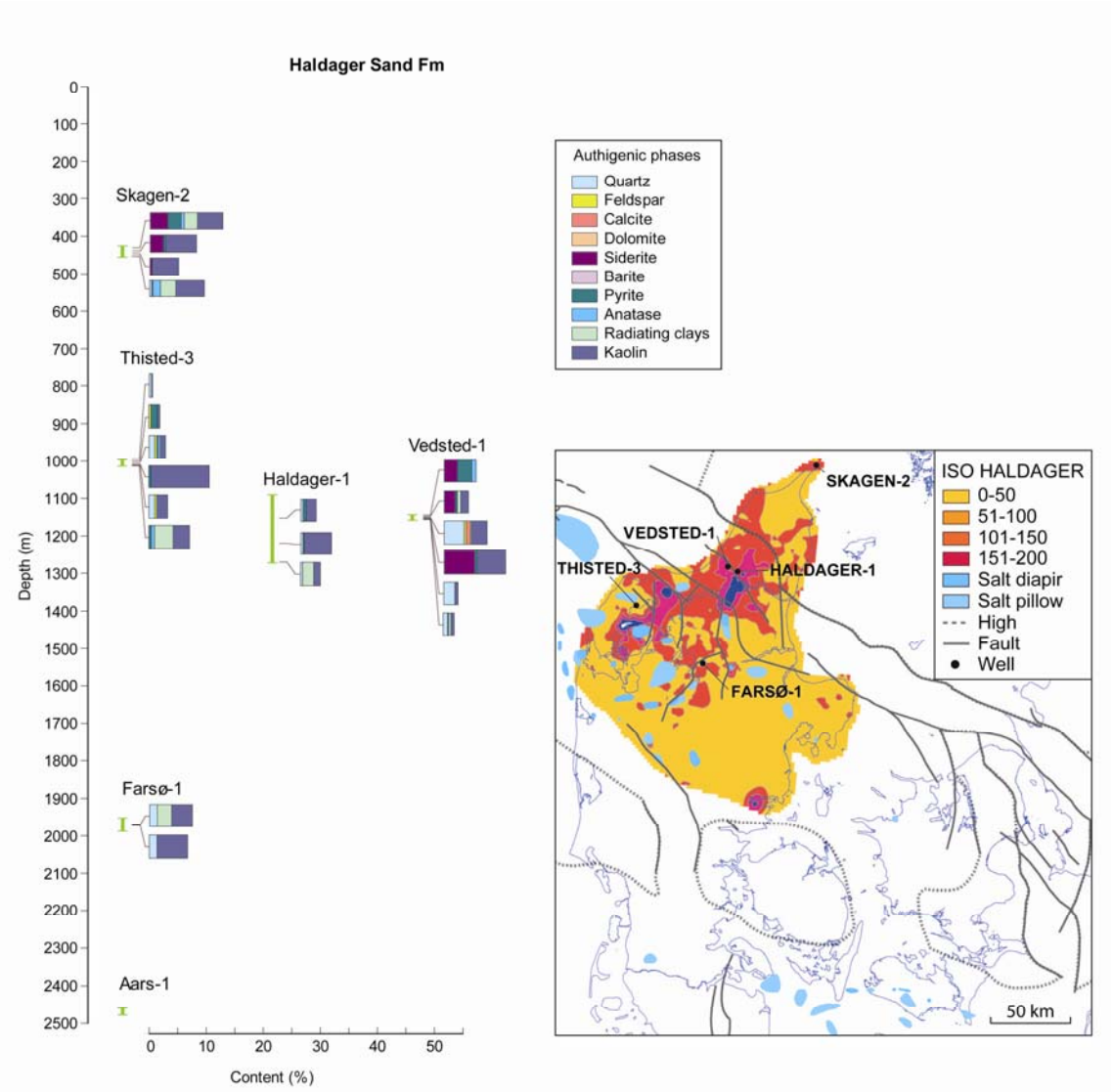

Figure 6.24. *Authigenic phases, quantified by point counting, in the Haldager Sand Formation for different wells and consequently different burial depths*.

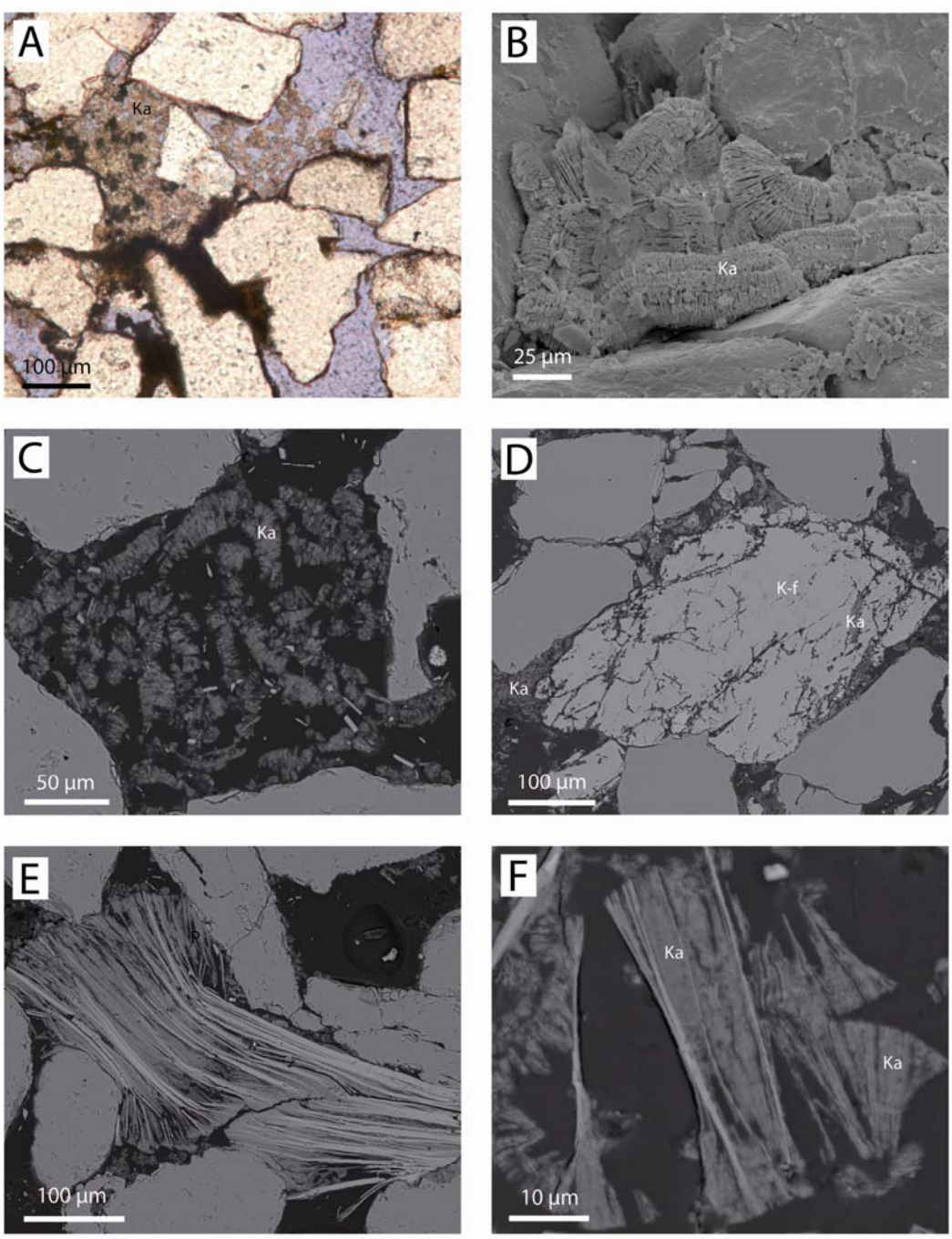

Figure 6.25. *Kaolin precipitation in the Haldager Sand Formation. A. Local area with pore filling kaolin, Vedsted-1, 1151.35 m. B. Pore filling vermicular kaolin, Vedsted-1, 1155.50 m, scanning electron micrograph. C. Pore filling kaolin in over-size pore, Vedsted-1, 1155.50 m, backscatter electron micrograph. D. Vermicular kaolin growing within cleavage planes of K-feldspar and in the adjacent pore space, Vedsted-1, 1155.44 m, backscatter electron micrograph. E. Kaolin precipitating between the cleavage planes of muscovite and in the adjacent pore space, Vedsted-1, 1155.50 m, backscatter electron micrograph. F. Kaolin precipitating between the cleavage planes of muscovite, Vedsted-1, 1155.50 m, backscatter electron micrograph.*

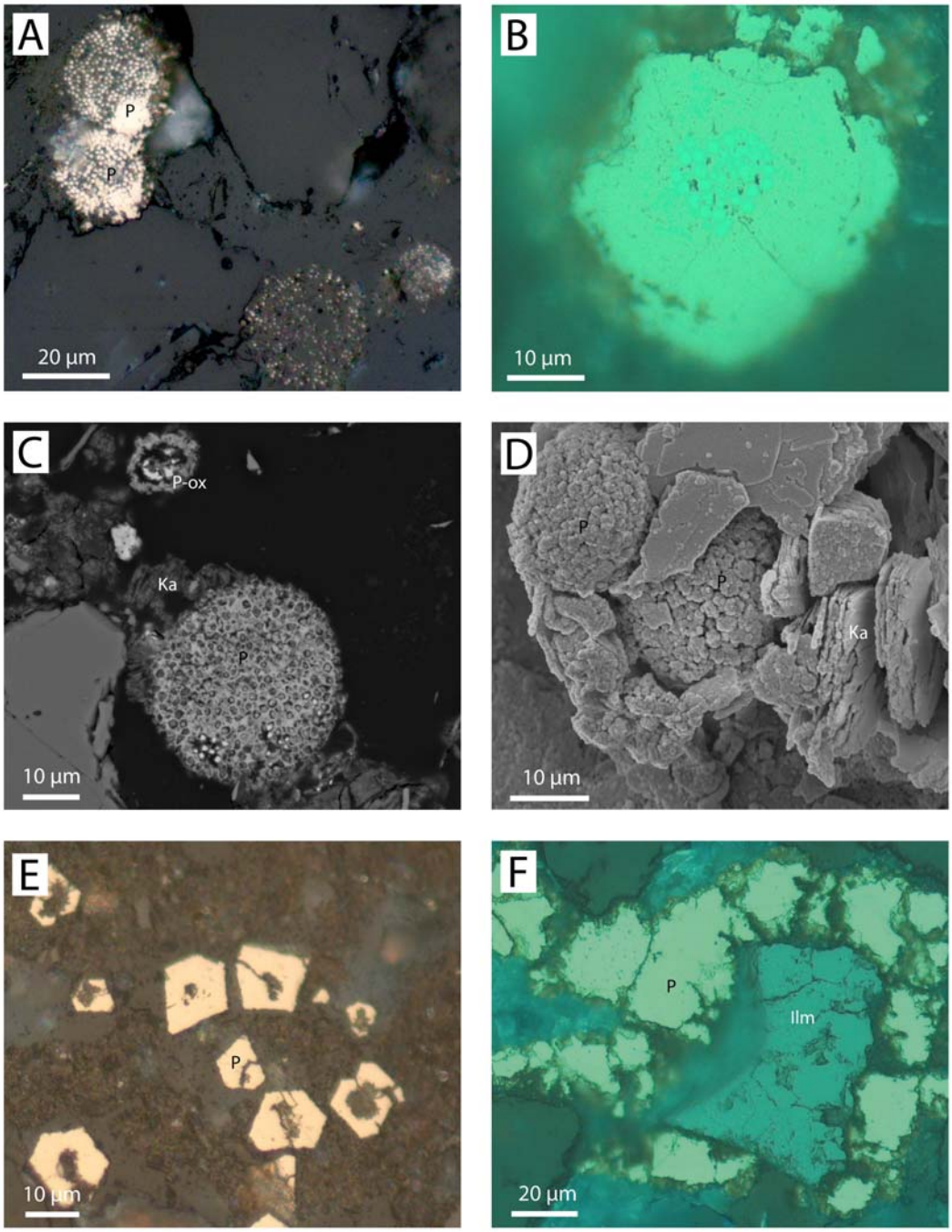

Figure 6.26. *Pyrite in the Haldager Sand Formation. A. Framboidal pyrite in pore space, Vedsted-1, 1151.12 m, reflected light. B. Framboidal pyrite enclosed in euhedral pyrite, Vedsted-1, 1147.95 m, reflected light. C. Framboidal pyrite with an oxidation rim partly enclosed by kaolin minerals, Vedsted-1, 1155.50 m, backscatter electron micrograph. D. Framboidal pyrite with an outer oxidation rim surrounded by kaolin minerals, Vedsted-1, 1155.50 m, scanning electron micrograph. E. Euhedral pyrite with round internal dissolution voids, possibly after framboidal pyrite, Vedsted-1, 1148.90 m, reflected light. F. Euhedral pyrite formed around leucoxene altered ilmenite grain, Vedsted-1, 1147.95 m, reflected light.*

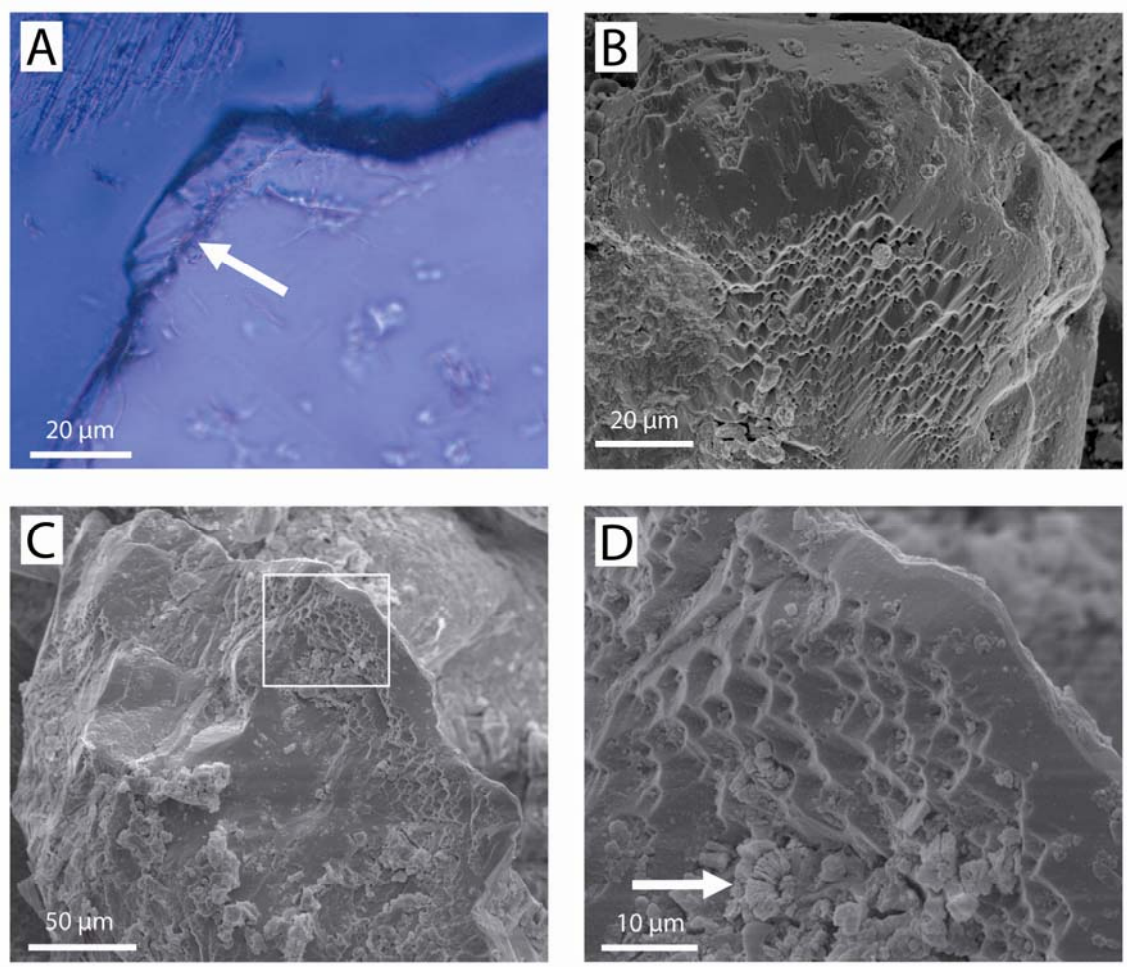

Figure 6.27. *Quartz diagenesis in the Haldager Sand Formation. A. Small quartz overgrowth, Vedsted-1, 1147.95 m. B. Quartz mountains merging into small overgrowth, Vedsted-1, 1155.50 m, scanning electron micrograph. C. Quartz mountains, Vedsted-1, 1155.47 m, scanning electron micrograph. D. Close up of C. Note that the vermicular kaolin (arrow) seem to have inhibited the authigenic quartz growth, scanning electron micrograph.*

6.6.3.4 Mineralogical changes with burial depth

An approximately diagentic sequence for the Haldager Sand Formation is presented in Fig. 5.32.

Immediately after deposition begins the first, volumetric insignifican diagenetic changes. Abundant organic matter creates reducing and weakly acid conditions. Pyrite forms due to the activity of sulphate reducing bacteria, and is therefore commonly associated with organic matter. The common oxidation rim on pyrite is likely to have formed in the cores, and consequently not necessarily a diagenentic event related to burial.

Flushing by meteoric water, undersaturated by most ionic species, promotes the dissolution of feldspar and mica and the formation of kaolin minerals (see Bjørlykke 1993). Mica is intensely altered and replaced by kaolin probably due to the mature detrital composition of the sediments.

Other authigenic phases is not identified in the Haldager Sand Formation, though calcite cement has been described as important in the marine deposits (Nielsen and Friis 1984), whereas this investigation has focused on the fluvio-deltaic sediments.

The general shallow burial and the mature detrital composition of the Haldager Sand Formation result in a less significant diagenetic imprint compared to the other reservoir sandstones. The mature detrital composition, with dominance of quartz, few feldspar grains and rock fragments and very stable heavy mineral assemblage, also means that fewer unstable grains could enter into the diagenetic reactions.

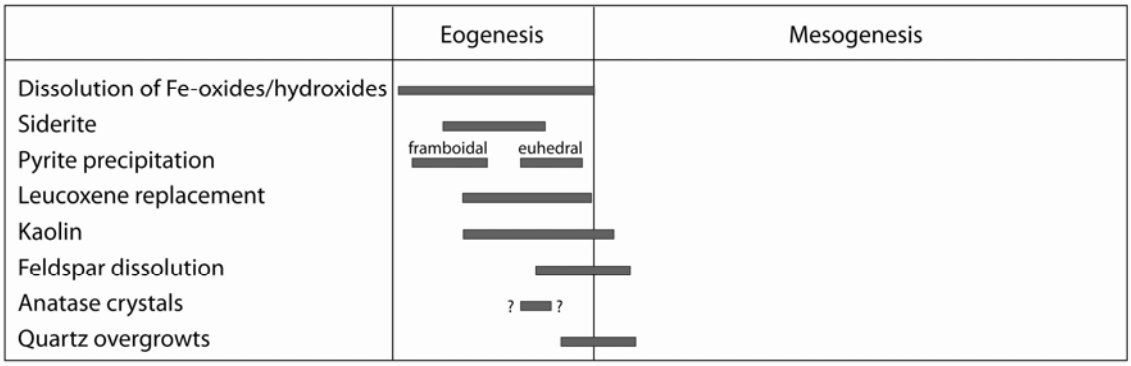

Figure 6.28. *Diagenetic sequence for the Haldager Sand Formation.*

6.7 Mineralogical similarities and differences

The detrital mineralogy and the diagenetic alterations of the Skagerrak, Gassum and Haldager Sand formations are discussed in the following.

6.7.1 The Skagerrak Formation

The proximal Skagerrak Formation deposits are immature containing a high abundance of feldspar, heavy minerals and igneous rock fragments. A possible Norwegian volcanic source may have supplied material to the western part of the Norwegian-Danish Basin during deposition. K-feldspar is the dominating feldspar.

The diagenetic sequence of the Skagerrak Formation represents several diagenetic events tied to the arid depositional environment i.e. mineral reactions related to the eogenesis in an arid to semi-arid climate, such as iron-oxide/hydroxide coatings, hematisation, calcrete, authigenic clay minerals dominated by illite and mixed-layer illite/smectite, carbonates and anhydrite. Dolomite and ankerite is common whereas only rare anhydrite has been recognized.

The high clay mineral abundance is partly related to its in places deep burial (higher burial temperatures) in connection with the immature detrital composition (rock fragments, including volcanic rock fragments, and unstable heavy minerals). Prismatic quartz outgrowths are common in the Skagerrak Formation due to the thick clay coatings.

6.7.2 Comparison of the Gassum and Haldager Sand Formations

The detrital mineralogy of the Gassum Formation in the eastern part of the Norwegian-Danish Basin (Stenlille wells) resembles that of the Haldager Sand Formation with dominance by quartz and low abundances of feldspar and rock fragments. Towards west feldspar grains seem to be a more common part of the detrital mineralogy of the Gassum Formation. Mineral difference (different heavy mineral composition and K-feldspar content) could indicate contribution from different sediment sources of the eastern and western parts of the Gassum Formation, where high quartz amounts in the eastern part could be sourced by a kaolinised basement for example in southern Sweden (Ahlberg et al. 2003).

The Gassum and Haldager Sand formations have almost similar diagenetic sequences and mainly differ with the amount of authigenic phases. Dominance of quartz and stable grains in the Haldager Sand Formation means less reactive minerals which can enter the diagenetic reactions and lead to new authigenic minerals. Similar climate and depositional environment results in eogenetic pyrite, siderite and kaolin formation.

6.7.3 Comparison of the hot dry deposits with the vegetated (humid) deposits

The eogenesis reflects the depositional environment to such a degree that the Gassum and Haldager Sand formations have almost similar diagenetic sequences, though the abundance differs. Both formations were deposited in a vegetated warm wet climate in fluvial, deltaic, estuarine and shallow marine environments. In contrast, the Skagerrak Formation was deposited in ephemeral fluvial and lacustrine environments in an arid to semi-arid climate. The diagenetic alterations are markedly different between the deposits from arid and humid climates.

The iron-rich minerals formed in the eogenetic regime vary according to the depositional environments, as iron-oxide/hydroxide coatings form in the arid Triassic alluvial fan, ephemeral fluvial and lacustrine environments, whereas siderite and pyrite are characteristic for the humid fluvial, parallic and shallow marine deposits. Abundant organic matter in the humid vegetated sediments leads to reducing conditions, whereas the arid to semi-arid conditions typically have oxidising conditions. Oxidised iron precipitates as iron-oxide/hydroxides close to its source (altered iron silicates or Fe-Ti oxides), whereas reduced iron can be transported longer and results in dispersed or concretionary pyrite and siderite formation. Concretionary pyrite and siderite growth can be associated with microbial populations.

The dominating clay minerals vary between the arid deposits and the humid deposits. Kaolin is the dominating clay mineral in both the Gassum and the Haldager Sand formations, whereas it occurs only in the reduced parts of the Skagerrak Formation. Illite and mixed-layer illite/smectite are the typical clays in the Skagerrak Formation, though the abundance of chlorite seems to increase with burial depth. In sediments rich in rock fragments and heavy minerals (Skagerrak Formation), the pore fluid will easily become enriched by several ions. The dissolution of feldspar grains will therefore not be as intensive as in sediments dominated by quartz and feldspar (arkoses), where the pore fluids will be diluted in respect to most ions and consequently will be very corrosive towards the feldspar grains (Gassum

Formation). The dominating clay mineral, associated with feldspar dissolution, is therefore kaolin.

Authigenic albite precipitation and albitisation is generally considered a process occurring at high temperatures (Saigal et al. 1988; Morad et al. 1990; Baccar et al. 1993), though few authors has suggested that albite may precipitate at low temperatures in pore fluids of high sodium concentration (Parcerissa et al. 2010). Albitisation is clearly a temperature dependent (deep burial) process. Authigenic albite precipitation and albitisation are more pronounced in the Gassum Formation than in the Skagerrak Formation at corresponding burial depth. Consequently, the abundance of plagioclase may also be important, as its skeletal remnants form excellent precipitation sites for albite. Organic matter leads to liberation of CO_2 and formation of carboxylic acid in the pore fluids and thus promotes dissolution of feldspar grains (Surdam et al. 1984). Therefore a more intensive dissolution of feldspar grains occurs in the Gassum Formation compared to the Skagerrak Formation.

Prismatic quartz overgrowths occur in the Skagerrak Formation, whereas authigenic quartz occurs with the morphology named ‘quartz mountains’ by Weibel et al. (2010) in shallow samples of the Haldager Sand and Gassum formations. The pore lining clay coatings on all detrital grains in the Skagerrak Formation inhibit authigenic quartz growth, which therefore becomes prismatic or wider but with few contact points. The pore filling kaolin in the Gassum and Haldager Sand formations has less influence on the growth of authigenic quartz on the detrital quartz grains. Authigenic quartz therefore begins on most detrital quartz grains, though only forming limited thin quartz overgrowths (as quartz mountains), which eventually during deeper burial evolve into full macroquartz overgrowths (see Weibel et al. 2010).

Abundance authigenic quartz is controlled by several factors:
Burial depth.
Thickness and continuity of the pore lining chlorite, which may inhibit authigenic quartz formation.
Stylolite formation and pressure solution, which sources silica for authigenic quartz formation. Pressure solution will only occur in sandstones with few ductile grains and only thin clay coatings on the detrital quartz grains. Stylolite formation seems to be associated with detrital mica.
Silica sources. Dissolution of feldspar liberating silica for authigenic quartz formation. Feldspar occurs with highest abundance in fluvial sediments.
Monocrystalline or polycrystalline detrital quartz grains’ relative abundance, as the crystal size of authigenic quartz is related to the ‘type’ of detrital quartz grains, as larger overgrowths tend to form on monocrystalline quartz grains contrary to polycrystalline quartz grains (Lander et al. 2008). On the other hand pressure solution is much more common in coarse-grained sandstones with limited amounts of ductile detrital grains and detrital and authigenic clays.

6.8 Additional reservoirs

The Mesozoic succession of the Norwegian-Danish Basin contains additional sandstones to those described here. The upper part of the F-II Member in the Skagerrak-Kattegat Plat-

form consists of muddy sandstones, 20–30 m thick, deposited by coastal progradation and ensuing transgression (Figs 5.2, 5.6; sequence Fj 4 & Fj 5). The sandstones are only well developed northeast of the Børglum Fault, where they show good porosity. Thin and fine-grained sandstones may be present in the Farsund Basin at this stratigraphic level, but are not expected to be present in the license area except as very thin, fine-grained or silty intercalations.

The shoreface sandstones in the lower and upper parts of the Upper Jurassic Flyvbjerg Formation are expected from the regional geological model discussed above to show a marked thinning from north to south and from east to west (Fig. 5.2, 5.6). This trend is also indicated by the Felicia-1, K-1 and F-1 wells. In K-1 and F-1 the Flyvbjerg Formation consists mainly of sandy mudstones, whereas ca. 12–14 m of fine-grained, muddy sandstones with shell fragments occur in Felicia-1 separated by 5–7 m of mudstones from the underlying Haldager reservoir (Fig. 5.8). The thickness and quality of the Flyvbjerg sandstones are expected to be best in the northeastern part of the Licence area.

On the Skagerrak-Kattegat Platform the Frederikshavn Formation contains shallow marine and fluvial sandstones which posse reservoir properties. However, the sandstones shale out rapidly toward the basin and are not expected to be present in the licence area.

6.9 Conclusion

The focus of the investigation of mineralogical composition and the diagenetic alterations has been directed toward the potential reservoir rocks for CO_2 storage in the Norwegian-Danish Basin, which comprise the Skagerrak Formation, Gassum Formation and Haldager Sand Formation. The investigation has indicated major differences between the three formations, which influence the quality of the potential reservoirs and thus need to be evaluated in detail for reservoir assessments.

The Fennoscandian Shield constitutes the major sediment source area for the sediments in the eastern part of the Norwegian-Danish Basin. Different climate, depositional environments, transport distances and alterations lead to differences in the detrital composition. The proximal Skagerrak Formation, which was deposited in the alluvial fans and braided streams, has the highest content of unstable minerals, such as heavy minerals, rock fragments and feldspar grains. Only minor alteration of feldspar grains occurred in the arid climate. The Gassum and Haldager Sand formations were deposited in fluvial, parallic and shallow marine environments under a humid, wet climate. Under these conditions detrital mineral alteration probably took place in the hinterland as well as in situ the sediment. The Gassum and the Haldager Sand formations therefore contain more stable minerals than the Skagerrak Formation.

During burial the porosity is reduced due to mechanical compaction and precipitation of authigenic minerals. Dissolution of unstable minerals (formation of secondary porosity) may counteract some of the porosity reduction. The porosity reduction in the Skagerrak Formation is mainly due to carbonate cement and clay minerals. Deep burial in places of the Skagerrak Formation in combination with a high proportion of unstable minerals have lead to abundant clay precipitation. The porosity changes in the Gassum Formation are influenced by carbonate cement, precipitation of clay minerals, quartz diagenesis and feldspar

dissolution. Porosity gain from feldspar dissolution is partly destroyed by authigenic phases growing into th secondary porosity. Quartz diagenesis becomes more intensive with burial, as pressure solution of detrital quartz leads to abundant precipitation of authigenic quartz. The porosity reduction of the Haldager Sand Formation is due to its shallow burial mainly related to mechanical compaction. Precipitation of clay minerals (kaolin) played an insignificant role in the porosity reduction. The Haldager Sand Formation can approximately be considered as a shallow equivalent to the Gassum Formation.

Appendix 1. Bulk rock XRD analyses: Bulk mineralogy of the investigated reservoir rocks.

Formation	Sample	Lab*	Quartz	K-feldspar	Plagioclase	Ankerite	Dolomite	Calcite	Siderite	Barite	Anhydrite	Analcime	Pyrite	Hematite	Clay minerals	Kaolinite	Chlorite	Illite
			%	%	%	%	%	%	%	%	%	%	%	%	%	%	%	%
Bunter Sand-	TØ4-Bu166321	KU	48.3	11.6	21.5			4.7			5.0	4.6					2.1	2.1
stone	TØ4-Bu166331	KU	49.9	10.7	19.7			5.9				5.6					2.8	5.5
	TØ4-Bu166313	AU	54.3	13.4	20.5	1.8		5.3						1.9	2.8			
Skagerrak	VE1-Sk206487	KU	81.2	0.7	10.3	6.6										1.2		
	VE1-Sk206494	KU	73.2	2.2	13.7	7.1										3.8		
	VE1-Sk 206501	AU	66.6	4.1	14.9	7.0									7.4			
Gassum	ST18-Ga166240	KU	96.2	1.7	0.4			1.3					0.1			0.3		
	ST18-Ga166240	KU	96.2	1.2				1.3								1.3		
	ST18-Ga166245	AU	93.2	1.5	2.0	0.0		1.1	0.0	0.5			0.6	0.0	1.1			
	ST18-Ga166233	AU	89.0	2.7	1.4	0.0		1.9	1.7	0.6			0.8	0.0	2.0			
	ST18-Ga166264	AU	84.8	2.4	0.6	0.5		1.3	2.2	0.0			0.4	0.0	7.8			
	ST18-Ga167211	AU	85.5	1.4	3.8	0.0		1.3	6.5	0.0			0.6	0.0	1.0			
	ST18-Ga167245	AU	88.5	2.3	5.1	0.0		0.9	0.0	0.9			0.4	0.0	1.9			
	ST18-Ga167439	AU	78.3	7.9	1.9	0.6		1.4	4.1	0.0			0.3	0.0	5.5			
	ST18-Ga167811	AU	88.9	3.3	5.6	0.5		0.8	0.0	0.0			0.0	0.0	1.0			
	VE1-Ga201006	KU	80.3	4.1	10.4				0.1							3.9		1.2
	VE1-Ga201009	KU	81.6	4.8	9.2				0.8							3.8		
	VE1-Ga201010	AU	74.9	3.7	10.9	1.9			6.3						2.4			
	VE1-Ga201016	AU	76.6	6.0	3.3	0.8		0.0	5.2	0.0			2.0	0.0	6.0			
	VE1-Ga177566	AU	84.4	5.3	2.1	4.9		1.0	0.5	0.0			0.6	0.0	1.1			
	VE1-Ga200777	AU	56.7	6.6	7.7	0.0		0.6	7.8	0.0			0.0	0.0	20.6			
	VE1-Ga201010	AU	74.9	3.7	10.9	1.9		0.0	6.3	0.0			0.0	0.0	2.4			

Formation	Sample	Lab*	Quartz	K-feldspar	Plagioclase	Ankerite	Dolomite	Calcite	Siderite	Barite	Anhydrite	Analcime	Pyrite	Hematite	Clay minerals	Kaolinite	Chlorite	Illite
			%	%	%	%	%	%	%	%	%	%	%	%	%	%	%	%
Haldager Sand	VE1-Ha115083	KU	93.9	4.2												2.0		
	VE1-Ha115544	KU	91.9	5.8												2.3		
	VE1-Ha115550	AU	83.2	12.3	0.0	0.6		0.0	1.4	0.0			0.0	0.0	2.5			
	VE1-Ha115162	AU	87.4	8.3	0.0	1.2		0.0	1.8	0.0			0.0	0.0	1.3			
	FA1-Ha196816	AU	88.9	0.0	0.0	0.1		0.0	0.0	0.0			0.0	0.0	11.0			
	FA1-Ha196863	AU	91.1	0.0	0.0	0.0		0.0	0.0	0.0			0.0	0.0	8.9			
	FA1-Ha196660	AU	94.4	0.0	0.0	0.0		0.5	0.0	0.0			0.0	0.0	4.9			
	HA1-Ha122056	AU	76.5	0.0	1.8	0.0		0.4	0.0	0.0			0.0	0.0	21.3			
	HA1-Ha115450	AU	84.9	6.1	0.0	1.1		0.4	1.6	0.0			0.0	0.0	4.3			

* Two different methods of quantifying the XRD results have been attempted. Samples analysed at University of Aarhus (AU) has been semi-quantified by application of corrections factors determined for the applied X-ray diffractometer. Samples analysed at University of Copenhagen (KU) has been quantified by use of Rietveld refinement. The quantification method using corrections numbers it a relatively fast semi-quantitative method, but has its drawback when large amounts of poorly crystalline phases are present.

Appendix 2. Microprobe analyses

Feldspar composition measured by microprobe.

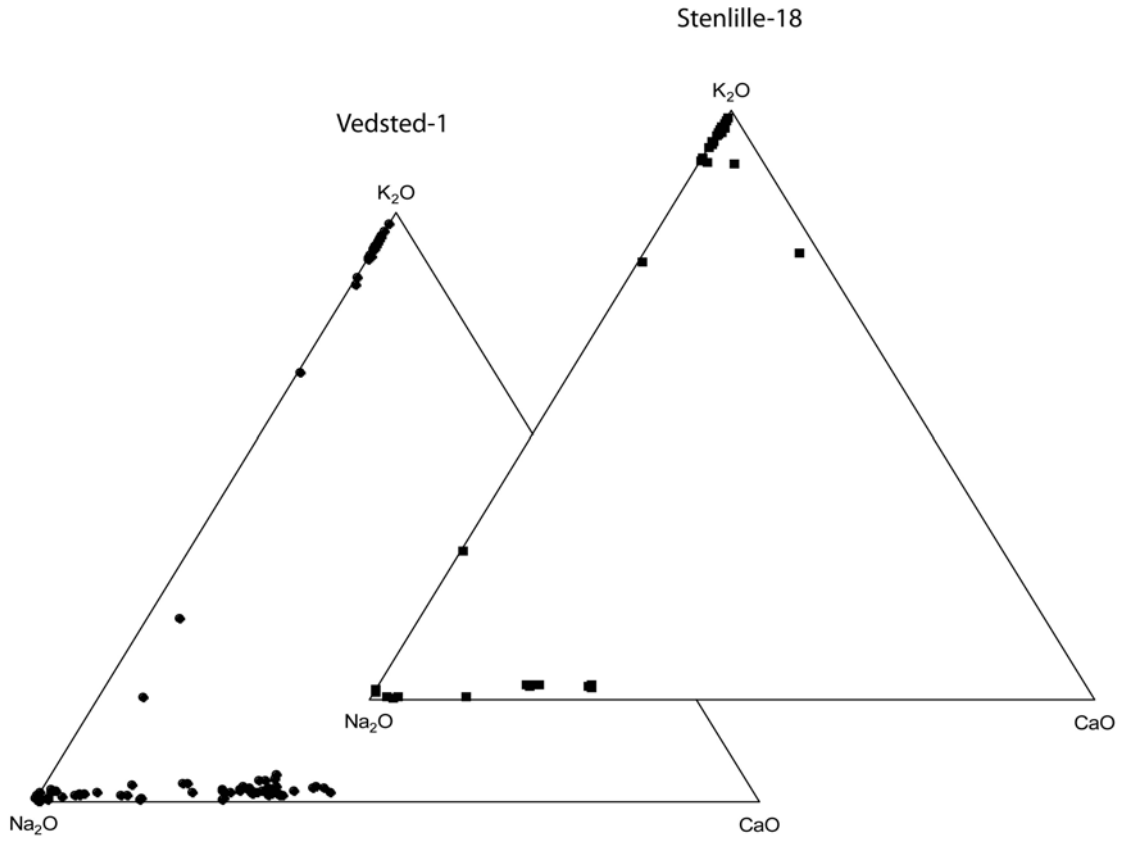

Tables of mineralogy data

The petrographic identification of the mineralogy is based on systematic point counting of thin sections from the Haldager Sand, Gassum and Skagerrak formations from a number of wells situated in the northern part of Jutland north of Limfjorden. The data are not yet published as they form part of an ongoing PhD-study, which aims at covering the potential for geothermal energy in the Mesozoic sandstones onshore Denmark.

Petrographic data have been included from the following wells:

Haldager Sand Fm: Haldager-1, Skagen-2, Thisted-3, Vedsted-1
Gassum Fm: Thisted-3, Vedsted-1
Skagerrak Fm: Frederikshavn-1, Frederikshavn-2, Thisted-2, Thisted-4, Vedsted-1
The subdivision into formations is based on the lithostratigraphy in Nielsen and Japsen (1991).

The mineralogy has been grouped in 15 categories summing up to 100%, whereas the values of primary and secondary porosity are additional to the mineralogy values. The average, minimum and maximum values are included for each well. Merging has been made of the detrital and authigenic phases of quartz and feldspar, respectively. The Ca-carbonates comprise calcite, dolomite and ankerite. The rocks fragments are of sedimentary, metamorphic, volcanic and plutonic origin. The local high amounts of heavy minerals in the Skagerrak Fm include mainly opaque minerals. Others primarily comprise red coatings of hematite besides some anhydrite and analcime. The detrital clays consist of allogenic clays and intraclasts.

Haldager Sand Fm: Haldager-1 well, 2 samples in the depth 1154-1219 m

	Quartz	K-feldspar	Plagioclase	Mica	Ca-carbonates	Siderite	Rock fragments	Heavy minerals	Organic matter	Others	Detrital clays	Infiltration clays	Illite and chlorite	Smectite	Kaolin	Primary porosity	Secondary porosity
Average	75.6	4.4	0.0	3.6	0.0	0.0	6.9	1.0	0.0	0.0	5.2	0.0	0.0	0.0	3.3	14.7	1.7
Min	66.1	0.3	0.0	0.7	0.0	0.0	0.0	0.7	0.0	0.0	2.0	0.0	0.0	0.0	1.7	13.5	1.4
Max	85.0	8.5	0.0	6.4	0.0	0.0	13.9	1.4	0.0	0.0	8.3	0.0	0.0	0.0	5.0	16.0	2.0

Haldager Sand Fm: Skagen-2 well, 3 samples in the depth 434-438 m

	Quartz	K-feldspar	Plagioclase	Mica	Ca-carbonates	Siderite	Rock fragments	Heavy minerals	Organic matter	Others	Detrital clays	Infiltration clays	Illite and chlorite	Smectite	Kaolin	Primary porosity	Secondary porosity
Average	59.8	4.6	0.9	8.6	0.0	1.9	3.6	2.0	0.0	0.0	13.2	0.0	0.8	0.0	4.8	14.0	4.0
Min	53.3	0.3	0.0	4.0	0.0	0.3	2.0	0.7	0.0	0.0	11.7	0.0	0.0	0.0	4.3	1.5	1.6
Max	63.3	9.3	2.3	14.7	0.0	3.0	6.0	3.3	0.0	0.0	15.7	0.0	2.3	0.0	5.3	20.7	7.3

Haldager Sand Fm: Thisted-3 well, 2 samples in the depth 998-999 m

	Quartz	K-feldspar	Plagioclase	Mica	Ca-carbonates	Siderite	Rock fragments	Heavy minerals	Organic matter	Others	Detrital clays	Infiltration clays	Illite and chlorite	Smectite	Kaolin	Primary porosity	Secondary porosity
Average	71.6	8.2	1.0	6.3	0.0	0.0	2.2	2.0	0.0	0.0	8.3	0.0	0.0	0.0	0.3	23.7	2.0
Min	65.7	6.4	0.7	3.7	0.0	0.0	2.0	1.7	0.0	0.0	7.4	0.0	0.0	0.0	0.3	23.4	1.0
Max	77.6	10.0	1.3	9.0	0.0	0.0	2.3	2.3	0.0	0.0	9.3	0.0	0.0	0.0	0.3	23.9	2.9

Haldager Sand Fm:Vedsted-1 well, 3 samples in the depth 1148-1151 m

	Quartz	K-feldspar	Plagioclase	Mica	Ca-carbonates	Siderite	Rock fragments	Heavy minerals	Organic matter	Others	Detrital clays	Infiltration clays	Illite and chlorite	Smectite	Kaolin	Primary porosity	Secondary porosity
Average	81.0	1.9	1.5	0.6	0.0	3.3	0.7	1.3	0.0	0.0	7.4	0.0	0.2	0.0	2.2	20.9	1.3
Min	77.2	0.3	0.0	0.3	0.0	2.0	0.3	0.3	0.0	0.0	5.9	0.0	0.0	0.0	0.0	15.3	0.0
Max	83.3	3.3	4.1	0.7	0.0	5.5	1.0	3.3	0.0	0.0	8.7	0.0	0.7	0.0	5.2	25.3	2.8

Gassum Fm:Thisted-3 well, 12 samples in the depth 1174-1233 m

	Quartz	K-feldspar	Plagioclase	Mica	Ca-carbonates	Siderite	Rock fragments	Heavy minerals	Organic matter	Others	Detrital clays	Infiltration clays	Illite and chlorite	Smectite	Kaolin	Primary porosity	Secondary porosity
Average	62.4	9.9	10.6	0.8	0.5	1.9	1.8	2.2	0.5	0.0	8.7	0.0	0.3	0.0	0.5	20.1	0.3
Min	49.4	4.0	6.0	0.0	0.0	0.0	0.2	0.8	0.0	0.0	0.2	0.0	0.0	0.0	0.0	9.9	0.0
Max	77.4	14.0	18.0	2.2	4.0	21.8	4.0	6.4	4.6	0.0	25.0	0.0	1.4	0.0	3.2	33.6	1.2

Gassum Fm:Vedsted-1 well, 5 samples in the depth 1776-2010 m

	Quartz	K-feldspar	Plagioclase	Mica	Ca-carbonates	Siderite	Rock fragments	Heavy minerals	Organic matter	Others	Detrital clays	Infiltration clays	Illite and chlorite	Smectite	Kaolin	Primary porosity	Secondary porosity
Average	59.1	7.9	5.7	3.0	1.6	3.5	3.6	2.8	0.0	0.1	7.9	0.0	1.7	0.0	2.9	5.5	1.9
Min	41.5	5.3	2.0	0.0	0.0	0.4	2.7	0.7	0.0	0.0	0.2	0.0	0.0	0.0	0.0	0.0	0.0
Max	70.3	14.5	9.6	12.5	3.7	7.7	4.7	4.0	0.0	0.5	15.3	0.0	6.0	0.0	8.3	9.0	4.9

Skagerrak Fm: Frederikshavn-1 well, 1 sample in the depth 1239 m

	Quartz	K-feldspar	Plagioclase	Mica	Ca-carbonates	Siderite	Rock fragments	Heavy minerals	Organic matter	Others	Detrital clays	Infiltration clays	Illite and chlorite	Smectite	Kaolin	Primary porosity	Secondary porosity
values	39.3	18.7	2.7	7.0	0.0	0.0	4.0	1.3	0.0	0.0	4.0	0.0	0.0	14.3	8.7	0.0	0.0

Skagerrak Fm: Frederikshavn-2 well, 2 samples in the depth 1051 m

	Quartz	K-feldspar	Plagioclase	Mica	Ca-carbonates	Siderite	Rock fragments	Heavy minerals	Organic matter	Others	Detrital clays	Infiltration clays	Illite and chlorite	Smectite	Kaolin	Primary porosity	Secondary porosity
average	34.7	10.3	0.2	4.3	18.5	0.0	7.2	2.3	0.0	12.8	0.0	0.0	0.2	6.3	3.2	1.5	0.0
min	28.7	5.0	0.0	2.3	17.3	0.0	6.3	2.0	0.0	0.0	0.0	0.0	0.0	0.0	1.0	1.3	0.0
max	40.7	15.7	0.3	6.3	19.7	0.0	8.0	2.7	0.0	25.7	0.0	0.0	0.3	12.7	5.3	1.7	0.0

Skagerrak Fm: Thisted-2 well, 5 samples in the depth 2763-3165 m

	Quartz	K-feldspar	Plagioclase	Mica	Ca-carbonates	Siderite	Rock fragments	Heavy minerals	Organic matter	Others	Detrital clays	Infiltration clays	Illite and chlorite	Smectite	Kaolin	Primary porosity	Secondary porosity
average	43.2	13.3	0.3	0.3	7.9	0.0	14.3	9.5	0.0	6.0	0.1	0.0	4.0	0.0	1.1	4.9	0.4
min	30.3	11.0	0.0	0.0	1.7	0.0	7.0	2.0	0.0	0.0	0.0	0.0	0.0	0.0	0.0	1.3	0.0
max	58.7	16.7	1.0	0.7	21.0	0.0	28.3	26.7	0.0	12.0	0.3	0.0	9.3	0.0	5.3	13.0	1.0

Skagerrak Fm: Thisted-4 well, 1 sample in the depth 1238 m

	Quartz	K-feldspar	Plagioclase	Mica	Ca-carbonates	Siderite	Rock fragments	Heavy minerals	Organic matter	Others	Detrital clays	Infiltration clays	Illite and chlorite	Smectite	Kaolin	Primary porosity	Secondary porosity
values	14.7	18.3	1.3	0.0	49.7	0.0	4.0	1.0	0.0	4.3	6.7	0.0	0.0	0.0	0.0	6.0	0.0

Skagerrak Fm: Vedsted-1 well, 1 sample in the depth 2063 m

	Quartz	K-feldspar	Plagioclase	Mica	Ca-carbonates	Siderite	Rock fragments	Heavy minerals	Organic matter	Others	Detrital clays	Infiltration clays	Illite and chlorite	Smectite	Kaolin	Primary porosity	Secondary porosity
values	64.3	12.3	1.7	0.0	1.3	0.0	6.7	1.7	0.0	0.0	5.7	0.0	1.7	0.0	4.7	1.7	0.3

7. Reservoir evaluation and parameters

This section deals with an assessment of the reservoir parameters characterizing the Skagerrak, Gassum and Haldager Sand Formations within the Danish part of the Eastern North Sea, Skagerrak, Kattegat and the Northern part of Jutland. The evaluation is based on well log data and core analysis data from selected Danish and Norwegian wells. The parameters are presented in tables below. Comments on each parameter along with additional geological and technical information are given in the following text.

7.1 Wells analysed

The following wells have been evaluated:
Haldager Sand Fm.: F-1x, K-1x, J-1x, Felicia-1.
Gassum Fm.: F-1x, K-1x, J-1x, Felicia-1, Inez-1, Børglum-1, Thisted-1, Mors-1, Terne-1, Rønde-1 and Vedsted-1.
Skagerrak Fm.: F-1x, K-1x, J-1x, Felicia-1A, Thisted-2, Mors-1, Sæby-1 and Hans-1.
The subdivision into formations is based on the lithostratigraphic subdivision given in Nielsen and Japsen (1991).

7.2 Temperature model

The determination of the temperature is based on a surface temperature of 8°C and a temperature gradient of 30°C/km; this model is normally considered applicable to the Danish onshore area. The temperature is thus calculated as:
Onshore DK: Approximate temperature (in Centigrade) = 0.030*Depth (in metres) + 8ºC.
For comparison it may be mentioned that corresponding offshore temperatures are slightly higher within certain areas, e.g. for the Danish Central Graben (DCG) area:
Offshore DCG: Approximate temperature (in Centigrade) = 0.036*Depth (in metres) + 8ºC

7.3 Salinity model

The salinity of the formation water has been measured in the wells Thisted-2, Farsø-1, Aars-1, Stenlille-1, Gassum-1, and Margretheholm-1. Generally, the analysed data reflect the composition of formation waters produced during well tests. The salinity may be estimated on the basis of these measurements, utilising Salinity versus Depth trends, as e.g. presented by Laier (1989). Furthermore, information from Pickett plots (example in **Figure 7.1**) combined with general geological information, e.g. subsidence history and/or the presence of Triassic / Zechstein salt, has been used in estimating salinity. The relations listed below are suggested for estimating the formation water salinity when considering the Danish onshore area. The first equation is derived from Laier (1989); the remaining three equations are calculated by the author:

Salinity (*in Mol* Cl^-) = 0.00152*Depth (*in metres*) + 0.62 Mol/l

Salinity (*in g/l Cl^-*) = 0.054*Depth (*in metres*) + 22 g/l
Salinity (*in ppm Cl^-)* = 54.0*Depth (*in metres*) + 22,000 ppm
Salinity (*in ppm NaCl*) = 75.6*Depth (*in metres*) + 28,000 ppm.

7.4 Thicknesses of reservoir sandstones

The following cut-offs have been applied prior to calculating thicknesses:
Net sand: 30% Vshale cut-off.
Net reservoir: 30% Vshale cut-off and 15% porosity cut-off.

7.5 Porosity determination

Initially, a petrophysical evaluation of relevant well logs was carried out and then calibrated to core analysis data, if available. The porosity has normally been determined from a shale-corrected density log (information about the shale content is provided by the GR log). Exceptions are the Børg-lum-1, Vedsted-1 and Terne-1 wells, as no density logs were acquired in these wells. The porosity evaluation is based either on the resistivity log (Børglum-1; Vedsted-1) or the sonic log (Terne-1). The porosity values listed in the tables refer to the *average* porosity of the net sand and the net reservoir, respectively.

7.6 Permeability estimates

So far no porosity-permeability model has been published for the various formations within Danish part of the UiO-GEUS study area. GEUS is currently compiling data on porosity-permeability relations in order to establish a well-constrained database that will be published when ready. For the present study, GEUS compiled a number of porosity-permeability data assumed to be representative of the eastern North Sea – Skagerrak – Kattegat – N. Jutland areas (**Fig. 7.2**). The database consists of porosity and permeability measurements available from a number of Danish onshore wells located in the Northern part of Jutland, one Zealand well (Stenlille-13) along with two Norwegian wells (9/2-1 and 9/2-2). In order to ensure a reasonably large and representative database, data from four formations are included in plot: the Skagerrak Fm (Danish part), Gassum Fm and Haldager Sand Fm plus the Norwegian Sandnes Formation. On the basis of this *regional database*, the following relationship between porosity and permeability is suggested:

$$Permeability = 1{,}000{,}000 \cdot (Porosity)^{5.8577}$$

where the permeability is in mD and the porosity is in fraction. The assumed correlation between porosity and permeability can thus be expressed by a power function. The data points plotted in **Figure 7.2** are rather scattered – some the outliers are, however, related to shaly sand lithology (low perm.) or fractured plugs (high perm.). The use of a functional equation ("regression line") for modelling permeabilities implies that modelled permeabilities may deviate significantly from permeabilities measured on core plugs. Also on a local

scale, the actual and modelled permeability levels may deviate, due to e.g. uplift or atypical sediment source.

7.6.1 Log-derived permeability

The permeability has not been logged, but the equation listed above provides a reasonable link between log-porosity and permeability. This relationship forms the basis of calculating log-derived permeabilities using the log-porosities, i.e. the porosities interpreted from the well log data, as input data. Log-derived permeabilities are to be used in the Petrel modelling work, primarily because the amount of core permeability measurements is (very) limited.

A log-derived permeability value is an *acceptable permeability estimate*, but it may be associated with rather large uncertainty.

Tables of reservoir parameters

Haldager Sand Fm. Net sand cut-off(s): 30% Vshale cut-off, no porosity cut-off

Well	F-1x	K-1x	J-1x	Felicia-1
Depth (m), c	1800	1400	1100	1000
Temperature, deg.C	62	50	41	38
Salinity (ppm NaCl)	150,000	130,000	110,000	100,000
Gross thickness (m)	48	14	19	34
Net sand thickness (m)	24	12	3	21
Net-to-gross	0.50	0.86	0.16	0.62
Net Porosity, avg. (%)	26.4	28.6	26	29.8
Estimated Perm. (mD)	400	650	375	825

Haldager Sand Fm Net reservoir cut-off(s): 30% Vshale cut-off and 15% porosity cut-off

Well	F-1x	K-1x	J-1x	Felicia-1
Gross thickness (m)	48	14	19	34
Net reservoir thick-ness (m)	23	11.5	3	21
Net-to-gross	0.48	0.82	0.16	0.62
Net Porosity, avg. (%)	26.7	29.6	26	30.0
Estimated Perm. (mD)	440	800	375	850

Formation: Gassum Fm: Net sand cut-off(s): 30% Vshale cut-off, no poros-ity cut-off

Well	F-1x	K-1x	J-1x	Felicia-1
Depth (m), c.	2100	2000	1800	1600
Temperature, deg.C	71	68	62	56
Salinity (ppm NaCl)	175,000	175,000	160,000	150,000
Gross thickness (m)	76	67	72	230
Net sand thickness (m)	37	47	54	98
Net-to-gross	0.49	0.70	0.75	0.30
Net Porosity, avg. (%)	18.7	22.9	19.4	Poor logs
Estimated Perm. (mD)	55	175	70	N/A

Formation: Gassum Fm: Net sand cut-off(s): 30% Vshale cut-off, no porosity cut-off

Well	Børglum-1	Thisted-1	Mors-1	Inez-1
Depth (m), c.	1450	800	2800	1700
Temperature, deg.C	51	32	92	60
Salinity (ppm NaCl)	140,000	90,000	240,000	150,000
Gross thickness (m)	115	125	167	71
Net sand thickness (m)	91	59	127	37
Net-to-gross	0.79	0.47	0.76	0.52
Net Porosity, avg. (%)	28.2	26.8	13.6	21.1
Estimated Perm. (mD)	600	450	10	110

Formation: Gassum Fm: Net sand cut-off(s): 30% Vshale cut-off, no porosity cut-off

Well	Sæby-1	Terne-1*	Rønde-1	Vedsted-1
Depth (m), c.	1100	1200	2700	1900
Temperature, deg.C	41	44	90	65
Salinity (ppm NaCl)	110,000	120,000	160,000	170,000
Gross thickness (m)	88	133	140	288
Net sand thickness (m)	9.5	100	31	109
Net-to-gross	0.11	0.75	0.22	0.37
Net Porosity, avg. (%)	23.3	15.0	12.9	23.0
Estimated Perm. (mD)	200	15	6	190

* Compare to well Hans-1; in Hans-1 the Gassum Fm is located too shallow (296-666m MD) for CO2 injection.

Gassum Fm: Net reservoir cut-off(s): 30% Vshale cut-off and 15% porosity cut-off

Well	F-1x	K-1x	J-1x	Felicia-1
Gross thickness (m)	76	67	72	230
Net reservoir thickness (m)	31	44	48	N/A
Net-to-gross	0.41	0.66	0.67	-
Net Porosity, avg. (%)	20.4	23.7	20.1	Poor logs
Estimated Perm. (mD)	90	220	85	N/A

Gassum Fm: Net reservoir cut-off(s): 30% Vshale cut-off and 15% porosity cut-off

Well	Børglum-1	Thisted-1	Mors-1	Inez-1
Gross thickness (m)	115	125	167	71
Net reservoir thickness (m)	89	58	49	32
Net-to-gross	0.77	0.46	0.29	0.45
Net Porosity, avg. (%)	28.6	27.0	21.8	22.7
Estimated Perm. (mD)	650	470	130	170

Gassum Fm: Net reservoir cut-off(s): 30% Vshale cut-off and 15% porosity cut-off

Well	Sæby-1	Terne-1	Rønde-1	Vedsted-1
Gross thickness (m)	88	133	140	288
Net reservoir thickness (m)	9	57	15	98
Net-to-gross	0.10	0.43	0.11	0.34
Net Porosity, avg. (%)	23.4	17.7	15.1	24.1
Estimated Perm. (mD)	200	40	15	240

Skagerrak Fm: Net sand cut-off(s): 30% Vshale cut-off, no porosity cut-off

Well	F-1x	K-1x	J-1x	Felicia-1A
Depth (m), c.	2200	2100	1800	2800
Temperature, deg.C	75	70	65	95
Salinity (ppm NaCl)	175,000	175,000	165,000	200,000
Gross thickness (m)	>267	>200	>183	2281
Net sand thickness (m)	-	-	-	326
Net-to-gross	-	-	-	0.14
Net Porosity, avg. (%)	Fm not	Fm not	Fm not	Poor logs
Estimated Perm. (mD)	Penetrated	Penetrated	penetrated	N/A

Skagerrak FmNet sand cut-off(s): 30% Vshale cut-off, no porosity cut-off

Well	Thisted-2	Mors-1	Sæby-1	Hans-1
Depth (m), c.	2800	4500	1300	1000
Temperature, deg.C	92	140	47	38
Salinity (ppm NaCl)	240,000	250,000	125,000	100,000
Gross thickness (m)	1682	1500	538	1119
Net sand thickness (m)	1036	452	336	276
Net-to-gross	0.62	0.30	0.62	0.25
Net Porosity, avg. (%)	9	1	15.0	9
Estimated Perm. (mD)	1	0.01	15	1

Skagerrak Fm Net reservoir cut-off(s): 30% Vshale cut-off and 15% porosity cut-off

Well	Thisted-2	Mors-1	Sæby-1	Hans-1
Gross thickness (m)	1638	1500	538	1119
Net reservoir thickness (m)	227	0	175	46
Net-to-gross	0.14	0	0.33	0.04
Net Porosity, avg. (%)	18.0	-	20.8	21.8
Estimated Perm. (mD)	45	-	100	135

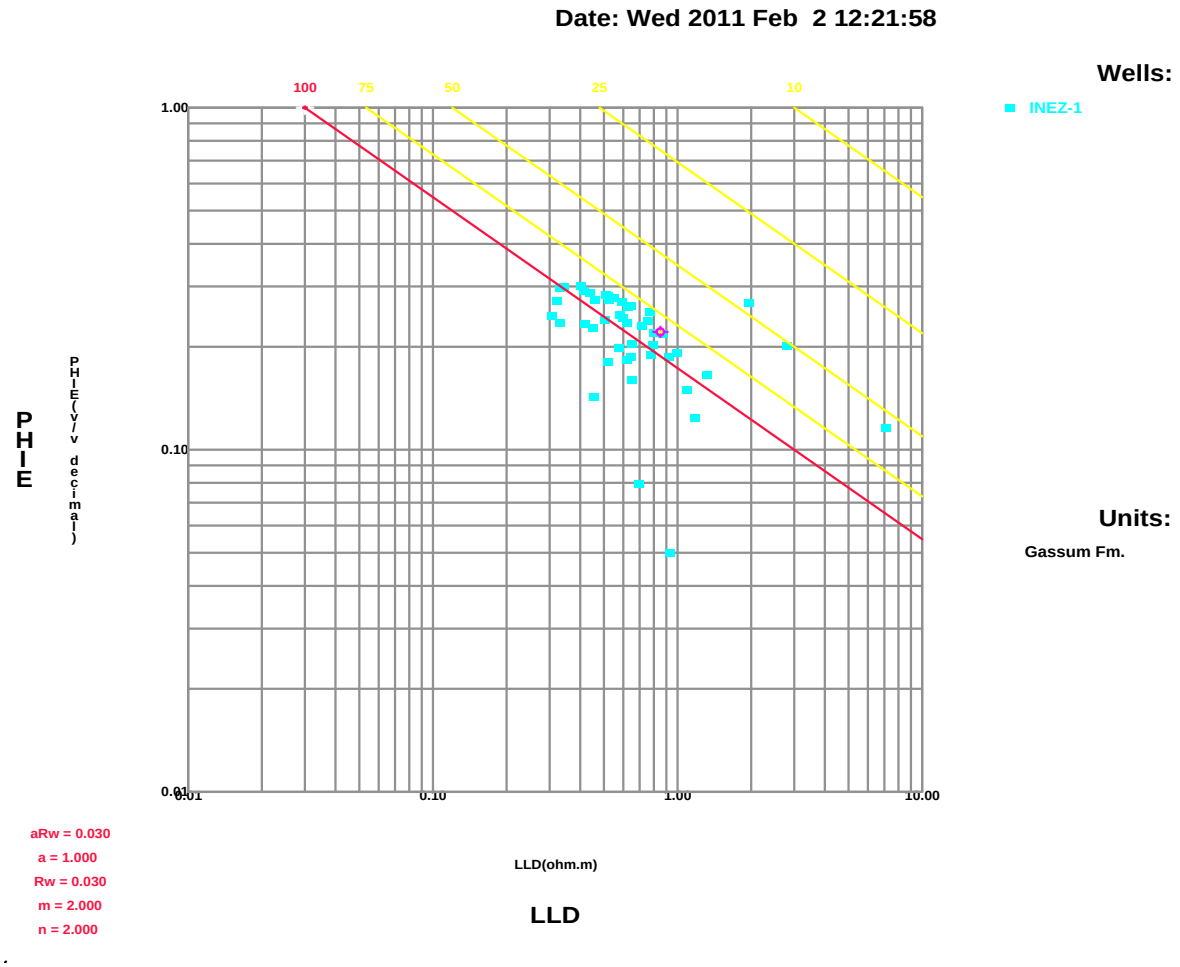

Figure 7.1: *Pickett plot for the Gassum Formation in the Inez-1 well. Reservoir depth c. 1700m; reservoir temperature c. 60°C. The formation water resistivity is about 0.03 ohmm corresponding to a salinity of c. 150,000 ppm NaCl. PHIE: Effective porosity as interpreted from the log data, LLD: deep-reading resistivity log (LateroLog).*

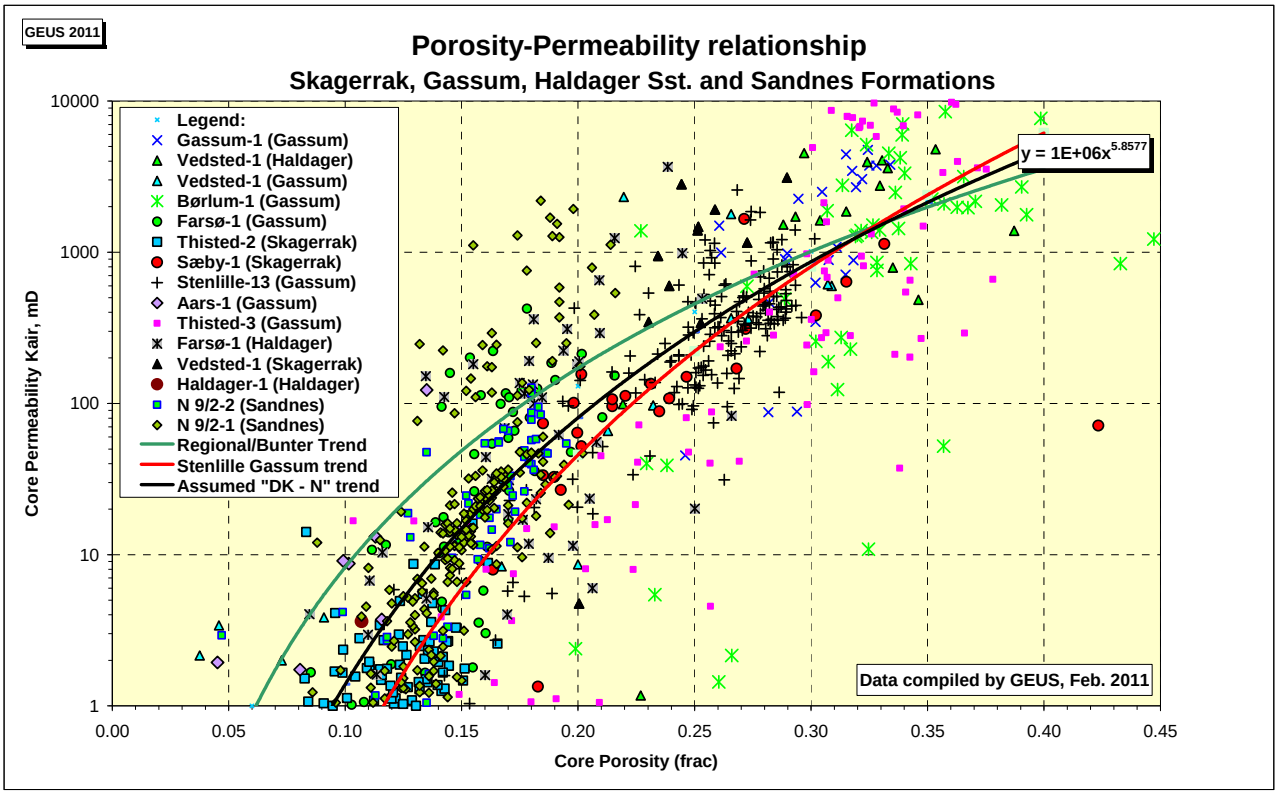

Figure 7.2: *Suggested porosity-permeability relationship for the Danish part of the study area and parts of the Norwegian area (**black curve**). Two additional curves are included for comparison: the red curve represents a local model (the Gassum Fm at the Stenlille gas storage area, Zealand) and the green curve represents a regional model valid for the Danish onshore area south of the Fjerritslev fault. The red and green curves are, in general, not considered representative of the UiO-GEUS study area. The trend line in black colour is based on core analysis data from selected Danish and Norwegian wells. Data from four formations are included.*

8. Biostratigraphic and palynofacies analyses of selected parts of the Iku/Sintef core 13/1-U-1

8.1. Biostratigraphy

A total of 17 samples representing the interval from 196 to 121 m were selected for analysis in order to establish a well-documented biostratigraphic subdivision of this part of the succession to support the sequence stratigraphic breakdown and the regional geological model. Based on sedimentological core description and correlation to Danish well sections this interval was assumed to represent the upper Lower Jurassic, Middle Jurassic and the lowermost Upper Jurassic. The resulting palynological data is discussed below.

Several palynological studies of the Lower to Middle Jurassic succession in the Danish Basin and nearby areas (Scania, Bornholm, North Germany) (e.g. Nilsson 1958; Lund 1977; Hoelstad 1985; Guy-Ohlson 1986; Dybkjær 1988, 1991; Koppelhus 1991; Koppelhus and Nielsen 1994; Koppelhus and Batten 1996) has resulted in a solid miospore zonation. The dinocyst zonation erected for the British Lower and Middle Jurassic (Woolam and Riding 1983; Riding and Thomas 1992) has proven very useful for the Norwegian-Danish Basin, with a few additional zones and subzones included (Koppelhus and Nielsen 1994; Poulsen 1996). The studied succession from the N-13/1-U-1 core has been subdivided using the established miospore- and dinocyst zonation.

8.1.1. Miospore zones

8.1.1.1 Chasmatosporites Zone (Koppelhus and Nielsen 1994)

Occurrence: ?195.34 m (lowest sample studied) to 154.55 m.

Base: where the assemblages become rich in *Chasmatosporites* and *Corollina torosus*, and where *Cerebropollenites macroverrucosus* is present. The base is not reached in the present study.

Top: below a distinct increase of *Spheripollenites* and the first appearance of *Leptolepidites*.

Characteristics: abundance of different species of Chasmatosporites (especially C. hians and C. major) and presence of Corollina torosus, Cerebropollenites thiergartii and C. macroverrucosus.

Suggested age: Pliensbachian.

8.1.1.2 Spheripollenites - Leptolepidites Zone (Dybkjær 1991)

Occurrence: 154.55 m to 142.0 m

Base: at a distinct increase in *Spheripollenites* and the first appearance of *Leptolepidites* and/or *Ischyosporites*.

Top: immediately below a distinct increase in *Perinopollenites elatoides* and a decrease in *Spheripollenites psilatus*.
Characteristics: abundant Spheripollenites and Corollina. Presence of Leptolepidites and/or Ischyosporites. In the boreholes studied by Dybkjær (1991) the species Manumia delcourtii, Staplinisporites caminus, Klukisporites and Clavatipollenites hughesii appear within this zone but in the present study these species appear in the upper part of the underlying zone.

In the middle part of the basin this zone is further characterised by the occurrence of several taxa of dinoflagellate cysts, prasinophycean algae and acritarchs. In the succession at Bornholm, which represents the more marginal parts of the basin, hardly any marine palynomorphs were recorded, while freshwater algae, especially *Botryococcus*, are common (Koppelhus & Nielsen 1994). The palynomorph assemblage recorded from this zone in the N-13/1-U1 well corresponds closely to the assemblage from Bornholm, indicating a corresponding marginal position in the basin.
Suggested age: Toarcian (Dybkjær 1991)

8.1.1.3 Perinopollenites elatoides Zone (Dybkjær 1991)

Occurrence: 142.0 m to 139.60 m
Base: at a distinct increase in abundance of *Perinopollenites elatoides* and a concurrent decrease in *Corollina* and *Spheripollenites*.
Top: not defined.
Characteristics: dominance of *Perinopollenites elatoides* and a relatively low abundance of *Corollina torosus* and of bisaccate pollen.
Suggested age: Middle Jurassic.

The upper part of the studied interval cannot be referred to any of the established miospore and dinocyst zonations due to the lack of diagnostic spores and pollen and the absence of dinoflagellate cysts.

8.1.2. Dinoflagellate cyst zones

8.1.2.1 Mendicodinium reticulatum Zone (Koppelhus and Nielsen1994)

Occurrence: ?195.34 m (lowest sample studied) to 182.50 m.
Base: first appearance of *Mendicodinium reticulatum*. Younger palynomorphs such as *Luehndea spinosa* and *Nannoceratopsis* spp. are lacking. The base is not reached in the present study.
Top: first appearance of either *Luehndea spinosa* or *Nannoceratopsis* spp.
Suggested age: Early to early late Pliensbachian (Morgenroth 1970; Koppelhus and Nielsen 1994).

8.1.2.2 Luehndea spinosa Total Range Biozone (Woollam and Riding 1983, emended Riding and Thomas 1992)

Occurrence: 182.50 m to 165.87 m.

Base: first appearance of Luehndea spinosa. Mancodinium semitabulatum, Nannoceratopsis gracilis, Scriniocassis weberi and Valveodinium armatum appear within this zone.

Suggested age: Late Pliensbachian to earliest Toarcian (Riding and Thomas 1992).

8.1.2.3 Luehndea spinosa Total Range Biozone (Woollam and Riding 1983, emended Riding and Thomas 1992) or Nannoceratopsis gracilis Interval Biozone (Woollam and Riding 1983, emended Riding and Thomas 1992)

Occurrence: 165.87 m to 146.37 m.

The characteristics and the stratigraphic range of the *Luehndea spinosa* Zone is discussed above. The base of the *Nannoceratopsis* Zone is defined by the presence of several species of *Nannoceratopsis* and a dominance of *Nannoceratopsis*. The *Nannoceratopsis* Zone is referred to the Early Toarcian to Early Bajocian (Riding and Thomas 1992).

This interval is referred to either the *Luehndea spinosa* Zone or the *Nannoceratopsis* Zone on the basis of the occurrence of *Luehndea spinosa*, *Nannoceratopsis senex* and *N. gracilis* at 165.87m, the lack of these species above this level and the sporadic occurrences of *Mancodinium semitabulatum* and *Scriniocassis weberi* at 148.03 m (Riding and Thomas 1992; Koppelhus and Nielsen 1994). The referring of this interval to the upper part of the *Chasmatosporites* Zone and to the *Spheripollenites - Leptolepidites* Zone further supports a correlation to either the *Luehndea spinosa* Zone or the *Nannoceratopsis* Zone (e.g. Koppelhus and Nielsen 1994). The lack of *Luehndea spinosa* as well as *Nannoceratopsis* among the few dinocysts present in the samples at 162.95 m, 148.03 m and 146.37 m may be due to environmental factors unfavourable for those taxa.

No dinocysts were recorded from the sample at 154.55 m and in the interval between the samples at 146.37 m and 121.95 m.

8.1.3. Biostratigraphic conclusions, this study

The stratigraphically most important bioevents (first appearance datums, FAD´s, last occurrence datums, LOD´s, and consistent, common or frequent occurrences) were determined. The chronostratigraphic subdivision shown in the rightmost column in the enclosure and discussed below is based on these events. The results have been integrated with the sequence stratigrapic framework previously established for the eastern Norwegian-Danish Basin (Nielsen 2003) for strengthening of the geological model of the area.

8.1.3.1 195.34 m –185.35 m: Lower and/or Upper Pliensbachian.

The presence of *Mendicodinium reticulatum* in the lowermost sample, at 195.34 m, strongly indicates an age not older than Pliensbachian (Morgenroth 1970; Koppelhus and Nielsen 1994)

8.1.3.2 182.50 m – 154.55 m: Upper Pliensbachian.

The first appearances of *Luehndea spinosa*, *Mancodinium semitabulatum* and *Nannoceratopsis gracilis* at 182.50 m strongly indicate an age not older than Late Pliensbachian (Rid-

ing and Thomas 1992; Poulsen 1996; Bucefalo Palliani and Riding 2000). The last occurrence of *Luehndea spinosa* at 165.87 m indicates a Late Pliensbachian or earliest Toarcian age (Riding and Thomas 1992). The common occurrence of *Chasmatosporites* up to 154.55 m, defining the presence of the *Chasmatosporites* Zone, indicates an age not younger that the Pliensbachian (Koppelhus and Nielsen 1994).

8.1.3.3 154.55 m – 142.22 m: Lower Toarcian.

The common occurrence of *Spheripollenites* spp. at 154.55 m and the frequent occurrence in the samples at 144.66 m and 142.22 m strongly indicate an Early Toarcian age. Abundance of small, spherical, psilate to subgranulate bodies (here referred to *Spheripollenites*) is a well-documented characteristic of the Lower Toarcian in widespread areas (e.g. England: Wall 1965; Bucefalo Palliani *et al.*1998, 2000, Germany: Wille 1982; Loh *et al.* 1986; Prauss *et al.* 1991, East Greenland: Lund and Pedersen 1985, Denmark: Dybkjær 1991; Koppelhus and Nielsen 1994, northern North Sea: Charnock *et al.* 2001), known to be coincident with a widespread Total Organic Carbon (TOC) maximum in the lower part of the *H. falciferum* Ammonite Zone (Bucefalo Palliani, Mattioli and Riding 1998). The TOC maximum is possibly related to an anoxic event resulting from stratification of the water masses connected with the Early Toarcian marine flooding (named MFS 15 by Nielsen 2003). See further discussion in Dybkjær (1991, p.39) and Bucefalo Palliani and Riding (2000).

The small spherical bodies have been interpreted as sphaeromorph acritarchs (Charnock *et al.* 2001), pollen of either *Inaperturopollenites* (Wall 1965; Wille 1982) or *Spheripollenites* (Lund and Pedersen 1985; Dybkjær 1988, 1991, Koppelhus and Nielsen 1994 and herein) and Prasinophycean algae of the species *Halosphaeropsis liassica* (Mädler 1963, see further Bucefalo Palliani and Riding 2000).

A Toarcian age is supported by the first appearances of *Leptolepidites major* and *Ischyosporites variegatus* at 154.55 m and of *Callialasporites turbatus*, *Leptolepidites bossus* and *Neoraistrickia gristhorpensis* at 146.37 m (Batten and Koppelhus 1996).

8.1.3.4 141.55 m – 128.18 m: mid-Bajocian and/or Bathonian.

The first appearance of *Leptolepidites equatibossus* at 134.95 m indicates an age not older than the mid-Bajocian, while the occurrence of *Quadraeculina anellaeformis* at 141.55 m and of *Chasmatosporites apertus* at 128.18 m indicate an age not younger than Bathonian (Batten and Koppelhus 1996).

8.1.3.5 121.95 m: Middle Oxfordian – Kimmeridgian.

The occurrences of *Glossodinium dimorphum* and *Cribroperidinium globatum* group indicate an age not older than Middle Oxfordian (Riding 1987; Riding and Thomas 1992). The occurrence of *Endoscrinium luridum* at 114 m according to IKU/Sintef indicates an age not younger than the Kimmeridgian (Riding and Thomas 1992).

8.1.4. Comparison between the stratigraphic conclusions of the present study and the IKU/Sintef-report

A comparison of the stratigraphic conclusions in the IKU/Sintef report and those of the present study are shown in figure 8.1.

- The present study narrows the possible age of the interval from 182.5 m to 154.55 m to the Late Pliensbachian rather than a broad Late Sinemurian to Late Pliensbachian age as indicated by IKU/Sintef.

- Strong evidence for an Early Toarcian age of the interval between 154.55 m and 142.22 m is presented in the present study, while no indications of Aalenian deposits were found. A mid-Bajocian and/or Bathonian age are suggested for the interval 141.55 m – 128.18 m. IKU/Sintef indicates an undifferentiated Toarcian – Aalenian age of the interval from 159.2 m – 124.32 m.

- According to IKU/Sintef the Lower/Middle Jurassic transition is located around 123.15 m. This transition is located around 142 m according to the present study.

- There is a general agreement to a Middle Oxfordian – Kimmeridgian age of the deposits around 122 m. Studies of more samples from this level could possibly narrow the suggested stratigraphic relationship.

Some of the explanations for these discrepancies may be that the only dinocyst taxa recorded by IKU/Sintef in the interval below 142.51 m is *Nannoceratopsis* sp. In the present study additional stratigraphically very useful dinocyst species (e.g. *Mendicodinium reticulatum* and *Luehndea spinosa*) were recorded. Furthermore, the IKU/Sintef report does not show abundance variations in the range chart for spores and pollen and does not mention abundance of *Spheripollenites* in any samples.

8.2 Palynofacies

The assemblage of organic sedimentary particles (the palynofacies) was studied in 7 samples from the interval from 182.50 m to 134.95 m in order to add information to the interpretation of the depositional environment and to aid in the identification and characterisation of the Lower Toarcian. A minimum of 500 organic sedimentary particles were referred to one of the following five categories; amorphous organic matter (AOM), black wood (carbonised wood fragments), brown wood, cuticles and membranes, and palynomorphs. Then a minimum of 200 palynomorphs was referred to one of the groups: microspores, non-saccate pollen, bisaccate pollen, freshwater algae, acritarchs, dinoflagellate cysts and other marine algae. The environmental indications of these groups are summarised in table 1 and 2 in Rasmussen & Dybkjær (2005) and the results are presented in fig. 10.2. Tyson (1995) gives a thorough discussion of the use of organic sedimentary particles as indicators of palaeoenvironments.

8.2.1. General description

The organic sedimentary particles are dominated by brown wood and terrestrial palynomorphs (mainly bisaccate and non-saccate pollen). The two lowermost and the two uppermost samples (182.50 m, 162.95 m, 141.55 m and 134.95 m) are dominated by brown wood, while the three middle samples (146.37 m, 144.66 m, 142.76 m) are dominated by terrestrial palynomorphs. In the sample at 141.55 m no less than 90% of the organic sedi-

mentary particles are brown wood particles and the black wood particles show a coinciding maximum of 6%.

The palynomorphs are dominated by non-saccate pollen, except for the sample at 134.95 m, which is dominated by microspores, especially *Deltoidospora toralis* (Enclosure 3). Dinoflagellate cysts only occur in the lower three samples (182.50 m, 162.95 m, 146.37 m). Acritarchs comprise 12% of the palynomorphs in the lowermost sample and occur up to 144.66 m. No marine palynomorphs were recorded from the samples in the interval 142.76 m to 134.95 m - that is if the small, round spheres here referred to *Spheripollenites* (a pollen genus) are not interpreted as marine algae as suggested by Bucefalo Palliani and Riding (2000).

8.2.2. Interpretation

Generally the high influx of wood particles and terrestrial palynomorphs in all the studied samples indicate a marginal marine to non-marine depositional environment.

The strong dominance of wood particles and terrestrial palynomorphs in the lower two samples (182.50 m, 162.95 m) combined with the occurrence of acritarchs and dinocysts strongly indicate a near-shore, shallow marine environment with a high influx of terrestrial organic matter and a relatively high energy level.

The increase in relative abundance of palynomorphs in the three middle samples probably reflects a change towards a lower energy environment compared with the samples below. The occurrence of a few dinocysts in the samples at 146.37 m and 144.66 m and of a few acritarchs in the sample at 142.76 m (see Enclosure 3) indicates that the depositional environment continuously were marine.

The sudden increased relative abundance of AOM in the sample at 144.66 m indicates anoxic to dysoxic conditions at the seafloor (e.g. Tyson 1995). A corresponding peak in relative abundance of AOM was also recorded by Dybkjær (1991) in the Lower Toarcian of the Stenlille-1 well and was related to the Early Toarcian marine flooding. The lack of dinocysts in this sample and in the sample at 142.76 m, may be related to the widespread dysoxic or anoxic conditions being unfavourable for the dinocysts and resulting in a distinct turnover in the dinocyst assemblage, see further discussion in Bucefalo Palliani and Riding (2000).

The strong dominance in the sample at 141.55 m of brown wood particles combined with the maximum of black wood particles strongly indicates a well-oxygenated, high energy depositional environment. The lack of marine palynomorphs indicates a non-marine depositional environment.

The spores referred to *Deltoidospora toralis*, which totally dominate the palynomorphs in the samples at 134.95 m, represent ferns. The majority of ferns that have been found in European Jurassic floras are considered to be part of moist lush vegetation, often occurring near river banks (e.g. Van Konijnenburg-Van Cittert 1984; Van Konijnenburg-Van Cittert and Van der Burgh 1989, see further Abbink 1998). This sample thus probably represents a floodplain environment.

8.2.3. Palynofacies summary

182.50 m: shallow water, near-shore marine. High influx of terrestrial organic matter. Relatively high energy-level.

162.95 m: shallow water, near-shore marine. High influx of terrestrial organic matter. Relatively high energy-level.

146.37 m: near-shore marine, low energy. High influx of terrestrial organic matter.

144.66 m: possibly marine, anoxic to dysoxic, low energy. High influx of terrestrial organic matter.

142.76 m: possibly marine, low energy, well-oxygenated. High influx of terrestrial organic matter.

141.55 m: non-marine, well-oxygenated, high energy depositional environment.

134.95 m: non-marine, well-oxygenated, high energy depositional environment. Possibly a floodplain environment.

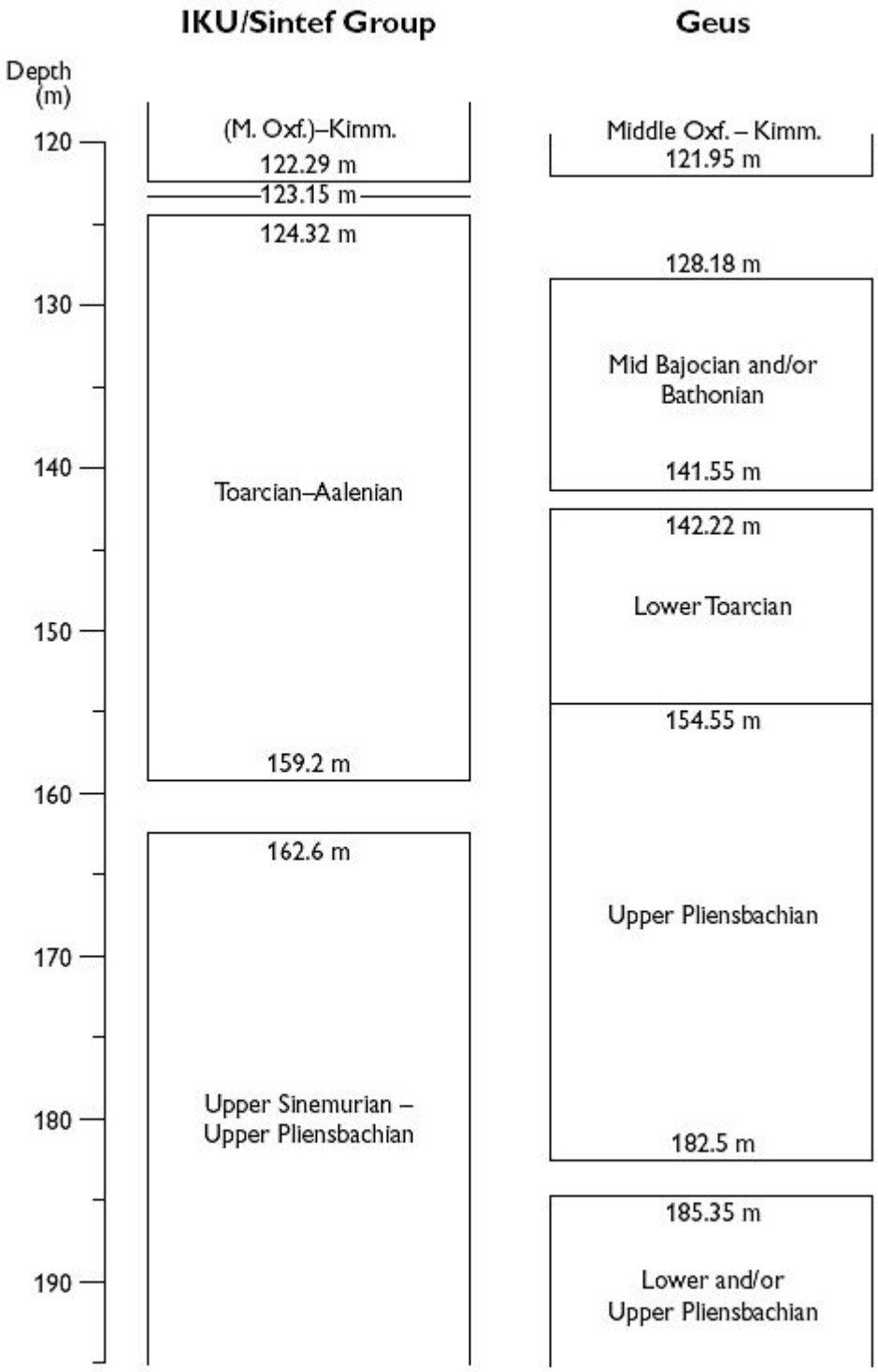

Figure. 8.1. *Biostratigraphic subdivision of N-IKU 13/1-U-1 according to IKU/Sintef Group and according to GEUS, respectively.*

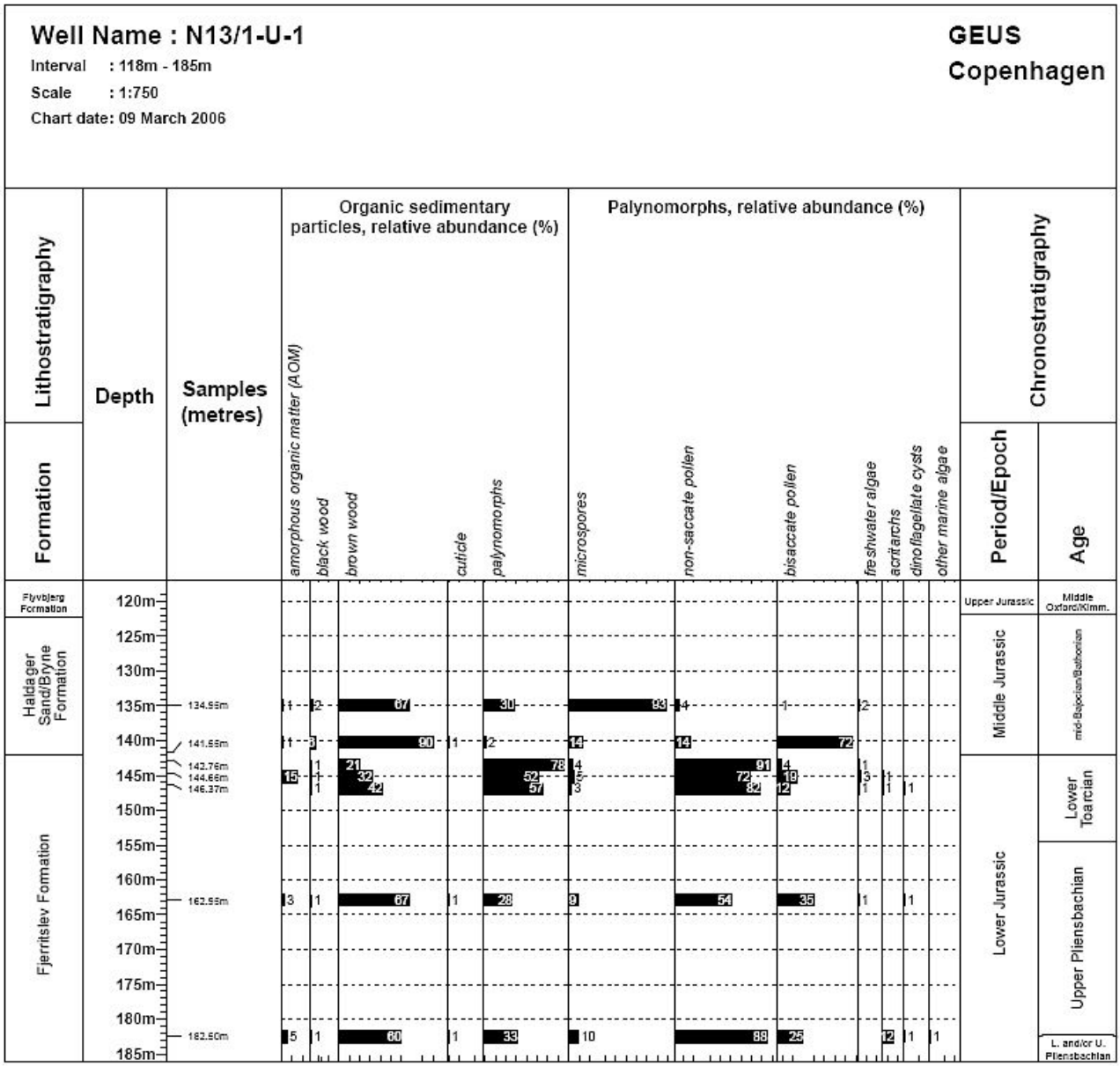

Figure. 8.2. *Relative abundance of organic sedimentary particles and palynomorphs.*

9.0 Neogene uplift and exhumation

This section aims to present an integrated interpretation of the magnitude of Cenozoic exhumation in Denmark. The results may be applied by correcting the present day burial depth for Neogene uplift when the quality of the potential reservoirs is predicted in undrilled area. The study combines “thermal history reconstruction”, based on apatite fission track analysis (AFTA) and vitrinite reflectance (VR) (e.g. Green et al. 2002) with exhumation studies based on sonic velocities and stratigraphic considerations (e.g. Japsen 1998, 2000; Japsen & Bidstrup 1999; Petersen et al. 2003; Japsen et al.2007). In particular the estimations are based on new AFTA data from eight Danish wells (e.g. from the Felicia-1 well; Green 2005). The results underline the advantages of exhumation studies based on palaeo-thermal and sonic data, and especially the benefits of integrating information from both approaches.
Table 1 shows the estimated amount of removed section and the estimated time of maximum burial for 8 wells based on thermal and sonic data: Års-1, Børglum-1, Farsø-1, Felicia-1, Gassum-1, Hans-1, Sæby-1 and Tønder-2,-3. Maximum burial of the Mesozoic succession occurred during the Cenozoic apart from the Hans-1 well where maximum burial of the pre-mid-Cretaceous section occurred during mid-Cretaceous time.

The map in Figure 1 shows the amount of section removed during the Cenozoic in the study area based on a revision of the work reported by Japsen & Bidstrup (1999). Compared to their values the following values have now been estimated: Års-1 600 m, Børglum-1 700 m, Farsø-1 600 m, Frederikshavn-1 750 m, Gassum-1 600 m, Hans-1 1000 m, J-1 800 m (based on basin modelling with a lower geothermal gradient than the previous estimate), Sæby-1 700 m, Terne-1 700 m (based on sonic data for the Skagerrak Fm), and Tønder-2,-3 200 m.

The map furthermore indicates the time of Cenozoic maximum burial:
1) In most of the area maximum burial occurred prior to late Neogene erosion. According to the AFTA data from Års-1, Farsø-1 and Gassum-1 onset of cooling occurred between 10 and 5 Ma. The presence of mid and late Miocene deposits in parts of the exhumed area indicates that the uplift occurred very late, probably at 5 Ma or even later i.e. during the Pliocene.
2) In the northern part of the area maximum burial occurred during the mid-Cenozoic (c. 25 Ma) based on the interpretation of AFTA data from the Hans-1 well, which suggest onset of cooling between 30 and 20 Ma. The constraints on the timing are poorer in the Felicia-1, 1A well, where the AFTA data suggest cooling between 45 and 20 Ma (Green 2005). The Felicia-1, -1A is located closely east of the Licence and closely southeast of the Farsund Basin, which contains the Lower Jurassic potential source rocks. Based on regional considerations it is likely that Early Oligocene delta and shelf deposits made up a substantial part of the section that was removed at the location of Felicia-1. It is thus assumed that the maximum burial at the Felicia-1, 1-A well occurred in the late part of the time period from 45 to 20 Ma. In the Hans-1 well cooling took place in Late Oligocene time and the cooling phase in both wells probably corresponds to the Late Oligocene hiatus that is recognised in wells and outcrops in the Danish Basin.

The time of maximum burial southwest of the Licence area at the F-1 and K-1 wells is not well constrained due to the lack of AFTA data, but in the area where the Oligocene wedges are likely to have been removed by erosion, the maximum burial is likely to have occurred around 25 Ma.

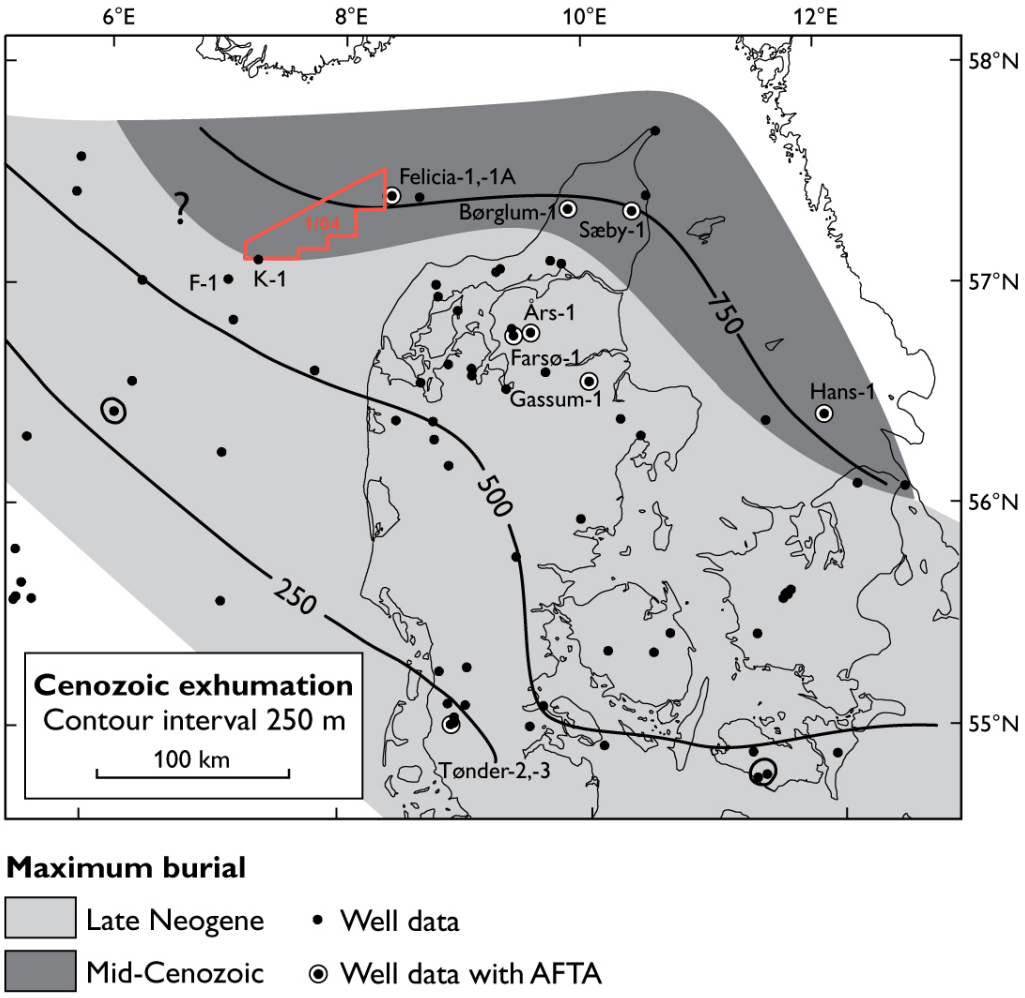

Figure. 9.1. *The map shows the estimated thickness of the section removed during Cenozoic exhumation based on numbers given by Japsen & Bidstrup (1999) with the modifications provided in this note (see Table 1). Maximum burial of the Mesozoic sediments (which contains the potential source rocks) generally occurred in late Neogene time in the areas south and west of the area where Oligocene wedges are prograding southwards from Norway based on the results from the Års-1, Farsø-1, Gassum-1 and Tønder-2, -3 wells. North and east of this area where the Chalk is deeply eroded or absent, the maximum burial is assumed to have occurred during the mid-Cenozoic as indicated by the presently available AFTA data from the Felicia-1, -1A, Børglum-1 and Hans-1 wells.*

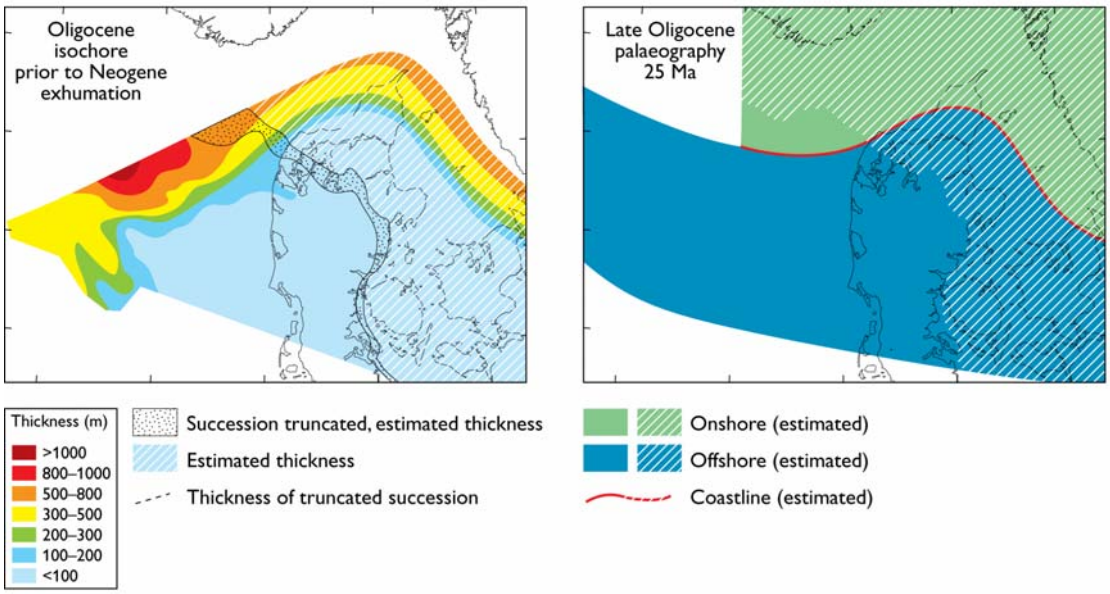

Figure.9.2. *Isochore and palaegeographic maps. The left figure shows Oligocene isochore; the western part shows preserved thickness while the isochore in the eastern part of the map is reconstructed based on estimates constrained by the total amount of section removed by exhumation (Table 1, Fig.1). The right figure shows Late Oligocene general paleogeography.*

9.1. Discussion

9.1.1. Reservoirs

Very limited direct information on the reservoir properties of the Upper Triassic–Lower Jurassic Gassum and the Middle Jurassic Haldager reservoirs are available from the Farsund Basin. Both reservoirs are proved to be present regionally and are expected to be present in the Farsund Basin sealed by Lower Jurassic and Upper Jurassic mudstones, respectively. Both reservoirs are present in much of the Norwegian-Danish Basin with fair to good porosities except over significant salt structures where the reservoirs are absent.

9.1.2 Cap rocks

The Gassum reservoir is overlain by laterally consistent, thick marine mudstones of the Fjerritslev Formation. Sandstone/siltstone stringers are present in the Fjerritslev Formation at several stratigraphic levels in Danish wells with increasing number and thickness toward the eastern and northern basin margins. Thin fine-grained shoreface sandstones formed during short-lived regressive events occur within the Lower Jurassic marine mudstones in the Fjerritslev Trough and Skagerrak-Kattegat Platform. The events can be traced relatively deep into the basin as thin silty intercalations in the mudstones. The sandstones are also expected to be present in the Farsund Basin. Their influence on seal capacity over the Gassum reservoir may be significant.

The Haldager reservoir is overlain by marine mudstones of the Flyvbjerg and Børglum formations. Sandstones are present in the lower and upper part of the Flyvbjerg Formation in places (e.g. Felicia-1, Fig. 5.8). Their thickness and grain size are expected to increase to north and east in the study area, where they locally may form an additional reservoir section. The middle part of the Flyvbjerg Formation is expected to be dominated by marine mudstones with some seal capacity, and the Flyvbjerg Formation it self is overlain by thick and regional continuous, marine mudstones of the Børglum Formation.

9.1.3 Neogene exhumation

Studies based on sonic velocity anomalies, vitrinite reflectance, geometric-stratigraphic considerations or apatite fission track analysis have all indicated a substantial Neogene exhumation of the northern and eastern part of the Norwegian-Danish Basin (e.g. Japsen 1993, 1998; Jensen & Schmidt 1992; Michelsen & Nielsen 1993; Japsen & Bidstrup 1999; Petersen et al. 2003). However, uncertainties exist when it comes to the precise amount of exhumation. The most comprehensive attempt to quantify the Neogene exhumation was presented by Japsen & Bidstrup (1999) who combined sonic data and 1D basin modelling from 68 Danish wells. Their results suggest ca. 750–1000 m of exhumation in the Farsund Basin being largest close to the Norwegian coast. The new vitrinite reflectance data from the Felicia-1/1A well indicates 800 m (Petersen & Nielsen 2005) compared to 800–1000 from the new AFTA data, 1020 m based on shale velocities and 712 m based on chalk velocities. Poor AFTA data from the IKU/Sintef shallow cores northeast of the Farsund Basin suggest erosion of 1.8–2.2 km of sediment, but constraints on the paleotemperature are

very poor. Jensen & Schmidt (1993; their Fig. 8) suggested 1500–1800 m in the same area. VR data suggest more exhumation in F-1 and K-1 than in Felicia-1/1A (as also suggested by Jensen & Schmidt 1993 based partly on the same data set), which seems to contradict the evidence from the thickness of preserved Cenozoic strata in these wells. On the other hand, the original thickness of the Cenozoic is unknown and the trend of the exhumation contours may be more complicated than previously thought. Hence, a number of considerations including sonic, VR, AFTA and stratigraphic data are recommended for the crucial estimation of Neogene exhumation of the Farsund Basin.

The apatite fission track analysis carried out on samples form Felicia-1/1A indicates that cooling (uplift/erosion) began in mid-Cenozoic time between 45–20 Ma, followed by a renewed subsidence phase and then a subsequent cooling from a lower temperature between 15–0 Ma. Thus the maximum temperature for the potential source rocks was reached between 45 and 20 Ma (Geotrack report 941; Japsen et al.2007).

10. Conclusion

The structural and stratigraphic development of eastern Norwegian-Danish Basin is relatively well documented by interpretations of the available seismic and well data. These data provides a framework for the predictions of undrilled stratigraphy. The data indicate several stratigraphic units which contain potential reservoirs for CO_2 storage. In this collection of information the emphasis has been on the Upper Triassic–Lower Jurassic Gassum Fomation and the Middle Jurassic Haldager Sand Formation, which both provides a large potential for CO_2 storage within the study area.

Well data is very sparse from the Norwegian sector in the eastern part of the basin. This report thus compiles a large amount of Danish well data, which in combination with available seismic data and new information from the IKU/Sintef core wells provide robust guidelines for the predictions of reservoir properties in undrilled areas. The scope of the report has mainly been to supplement previous reporting to the project group by integrating the data and to provide the group with the primary data that can facilitate predictions of reservoir properties at the local areas selected by Universitet i Oslo, UiO for detailed modelling.

11. References

Abbink, O., 1998. Palynological investigations in the Jurassic of the North Sea region. LPP Contributions Series 8, 192pp.

Ahlberg, A., Olsson, I., Simkevicius, P. 2003. Triassic-Jurassic weathering and clay minerals dispersal in basement areas and sedimentary basins of southern Sweden. Sedimentary Geology 161, 15-29.

Andsbjerg, J., Nielsen, L.H., Johannessen, P. & Dybkjær, K. 2001: Divergent development of depositional environments in the Danish Central Graben and the Norwegian-Danish Basin following the Jurassic North Sea Doming event. In: O.J. Martinsen & T. Dreyer (eds): Sedimentary environments offshore Norway – Palaeozoic to Recent. Norsk Petroleums Forening Special Publication 10, 175–197.

Anthonsen, K. L. and Nielsen, L. H. 2008: COC-02 Assessment of the potential for CO_2 storage in the Norwegian-Danish Basin, International Geological Conference, Olso, 2008 (Abstract).

Anthonsen, K.L., Vangkilde-Pedersen, T. & Nielsen, L.H. 2009: Estimates of CO2 storage capacity in Europe. Climate Change: Global Risks, Challenges & Decisions. 10-12 March, 2009. Copenhagen. University of Copenhagen & International Alliance of Research Universities (IARU). IOP Conference Series: Earth and Environmental Science 6, 1 p.

Anthonsen, K.L., Frykman, P. & Nielsen, L.H. 2011: The potential for geological storage of CO_2 in Denmark is very promising. Risø International Energy Conference 2011. Energy systems and technologies for the coming century. Risø DTU 10–12 May. Proceedings 48–55.

Audigane, P., Gaus, I., Czernichowski-Lauriol, I., Pruess, K. & Xu, T. 2007: Two-dimensional reactive transport modelling of CO_2 injection in a saline aquifer at the Sleipner site, North Sea. American Journal of Science **307**, 974–1008.

Baccar, M.B., Fritz, B. & Madé, B., 1993. Diagenetic albitization of K-feldspar and plagioclase in sandstone reservoirs: thermodynamic and kinetic modelling. Journal of Sedimentary Petrology 63, 6, 1100-1109.

Bailey, A. M., Roberts, H. H. & Blackson, J. H. 1998. Early diagenetic minerals and varables influencing their distribution in two long cores (> 40 m), Mississippi River delta plain. Journal of Sedimentary Research 68, 185-197.

Baines, S. J. and Worden, R. H. 2004. The long-term fate of CO_2 in the subsurface: natural analogues for CO_2 storage. In: Baines, S. J. and Worden, R. H. (eds.), Geological storage of carbon dioxide. Geological Society of London, Special Publication 233, 59-85.

Binot, F. Röhling, H. G. 1988: Lithostratigraphie und natürliche Gammastrahlung des Mittleren Buntsandsteins von Helgoland – Ein Vergleich mit der Nordseebohrung J/18-1. Zeitschrift der Deutschen Geologischen Gesellschaft 139, 33-49.

Barker, C.E., 2000. A paleolatitude approach to assessing surface temperature history for use in burial heating models. Int. J. Coal Geol. 43, 121–135.

Barker, C.E. and Pawlewicz, M.J., 1994. Calculation of vitrinite reflectance from thermal histories and peak temperatures. A comparison of methods. In: Mukhopadhyay, P.K. and Dow, W.G. (eds.), Vitrinite reflectance as a maturity parameter. Applications and limitations. ACS Symp. Ser. 570, 216–229.

Batten, D.J. and Koppelhus, E.B., 1996. Chapter 20D. Biostratigraphic significance of uppermost Triassic and Jurassic miospores in Northwest Europe. . In: Jansonius, J.

and McGregor, D.C. (ed.), *Palynology: principles and applications*; American Association of Stratigraphic Palynologists Foundation, Vol. 2, 795–806.

Bergström, J., Holland, B., Larsson, K., Norling, E. & Sivhed, U., 1982: Guide to excursions in Scania. Sveriges Geologiska Undersökning, Ser. Ca 54, 95 pp.

Bertelsen, F. 1978: The Upper Triassic – Lower Jurassic Vinding and Gassum Formations of the Norwegian–Danish Basin. Danmarks Geologiske Undersøgelse Serie B 3, 26 pp.

Bertelsen, F. 1980: Lithostratigraphy and depositional history of the Danish Triassic. Danmarks Geologiske Undersøgelse Serie B 4, 59 pp.

Berthelsen, A. 1992: From Precambrian to Variscan Europe. In: Blundell, D., Freeman, R. & Mueller, S. (eds): A continent revealed. The European geotraverse, 153–163. Cambridge: Cambridge University Press.

Bjørlykke, K., Aagaard, P., Dypvik, H., Hastings, D.S., Harper, A.S., 1986. Diagenesis and reservoir properties of Jurassic sandstones from the Haltenbanken area, offshore mid-Norway. In: Spencer, A.M., Holter, E., Campell, C.J., Hanslien, S.H., Nelson, P.H.H., Nysaether, E., Ormaasen, E.G. (Eds.), Habitat of Hydrocarbons on the Norwegian Continental Shelf. Graham and Trotman, London, pp. 275– 286.

Bjørlykke, K., 1998, Clay mineral diagenesis in sedimentary basins; a key to the prediction of rock properties, examples from the North Sea Basin. Clay Minerals 33, 15-34.

Boles, J. R. and Ramseyer, K. 1988: Albitization of plagioclase and vitrinite reflectance as paleothermal indicators, Sand Joaquin Basin. SEPM Pacific Section, 219-139.

Bridges, E. M. 1997: World soils, 3rd edition, University Press, Cambridge, United Kingdom, 170p.

Burley, S. 1984: Patterns of diagenesis in the Sherwood Sandstone Group (Triassic), United Kingdom. Clay Minerals 19, 403-440.

Burley, S., Kantorowicz, J. D. and Waugh, B. (1985). "Clastic diagenesis." Journal of Sedimentary Petrology 49, 53-70.

Bonde, N., 1979. Palaeoenvironment in the “North Sea” as indicated by the fish bearing Mo clay deposits (Paleocene/Eocene), Denmark. Meded. Wekgrp. Tert. Kwart. Geol. 2 29–36.

Britze, P. & Japsen, P. 1991: Geological map of Denmark 1:400 000. The Danish Basin. "Top Zechstein" and the Triassic. Danm. geol. unders. Map series 31.

Bucefalo Palliani, R., Mattiole, E. and Riding, J.B., 1998. Timing and palaeoceanography of Lower Toarcian (Jurassic) marine anoxic events: a comparison between the Boreal and Tethyan realms. Abstract volume for the symposium “Strata 2000”, Paris, September 1998.

Bucefalo Palliani, R. and Riding, J.B., 2000. A palynological investigation of the Lower and lowermost Middle Jurassic strata (Sinemurian to Aalenian) from North Yorkshire, UK. Proceedings of the Yorkshire Geological Society 53 (1), 1–16.

Chadwick, A., Arts, R., Bernstone, C., May, F., Thibeau, S. & Zweigel, P. 2009: Best practice for the storage of CO_2 in saline aquifers. British Geological Survey Occasional Publication **14**, 267p.

Charnock, M.A., Kristiansen, I.L., Ryseth, A. and Fenton, J.P.G., 2001. Sequence stratigraphy of the Lower Jurassic Dunlin Group, northern North Sea. In: O.J. Martinsen & T. Dreyer (eds) Sedimentary Environments Offshore Norway – Palaeozoic to Recent. NPF Special Publication 10, 145–174.

Choi, K. S., Khim, B. K. & Woo, K. S. 2003: Spherulitic siderites in the Holocene coastal deposits of Korea (eastern Yellow Sea). Elemental and isotopic composition and depositional environment. Marine Geology 202, 17-31.

Christensen, O.B., 1971: Den stratigrafiske inddeling af præ-zechstein aflejringerne i Rønde nr. 1. In Rasmussen, L.B. (ed.): Dybdeboringen Rønde nr. 1 på Djursland. Danmarks geologiske Undersøgelse III Række 40, 119-123.

Christensen, O.B., 1973: Rønde og Nøvling formationerne (silur) i Nøvling nr. 1 (3534-3762 m). In Rasmussen, L.B. (ed.): Dybdeboringen Nøvling nr. 1 i Midtjylland. Danmarks geologiske undersøgelse III Række 40, 150-157.

Christensen, J.E. & Korstgård J.A. 1994: The Fjerritslev Fault offshore Denmark – salt and fault interactions. First Break 12, 31–42.

Clausen, O. R. and Pedersen, P. K. 1999: Late Triassic structural evolution of the southern margin of the Ringkøbing-Fyn High, Denmark. Marine and Petroleum Geology **16**, 653-665.

Clemmensen, L. B. 1979. Triassic lacustrine red-beds and palaeoclimate: The "Buntsandstein" of Helgoland, Geologische Rundschau 74, 519-536.

Clemmensen, L.B., 1985. Desert sand plain and sabkha de- posits from the ***Bunter*** Sandstone Formation (L. Triassic) at the northern margin of the German Basin. Geologische Rundshau 74, 519-536.

Coleman, M. L. and Raiswell., R. 1981: "Carbon, oxygen and sulphur isotope variations in concretions from the Upper Lias of N. E. England." Geochimical et Cosmochimical Acta 45, 329-340.

Coleman, M. L. 1993: Microbial processes: Controls on the shape and composition of carbonate concretions. Marine Geology 113, 127-140.

Cohen, A.D., Raymond, Jr., Archuleta, L.M. and Mann, D.A., 1987. Preliminary study of the reflectance of huminite macerals in recent surface peats. Org. Geochem. 11, 429–430.

Dinesen, A., Michelsen, O. & Liberkind, K., 1977. A survey of the Paleocene and Eocene deposits of Jylland and Fyn. Danm. Geol. Unders., Ser. B.1, 15 pp.

Dow, W.G., 1977. Kerogen studies and geological interpretations. J. Geol. Explo. 7, 79–99.

Dybkjær, K., 1988. Palynological zonation and stratigraphy of the Jurassic section in the Gassum No. 1-borehole, Denmark. D.G.U. Ser. A 21. 73pp.

Dybkjær, K., 1991. Palynological zonation and palynofacies investigation of the Fjerritslev Formation (Lower Jurassic – basal Middle Jurassic) in the Danish Subbasin. D.G.U. Ser. A 30. 150 pp.

Ehrenberg, S.N., 1990. Relationship between diagenesis and reservoir quality in sandstones of the Garn Formation, Haltenbanken, mid-Norwegian continental shelf. AAPG Bull. 74, 1538– 1558

Ehrenberg, S**. N. 1993.** Preservation of anomalously high porosity in deeply buried sandstones by grain-coating chlorite; examples from the Norwegian continental shelf. AAPG Bulletin 77, 1260-1286.

Erlström, M.,1990. Petrology and deposition of the Lund Sandstone, Upper Cretaceous, southwestern Scania. Sveriges Geologiska Undersökning Forskningsrapporter, Ca 74, 1–91.

Erlström, M., 1994. Evolution of Cretaceous sedimentation in Scania. Lund Publications in Geology No 122, 38 pp.

Erlström, M., Thomas, S.A., Deeks, N. & Sivhed, U. 1997. Structure and tectonic evolution of the Tornquist Zone and adjacent sedimentary basins in Scania and the southern Baltic Sea area. Tectonophysics 271, 191–215.

Erlström, M. & Sivehed, U., 2001. Intra-cratonic dextral transtension and inversion of the southern Kattegat on the southwest margin of Baltica – Seismostratigraphy and structural development. Sveriges Geologiska Undersökning C 832, 33 pp.

EUGENO-S Working Group 1988: Crustal structures and tectonic evolution of the transition between the Baltic Shield and the North German Caledonides (the EUGENO-S Project). Tectonophysics 150, 253–348.

Fine, S. 1986: The diagenesis of the Lower Triassic Bunter Sandstone Formation, Onshore Denmark: Geological Survey of Denmark, A 15.

Friis, H. 1987: Diagenesis of the Gassum Formation Rhaetian-Lower Jurassic, Danish Subbasin. Geological Survey of Denmark **A 18**, 41pp.

Friis, H., Mikkelsen, J. & Sandersen, P. 1998, Depositional environment of the Vejle Fjord

Formation of the Upper Oligocene-Lower Miocene of Denmark: A backisland/barrier-protected depositional complex: Sedimentary Geology 17, p. 221–244.

Frykmann, P., Nielsen, L.H., Vangkilde-Petersen, T. & Anthonsen, K. 2009: The potential for large-scale, subsurface geological CO_2 storage in Denmark.In: Bennike, O., Garde, A.A. & Watt, W.S. (eds): Review of Survey activities 2008. Geological Survey of Denmark and Greenland Bulletin 17, 13-16.

Gaus, I., Azaroual, M. & Czernichowski-Lauriol, I. 2002: Preliminary modelling of the geochemical impact of CO_2 injection on the caprock at Sleipner. Confidential report, BRGM/RP-52081, 44pp.

Green, P. F. 2005. Thermal history reconstruction in offshore Denmark well Felicia-1 based on AFTA and VR data. A report prepared for GEUS, Copenhagen, on behalf of DONG. Geotrack Report 941, 30 pp.

Green, P. F., Duddy, I. R. & Hegarty, K. A. 2002. Quantifying exhumation from apatite fission-track analysis and vitrinite reflectance data: precision, accuracy and latest results from the Atlantic margin of NW Europe. In: Doré, A. G., Cartwright, J., Stoker, M. S., Turner, J. P. and White, N. Exhumation of the North Atlantic Margin: Timing, mechanisms and Implications for Petroleum Exploration. Geological Society Special Publication, 196, 331–354.

Guy-Ohlson, D., 1986. Jurassic palynology of the Vilhelmsfält Bore No. 1, Scania, Sweden, Toarcian – Aalenian. Sec. Palaeobot., Swedish Mus. Nat. Hist., Stockholm. 127 pp.

Harris, N. B. 1992. Burial diagenesis of the Brent sandstones: a study of the Statfjord, Hutton and Lyell fields. In Moron, A. C., Haszeldine, R. S., Giles, M. R., Brown, S. Geology of the Brent Group. Special Publications of the Geological Society of London 61, 351-375.

Hendry, J. P., Wilkinson, M., Fallick, A. E. and Haszeldine, R. S. 2000: Ankerite cementation in deeply buried Jurassic sandstone reservoirs of the Central North Sea. Journal of Sedimentary Research 70, 227–239.

Hesselbo, S.P., Gröcke, D.R., Jenkyns, H.C., Bjerrum, C.J., Farrimond; P. Morgans, H.S. & Green, O.R., 2000. Massive dissociation of gas hydrate during a Jurassic oceanic anoxic event. Nature 406, 392–395.

Hoelstad, T., 1985. Palynology of the uppermost Lower to Middle Jurassic strata on Bornholm, Denmark. Bull. Geol. Soc. Denmark 34, 111–132.

Japsen, P., 1993. Influence of lithology and Neogene uplift on seismic velocities in Denmark: Implications for depth conversions on maps. AAPG Bull. 77, 194–211.

Japsen, P., 1998. Regional velocity-depth anomalies, North Sea chalk: A record of overpressure and Neogene uplift and erosion. AAPG Bull. 82, 2031–2074.

Japsen, P. 2000. Investigation of multi-phase erosion using reconstructed shale trends based on sonic data. Sole Pit axis, North Sea. Global and Planetary Change 24, 189-210.

Japsen, P. & Langtofte, C. 1991: Geological map of Denmark 1:400 000 "Top Trias" and the Jurassic-Lower Cretaceous. Danmarks geologiske undersøgelse Map series 30.

Japsen, P. & Bidstrup, T. 1999. Quantification of late Cenozoc erosion in Denmark based on sonic data and basin modelling. Bulletin of the Geological Society of Denmark 46, 79–99.

Japsen, P., Bidstrup, T. & Lidmar-Bergström, K., 2002a. Neogene uplift and erosion of southern Scandinavia induced by the rise of the South Swedish Dome. From Doré, A.G. et al.: Exhumation of the North atlantic Margin: Timing, Mechanisms and Implications for Petroleum Exploration. Geological Society. London. Spec. Publ. 196, 183–207.

Japsen, P., Bidstrup, T. and Rasmussen, E.S., 2002b:.Cenozoic evolution of the eastern Danish North Sea. Discussion, Mar. Geol. 186, 571-575.

Japsen, P., Green, P. F., Nielsen, L. H., Rasmussen, E. S. and Bidstrup, T. 2007: Mesozoic–Cenozoic exhumation events in the eastern North Sea Basin A multi-disciplinary study based on palaeothermal, palaeoburial, stratigraphic and seismic data. Basin Research 19, 451–490.

Jensen, L.N. and Schmidt, B.J., 1993. Neogene uplift and erosion offshore south Norway: Magnitudes and consequences for hydrocarbon exploration in the Farsund Basin. In: Spencer, A.M. (ed.), Generation, accumulation and production of Europe's hydrocarbons III. Spec. Publ. Euro. Assoc. Petrol. Geosc. 3, Springer-Verlag Berlin Heidelberg, 79–88.

Kastner, M. and Siever., R. 1979: "Low temperature feldspars in sedimentary rocks." American Journal of Science 279, 435-479.

Krabbe, H. & Nielsen, S. 1984: Rapport om bulk- og lermineralogien i de danske landboringer Års-1 og Farsø-1. Geologisk Institut, Aarhus Universitet, 66pp.

Koch, B.E. 1989. Geology of the Søby-Fsterholt area. Geological Survey Denmark, Series A 22 177 pp.

Koch, J.-O., 1983. Sedimentology of Middle and Upper Jurassic sandstone reservoirs of Denmark. Geologie en Mijnbouw 62, 115–129.

Koppelhus, E.B., 1991. Palynology of the Lower Jurassic Rønne formation on Bornholm, eastern Denmark. Bulletin of the Geological Society of Denmark 39, 91–110.

Koppelhus, E.B. and Nielsen, L.H., 1994. Palynostratigraphy and palaeoenvironments of the Lower to Middle Jurassic Bagå Formation of Bornholm, Denmark. Palynology 18, 139–194.

Koppelhus, E.B. and Batten, D.J., 1996. Chapter 20C. Application of a palynomorph zonation to a series of short borehole sections, Lower to Middle Jurassic, Øresund, Denmark. In: Jansonius, J. and McGregor, D.C. (ed.), *Palynology: principles and applications*; American Association of Stratigraphic Palynologists Foundation, Vol. 2, 779–793.

Kristin and Lavrans fields, offshore Mid-Norway. Marine and Petroleum Geology 19, 767-781.

Land, L.S., Fisher, R.S., 1987. Wilcox sandstone diagenesis, Texas Gulf coast: a regional isotopic comparison with the Frio Formation. In: Marshall, J.D. (Ed.), Diagenesis of Sedimentary Sequences. Spec. Publ.-Geol. Soc. London, vol. 36, pp. 219–235.

Lander, R.H., Larese, R.E. and Bonell, L.M., 2008. Toward more accurate quartz cement models: The importance of euhedral versus noneuhedral growth rates. AAPG Bulletin, 92: 1537-1563

Laier, T. 1989: Mapping of low enthalpy brines in Denmark for geothermal exploitation. Water-Rock Interaction.

Larsen, G. & Dinesen, A., 1959: Vejle Fjord Formationen ved Brejning. Sedimenterne og foraminiferfaunaen (Oligocæn-Miocæn). Danmarks Geologiske Undersøgelse 2. Række **82**, 114 pp.

Larsen, F. 1986: En sedimentologisk og diagenetisk undersøgelse af Gassum Formationen – II. Kvartscementering af sandsten i Gassum Formationen. Upubliceret Speciale ved Københavns Universitet, 100pp.

Larsen, O. 1971: K/Ar age determinations from the Precambrian of Denmark. Danmarks geologiske undersøgelse II Række 97, 37 pp.

Larsen, O. 1972: Kalium/argon datering af prøver fra danske dybdeboringer. Dansk geol. Fören. Årsskrift for 1971, 91-94.

Liboriussen, J., Ashton, P. & Tygesen, T. 1987: The tectonic evolution of the Fennoscandian Border Zone in Denmark. Tectonophysics 137, 21-29.

Loh, H., Maul, B., Prauss, M. and Riegel, W., 1986. Primary production, maceral formation and carbonate species in the Posidonia shales of NW Germany. Mitteilungen aus dem Geologisch-Paläontologischen Institüt der Universitat Hamburg 60, 397–421.

Lund, J.J., 1977. Rhaetic to Lower Liassic palynology of the onshore south-eastern North Sea Basin. Danm. Geol. Unders. II Række 109. 130pp

Lund, J.J. and Pedersen, K.R., 1985. Palynology of the marine Jurassic formations in the Vardekløft ravine, Jameson Land, East Greenland. Bull. Geol. Soc. Denmark 33(3–4), 371–399.

Machemer, S. D. & Hutcheon, I. E.. 1988. Geochemistry of early carbonate cements in the Cardium Formation, Central Alberta. Journal of Sedimentary Petrology **58**, 136-147.

Majorowicz, J.A., Jones, F.W., Ertman, M.E., Osadetz, K.G. and Stasiuk, L.D., 1990. Relationship between thermal maturation gradients, geothermal gradients and estimates of the thickness of the eroded foreland section, southern Alberta Plains, Canada. Mar. Petrol. Geol. 7, 138–152.

Mansurbeg, H., Morad, S., Salem, A., Marfil, R., El-ghali, M.A.K., Nystuen, J.P., Caja, M.A. Amorosi, A., Garcia, D. & La Iglesia, A., 2008. Diagenesis and reservoir quality evolution of palaeocene deep-water, marine sandstones, the Shetland-Faroes Basin, British continental shelf. Marine and Petroleum Geology 25, 514-543.

Marcussen, Ø., Maast, T. E., Mondol, N. H., Jahren, J, Bjørlykke, K. 2010: Changes in physical properties of a reservoir sandstone as a function of burial depth – The Etive Formation, northern North Sea. Marine and Petroleum Geology 27, 1725-1735.

Mathiesen, A., Kristensen, L., Bidstrup, T. & Nielsen, L. H. 2009: Vurdering af det geotermiske potentiale i Danmark. Danmark og Grønlands geolgosiek undersøgelse Rapport **2009/59**, 30p.

McBride, E. F. 1963: A classification of common sandstones. Journal of Sedimentary Petrology **33**, 664-669.

Michelsen, O. 1978. Stratigraphy and distribution of Jurassic deposits of the Norwegian–Danish Basin. Danmarks Geologiske Undersøgelse Serie B 2, 28 pp.

Michelsen, O. 1989a. Revision of the Jurassic lithostratigraphy of the Danish Subbasin. Danmarks geologiske undersøgelse Ser. A 24, 21 pp.

Michelsen, O. 1989b. Log-sequence analysis and environmental aspects of the Lower Jurassic Fjerritslev Formation in the Danish Subbasin. Danmarks geologiske undersøgelse Ser. A, 25, 23 pp.

Michelsen, O., 1997. Mesozoic and Cenozoic stratigraphy and structural development of the Sorgenfrei-Tornquist Zone. Z. dt. Geol. Ges. 148, 33–50.

Michelsen, O. & Nielsen, L.H. 1991: Well records on the Phanerozoic stratigraphy in the Fennoscandian Border Zone, Denmark. Danmarks Geologiske Undersøgelse Serie A 29, 37 pp.

Michelsen, O. & Nielsen, L.H. 1993: Structural development of the Fennoscandian Border Zone, offshore Denmark. Marine and Petroleum Geology 10, 124–134.

Michelsen, O., Nielsen, L.H., Johannessen, P.N., Andsbjerg, J. & Surlyk, F. 2003: Jurassic lithostratigraphy and stratigraphic development onshore and offshore Denmark. In: Ineson, J.R. & Surlyk, F. (eds): The Jurassic of Denmark and Greenland. Geology of Denmark Survey Bulletin 1, 147–216.

Morad, S., Bergen, M., Knarud, R., Nystuen, J.P., 1990. Albitization of detrital plagioclase in Triassic reservoir sandstones from the Snorre field, Norwegian North Sea. Journal of Sedimentary Petrology 60, 411-425

Michelsen, O. & Clausen, O.R. 2002: Detailed stratigraphic subdivision and regional correlation of the southern Dansih Triassic succession. Marine and Petroleum Geology 19 563–587.

Michelsen, O., Thomsen, E., Danielsen, M., Heilmann-Clausen, C., Jordt, H. & Laursen, G.V. 1998: Cenozoic sequence stratigraphy in the eastern North Sea. In: De Graciansky P.C. *et al.* (eds): Mesozoic–Cenozoic sequence stratigraphy of western European basins. Society of Economic Paleontologists and Mineralogists Special Publication 60, 91–118**.**

Mogensen, T.E. 1994: Palaeozoic structural development along the Tornquist Zone, Kattegat area, Denmark. In: Cloetingh *et al*. (eds): Dynanmics of extensional basin formation and inversion. Tectonophysics 240, 191–214.

Mogensen, T.E. 1996: Triassic and Jurassic structural development along the Tornquist Zone, Kattegat, Denmark. Tectonophysics 252, 197-220.

Mogensen, T.E. & Korstgård 2003: In: Ineson, J.R. & Surlyk, F. (eds): The Jurassic of Denmark and Greenland. Geology of Denmark Survey Bulletin 1**,** 439–458.

Mogensen, T.E. & Jensen, L.N. 1994: Cretaceous subsidence and inversion along the Tornquist Zone from Kattegat to the Egersund Basin. First Break 12, 211–222.

Morgenroth, P., 1970. Dinoflagellate cysts from the Lias Delta of Lühnde/Germany. Neues Jahrbuch für Geologie und Paläontologie Abhandlungen 136, 345–359.

Mädler, K., 1963. Die figurierten organischen Bestandteile der posidonienschiefer. In: Schmitz, H.H. (Ed.) Zur kenntnis des nordwestdeutschen Posidonienschiefers. Beih. Geol. Hahrb. 58, 1–119.

Nielsen, B. L. & Friis, H. 1985: Diagenesis of Middle Jurassic Haldager Sand Formation sandstone in the Danish Subbasin, north Jutland. Bulletin of Geological Society of Denmark 33, 273-285.

Nielsen, L. H. 1995: Genetic stratigraphy of Upper Triassic- Middle Jurassic deposits of the Danish Basin and Fennoscandian Border Zone 1, 2, 3, 162pp. Unpublished PhD, University of Copenhagen, Denmark.

Nielsen, L.H. 2003. Late Triassic – Jurassic development of the Danish Basin and the Fennoscandian Border Zone, southern Scandinavia. In: Ineson, J.R. & Surlyk, F. (eds): The Jurassic of Denmark and Greenland. Geological Survey of Denmark and Greenland Bulletin 1, 459–526.

Nielsen, L.H. & Japsen, P. 1991: Deep wells in Denmark 1935–1990. Lithostratigraphic subdivision. Danmarks Geologiske Undersøgelse Serie A 31, 179 pp.

Nielsen, L.H., Petersen, H.I., Bojesen-Koefoed, J., Mathiesen, A., Dybkjær, K., Dalhoff, F., Kristensen, L. & Nytoft, H.P. 2006: Geological aspects relevant for an evaluation of the hydrocarbon potential of the Skagerrak Licence 1/4. Danmarks og Grønlands Geologiske Undersøgelse Rapport 2006/10 183 pp, 3 encl.

Nilsson, T., 1958. Über das vorkommen eines mesozoischen Sapropelgesteins in Schonen. Lunds Univ. årsskr. N.R. Avd. 2, 54(10). 112pp.

Norling, E. & Bergström, J. 1987. Mesozoic and Cenozoic tectonic evolution of Scania, southern Sweden. In: Ziegler, P.A. (ed.): Compressional inter-plate deformations in the Alpine Foreland. Tectonophysics 137, 7–19

Olsen, H. 1987: Ancient ephemeral stream deposits: a local terminal fan model from the Bunter Sandstone Formation (L. Triassic) in the Tønder-3, -4 and -5 wells, Denmark. In: Frostick, L., Reid, I. (Eds.), Desert Sediments: Ancient and Modern. Geological Society of London Special Publication, 35, 69-86.

Overeem, I., Weltje, G. J., Bishop-Kay, C. & Kroonenberg, S. B. 2001, The Late Cenozoic Eridanos delta system in the Southern North Sea Basin: a climate signal in sediment supply?: Basin Research 13(3), p. 293–312.

Parcerisa, D., Thiry, M. & Schmitt, J. M. 2010: Albitisation related to the Triassic unconformity in igneous rocks of the Morvan Massif (France). International Journal of Earth Science 99, 527-549.

Pearce, J. M, Holloway, S. Wacker, H., Nelis, M. K., Rochelle, C. and Bateman, K. 1996. Natural occurrences as analogues for the geological disposal of carbon dioxide. Energy Conversion and Management 37, 1123-1128.

Pearce, J. M., Kemp, S. J. & Wetton, P. D. 1999: Mineralogical and petrographical characterisation of a 1 m core from the Utsira Formation, Central North Sea. British Geological Survey Technical Report, Mineralogy & Petrography Series, 17pp.

Pegrum, R.M. 1984. The extension of the Tornquist Zone in the Norwegian North Sea. Norsk Geologisk Tidsskrift 64, 39–68.

Priisholm, S. 1983: Gethermal reservoir rocks in Denmark. Geological Survey of Denmark and Greenland, Årbog 1982, 73-86.

Pedersen, G.K., 1981. Anoic events during sedimentation of a Palaeogene diatomite in Denmark. Sedimentology 28, 487–504.

Petersen, H.I. and Nielsen, L.H., 2005. Vitrinite reflectance profile of the Felicia-1/1A well. Danm. Grønl. Geol. Unders. Rap. 2005/70, Confidential.

Petersen, H.I., Nielsen, L.H., Bidstrup, T. and Thomsen, E., 2003. Burial depth and post-Early Cretaceous uplift of Lower–Middle Jurassic strata in the Fennoscandian Border Zone based on organic maturity. In: Ineson, J.R. and Surlyk, F. (eds.), The Jurassic of Denmark and Greenland. Geol. Surv. Denm. Greenl. Bull. 1, 611–630.

Pedersen, G.K. & Andersen, P.R. 1980. Depositional environments, diagenetic history and sorce areas of some Bunter sandstones in northern Jutland. Danm. geol. Unders., Årbog 1979, 69–93.

Petersen, H.I., Nielsen, L.H., Mathiesen, A. and Bojesen-Koefoed, J.A., 2005. Assessment of the petroleum generation potential in the Danish Basin and Fennoscandian Border Zone. Danm. Grønl. Geol. Unders. Rap. 2005/65, Confidential.

Petersen, H.I, Nielsen, L.H., Bidstrup, T. & Thomsen, E. 2003: Burial depth and post-Early Cretaceous uplift of Lower–Middle Jurassic strata in the Fennoscandian Border Zone based on organic maturity. In: Ineson, J. R. & Surlyk, F. (eds): The Jurassic of

Denmark and Greenland. Geological Survey of Denmark and Greenland Bulletin 1, 611–630.

Poulsen, C. 1969: The Lower Cambrium from Slagelse No. 1, Western Sealand. Danmarks geologiske undersøgelse II Række 93, 29 pp.

Poulsen, C. 1974: Further contribution to the knowledge of the Palaeozoic of Slagelse No. 1, Western Sealand. Danmarks geologiske undersøgelse II Række 101, 72 pp.

Poulsen, N.E., 1996. Dinoflagellate Cysts from Marine Jurassic Deposits of Denmark and Poland. AASP Contribution Series 31, 227pp.

Prauss, M., Ligouis, B. and Luterbacher, H., 1991. Organic matter and palynomorphs in the "Posidonienschiefer" (Toarcian, Lower Jurassic) of southern Germany. In: Tyson, R.V. & Pearson, T.H. (eds) Modern and ancient continental shelf anoxia. Geological Society London, Special Publication 58, 335–351.

Ramseyer, K., Boles, J. R., Lichtner, P. C. 1992: Mechanism of plagioclase albitization. Journal of Sedimentary Petrology 62, 349-356.

Rasmussen, E.S. 2004: The interplay between true eustatic sea-level changes, tectonics, and climate changes: what is the dominating factor in sequence formation of the Upper Oligocene–Miocene succession in the eastern North Sea Basin, Denmark? Global and Planetary Change **41**, 15–30.

Rasmussen, E.S. and Dybkjær, K., 2005. Sequence stratigraphy of the Upper Oligocene–Lower Miocene of eastern Jylland, Denmark: role of structural relief and variable sediment supply in controlling sequence development. Sedimentology 52, 25–63.

Rasmussen, E.S., Vejbæk, O.V., Bidstrup, T., Piasecki, S and Dybkjær, K., 2005. Late Cenozoic depositional history of the Danish North Sea Basin: implications for the petroleum systems in the Kraka, Halfdan, Siri and Nini fields. In: Dore, A.G. & Vinding, B.A. (eds) Petrileum geology: North-West Europe and global perspectives–Proceedings of the 6th petroleum geology conference, 1347-1358. Geological Society, London.

Riding, J.B., 1987. Dinoflagellate cyst stratigraphy of the Nettleton Bottom Borehole (Jurassic: Hettangian to Kimmeridgian), Lincolnshire, England. Proceedings of the Yorkshire Geological Society 46, 231–266.

Riding, J.B. and Thomas, J.E., 1992. Dinoflagellate cysts of the Jurassic System. In: Powell, A.J. (ed.): A stratigraphic index of dinoflagellate cysts, 7–97. British Micropaleontological Society Publication Series. London: Chapman & Hall.

Ro, H.E., Larson, F.R., Kinck, J.J. & Husebye, E.S. 1990: The Oslo Rift - its evolution on the basis of geophysical observations. In: Neuman, E.-R. (ed.): Rift Zones in the Continental Crust of Europe - Geophysical, Geological and Geochemical Evidence: Oslo-Horn Graben. Tectonophysics 178, 11-28.

Rossi, C., Nielsen, B. L., Ramseyer, K. & Permanyer, A. 2001: Faceis-related diagenesis and multiphase siderite sementation and dissolution in the reservoir sandstones of the Khatatba Formationm Egypt's Western Desert. Journal of Sedimentary Research 71, 459-472.

Röhl, H.-J., Röhl, A.-S, Oshmann, W., Frimmel, A. & Schwark, L. 2001: The Posidonia Shale (Lower Toarcian) of SW-Germany: an oxygen-depleted ecosystem controlled by sea level and palaeoclimate. Palaeogeography, Palaeoclimatology, Palaeoecology 165, 27–52.

Saigal, G. C., Morad, S., Bjørlykke, K., Egeberg, P. K., Aagaard, P. 1988: Daigenetic albitization of detrital K-feldspar in Jurassic-Lower Cretaceous, and Tertiary clastic reservoir rocks from offshore Norway, I. Textures and origin. Journal of Sedimentary Petroloty 58, 1003-1013.

Schmid, V. and MacDonald, D. A. 1979: The role of secondary porosity in the course of sandstone diagenesis. In Scholle, A. P. & Schuldger, P. R. (eds.), Aspects of diagenesis. Soc. Econ. Paleont. Miner Spec. Publication 29, 175-207.

Schmidt, B.J., 1988. A source rock evaluation of the Mesozoic sediments of the well Hyllebjerg-1, Danish Subbasin. Danm. Geol. Unders. Ser. C 9, 105 pp.

Schmidt, B.J., 1989. Maturity and source-rock evaluation of the Mesozoic sequence in some Danish off-shore wells outside the Central Trough. Unpublished Ph.D. thesis, University of Aarhus, Århus, Denmark, 429 pp.

Sivhed, U., Wikman, H. & Erlström; M. 1999. Beskrivning till berggundskartona 1C Trelleborg NV och NO samt 2C Malmö SV, SO, NV och NO, 1: 50.000. SGU serie Af 191, 192, 193, 194, 196, 198.

Sorgenfrei, T. & Buch, A. 1964: Deep tests in Denmark, 1935–1959. Danmarks Geologiske Undersøgelse III. Række 36, 146 pp.

Spötl, C. and Pitman, J. K. (2009) Saddle (Baroque) Dolomite in Carbonates and Sandstones: A Reappraisal of a Burial-Diagenetic Concept. In: Morad, S. (ed.) Carbonate Cementation in Sandstones: Distribution Patterns and Geochemical Evolution, Blackwell Publishing Ltd., Oxford, UK.

Stemmerik, L., Frykman, P., Christensen, O.W. & Stentoft, N. 1987: The Zechstein carbonates of southern Jylland, Denmark. In: Brooks, J. & Glennie, K. (eds): Petroleum Geology of North West Europe, 365–374. London: Graham & Trotman.

Stenestad, E. 1972: Træk af det danske bassins udvikling i Øvre Kridt. Dansk geol. Foren., Årskrift for 1971, 63–69.

Storvold, V., Bjørlykke, K., Karlsen, D., Saigal, G. 2002: Porosity preservation in reservoir sandstones due to grain-coating illite: a study of the Jurassic Garn Formation from the

Schmidt, B.J., 1985. A coal petrographic source rock evaluation of the Rhaetic – Jurassic – Lower Cretaceous sediments of the Børglum-1 and Uglev-1 wells, Denmark. Bull. Geol. Soc. Denm. 33, 239–252.

Suggate, R.P., 1998. Relations between depth of burial, vitrinite reflectance and geothermal gradient. J. Petrol. Geol. 21, 5–32.

Surdam, R. C., Boese, S.W. & Crossey, L.J. 1984: The chemistry of secondary porosity. In: McDonald, D.A. & Surdam, R.C. (Eds), Clastics Diagenesis, American Association of Petroleum Geologists Memoir **37,** 127–149.

Surlyk, F. 1980: Demark. In: The geology of the European Countries, Denmark, Finland, Norway, Sweden, pp. 1-50. Graham and Trotman Ltd, Dunod.

Surlyk, F., 1997. A cool-water carbonate ramp with bryozoan mounds; Late Cretaceous-Danian of the Danish Basin. In: N.P. James and J.A.D. Clarke (Editors), Cool-water carbonates. Society of Economic Paleontologists and Mineralogists Special Publication. Society for Sedimentary Geology, Tulsa, pp. 293-307.

Surlyk, F. and Håkansson, E., 1999. Maastrichtian and Danian strata in the southeastern part of the Danish Basin. In: G.K. Pedersen and L.B. Clemmensen (Editors), 19th Regional European Meeting of Sedimentology, Copenhagen. Excursion A3, Copenhagen, pp. 29-58.

Thomsen, E., 1980. Rank of coal and dispersed organic matter in Rhaetian – Jurassic – L. Cretaceous deposits from the onshore part of the Danish Subbasin: Interpretation and implications for the maturity of potential hydrocarbon source rocks. Unpublished Ph.D. thesis, University of Aarhus, Århus, Denmark, 269 pp.

Thomsen, E., 1983. A coal petrographical investigation of the well Farsø-1. DGU Internal report. Geological Survey of Denmark, 14 pp.

Thomsen, E., 1984. A coal petrographical investigation of the well Års-1. DGU conf. report 1, 19 pp.

Thyne, G. D. & Gwinn, C. J. 1994. Evidence for a paleaoaquifer from early diagentic siderite of the Cardium Formation, Alberta, Canada. Journal of Sedimentary Research 64, 726-732.

Tyson, R.V., 1995. Sedimentary Organic Matter – Organic Facies and Palynofacies. Chapman & Hall, London, 615pp.

Van Konijnenburg-Van Cittert, J.H.A. and Van der Burgh, J., 1989. The flora from the Kimmeridgian (Upper Jurassic) of Culgower, Sutherland, Scotland. Rev. Palaeobot. Palynol. 61, 1–51.

Van Konijnenburg-Van Cittert, J.H.A. and Van der Burgh, J., 1996. Review of the Kimmeridgian flora of Sutherland. Scotland, with reference to the ecology and *in situ* pollen and spores. Proc. Geologists Assoc., 107, 97–105.

Vejbæk, O.V. 1989: Effects of asthenospheric heat flow in basin modelling exemplified with the Danish Basin. Earth and Planetary Science Letters 95, 97–114.

Vejbæk, O.V. 1997: Dybe strukturer i danske sedimentære bassiner. Geologisk Tidsskrift 4, 1–31.

Vejbæk, O.V. & Britze, P. 1994: Geological map of Denmark 1:750000. Top pre-Zechstein. Geological Survey of Denmark, Map series no. 45.

Wall, D., 1965. Microplankton, pollen, and spores from the Lower Jurassic in Britain. Micropaleontology 11(2), 151–190.

Waugh, B. 1978: "Authigenic K-feldspar in British Permo-Triassic sandstones." Journal of Geological Society London 135, 51-56.

Wille, W., 1982. Evolution and ecology of Upper Liassic dinoflagellates from SW Germany. N. Jb. Geol. Paläont. Abh. 164 (1–2), 74–82.

Woollam, R. and Riding, J.B., 1983. Dinoflagellate cyst zonation of the English Jurassic. Institute of Geological Sciences, Report 83/2, 1–42.

Weibel, R. 1998: Diagenesis in oxidising and locally reducing conditions – an example from the Triassic Skagerrak Formation, Denmark. Sedimentary Geology **121**, 259–276.

Weibel, R. 1999: Effects of burial on the clay assemblages in the Triassic Skagerrak Formation, Denmark. Clay Minerals **34**, 619–635.

Weibel, R. & Groberty, B. 1999: Pseudomorphous transformation of geothite needles into hematite in sediments of the Triassic Skagerrak Formation, Denmark. Clay Minerals **34**, 657–661.

Weibel, R. & Friis, H. 2004: Opaque minerals as keys for distinguishing oxidising and reducing diagenetic conditions in the Lower Triassic Bunter Sandstone, North German Basin. Sedimentary Gelogy **169**, 129–149.

Weibel, R. & Friis, H. 2007: Alteration of opaque heavy minerals as reflection of geochemical conditions in depositional and diagenetic environments. In: Mange, M. A. and Wright, D. T. (eds.) Heavy minerals in use. Developments in Sedimentology, Elsevier **58**, 305–333.

Wilkinson, M., Haszeldine, R. S., Fallick, A. E., Odling, N., Stoker, S. J., Gatliff, R. W. 2007. CO_2-mineral reaction in a natural analogue for CO2 storage – implications for modeling. Journal of Sedimentary Research 79, 486-494.

Wright, V. P. 1990: Soil micromorphology: A basic and applied science. Developments in Soil Scien 19, Elsevier, Amsterdam, 401-407.

Zachos, J.C., Pagani, M., Sloan, L.C., Thomas, E. & Billups, K. 2001: Trends, rhythms, and aberrations in global climate 65 Ma to present. Science 292, 686–693.

Ziegler, P.A. 1982: Geological atlas of western and central Europe. Shell International Petroleum Maatschappij B. V. 130 pp.

Ziegler, P.A. 1990: Geological atlas of western and central Europe, 2nd edition, 239 pp. Amsterdam: Elsevier for Shell Internationale Petroleum Maatschappij.

11. Enclosures

Seven log panels primarily showing lithostratigraphic correlation of the Skagerrak, Vinding, Gassum and Haldager Sand Formation have made been constructed and in included here in A4-format.

The logpanels have been forwarded to Universitet i Oslo in large scale hardcopy print for further consideration. The log panels are designed as contribution for discussions among the project participants for a coming project meeting.

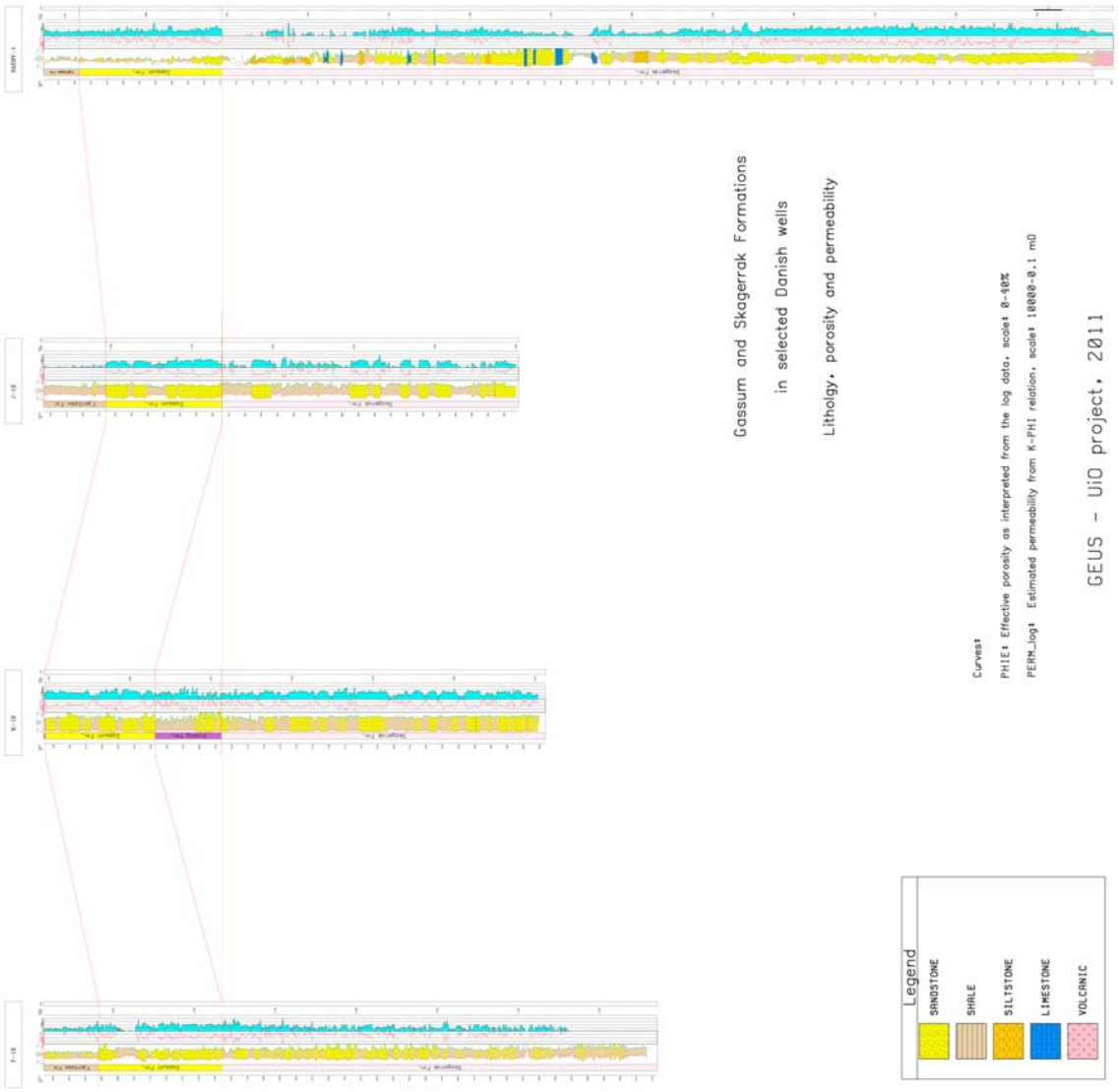
Gassum and Skagerrak Formations
in selected Danish wells
Lithology, porosity and permeability
Curves:
PHIE: Effective porosity as interpreted from the log data, scale: 0-40%
PERM_log: Estimated permeability from K-PHI relation, scale: 10000-0.1 mD
GEUS - UiO project, 2011
Legend
SANDSTONE
SHALE
SILTSTONE
LIMESTONE
VOLCANIC

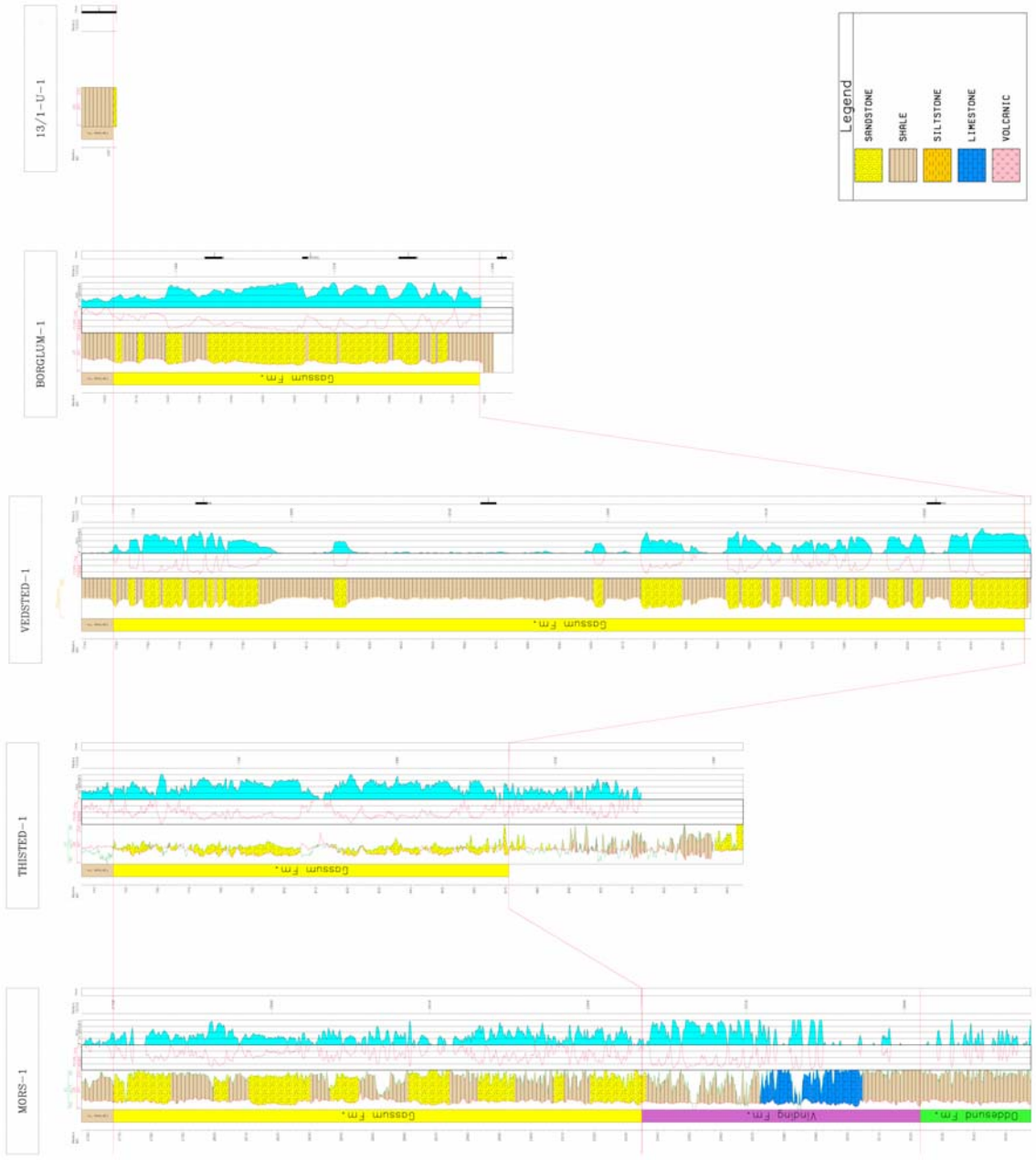
13/1-U-1
BORGLUM-1
VEDSTED-1
THISTED-1
MORS-1
Legend
SANDSTONE
SHALE
SILTSTONE
LIMESTONE
VOLCANIC
Gassum Fm.
Vinding Fm.
Oddesund Fm.


13/1-U-1
TERNE-1
ROENDE-1
Legend
SANDSTONE
SHALE
SILTSTONE
LIMESTONE
VOLCANIC
Gassum Fm.
Gassum Fm.

F-1X
K-1X
FELICIA-1
J-1X
13/1-U-1
Haldager Sand Fm.
Fjerritslev Fm
Legend
SANDSTONE
SHALE
SILTSTONE
LIMESTONE
VOLCANIC


J-1X
FELICIA-1A
Skagerrak Fm.
K-1X
F-1X
Legend
SANDSTONE
SHALE
SILTSTONE
LIMESTONE
VOLCANIC

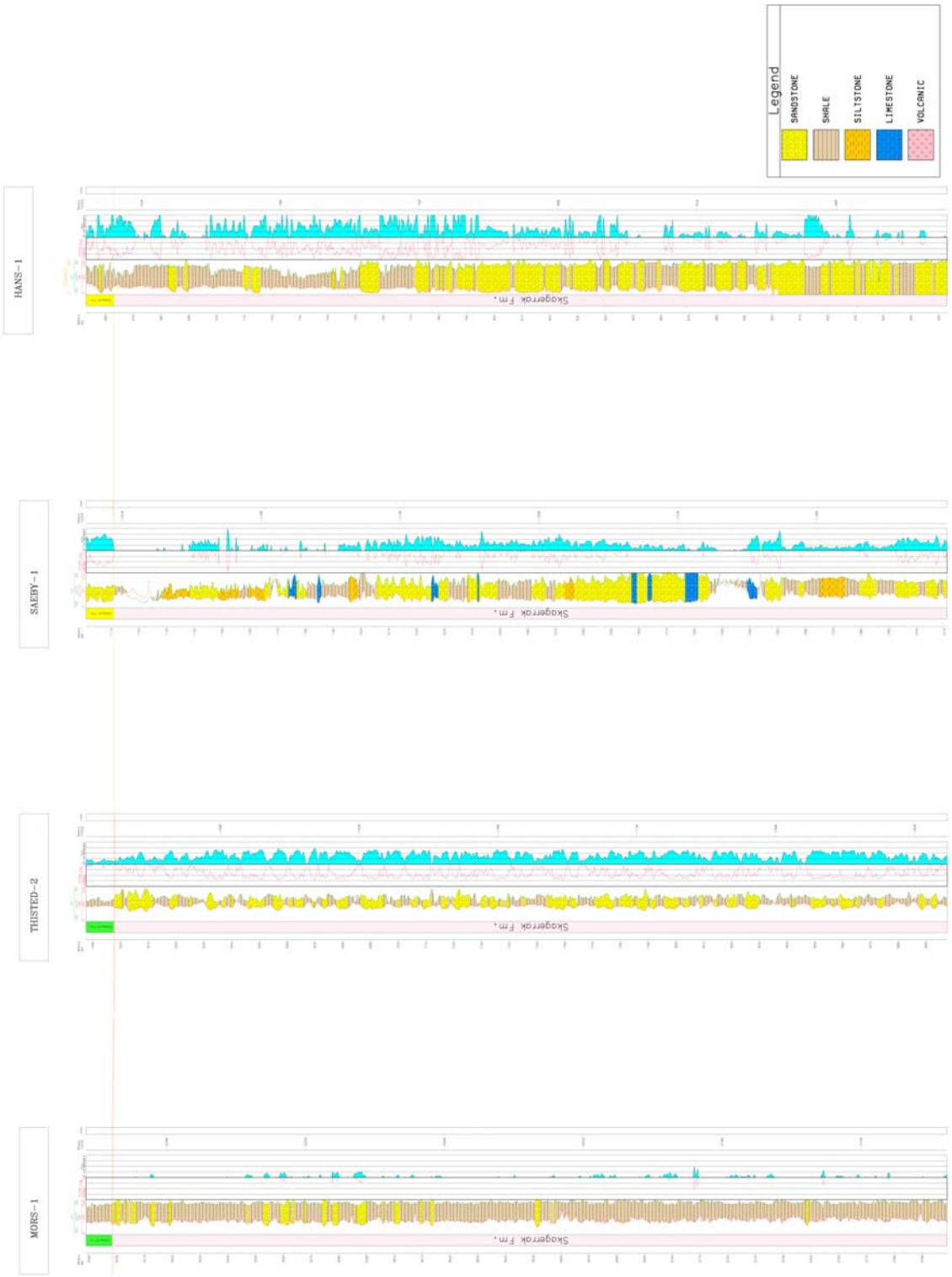
Legend
SANDSTONE
SHALE
SILTSTONE
LIMESTONE
VOLCANIC
HANS-1
SAEBY-1
THISTED-2
MORS-1
Skagerrak Fm.

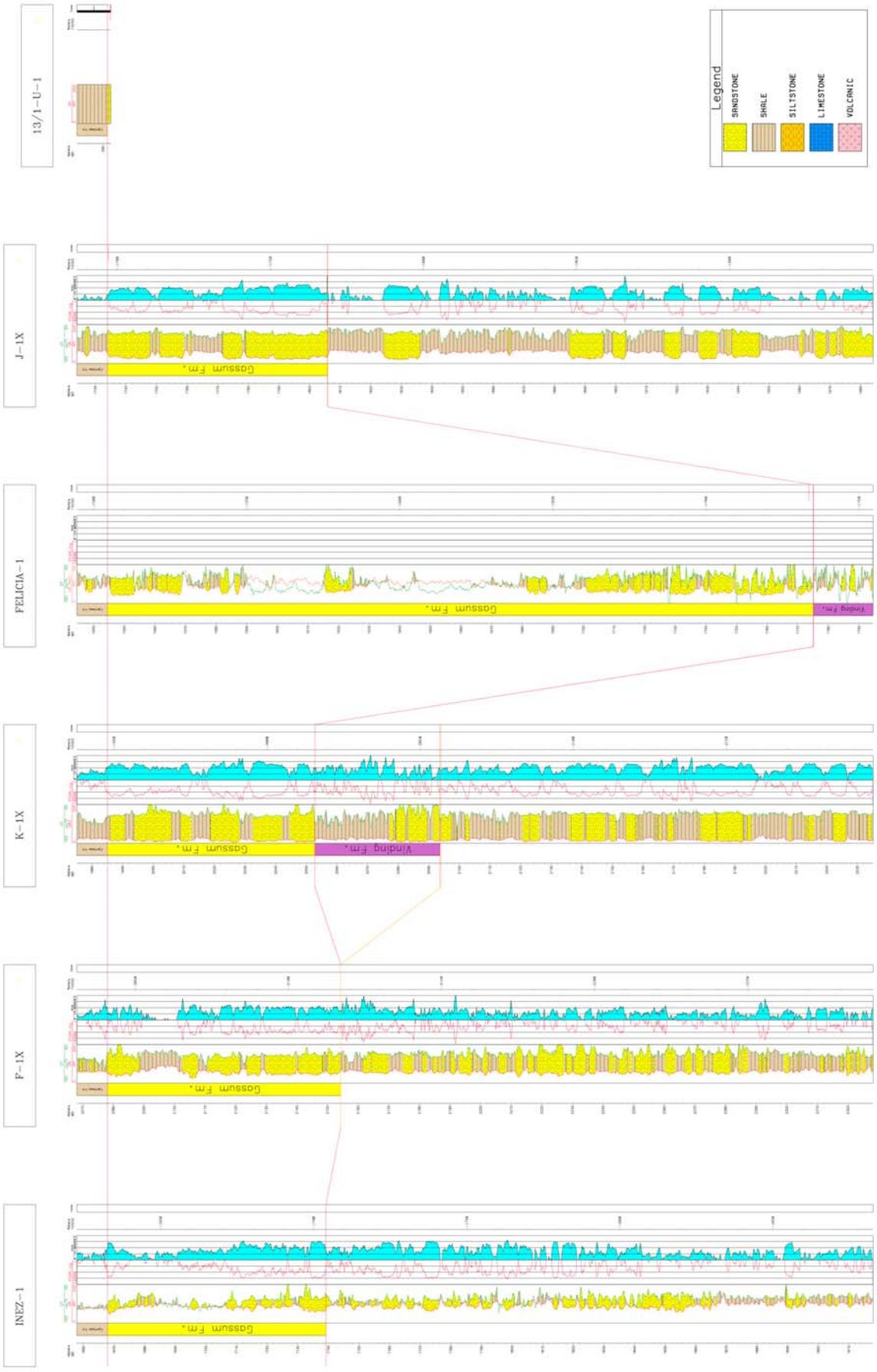
13/1-U-1
Legend
SANDSTONE
SHALE
SILTSTONE
LIMESTONE
VOLCANIC
J-1X
Gassum Fm.
FELICIA-1
Gassum Fm.
Vinding Fm.
K-1X
Gassum Fm.
Vinding Fm.
F-1X
Gassum Fm.
INEZ-1
Gassum Fm.